Random Planar Maps coupled to Spin Systems

Linxiao Chen

NNT : 2018SACLS096

THÈSE DE DOCTORAT

de

l'Université Paris-Saclay

École doctorale de mathématiques Hadamard (EDMH, ED 574)

Établissement d'inscription : Université Paris-Sud

Établissement d'accueil : Commissariat à l'énergie atomique et aux énergies alternatives

Laboratoire d'accueil : Institut de physique théorique de Saclay, URA 2306 CNRS

Spécialité de doctorat : Mathématiques appliquées

Linxiao CHEN

Cartes planaires aléatoires couplées aux systèmes de spins

Date de soutenance : 16 avril 2018

Après avis des rapporteurs :
Nathanaël Berestycki (University of Cambridge)
Gaëtan Borot (Max Planck Institute for Mathematics)

Jury de soutenance :

Marie Albenque	École polytechnique	Examinatrice
Nathanaël Berestycki	University of Cambridge	Rapporteur
Gaëtan Borot	Max Planck Institute for Mathematics	Rapporteur
Jérémie Bouttier	CEA Saclay et ENS Lyon	Directeur de thèse
Nicolas Curien	Université Paris-Sud	Directeur de thèse
Nathanaël Enriquez	Université Paris-Sud et UPMC	Président du jury
Antti Kupiainen	University of Helsinki	Examinateur

Remerciements – *Acknowledgements*

Je voudrais exprimer ma profonde gratitude à tous ceux qui ont contribué, directement ou indirectement, sur le plan scientifique ou moral, à la réalisation de cette thèse. Je regrette de ne pas pouvoir prononcer le nom de chacun d'entre eux, puisqu'il sera impossible de réciter proprement leurs actes de bienveillance dans ces courtes pages.

Le plus grand merci va naturellement à Jérémie et Nicolas, pour m'avoir fait découvrir un sujet aussi riche et joli que les cartes planaires décorées. À la réception de mes sollicitations d'un stage de Master, ils se sont mis spontanément en contact pour me proposer un stage en codirection, qui est devenu plus tard le début de cette thèse. Grâce à cela, j'ai pu bénéficié non seulement d'un double d'attention et de soutien, mais aussi de leurs grandes compétences sur les aspects complémentaires du sujet de thèse. Je voudrais aussi les remercier pour m'avoir laissé une grande liberté à organiser mes recherches, à participer à de nombreuses écoles et conférences, tout en créant les meilleurs conditions pour les réaliser. Dès le premier jour de notre rencontre, j'étais impressionné par leur dynamisme et leur passion à la recherche. Je ne sais combien de fois j'entre dans leurs bureaux confus et découragé, et sors éclairé et pleine d'énergie. Merci !

Je suis extrêmement reconnaissant à Nathanaël Berestycki et Gaëtan Borot pour avoir accepté la lourde tache d'être rapporteurs de ma thèse, et pour leur grande patience pendant mes délais de rédaction. Leurs commentaires précieux ont beaucoup contribué à la clarté de ce manuscrit. Je tiens aussi à remercier chaleureusement Marie Albenque et Nathanaël Enriquez avoir aimablement accepté à faire partie de mon jury, malgré des difficultés personnelles et une date de soutenance au milieu des vacances scolaires. *Special thanks go to Antti Kupiainen for allowing me to finish this thesis while working in the mathematical physics group at University of Helsinki, and for his cheerful support during the hard winter time of writing.*

This thesis is based on joint works with Timothy Budd, Nicolas Curien, Pascal Maillard and Joonas Turunen. It was a great pleasure to collaborate with them and I deeply appreciate their help and encouragement during the work. I feel indebted to the following people, as many ideas in this thesis grew out of the enlightening discussions with them: Marie Albenque, Nathanaël Berestycki, Mireille Bousquet-Mélou, Bertrand Eynard, Emmanuel Guitter, Yichao Huang, Konstantine Izyurov, Benoît Laslier, Laurent Ménard and Gourab Ray. I thank also all the regular participants of the "journée cartes" for sharing their latest advances in the domain during our frequent and convivial meetings.

Cette thèse n'aurais pas été possible sans la formation de grande qualité livrée par les professeurs du Master 2 "Probabilités et Modèles Aléatoires" 2013/2014 à l'UPMC. Je remercie particulièrement Prof. Zhan Shi pour ses conseils précieux qui m'ont poussé à découvrir le stage qui prélude cette thèse. Je tient aussi à remercier Jean-François Allemand, Alberto Rosso et Guilhem Semerjian du Master de physique théorique de l'ENS pour m'initier à la recherche scientifique et pour leurs conseils d'orientation.

Je voudrais aussi exprimer mes gratitudes à mes amis et collègues de l'Institut de Physique Théorique et du Laboratoire de Mathématiques d'Orsay, où j'ai passé trois années de thèse dans une atmosphère dynamique et conviviale. Je suis reconnaissant à Emmanuel, Jean-Marc et Jérémie pour leur accueil chaleureux à l'IPhT et de nombreux trajets en voiture à la cantine du CEA. Je remercie tous les habitués des séminaires de Proba-Stat et "Trucs et Astuces" au LMO pour les échanges enrichissant au tableau ou bien autour d'un café. C'était heureux de faire partie du troupeau de doctorants qui migrent ensemble chaque midi entre le bâtiment 430 et le CESFO. J'apprécie beaucoup les conversations (et parfois de vifs débats !) à la table et sur les chemins. Je remercie en particulier mes co-bureaux Emilien, Zheng, Sasha, Salim, Antoine et co-bureau-connecté-par-le-balcon Çagr et Weikun pour leurs coups de main au quotidien sur des problèmes mathématiques ou non-mathématiques. Ils ont fait le bureau un lieu de travail idéal. Enfin, je dois aussi un grand merci aux équipes administratives de l'IPhT et du LMO pour leur très grande efficacité, et pour avoir toléré ma tendance de prendre les démarches au dernier moment. En particulier j'ai beaucoup bénéficié du "PhD-coaching" de Stéphane Nonnenmacher à l'IPhT et au LMO.

Une mention particulière pour le chat du bureau 014 du bâtiment 430, qui a porté beaucoup de joie à moi et à son entourage pendant ces dernières années de thèse. Je suis aussi très reconnaissant à Chen Hu pour son accompagnement et encouragement au fil des années. Enfin et surtout, je remercie ma famille pour leur soutien permanent et inconditionnel: 最后，感谢我的家人，对我一直以来无条件的支持与鼓励。

献给我的(外)祖父母

To my grandparents.

Contents

Chapter I

Introduction

Cette introduction est divisée en quatre sections. La section 1 rappelle les définitions de base sur les cartes planaires sans aléa ni décoration. La section 2 introduit les cartes aléatoires non décorées avec quelques exemples. On essaie de dégager l'idée de l'universalité en s'appuyant sur la classe d'universalité de la carte brownienne. On retrace aussi les premières étapes de sa construction, qui servira comme repère pour la discussion à propos des cartes décorées. La section 3 définit les modèles de cartes décorées abordés dans ce mémoire, et explique les motivations (surtout physiques) pour leur étude. Enfin la section 4 donne un résumé par chapitre du reste de ce mémoire, et explicite des liens précis entre les modèles abordés.

1 Définitions et conventions de base

On regroupe dans cette section les définitions nécessaires pour que cette introduction puisse être lue de façon autonome. Pour un panorama plus détaillé, on réfère aux nombreux livres et notes de cours dédiés à ce sujet, par exemple [LZ04, Mie14, Cur17, Eyn16].

Grosso modo, une carte planaire est un graphe muni d'une structure planaire. Il y a plusieurs façons de formaliser cela, voir par exemple [LZ04, Section 1.3]. La définition la plus intuitive est probablement la suivante :

Definition. Considérons les plongements *propres* (i.e. sans croisement d'arêtes) d'un graphe *fini* et *connexe* dans la sphère. Une carte planaire est une classe d'équivalence de ces plongements modulo les homéomorphismes de la sphère qui préservent l'orientation.

La Figure I.1(a) donne trois plongements propres d'un même graphe dans le plan, dont les deux derniers représentent la même carte planaire,[1] mais pas le premier. Pour mettre en évidence la différence entre les deux premiers dessins, on peut les découper le long des arêtes, et observer que les composantes connexes ainsi obtenues ne sont pas entourées du même nombre d'arêtes.

1.1 Les faces et leurs degrés

On appelle les composantes connexes ainsi obtenues les *faces* de la carte, et le nombre d'arêtes qui entourent une face le *degré* de la face. L'ensemble des sommets et l'ensemble des arêtes d'une carte sont hérités de son graphe sous-jacent. Au contraire, l'ensemble des faces est une structure propre à la carte. Les cardinaux de ces trois ensembles sont reliés par la relation d'Euler:

$$\#\,\text{sommet} + \#\,\text{face} - \#\,\text{arête} = 2 \tag{I.1}$$

La constante 2 à droite est appelée *caractéristique d'Euler* de la sphère. D'autre part, un simple comptage du nombre d'arêtes donne la contrainte suivante, qui est utile pour étudier les cartes avec degrés des faces contrôlés :

$$\sum_{f\in\text{face}} \deg(f) = 2\cdot\#\,\text{arête}\,. \tag{I.2}$$

On peut inverser la procédure de découpage ci-dessus pour donner une définition alternative des cartes planaires : une carte planaire est un recollement de polygones (i.e. un couplage parfait entre les arêtes des polygones) tel que la surface qui en résulte est homéomorphe à la sphère.[2] La Figure I.1 donne un exemple d'un tel recollement. Cette définition met en évidence le fait que pour tout n fixé, le nombre des cartes planaires ayant n arêtes est fini.

1.2 Dual d'une carte

À chaque carte planaire $\mathfrak{m}$ on peut associer une *carte duale* $\mathfrak{m}^\dagger$ qui échange les rôles des sommets et des faces de $\mathfrak{m}$. Plus précisément, on place un sommet dual dans chaque face

[1] On représente une carte planaire, objet qui vit sur la sphère, dans le plan en utilisant la projection stéréographique. Cela revient à choisir arbitrairement une face de la carte comme la face externe.

[2] La sphéricité est caractérisée par le caractéristique d'Euler 2. Voir [MT01, Section 3.1].

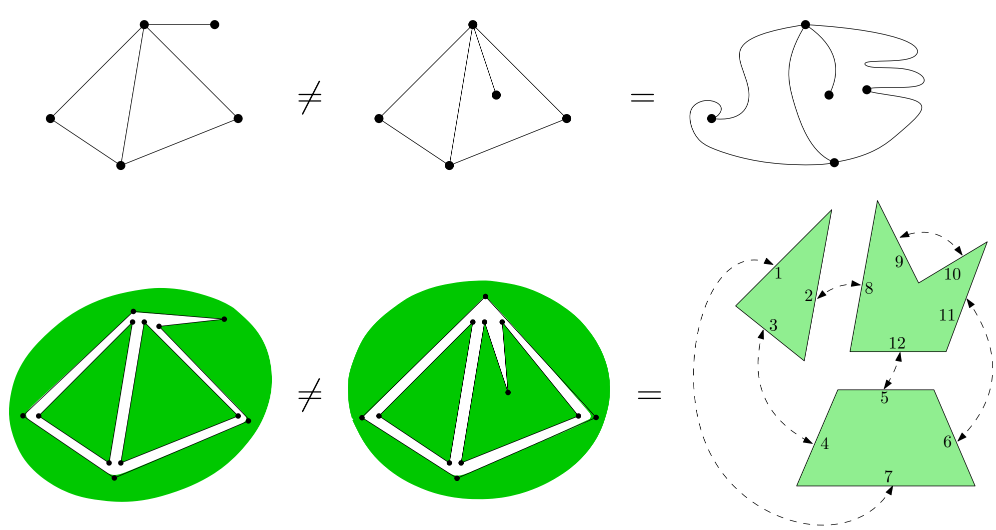

Figure I.1 – *Trois différents plongements propres d'un même graphe dans le plan. Les deux premiers plongements ne correspondent pas à la même carte: en découpant les dessins le long des arêtes, on observe que les degrés des faces sont* $\{3,3,6\}$ *dans le premier cas, mais* $\{3,4,5\}$ *dans le deuxième cas.*

de $\mathfrak{m}$, et pour chaque arête e de $\mathfrak{m}$, on trace une arête duale $e^\dagger$ qui relie les sommets duaux dans les deux faces adjacentes à e comme dans la Figure I.2. Chaque face de la carte duale contient exactement un sommet de $\mathfrak{m}$. (Cela est témoigné par la symétrie de rôle du nombre de sommets et du nombre de faces dans la relation d'Euler.) Le passage au dual est une involution sur l'ensemble des cartes planaires. Un point fixe de cette involution est dit *autodual*.

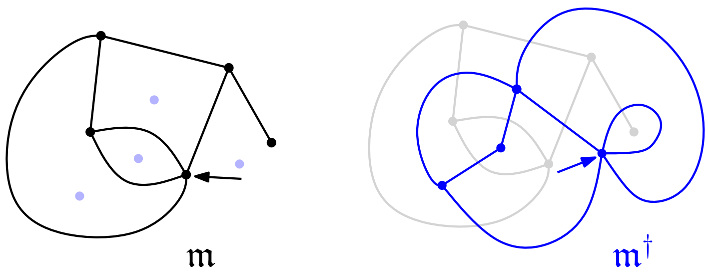

Figure I.2 – *Une carte* $\mathfrak{m}$ *et son dual* $\mathfrak{m}^\dagger$*. Les flèches indiquent les coins racines.*

1.3 Carte enracinée: absence de symétrie

Une carte peut admettre des automorphismes non triviaux. (Par exemple la première carte dans la Figure I.1 est invariante sous la symétrie miroir.) Cela rend compliqué leur énumération, ou plus généralement la construction de bijections sur les cartes. Pour contourner ce problème, on considère les cartes *enracinées*, i.e. munies d'un *coin distingué* (la racine).[3] On

[3] Un coin désigne la section angulaire entre deux arêtes consécutives autour d'un sommet. Une autre convention couramment utilisée consiste à distinguer une arête orientée pour enraciner la carte. On peut bien sûr passer de l'un à l'autre bijectivement. L'avantage d'utiliser un coin racine est que le choix de la racine de la carte duale est canonique, voir la Figure I.2.

appelle la face contenant ce coin la *face racine*, et le sommet incident à ce coin le *sommet racine*.

Une carte enracinée n'a pas d'automorphisme non trivial. En effet, la racine permet de définir une numérotation canonique des sommets (par exemple à l'aide d'un parcours en largeur), des arêtes et des faces de la carte. Donc un automorphisme de la carte qui fixe la racine fixe aussi tous les sommets, arêtes et faces, i.e. il est égal à l'identité. En pratique, cette absence d'automorphisme est souvent utilisée pour choisir de façon arbitraire (mais déterministe) un sommet/arête/face parmi tous ceux qui satisfont une certaine propriété : il suffit de choisir celui du plus petit numéro sous une certaine numérotation canonique fixée en avance. Dans les Chapitres II et V, c'est cet argument qui nous permettra d'enraciner les petites cartes issues de certaines décompositions récursives de cartes.

1.4 Cartes à bord

Les décompositions récursives des cartes, qui sont à la base de très nombreuses études combinatoires des cartes, nécessitent la considération des cartes avec un bord. On définit une *carte à bord enracinée* comme la même structure qu'une carte planaire enracinée sans bord, mais avec un point de vue différent: dans une carte enracinée à bord, on considère la face racine comme la *face externe* et les autres faces comme les *faces internes*. Le degré de la face externe est appelé *périmètre* de la carte à bord. Par définition, le sommet racine est toujours sur le bord.

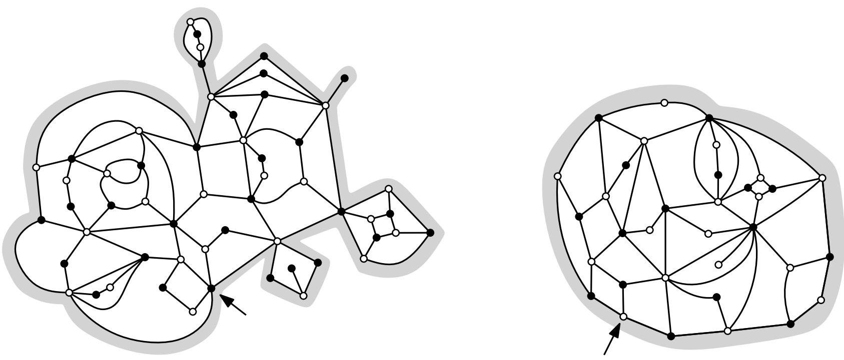

(a) (b)

Figure I.3 – *(a) Une carte bipartie avec un bord général, et des faces internes de degrés 2, 4 et 6. (b) Une quadrangulation à bord simple. Dans les deux cas, la flèche représente la racine.*

La face externe d'une carte à bord peut avoir des points de pincement comme dans l'exemple de la Figure I.3(a), autrement dit, plusieurs coins de la face externe peuvent partager le même sommet. Parfois il est commode de se restreindre aux cas où cela n'arrive pas. On dit alors que le bord de la carte est *simple*. Une carte à bord simple est aussi appelée *carte du polygone*, ou *carte du p-gone* si l'on veut spécifier le périmètre p.

1.5 Cartes biparties, p-angulations

Comme pour les graphes, une carte est dite *bipartie* si ses sommets peuvent être coloriés par deux couleurs de sorte qu'une arête relie toujours deux sommets de couleurs différentes. Une carte planaire est bipartie si et seulement si toutes ses faces sont de degré pair. Si toutes les faces sont du même degré p, la carte est appelée *p-angulation* (*triangulation* si $p = 3$, *quadrangulation* si $p = 4$, etc.). Lorsque cela est vrai à l'exception de la face externe, on parle d'une *p-angulation à bord*. La Figure I.3 donne un exemple (a) d'une carte bipartie avec un bord non simple, et (b) d'une quadrangulation du 12-gone (bord simple).

Dans ce mémoire, une carte sera toujours supposée *planaire* et *enracinée*. Le graphe sous-jacent d'une carte peut contenir des cycles (arêtes dont les deux extrêmités coïncident) et des arêtes multiples.

2 Rappels sur les cartes aléatoires non décorées

2.1 La classe d'universalité des cartes uniformes

Cartes aléatoires uniformes La classe la plus naturelle — et en effet la plus étudiée — de carte aléatoire est celle de *carte aléatoire uniforme*. Au sens strict, une carte aléatoire uniforme est un élément choisi uniformément dans un ensemble fini de cartes. Les ensembles les plus souvent considérés sont ceux définis par une contrainte sur les degrés de faces, plus la valeur d'un ou plusieurs *paramètres de taille*.[4] On notera par N l'ensemble de ces paramètres. Voici quelques exemples.

(i) L'ensemble des *cartes générales* ayant n arêtes. ($N = n$)

(ii) L'ensemble des *quadrangulations* ayant n faces. ($N = n$)

(iii) L'ensemble des *triangulations du p-gone* ayant n faces. ($N = (n, p)$)

(iv) L'ensemble des *cartes biparties à bord de périmètre* $2p$ ayant n_1 faces de degré 2, n_2 faces de degré 4, …, et n_d faces de degré $2d$. ($N = (n_1, \dots, n_d, p)$)

Les paramètres de taille consistent en un seul entier n dans les cas (i) et (ii), mais un couple d'entiers (n, p) dans le cas (iii).[5]

Cartes aléatoires de Boltzmann Au sens large, la *classe d'universalité* des cartes aléatoires uniformes inclut aussi certaines *cartes aléatoires de Boltzmann*. La loi d'une carte aléatoire de Boltzmann est construite à partir d'une carte aléatoire uniforme en remplaçant une ou plusieurs contraintes de taille par des poids de Boltzmann qui pénalisent les grandes cartes. Dans l'exemple (iii) ci-dessus, on peut relâcher la contrainte sur le nombre de faces n, et donner un poids t à chaque face. Alors on obtient une *triangulation de Boltzmann du p-gone* $\mathfrak{t}$ de loi

$$\mathbb{P}_p(\mathfrak{t} = \mathfrak{t}_0) = \frac{t^{\#\mathrm{face}(\mathfrak{t}_0)}}{Z_p(t)} \qquad \text{où} \qquad Z_p(t) = \sum_{\mathfrak{t}_0} t^{\#\mathrm{face}(\mathfrak{t}_0)}$$

et la somme porte sur toutes les triangulations du p-gone. On dit que la valeur du paramètre $t > 0$ est *admissible* si la fonction de partition $Z_p(t)$ est finie. De la même façon, on peut

[4]Le cardinal d'un tel ensemble de cartes a systématiquement une expression simple en intégrale de matrices. Cela explique pourquoi ces ensembles de cartes sont relativement facile à étudier.

[5]On ne peut pas fixer le nombre de faces comme paramètre de taille dans le cas (i) puisque, sans constrainte sur les degrés des faces, l'ensemble des cartes ayant n faces est infini. Ce problème n'existe pas dans le cas (ii) puisque la relation (I.2) donne $\#\,\text{arête} = 2 \cdot \#\,\text{face}$.

définir une *carte bipartie de Boltzmann à bord de périmètre* $2p$ en donnant un poids q_k à chaque face de degré $2k$ ($k = 1, \dots, d$) dans l'exemple (iv) ci-dessus:

$$\mathbb{P}_p(\mathfrak{m} = \mathfrak{m}_0) = \frac{1}{F_p(\mathbf{q})} \prod_{k=1}^{d} q_k^{\#\,\text{face de degré } 2k(\mathfrak{m}_0)} \tag{I.3}$$

où le jeu de poids $\mathbf{q} = (q_1, \dots, q_d)$ est dit admissible si la fonction de partition $F_p(\mathbf{q}) := \sum_{\mathfrak{m}_0} \prod_{k=1}^{d} q_k^{\#\,\text{face de degré } 2k(\mathfrak{m}_0)}$ est finie.

Dans la suite de cette introduction, on utilisera la notation générique $\mathcal{C}_N$ pour désigner une famille de cartes de taille N, et l'on notera par $w(\mathfrak{m})$ un poids de Boltzmann défini sur les cartes $\mathfrak{m} \in \mathcal{C}_N$. Alors la loi d'une carte de Boltzmann générique s'écrit

$$\mathbb{P}_N(\mathfrak{m} = \mathfrak{m}_0) = \frac{w(\mathfrak{m}_0)}{Z_N} \qquad \text{où} \qquad Z_N = \sum_{\mathfrak{m}_0 \in \mathcal{C}_N} w(\mathfrak{m}_0)\,.$$

Les deux exemples ci-dessus correspondent respectivement aux poids $w(\mathfrak{t}) = t^{\#\,\text{face}(\mathfrak{t})}$ et $w(\mathfrak{m}) = \prod_{k=1}^{d} q_k^{\#\,\text{face de degré } 2k(\mathfrak{m})}$. Notons que cela inclut aussi les cartes aléatoires uniformes, qui correspondent au cas où $w(\mathfrak{m}) = 1$.

Universalité des cartes uniformes Du point de vue de la physique statistique, les cartes uniformes et les cartes de Boltzmann ne sont que deux descriptions microscopiques (i.e. description *micro-canonique* et description *canonique*) d'un même système macroscopique. On s'attend donc à l'émergence d'un même objet aléatoire dans la limite thermodynamique. Cela signifie qu'une carte uniforme et ses cartes de Boltzmann associées, proprement remises à l'échelle, doivent converger vers la même limite quand leurs tailles convergent vers l'infini. De plus, on s'attend à ce que cet objet limite soit *universel*, i.e. il ne dépend pas de la plupart des détails microscopiques du modèle. Il est en général difficile de prouver rigoureusement la convergence d'une classe de modèle de physique statistique vers une limite thermodynamique *universelle*. Remarquablement, cela a été fait en grande partie pour les modèles dans la classe d'universalité des cartes uniformes, et dans un sens très fort de *limite d'échelle* des cartes.

2.2 La carte brownienne et ses variantes

Plus précisément, considérons l'ensemble $\mathcal{C}_N$ des cartes biparties *sans bord* ayant N faces de degrés bornés par $2d$. Soit $\mathfrak{m}_N$ la carte de Boltzmann définie sur $\mathcal{C}_N$ par le poids $w(\mathfrak{m}) = \prod_{k=1}^{d} q_k^{\#\,\text{face de degré } 2k(\mathfrak{m})}$. Si les paramètres $(q_1, \dots, q_d)$ sont *critiques* (on reviendra dans la section 2.4 sur la définition de la criticité), alors on a le résultat de limite d'échelle suivant:

Theorem I.A (convergence vers la carte brownienne [LG13]). *Soit $V(\mathfrak{m}_N)$ l'ensemble des sommets de $\mathfrak{m}_N$, vu comme un espace métrique sous la distance de graphe $d_{\mathtt{gr}}$. Alors il existe une constante $c > 0$ dépendant de la famille $(\mathfrak{m}_N)_{N\geq 1}$ telle que*

$$\left(V(\mathfrak{m}_N), \frac{c}{N^{1/4}} d_{\mathtt{gr}} \right) \xrightarrow[N\to\infty]{} (\mathbb{M}, D)$$

en loi par rapport à la distance de Gromov-Hausdorff,[6] *où* $(\mathbb{M}, D)$ *est la* carte brownienne*, un espace métrique compact (aléatoire) défini indépendemment de* $(\mathfrak{m}_N)_{N\geq 1}$.

Ce théorème contient en particulier le résultat fondateur de la limite d'échelle de la quadrangulation uniforme à N faces [LG13, Mie13], qui correspond au cas où $q_k = g\delta_{k,2}$. Il a aussi été démontré que d'autres familles de cartes convergent dans le sens de Gromov-Hausdorff vers la carte brownienne, confirmant l'universalité de cette dernière. Citons ici la triangulation uniforme [LG13], les triangulations et quadrangulations uniformes avec contraintes locales [BLG13, ABA17, ABW17], les cartes uniformes [BJM14] ou les cartes biparties uniformes [Abr16] (à N arêtes). Voir aussi [Mar16] pour une généralisation du théorème I.A où la famille $(\mathfrak{m}_N)_{N\geq 1}$ est remplacée par une famille de cartes à degrés de faces prescrits.

Les résultats de convergence ci-dessus traitent des cartes planaires sans bord, i.e. cartes définies sur la sphère. Des convergences similaires ont aussi été établies pour les familles de cartes définies sur une surface $\mathcal{S}$ autre que la sphère, comme le disque [BM17], le plan [CLG14] ou le demi-plan [BMR16][7] et, si l'on se contente de la convergence le long des sous-suites, toutes les surfaces compactes orientables [Bet10]. Les limites d'échelles ainsi obtenues sont en général homéomorphes à la surface de départ $\mathcal{S}$ [LGP08, CLG14, Bet15b, Bet12], à condition que la normalisation des distances soit "standard" (voir discussions dans [Bet15b, BMR16]). Mise à part cette différence de la topologie globale, ces surfaces continues sont similaires localement autour d'un point typique. Elles représentent donc la même classe d'universalité. Elles sont appelées *surfaces browniennes* dues à leurs constructions qui s'appuient sur l'*arbre continu brownien* (voir [Ald91]).

Une feuille de route vers la carte brownienne D'un point de vue physique (qui sera expliqué dans la section 3.2), le but de l'étude des cartes aléatoires *décorées* est la construction des limites d'échelle similaires à la carte brownienne. Cependant, ce but semble hors de portée à l'heure actuelle. Pour comprendre les obstacles qui empêchent la généralisation du résultat de limite d'échelle aux cartes aléatoires décorées, soulignons quelques étapes clés dans la démonstration des convergences vers la carte brownienne:

(i) **Énumération** de différentes familles de cartes.

(ii) Construction de **bijections** entre cartes et *arbres étiquetés* qui encodent bien la **distance de graphe** dans la carte.

(iii) Limite d'échelle du **diamètre** et du **profil de distance**.

(iv) Convergence au sens de **Gromov-Hausdorff** de cartes le long de sous-suites.

(v) Propriétés des **géodésiques** dans les limites des sous-suites.

(vi) **Unicité** de la limite.

---

[6] La distance de Gromov-Hausdorff $d_{\mathtt{G.H.}}$ entre deux espaces métriques compacts (E, d) et (E', d') mesure l'erreur minimale qu'il faut commettre sur la métrique pour déformer (E, d) en (E', d'). En particulier, elle est définie de façon intrinsèque, i.e. indépendemment de toute paramétrisation de E et E'. L'ensemble des (classes d'isométrie d') espaces métriques compacts muni de $d_{\mathtt{G.H.}}$ est un espace métrique polonais (séparable et complet). Pour ces raisons, la distance de Gromov-Hausdorff est la distance du choix pour formuler la convergence en loi des espaces métriques aléatoires. Cependant, ce mémoire ne prouvera aucun résultat de convergence sous $d_{\mathtt{G.H.}}$, et l'on renvoie les lecteurs à [BBI01] pour la définition précise de cette distance.

[7] Ces deux cas nécessitent une légère modification de la distance de Gromov-Hausdorff puisque le plan et le demi-plan ne sont pas compacts. Voir [BBI01].

À l'heure actuelle, la tentative d'appliquer ce schéma de preuve aux cartes décorées est bloquée à l'étape (ii): il existe bien des bijections qui encodent les cartes décorés par des objets plus simples (y compris des arbres étiquetés), mais aucune d'entre elles ne permet de lire facilement la distance de graphe dans la carte. Les paragraphes suivants détaillent davantage ce qui est connu sur l'énumération et le codage bijectif des cartes non décorées. On renvoie les lecteurs à [Mie14] pour de plus amples informations sur le reste de la liste.

2.3 Énumération de cartes

L'énumération (et l'étude mathématique en général) des cartes est initiée dans les années 1960 par une série de travaux de Tutte [Tut62b, Tut62c, Tut62a, Tut63] et Brown [Bro63, Bro64, BT64, Bro65a, Bro65b] motivés par le théorème (conjecture à l'époque) des quatre couleurs. L'approche de Tutte et Brown consiste à traduire une décomposition récursive d'une classe $\mathcal{C}_N$ de cartes en une équation fonctionnelle dite *à une variable catalytique* satisfaite par la série génératrice $f(x) := \sum_N \#\mathcal{C}_N \cdot x^N$. Ensuite, ils résolvent cette équation en utilisant une technique appelée la *méthode quadratique*. On renvoie à [GJ83, Section 2.9] pour une introduction à cette méthode. Cette méthode d'énumération est en général très calculatoire, mais aussi très robuste dans le sens où elle permet d'énumérer de nombreuses familles de cartes de façon quasi-systématique [BMJ06]. Elle a également été généralisée pour énumérer les cartes décorées. Voir [BBM17] et les références contenues. Dans le chapitre V, on l'appliquera dans le cas des triangulations décorées par le modèle d'Ising.

Une autre approche d'énumération des cartes a été développée par des physiciens dans les années 1970 [tH74, BIPZ78]. Cette approche réduit le problème d'énumération des cartes au calcul de certaines intégrales de matrices en exploitant le fait que les coefficients du développement asymptotique de ces intégrales comptent exactement les cartes. On renvoie à [LZ04, Chapter 3] pour une présentation introductive et à [Eyn16] pour un exposé plus complet.

Quelques formules énumératives Malgré la complexité calculatoire des deux méthodes d'énumération ci-dessus, les formules énumératives qu'elles génèrent s'avèrent souvent assez simples et explicites. Par exemple, on reverra dans le chapitre II que la fonction de partition de la quadrangulation de Boltzmann de périmètre $2p$ ($q_k = g\delta_{k,2}$ dans la définition (I.3)) s'écrit

$$Z_p(g) = \binom{2p}{p}\left(\frac{R}{p+1} - \frac{2(R-1)}{p+2}\right) R^p \tag{I.4}$$

où $R = \frac{1-\sqrt{1-12g}}{6g}$ est la solution positive minimale de l'équation $R - 3gR^2 = 1$. Lorsque $p = 1$, la formule ci-dessus devient $Z_1(g) = \frac{1}{3}(4R - R^2)$ avec $R - 1 = 3gR^2$. Puisque les quadrangulations à bord de périmètre 2 sont en bijection avec les quadrangulations sans bord, $Z_1(g)$ est aussi la fonction génératrice des nombres $\#\mathcal{Q}_n$ de quadrangulations à n faces. En utilisant la formule d'inversion de Lagrange, il n'est pas difficile d'en déduire que

$$\#\mathcal{Q}_n = \frac{2}{n+2} 3^n \frac{1}{n+1}\binom{2n}{n}. \tag{I.5}$$

Les résultats (I.4) et (I.5) sont connus (sous forme déguisée) depuis les premiers travaux de Tutte [Tut62c, Tut63]. Mais la raison derrière la simplicité de ces formules resta longtemps mystérieuse. Par exemple, l'expression (I.4) montre que $Z_p(g)$ admet une paramétrisation rationnelle, c'est-à-dire le graphe de la fonction $Z_p(g)$ est contenu dans une courbe paramétrée de la forme $\left\{(\hat{g}(R), \hat{Z}_p(R)) : R \in \mathbb{C}\right\}$, où $\hat{g}$ et $\hat{Z}_p$ sont deux fractions rationnelles que l'on lit facilement à partir de (I.4) et l'équation $R - 3gR^2 = 1$. Une paramétrisation similaire peut être écrite pour les fonctions de partition de beaucoup d'autres modèles de cartes de Boltzmann, et, comme on le verra dans le chapitre V, de cartes décorées par le modèles d'Ising. L'existence de la paramétrisation rationnelle est partiellement expliquée dans [Eyn16, Chapter 3] en utilisant le *paramètre de Zhukovsky*. Il sera intéressant de savoir dans quelle mesure cette preuve se généralise. Mentionnons aussi une approche alternative qui essaie de comprendre ces paramétrisations à l'aide des systèmes dynamiques intégrables en temps discret [Bro16].

Bijections Un autre aspect surprenant des résultats de Tutte est que les cardinaux de nombreuses familles de cartes s'écrivent comme un produit de facteurs simples comme dans (I.5), voir aussi [Fus15, Theorem 1–4] pour quelques formules générales. Cette observation invite à chercher une interprétation bijective de ces formules qui fera intervenir des objets combinatoires comptés par leurs facteurs. Par exemple, le nombre de Catalan $\mathrm{Cat}_n := \frac{1}{n+1}\binom{2n}{n}$ en facteur dans (I.5) suggère une bijection entre l'ensemble des quadrangulations à n faces et une modification de la famille des *arbres plans enracinés à n arêtes* (ou d'une des 65 autres familles combinatoires comptées par Cat_n, voir [Sta99, Exercise 6.19]).

Une telle bijection a effectivement été découverte par Cori et Vauquelin [CV81]. Mais elle ne fut popularisée que dix-sept ans plus tard, quand Schaeffer [Sch98] l'a généralisée et reformulée sous une forme plus maniable. Schaeffer a en fait développé deux types de bijections, l'une encode une carte par un arbre *étiqueté* (i.e. avec des nombres entiers attachés à certains sommets), et l'autre encode une carte par un arbre *bourgeonnant* (i.e. avec des flèches attachées à certains coins de l'arbre). Chacun des deux types de bijection a été repris et vastement généralisé par une longue liste de travaux ultérieurs que l'on ne va pas citer explicitement ici, voir [Fus15, Bet15a] et les références contenues.

Les bijections du premier type ci-dessus s'avèrent plus adaptées à l'étude de la limite d'échelle des cartes, puisqu'elles étiquettent un sommet de l'arbre directement par sa distance du graphe à la racine dans la carte correspondante.[8] Dans ce mémoire on utilisera une instance de ce type de bijections due à Bouttier, Di Francesco et Guitter [BDFG04], et l'on réfère à la section 2.2 du chapitre II pour une description plus précise.

2.4 Caractéristiques d'une carte aléatoire

Criticité d'une carte de Boltzmann Nous avons mentionné que le théorème I.A n'est vrai que si les poids $(q_1, \dots, q_d)$ des cartes de Boltzmann bipartie en question sont *critiques*. Dans le contexte de cartes à degrés de faces bornés, cela signifie que les poids $(q_1, \dots, q_d)$ sont *maximalement admissibles*, c'est-à-dire la fonction de partition $Z_p(q_1, \dots, q_d)$ est finie pour ces poids, mais ne le sera plus dès que l'on augmente l'un des q_k. Autrement dit, $(q_1, \dots, q_d)$ est sur le bord du domaine de convergence de la série multivariée $Z_p(q_1, \dots, q_d)$.

[8] Pour certaines familles particulières de cartes aléatoires, il est aussi possible d'utiliser les bijections aux arbres bourgeonnants pour approximer la distance du graphe pour ensuite établir la limite d'échelle, voir [ABA17].

Par exemple, la fonction de partition $Z_p(g)$ des quadrangulations de Boltzmann de périmètre $2p$ (équation (I.4)) est finie si et seulement si la série $R = R(g)$ converge, c'est-à-dire pour $g \leq \frac{1}{12}$. Donc une quadrangulation de Boltzmann critique a pour poids $g_c = \frac{1}{12}$, et sa fonction de partition vaut

$$Z_p(g_c) = \frac{2^{p+1}}{(p+2)(p+1)}\binom{2p}{p} \underset{p\to\infty}{\sim} \frac{2}{\sqrt{\pi}}\, 8^p\, p^{-5/2}. \tag{I.6}$$

On constate d'abord que $Z_p(g_c)$ est finie, donc la phase critique existe effectivement. Dans le cas $p = 1$ (le cas général est similaire), cela est une conséquence de l'exposant $5/2$ dans l'asymptotique suivante du nombre de quadrangulations à n faces:

$$\#\,\mathcal{Q}_n = \frac{2}{n+2} 3^n \frac{1}{n+1}\binom{2n}{n} \underset{n\to\infty}{\sim} \frac{2}{\sqrt{\pi}}\, 12^n\, n^{-5/2}. \tag{I.7}$$

En effet, l'exposant $5/2$ implique que la série $Z_1(g) = \sum_n g^n \#\,\mathcal{Q}_n$ est sommable à son rayon de convergence $g_c = \frac{1}{12}$. Remarquons que les deux asymptotiques ci-dessus ont le même exposant $5/2$. Mais ce n'est qu'une coïcidence dans la phase critique. Dans la phase sous-critique $g < g_c$, (I.4) implique immédiatement

$$Z_p(g) \underset{p\to\infty}{\sim} \frac{2-R}{\sqrt{\pi}}\,(4R)^p\, p^{-3/2}. \tag{I.8}$$

Lorsque les degrés de faces de la carte ne sont plus bornés, une suite de poids $(q_1, q_2, \ldots)$ est toujours dite critique si elle est maximalement admissible. Mais cela ne garantit plus la convergence de la carte de Boltzmann correspondante vers la carte brownienne comme dans le théorème I.A. Une condition de second moment supplémentaire (voir la section 2.3 du chapitre II) est nécessaire (et suffisante) pour assurer que la limite d'échelle soit la carte brownienne [Mar16]. Sans cette condition, on peut construire des exemples qui convergent vers d'autres limites [LGM11]. Au fond, c'est la condition de second moment qui permet l'application du théorème central limite.

L'exposant de périmètre et l'exposant de volume Nous allons voir dans le chapitre II (théorème II.1) que les exposants $5/2$ et $3/2$ dans (I.6) et (I.8) — appelés *exposants de périmètre* — sont universels parmi les cartes de Boltzmann (non décorées) qui satisfont la condition de second moment invoquée dans le paragraphe précédent. L'exposant $5/2$ dans (I.7) — appelé *exposant de volume* — est également universel, voir par exemple [AC15, Eq. (4)]. Les valeurs $5/2$ et $3/2$ de ces exposants sont donc une signature de la classe d'universalité de la carte brownienne. En général, ces exposants fournissent une caractéristique relativement accessible des modèles de cartes décorées qui permet d'identifier leurs classes d'universalité. Dans le chapitre II et V, on les calculera pour les cartes décorées par un modèle $O(n)$ ou par le modèle d'Ising, respectivement. Et on verra dans la section 4.5 que le résultat de ces calculs est en accord avec l'universalité de ces deux classes de cartes décorées.

Autres statistiques des cartes Il existe beaucoup d'autres statistiques des cartes qui permettent de caractériser la classe d'universalité de la carte brownienne. Mais le calcul de leurs analogues pour les cartes décorées peut s'avérer difficile, notamment quand ces derniers sont liés à la structure *métrique* de la carte, comme les exposants de la croissance du périmètre ou du volume associés à une boule métrique.

D'autre part, on peut souvent accéder aux statistiques de périmètre ou de volume associées aux composantes connexes de spins sur une carte décorée. Dans le chapitre III on calculera la loi de la limite d'échelle attendue du volume à l'intérieur d'une boucle (qui est la contrepartie de l'interface de spins dans un modèle de boucles) sur une quadrangulation décorée par un modèle $O(n)$ critique (théorème III.12). On prouvera aussi la limite d'échelle du périmètre d'une certaine interface de spins dans le chapitre V (théorème V.3). L'analogue de ces résultats pour les cartes non décorées est fourni par la percolation de Bernoulli sur une carte de Boltzmann, qui est maintenant un sujet bien étudié (voir [Ric17] et les références contenues).

3 Cartes aléatoires décorées

Dans ce mémoire, on appelle *carte aléatoire décorée* un modèle *recuit* de physique statistique défini sur une carte aléatoire, qui a la formulation générale suivante.[9]

> Soit $\mathcal{C}_N$ une famille de cartes de taille N comme dans notre discussion sur les cartes non décorées. On se donne un modèle de spin défini sur les cartes $\mathfrak{m} \in \mathcal{C}_N$, qui affecte un poids $w(\mathfrak{m}, \sigma)$ à chaque configuration σ dans un certain ensemble de configurations $\Theta(\mathfrak{m})$. Alors un modèle de carte aléatoire décorée est défini par la loi de probabilité
>
> $$\mathbb{P}_N((\mathfrak{m}, \sigma) = (\mathfrak{m}_0, \sigma_0)) = \frac{1}{Z_N} w(\mathfrak{m}_0, \sigma_0)\,, \tag{I.9}$$
>
> où $Z_N = \sum_{\mathfrak{m} \in \mathcal{C}_N} \sum_{\sigma \in \Theta(\mathfrak{m})} w(\mathfrak{m}, \sigma)$ est supposé finie.

Le modèle est *recuit* dans le sens où la configuration de spins σ est générée aléatoirement en même temps que la carte $\mathfrak{m}$ sous-jacent. Plus précisément, la loi du couple $(\mathfrak{m}, \sigma)$ est caractérisée par les deux conditions suivantes :

(i) La loi marginale de $\mathfrak{m}$ donne à chaque carte une probabilité proportionnelle à la fonction de partition $\mathcal{Z}(\mathfrak{m}) := \sum_{\sigma \in \Theta(\mathfrak{m})} w(\mathfrak{m}, \sigma)$, autrement dit, $\mathbb{P}_N(\mathfrak{m} = \mathfrak{m}_0) = \frac{\mathcal{Z}(\mathfrak{m}_0)}{Z_N}$.

(ii) Sachant $\mathfrak{m}$, la loi conditionnelle de σ est celle du modèle de spins classique sur $\mathfrak{m}$.

La condition (ii) signifie que le poids $w(\mathfrak{m}, \sigma)$ est défini par la même formule que le modèle de spins σ sur le réseau déterministe $\mathfrak{m}$, avec éventuellement un facteur supplémentaire $w_0(\mathfrak{m})$ du type Boltzmann.

3.1 Modèles abordés dans ce mémoire

Pour clarifier la discussion abstraite ci-dessus, donnons tout de suite les définitions des trois modèles spécifiques abordés dans ce mémoire.

[9] Pour alléger le langage, on utilisera délibérément le terme *modèle de spins* pour désigner un modèle de physique statistique général qui décore les cartes, bien que la configuration de ce dernier puisse ne pas être composée de spins.

Carte bipartie à bord avec un modèle $O(n)$ de boucles (chapitre II et III). On considère l'ensemble $\mathcal{C}_N$ des cartes biparties de périmètre $2p$, où le paramètre de taille $N \equiv p$ est le demi-périmètre. Une configuration du modèle $O(n)$ sur une carte $\mathfrak{m}$ est un ensemble $\sigma \equiv \boldsymbol{\ell} = \{\ell_1, \ell_2, \dots\}$ de chemins fermés disjoints sur le dual de $\mathfrak{m}$ et qui ne visitent que les faces internes de degré quatre.[10] Pour une suite $\mathbf{q} = (q_1, q_2, \dots)$ de réels positifs et $h, n \geq 0$, on définit le poids d'un couple $(\mathfrak{m}, \boldsymbol{\ell})$ par

$$w^{O(n)}_{\mathbf{q},h,n}(\mathfrak{m}, \boldsymbol{\ell}) := \left[\prod_{\ell \in \boldsymbol{\ell}} n\, h^{|\ell|} \right] \left[\prod_{f} q_{\deg(f)/2} \right], \tag{I.10}$$

où $|\ell|$ est la longueur (i.e. nombre de faces visitées) de la boucle ℓ, et le second produit parcourt toutes les faces internes non visitées par une boucle. Autrement dit, chaque face vide de degré $2k$ contribue un poids q_{2k} et chaque face visitée (de degré quatre) contribue un poids h. Finalement, un poids n est affecté à chaque boucle. Pour la différencier de son analogue pour les cartes non décorées, on notera par

$$F_p(\mathbf{q}, h, n) := \sum_{(\mathfrak{m}, \boldsymbol{\ell})} w^{O(n)}_{\mathbf{q},h,n}(\mathfrak{m}, \boldsymbol{\ell})$$

la fonction de partition des cartes biparties décorées de périmètre $2p$ par modèle $O(n)$.

Dans le chapitre III on restreindra ce modèle au cas où $q_k = g\delta_{k,2}$, c'est-à-dire les faces vides sont toutes de degré quatre. Dans ce cas, une configuration $(\mathfrak{q}, \boldsymbol{\ell})$ de poids non nul sera appelée une $O(n)$-*quadrangulation*.

Carte générale avec la percolation de Fortuin-Kasteleyn (chapitre IV). Pour ce modèle, $\mathcal{C}_N$ est l'ensemble des cartes (planaires et sans bord) ayant $N \equiv n$ arêtes. Une configuration de percolation de Fortuin-Kasteleyn (FK-percolation) sur une carte est simplement un sous-graphe — i.e. un sous-ensemble d'arêtes — de la carte. Dans sa généralité, le poids d'une carte $\mathfrak{m}$ décorée par un configuration $\mathfrak{g}$ de FK-percolation s'écrit

$$w^{\mathrm{FK}}_{p,q,t}(\mathfrak{m}, \mathfrak{g}) := \left(\frac{p}{1-p} \right)^{\#\,\text{arête}(\mathfrak{g})} q^{\#\,\text{c.c.}(\mathfrak{g})}\, t^{\#\,\text{sommet}(\mathfrak{m})} \tag{I.11}$$

où $\#\,\text{c.c.}(\mathfrak{g})$ est le nombre de composantes connexes du sous-graphe $\mathfrak{g}$, et $p \in (0,1)$, $q, t \geq 0$ sont des paramètres. Les lecteurs familiers avec la FK-percolation reconnaîtront que les deux premiers facteurs dans le membre de droite de (I.11) donnent la définition classique de la FK-percolation. Le dernier facteur $t^{\#\,\text{sommet}(\mathfrak{m})}$ ne change pas la loi conditionnelle de $\mathfrak{g}$ sachant $\mathfrak{m}$ et contribue seulement à un facteur du type Boltzmann dans la loi marginale de $\mathfrak{m}$.

Le chapitre IV est consacré au cas particulier de ce modèle où $\frac{p}{1-p} = \sqrt{q}$ et $t = 1/\sqrt{q}$. Comme on verra dans la discussion avant l'équation (I.17), ce choix de paramètres est *critique* dans le sens où la carte aléatoire décorée définie par ces paramètres est autoduale en loi. Dans ce cas on écrit w^{cFK}_q au lieu de $w^{\mathrm{FK}}_{p,q,t}$, et le couple $(\mathfrak{m}, \mathfrak{g})$ sera appelé *carte cFK*.

Triangulation du polygone avec le modèle d'Ising (chapitre V). Soit $\mathcal{C}_N$ l'ensemble des triangulations du l-gone pour un entier $l \geq 1$ fixé. On considère les configurations de

[10] On imposera aussi une condition de rigidité sur les boucles, mais elle est sans importance à ce stade de la discussion. Voir chapitre II pour les détails.

spins définies sur les *faces* de la triangulation : σ : face($\mathfrak{t}$) $\to$ {+, -}. Le poids du couple $(\mathfrak{t}, \sigma)$ est donné par

$$w_{\nu,t}^{\text{Ising}}(\mathfrak{t},\sigma) := \nu^{\#\,\text{mono}(\mathfrak{t},\sigma)}\, t^{\#\,\text{face}(\mathfrak{t})} \tag{I.12}$$

où $\#\,\text{mono}(\mathfrak{t},\sigma)$ est le nombre d'arêtes monochromatiques dans la configuration σ, c'est-à-dire le nombre d'arêtes de $\mathfrak{t}$ adjacentes à deux faces du même spin. De nouveau on voit que le facteur $\nu^{\#\,\text{mono}(\mathfrak{t},\sigma)}$ donne la définition du modèle d'Ising classique (sans champ extérieur), et le facteur supplémentaire $t^{\#\,\text{face}(\mathfrak{t})}$ ne dépend que du volume de la triangulation. Le couple $(\mathfrak{t}, \sigma)$ sera appelé *Ising-triangulation*.

Pour que la définition de $\#\,\text{mono}(\mathfrak{t},\sigma)$ ait du sens, on doit compléter le modèle avec une condition au bord. En effet, puisque les spins sont sur les faces de la triangulation, il faut préciser le signe du spin à l'extérieur de chacune des arêtes du bord pour savoir si cette arête est monochromatique ou non. On s'intéresse ici à la condition au bord de Dobrushin qui place p spins + et ensuite q spins - (avec $p + q = l$) dans le sens des aiguilles d'une montre autour du bord de la triangulation, voir la Figure I.6(a) sur la page 26. On appelle une Ising-triangulation munie d'une telle condition au bord *Ising-triangulation du* (p, q)*-gone*. On note

$$z_{p,q}(\nu,t) := \sum_{(\mathfrak{t},\sigma)} w_{\nu,t}^{\text{Ising}}(\mathfrak{t},\sigma)$$

la fonction de partition des Ising-triangulations du (p, q)-gone.

Nous allons revenir sur une comparaison entre ces trois modèles dans la section 4.5. Ces trois modèles font intervenir des modèles classiques de spins ou de boucles en physique. Il y a bien d'autres décorations intéressantes à étudier, dont la plupart correspondent aux (variantes de) diverses spécifications du *polynôme de Tutte* de la carte sous-jacente, voir par exemple [BBM11, BBM17].

3.2 Motivations pour l'étude des cartes décorées

Motivé par la démonstration du théorème des quatre couleurs, Tutte a naturellement étendu son étude énumérative de cartes aux cartes coloriées, qui fut ensuite généralisée aux cartes décorées par leurs polynômes de Tutte. Ceci a ouvert tout un champ de recherche en combinatoire. Toutefois, le but initial, qui était de montrer le théorème des quatre couleurs, n'a jamais été atteint de cette façon.

Suite à une observation de 't Hooft [tH74], Brézin, Itzykson, Parisi et Zuber [BIPZ78] se rendirent compte que la fonction de partition des cartes aléatoires de Boltzmann donne exactement le terme dominant du développement asymptotique de certaines intégrales de matrices.[11] Cela a été généralisé plus tard par Boulatov et Kazakov [Kaz86, BK87] aux cartes décorées par le modèle d'Ising. Cependant, ce lien avec les intégrales de matrices a servi comme un outil d'analyse des cartes plutôt qu'une motivation pour les étudier, puisqu'il existe de méthodes plus efficaces pour l'évaluation des intégrales de matrices (qui sont toutefois difficiles à rendre rigoureuses mathématiquement, voir [Dei99]).

[11] L'observation de 't Hooft était en fait plus précise et reliait tous les termes du développement asymptotique aux *cartes de genre supérieur*. Mais on va se concentrer aux cartes *planaires* (i.e. de genre zéro) ici.

La vraie motivation physique pour les cartes décorées n'est arrivée que dans les années 1980 comme une méthode de discrétisation de la théorie de gravité quantique de Liouville en deux dimensions (2D-LQG). Cette théorie modélise la fluctuation quantique du champ de gravité par une métrique aléatoire sur l'espace-temps en deux dimensions. L'interaction entre ce champ de gravité et la matière, traditionnellement modélisée par un autre champ décrit par la théorie conforme des champs (CFT), est alors incorporée comme un couplage entre la loi de cette métrique et la loi du champ de matière. Il est généralement accepté, et prouvé dans certains cas [Smi01, Smi10, CS12], que les modèles de spins comme le modèle $O(n)$ ou le modèle d'Ising convergent en limite d'échelle vers un champ décrit par la CFT. Alors une manière naturelle de construire la 2D-LQG est de définir une discrétisation de la métrique aléatoire de l'espace-temps, puis de la coupler avec un modèle de spins.

Il est connu, par exemple par l'étude numérique des équations différentielles partielles, que les triangulations, et par extension d'autre cartes, fournissent une bonne discrétisation de l'espace-temps. La distance géodésique dans l'espace-temps continu est devenue la distance du graphe dans sa discrétisation. Avec l'idée de couplage avec un modèle de spins, cela nous conduit à nous intéresser à la limite d'échelle des cartes aléatoires décorées au sens de Gromov-Hausdorff, mentionné dans la note 6 de bas de page. De ce point de vue, les cartes aléatoires non décorées sont une modélisation de la fluctuation quantique de l'espace-temps en absence de matière, appelée la *gravité pure*.[12] Cela explique le choix de la loi uniforme pour les cartes non décorées: en absence de l'influence de la matière, il n'y a pas de raison de préférer une géométrie de l'espace-temps plutôt qu'une autre.

Un autre aspect de l'étude des cartes décorées concerne les propriétés de la décoration, c'est-à-dire le modèle de spins qui vit sur la carte. Grâce à la moyenne sur la géométrie du réseau, ces modèles de spins sur réseaux aléatoires sont en général plus accessibles que leurs contreparties sur réseaux déterministes: par exemple ils sont souvent plus intégrables (dans le sens où la fonction de partition est explicite, voir la section suivante), la propriété de Markov spatiale est plus facile à formuler, etc. De plus, la physique théorique prédit une relation exacte — la fameuse **relation de KPZ** (Knizhnik-Polyakov-Zamolodchikov [KPZ88]) — qui relie les exposants critiques de modèles sur réseaux aléatoires à leurs contreparties sur réseaux déterministes. Une motivation pour étudier les cartes décorées est donc de vérifier si cette prédiction est toujours valide, et si oui, de comprendre le mécanisme derrière.

Dans les cas favorables, on peut calculer non seulement des exposants critiques, mais aussi des limites d'échelle de statistiques comme le périmètre ou le volume des composantes connexes de spins. Alors il sera intéressant de les comparer aux lois déduites directement des surfaces aléatoires continues décrites dans [She16a, DMS14, MS15, DKRV16], qui sont les limites d'échelle conjecturées des cartes décorées par modèles de spins.

Mises à part les motivations physiques, les cartes décorées sont aussi intéressantes en combinatoire et en probabilités grâce à leur riche structure qui permet de tester des nouvelles techniques applicables aux autres domaines des mathématiques. Quelques exemples de telles techniques abordées dans ce mémoire sont la résolution d'équations fonctionnelles *à plusieurs variables catalytiques*, *combinatoire analytique de séries génératrices multivariées*, ou l'étude asymptotique des marches aléatoires avec *distribution de pas à queue lourde*. Voir

[12] Il y a d'autres motivations physiques pour les cartes *non décorées*, en particulier la généralisation de l'intégrale de Feynman dans la dite "théorie des cordes" [Pol81], qui est en quelque sorte censée fournir aussi une théorie de gravité quantique.

l'appendice A du chapitre V.

3.3 Questions directrices de ce mémoire

D'un point de vue physique, une conclusion déduite d'un modèle de physique statistique n'est intéressante que si elle est universelle, c'est-à-dire indépendante des détails microscopiques du modèle, puisqu'un modèle malléable ne capture jamais tous les détails de la nature. Un modèle en physique statistique est dit exactement soluble ou *intégrable* si l'on peut calculer explicitement sa fonction de partition, puisqu'elle permet d'accéder facilement à beaucoup de propriétés macroscopiques du système. Il y a deux thèmes autour desquels tournent beaucoup de recherches en physique statistique. Le premier consiste à identifier et explorer les propriétés macroscopiques des classes d'universalité à l'aide des solutions des modèles intégrables, et le deuxième cherche à vérifier que l'universalité existe réellement pour un certain type de modèles.

Le deuxième problème est en général assez difficile. Heureusement pour les modèles de cartes aléatoires non décorées, on observe une abondance de modèles intégrables. Par exemple les modèles de cartes biparties de Boltzmann, qui forment une famille à une infinité de paramètres, sont tous intégrables et peuvent être résolus de façon uniforme (voir les sections 2.2–2.4 du chapitre II). Cette propriété d'intégrabilité est à la base de toute la théorie qui mène à la construction de la carte brownienne.

Il semble que cette intégrabilité persiste aussi dans beaucoup de modèles de cartes décorées. Cela nous mène au fil conducteur des travaux présentés dans ce mémoire: via l'étude d'exemples de modèles intégrables de cartes décorées, on essaie de

(i) Explorer les propriétés de différentes classes d'universalité du 2D-LQG.

(ii) Vérifier l'universalité en comparant les résultats obtenus à partir de différents modèles microscopiques qui appartiennent à la même classe d'universalité selon la prédiction physique.

Les travaux dans ce mémoire concernent principalement le point (i). Plus précisément, ils exploitent différentes méthodes de résolution exacte des trois modèles abordés, développées respectivement dans les travaux récents [BBG12c, She16b, BBM11], pour établir un nombre de propriétés géométriques de ces modèles. Dans la section suivante, on donnera la liste des propriétés étudiées pour chacun de ces modèles, en précisant leurs liens avec la limite d'échelle attendue du modèle. À la fin de la section, on abordera brièvement le point (ii) — la vérification d'universalité — en se penchant sur le lien entre les trois modèles étudiés.

4 Résumé des méthodes et des résultats

Cette section esquisse un plan des chapitres restants de ce mémoire en récapitulant les résultats principaux de chaque chapitre et les outils utilisés pour les obtenir.

4.1 II : Diagramme de phase de la carte de Boltzmann bipartie décorée par un modèle $O(n)$

Ce chapitre vise à clarifier quelques points techniques dans l'établissement du diagramme de phase du modèle de carte bipartie décorée par le modèle $O(n)$ défini par (I.10). Ce modèle est une légère extension de la quadrangulation décorée par un modèle $O(n)$ *rigide* examinée dans [BBG12c].

Le diagramme de phase des $O(n)$-quadrangulations est établi dans [BBG12c] en étudiant une équation fonctionnelle — appelée *équation de boucle* (*loop equation*) — satisfaite par la fonction résolvante du modèle (*grosso modo*, c'est la série génératrice des fonctions de partition $F_p(\mathbf{q}, h, n)$ indexées par le demi-périmètre p). Une étape de ce raisonnement consiste à identifier une solution *analytique* de l'équation de boucle, calculée explicitement dans [BBG12c], à la solution *combinatoire* définie par le modèle de cartes. Cette identification revient à supposer que l'équation de boucle a au plus une solution qui satisfait une contrainte de positivité (voir la proposition II.8). Cette hypothèse, bien que plausible, n'est pas immédiate vue la forme de l'équation. On en propose une justification qui s'appuie sur un critère d'*admissibilité* (i.e. finitude de la fonction de partition) dû à T. Budd (proposition II.A).

Dans le même chapitre on donne aussi la réponse affirmative, dans le contexte du modèle $O(n)$ *rigide*, à une conjecture sur la positivité de la densité spectrale associée à la fonction résolvante formulée dans [BBG12a]. La preuve de cette partie repose sur une équation intégrale satisfaite par la densité spectrale et sur un argument de continuité qui étend la positivitié de la densité spectrale du bord de son domaine de définition à tout le domaine (lemmes II.10 et II.14). Enfin, on combine ce résultat de positivité avec le paragraphe précédent pour donner une caractérisation des quatre phases du modèle en terme de la solution analytique de l'équation de boucle (proposition II.2). Cette caractérisation est utilisée dans [BBG12c] en conjonction avec la solution explicite de l'équation de boucle pour tracer le diagramme de phase du modèle sur quadrangulations ($q_k = g\delta_{k,2}$) donnée dans la Figure I.4. Le chapitre II n'entre pas dans le détail du tracé du diagramme de phase, mais justifie simplement l'existence des quatre phases non vides définies par leurs valeurs respectives de l'exposant de périmètre a données par

$$F_p(\mathbf{q}, h, n) \underset{p\to\infty}{\sim} C\,\gamma^{2p}\,p^{-a}$$

où $C, \gamma > 0$ et

$$a = \begin{cases} 3/2 & \text{si } (\mathbf{q}, h, n) \text{ est sous-critique} \\ 2-b & \text{si } (\mathbf{q}, h, n) \text{ est critique non générique et dense} \\ 2+b & \text{si } (\mathbf{q}, h, n) \text{ est critique non générique et dilué} \\ 5/2 & \text{si } (\mathbf{q}, h, n) \text{ est critique générique} \end{cases} \tag{I.13}$$

avec $n \in (0, 2)$ et $b := \frac{1}{\pi}\arccos(\frac{n}{2}) \in (0, \frac{1}{2})$.

Mis à part le critère d'admissibilité de Budd et l'argument de bootstrap de positivité, ce chapitre repose essentiellement sur l'analyse complexe classique appliquée à l'équation de boucle (II.4). Dans la section 2 du chapitre II, on détaille une manière d'obtenir l'équation de boucle à partir de la *décomposition en gasket*, la *bijection de Bouttier–Di Francesco–Guitter* (BDG), et une *transformation d'arbres* due à Janson et Stefánsson (JS). On décide d'inclure cette section parce que ces outils seront utilisés de façon essentielle dans le chapitre suivant pour étudier les tailles de boucles du modèle $O(n)$.

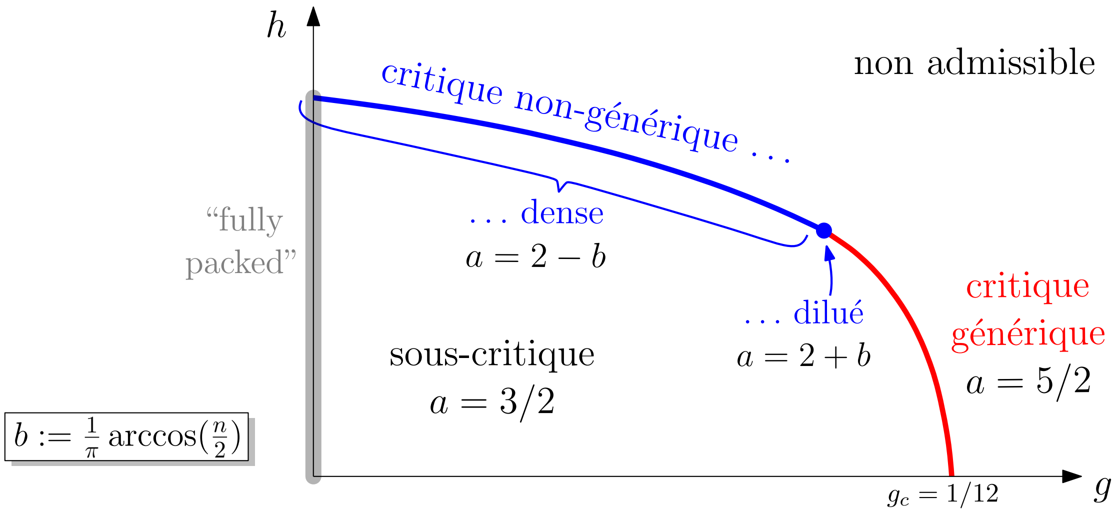

Figure I.4 – *Diagramme de phase du modèle des $O(n)$-quadrangulations pour une valeur donnée de $n \in (0, 2)$. (Le dessin reste qualitativement le même pour tout $n \in (0, 2)$.) Les trois phases critiques forment une ligne qui sépare la phase sous-critique et l'ensemble des paramètres non admissibles. Si $g = 0$, le modèle est dit* fully packed*, c'est-à-dire toutes les faces internes sont visitées par les boucles.*

4.2 III : La cascade des périmètres d'une $O(n)$-quadrangulation critique

Ce chapitre continue l'étude de la carte décorée par un modèle $O(n)$ rigide dans le cas des $O(n)$-quadrangulations ($q_k = g\delta_{k,2}$) et d'un point de vue probabiliste. On fixe un jeu de paramètres (g, h, n) critique non générique (dense ou diluée) et s'intéresse aux tailles et à la structure d'emboîtement des boucles du modèle $O(n)$. On encode cette structure d'emboîtement par un arbre plan enraciné dont chaque sommet est associé à une unique boucle du modèles $O(n)$ de la façon suivante: la racine de l'arbre est associée à une boucle virtuelle autour de la quadrangulation; les enfants de la racine sont associés aux boucles *les plus à l'extérieur* du modèle $O(n)$ — c'est-à-dire celles atteignables à partir du bord de la quadrangulation sans traverser d'autres boucles — classées par l'ordre décroissant de taille (en cas d'égalité, on ordonne selon une certaine règle déterministe); récursivement, si un sommet u de l'arbre est associé à la boucle l, alors on associe aux enfants de u les boucles à l'intérieur de l atteignables depuis l sans traverser d'autres boucles, et classées par l'ordre décroissant de taille. Ensuite, on affecte à chaque sommet de l'arbre une étiquette à valeurs entières qui est le demi-périmètre de sa boucle associée.

On obtient ainsi un arbre plan enraciné étiqueté comme dans la Figure I.5. On le complète en ajoutant récursivement un nombre infini dénombrable d'enfants d'étiquette zéro à chaque sommet. On dénote par $\mathcal{U}$ l'ensemble des sommets de l'arbre infini — connu comme *l'arbre de Ulam* — et voit l'étiquetage comme une fonction $\chi : \mathcal{U} \to \mathbb{N}$ que l'on appelle *la cascade des périmètres* de la $O(n)$-quadrangulation. Le résultat principal du chapitre III est la convergence en loi suivante: si $\chi^{(p)}$ est la cascade de périmètres de la $O(n)$-quadrangulation de Boltzmann de périmètre $2p$, alors

$$\frac{1}{p}\left(\chi^{(p)}(u)\right)_{u\in\mathcal{U}} \xrightarrow[p\to\infty]{(d)} \left(Z_\alpha(u)\right)_{u\in\mathcal{U}} \tag{I.14}$$

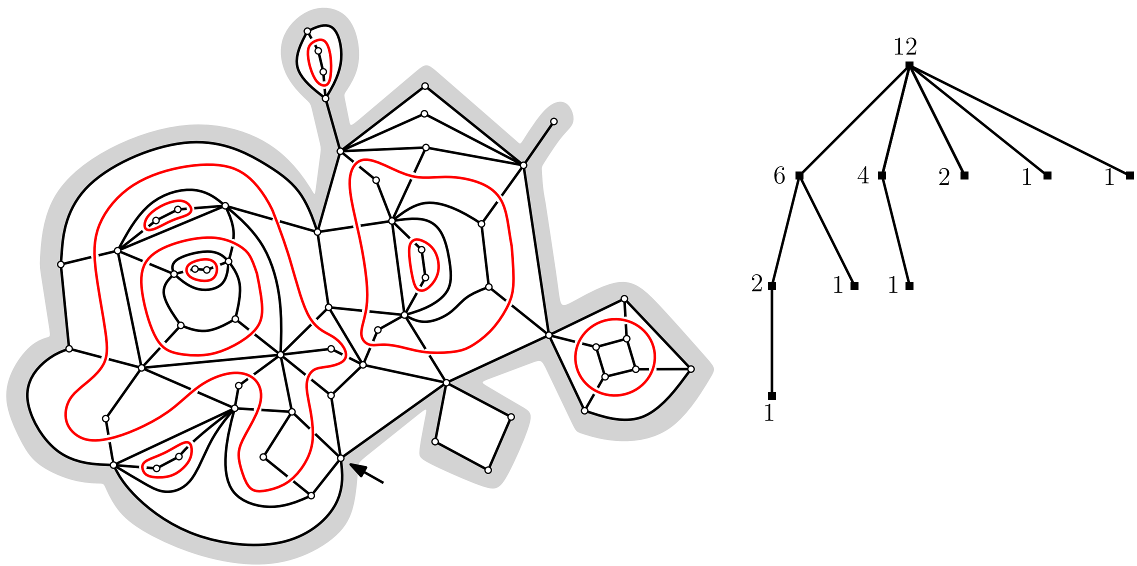

Figure I.5 – *À gauche : une $O(n)$-quadrangulation du 24-gone. À droite : l'arbre qui encode la structure d'emboîtement des boucles, étiqueté par les demi-périmètres.*

où Z_α est une *cascade multiplicative* (fonction aléatoire à valeurs réelles sur $\mathcal{U}$) dont la loi de reproduction est donnée en terme d'un processus de Lévy α-stable sans sauts négatifs, et α est lié à l'exposant de périmètre a dans (I.13) par $\alpha = a - 1/2$. La loi de reproduction explicite de Z_α permet aussi le calcul de la limite de la *martingale mathusienne* de la cascade multiplicative, qui fournit un candidat à la limite d'échelle du volume de la $O(n)$-quadrangulation.

La preuve de la convergence (I.14) est réalisée en trois temps. D'abord on utilise la décomposition en gasket et les bijections de BDG et de JS du chapitre précédent pour montrer (I.14) dans le sens des marginales fini-dimensionnelles. Ensuite, on l'améliore en une convergence en norme ℓ^∞ sur les k premières générations de l'arbre $\mathcal{U}$ en montrant la convergence de la *transformée de Biggins* de la cascade de périmètres $\chi^{(p)}$. Cette étape utilise une identité sur l'espérance d'une certaine fonctionnelle additive d'une marche aléatoire continue à gauche. Cette identité est intéressante en elle-même. Enfin on étend cette convergence en norme ℓ^∞ sur toutes les générations de l'arbre $\mathcal{U}$ à l'aide d'un argument de (sur-)martingale pour le processus de branchement $\chi^{(p)}$. Cette étape repose sur une estimée du volume de la $O(n)$-quadrangulation obtenue récemment par Budd [Bud17].

4.3 IV : Limite locale de la carte cFK

La plupart de ce court chapitre est consacrée à la démonstration de la convergence locale (voir la chapitre IV pour la définition) des cartes cFK. Notez que la définition de la criticité pour ce modèle, qui est synonyme d'*autodualité*, n'est pas le même que celle dans le chapitre précédent. Leur lien sera expliqué dans la section 4.5. La preuve de la convergence locale suit largement la méthode esquissée dans le papier original [She16b], mais utilise une reformulation de la *bijection de hamburger-cheeseburger* (aussi introduite dans [She16b]) qui permet d'encoder directement les cartes cFK infinies.

Après la preuve de la convergence locale, on utilise cette version de la bijection pour établir quelques propriétés de base de la limite locale (qui est une carte décorée infinie du plan): sa topologie, sa récurrence, et l'ergodicité de la loi sous la translation de la racine. Cette partie s'appuie d'une part sur la théorie ergodique de graphes aléatoires développée dans [BC12], et d'autre part sur un critère de récurrence de limites locales planaires dû à Gurel-Gurevich et Nachmias [GGN13].

4.4 V : Modèle d'Ising critique sur une triangulation de polygone

La première moitié du chapitre V traite la combinatoire énumérative des Ising-triangulations. Rappelons qu'on considère des triangulations du disque *à bord simple* et munies d'une condition au bord de Dobrushin. On commence par établir une équation fonctionnelle satisfaite par la série génératrice

$$Z(u,v;\nu,t) := \sum_{p,q\geq 0} z_{p,q}(\nu,t)u^p v^q\,,$$

où on rappelle que $z_{p,q}(\nu,t)$ est la fonction de partition des Ising-triangulations du (p,q)-gone. Cette équation est déduite d'une décomposition récursive classique de Tutte.[13] Deux équations essentiellement équivalentes à la nôtre (mais écrites pour deux modèles plus généraux qui ont des bords non nécessairement simples) ont déjà été résolues indépendamment dans [BBM11] et [Eyn16, Chapter 8]. La solution présentée ici est une simplification de la méthode d'*élimination de variables catalytiques* employée dans [BBM11]. La solution de [Eyn16] est en fait plus systématique et moins calculatoire, mais je n'était pas au courant de cette méthode lors de la résolution de l'équation fonctionnelle.

On se concentre ensuite sur un cas critique (ν_c,t_c) du couple de paramètres (ν,t). Il est choisi en vue du résultat suivant de [BBM11] qui suggère un comportement particulier à ces valeurs de paramètres: pour tout $\nu\geq 1$ fixé, le poids total des Ising-triangulations du $(1,0)$-gone ayant n faces satisfait

$$[t^n]z_{1,0}(\nu,t) \underset{n\to\infty}{\sim} C\,t_c^{-n}n^{-\beta} \tag{I.15}$$

où l'exposant de volume $\beta = 7/3$ si $\nu=\nu_c$ et $\beta=5/2$ sinon. On verra dans la section 4.5 que (ν_c,t_c) est le point critique non générique dilué d'une triangulation décorée par un modèle $O(1)$. La solution $Z(u,v)\equiv Z(u,v;\nu_c,t_c)$ de l'équation fonctionnelle est donnée par une paramétrisation rationnelle explicite de la forme $u=\hat{u}(H)$, $v=\hat{u}(K)$ et $Z=\hat{Z}(H,K)$. Dans l'appendice A.2 du chapitre V, on développe une méthode systématique pour l'analyse de singularité (plus précisément, pour la localisation des singularités dominantes) des séries génératrices données par une paramétrisation rationnelle.[14] Avec cette méthode, on extrait les asymptotiques suivantes de la fonction de partition d'Ising-triangulation :

$$\begin{aligned} z_{p,q}(\nu_c,t_c) &\underset{q\to\infty}{\sim} \tilde{a}_p\, u_c^{-q}q^{-7/3} \\ \tilde{a}_p &\underset{p\to\infty}{\sim} \tilde{b}\ \ u_c^{-p}p^{-4/3} \end{aligned} \tag{I.16}$$

[13] Le fait que l'on puisse obtenir une équation close dépend de manière cruciale de la stabilité de la condition au bord de Dobrushin sous la décomposition de Tutte. C'est la raison pour laquelle cette condition au bord est particulièrement intéressante.

[14] La classe des séries génératrices admettant une paramétrisation rationnelle n'est pas extrêmement grande, mais elle admet de bonnes propriétés de clôture, notamment par rapport aux équations de substitution comme $S(xG(x))=G(x)$: si dans cette équation $G(x)$ admet une paramétrisation rationnelle, alors $S(x)$ aussi. Ce type d'équations intervient naturellement quand on veut relier les cartes à bord simple aux cartes à bord général, ou relier les triangulations générales aux triangulations simples.

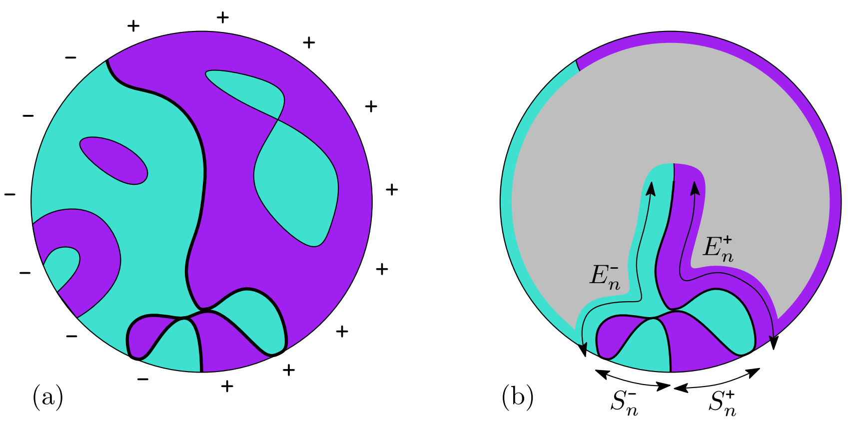

Figure I.6 – *(a) Une triangulation décorée par le modèle d'Ising avec une condition au bord de Dobrushin. (b) La région explorée après n étapes du processus d'épluchage. Le processus de périmètre est défini par les longueurs $E_n^{\pm}$ et $S_n^{\pm}$ comme $(X_n, Y_n) = (E_n^+ - S_n^+, E_n^- - S_n^-)$.*

La deuxième moitié du chapitre V exploite la série génératrice explicite de $z_{p,q}(\nu_c, t_c)$ et les asymptotiques ci-dessus pour étudier la géométrie des interfaces d'Ising dans une Ising-triangulation du (p, q)-gone dans la limite où $q \to \infty$ et ensuite $p \to \infty$. L'outil principal de cette étude est un *processus d'épluchage* (peeling process) qui explore les faces de la triangulation le long de l'interface macroscopique qui relie les deux points du bord où la condition au bord + et la condition au bord - se rencontrent.[15] On associe à ce processus d'épluchage un *processus de périmètres* $(X_n, Y_n)_{n\geq 0}$ qui compte les nombres nets d'arêtes + et d'arêtes - ajoutées au bord de la triangulation inexplorée après n étapes d'exploration, voir la Figure I.6(b).

La loi $\mathsf{P}_{p,q}$ du processus d'épluchage de l'Ising-triangulation du (p, q)-gone admet une expression explicite en terme des fonctions de partition $z_{p,q}(\nu_c, t_c)$. À l'aide des asymptotiques (I.16), on calcule facilement ses limites faibles $\mathsf{P}_{p,\infty} := \lim_{q\to\infty} \mathsf{P}_{p,q}$ et $\mathsf{P}_{\infty,\infty} := \lim_{p\to\infty} \mathsf{P}_{p,\infty}$. Puisque $(X_n, Y_n)_{n\geq 0}$ est une fonction mesurable du processus d'épluchage, on peut parler de sa loi sous $\mathsf{P}_{p,\infty}$ ou sous $\mathsf{P}_{\infty,\infty}$, qui s'interprète comme la loi du processus de périmètre sur la limite locale de l'Ising-triangulation du (p, q)-gone quand $q \to \infty$ ou quand $q, p \to \infty$. On verra dans le chapitre V :

(i) Sous $\mathsf{P}_{\infty,\infty}$, le processus $(X_n, Y_n)_{n\geq 0}$ est une marche aléatoire de dérive (μ, μ), où μ est *strictement positive*. Géométriquement, cela implique que presque sûrement, l'interface entre les spins + et les spins - du bord ne revient sur le bord qu'un nombre fini de fois. De plus, après renormalisation, la fluctuation $(X_n - \mu, Y_n - \mu)_{n\geq 0}$ converge en loi vers deux processus de Lévy 4/3-stables indépendants.

(ii) Sous $\mathsf{P}_{p,\infty}$, le processus $(P_n)_{n\geq 0} = (p + X_n)_{n\geq 0}$ est une chaîne de Markov récurrente, et par conséquent atteint zéro en temps fini presque sûrement. Géométriquement, cela signifie que la composante connexe des faces de spin + qui inclut le bord + est presque sûrement finie. De plus, on calculera la limite d'échelle en loi du temps de première visite de zéro par $(P_n)_{n\geq 0}$ (interprétée comme le périmètre de la composante connexe

[15] En réalité une telle interface n'est pas uniquement définie, puisqu'un nombre arbitraire d'arêtes non monochromatiques peuvent se rencontrer à un sommet. Pour fixer l'idée, dans le chapitre V on choisira soit l'interface la plus à gauche soit celle la plus à droite. Mais on s'attend à ce qu'il n'y ait pas de différence macroscopique entre tous les choix possibles.

des faces de spin +).

Enfin on esquisse une feuille de route vers la construction de limite locale de la triangulation aléatoire du (p,q)-gone, qui sera incluse dans la version finale du travail en cours d'où le contenu du chapitre V est tiré.

4.5 Relations entre les modèles abordés

On finit cette introduction avec une discussion sur le lien entre les trois modèles abordés. En fait les deux derniers modèles (carte cFK et Ising-triangulation) peuvent être vus comme des spécifications du premier ($O(n)$-quadrangulation) si l'on se permet de modifier les classes de cartes sur lesquelles vivent les modèles de spins. Plus précisément, considérons la variante suivante de $O(n)$-quadrangulation, définie toujours dans le cadre présenté au début de la section 3 :

Soit $\mathcal{C}_N$ l'ensemble des triangulations à bord de périmètre $N \equiv p$. Une configuration de boucles sur $\mathfrak{t} \in \mathcal{C}_p$ est un ensemble $\boldsymbol{\ell} = \{\ell_1, \ell_2, \dots\}$ de chemins fermés disjoints sur le dual de $\mathfrak{t}$ ne visitant pas la face externe, de sorte que les faces internes de $\mathfrak{t}$ soient de l'un des deux types suivants:

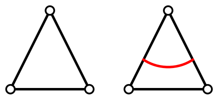 .

Pour $g, h, n \geq 0$, le poids du couple $(\mathfrak{t}, \boldsymbol{\ell})$ est défini par

$$w^{O(n),\Delta}_{g,h,n}(\mathfrak{t}, \boldsymbol{\ell}) := g^{\#\,\mathrm{face}(\mathfrak{t})} \prod_{\ell \in \boldsymbol{\ell}} n \left(\frac{h}{g}\right)^{|\ell|}.$$

Autrement dit, on donne un poids g à chaque face interne non visitée, un poids h à chaque face interne visitée, et un poids n à chaque boucle. On appellera ce modèle *$O(n)$-triangulation*. Sa fonction de partition sera notée $F^{\Delta}_p(g,h,n)$.

Cartes cFK comme $O(n)$-triangulations *fully packed*. Rappelons qu'une configuration de FK-percolation sur une carte $\mathfrak{m}$ est simplement un sous-graphe $\mathfrak{g}$ de $\mathfrak{m}$. Le sous-graphe dual de $\mathfrak{g}$ est le sous-graphe $\mathfrak{g}^\dagger$ de $\mathfrak{m}^\dagger$ tel qu'une arête duale $e^\dagger$ appartient à $\mathfrak{g}^\dagger$ si et seulement si e n'appartient *pas* à $\mathfrak{g}$, voir la Figure I.7(b).

Une bijection due à Tutte associe à chaque carte $\mathfrak{m}$ une quadrangulation $\mathfrak{q}$ en reliant chaque sommet de $\mathfrak{m}$ aux sommets duaux voisins et en oubliant les arêtes de $\mathfrak{m}$ comme dans la Figure I.7(c). Chaque face f de la quadrangulation correspond à une arête e de la carte $\mathfrak{m}$, qui divise f en deux triangles. Et l'arête duale $e^\dagger$ divise f en deux triangles le long de l'autre diagonale. Par conséquent, si $\mathfrak{g}$ est un sous-graphe de $\mathfrak{m}$, alors l'union de $\mathfrak{g}$, $\mathfrak{g}^\dagger$ et $\mathfrak{q}$ forme une triangulation. Elle est naturellement munie d'une configuration de boucles qui visite toutes ses faces en traversant toutes les arêtes de $\mathfrak{q}$, mais aucune arête de $\mathfrak{g}$ ou $\mathfrak{g}^\dagger$ comme dans la Figure I.7(d).

Modulo une subtilié concernant l'enracinement, la construction ci-dessus fournit une surjection de l'ensemble des configurations de la carte cFK dans l'ensemble des $O(n)$-triangulations du 2-gone *fully packed*, telle que chaque image a exactement deux antécédents. On verra dans le chapitre IV que la relation d'Euler implique que $w^{\mathrm{cFK}}_q(\mathfrak{m},\mathfrak{g}) = \sqrt{q}^{\#\boldsymbol{\ell}}$, où $\#\boldsymbol{\ell}$ est le nombre de boucles sur la triangulation correspondant à $(\mathfrak{m},\mathfrak{g})$. Noter que cela implique

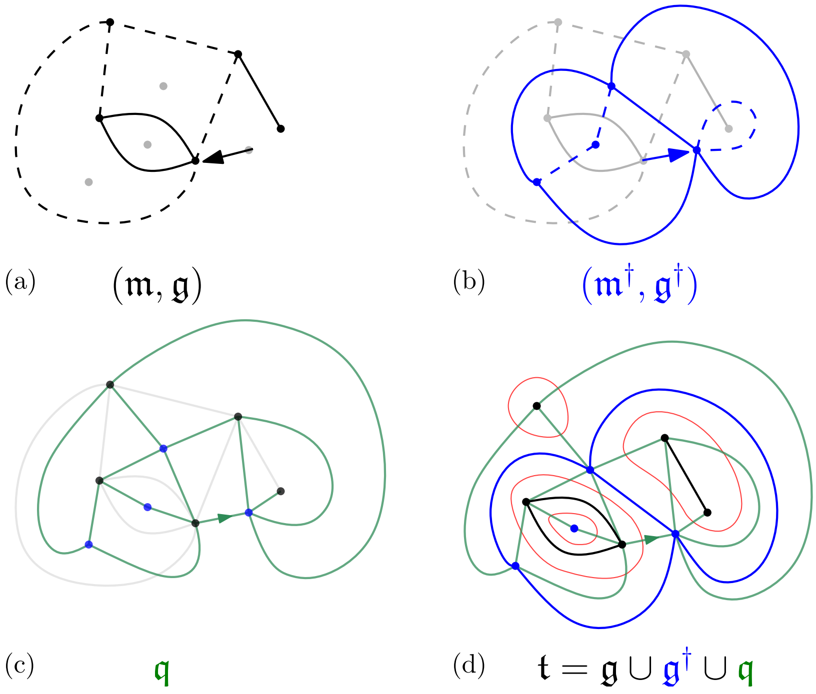

Figure I.7 – *(a) Une carte* $\mathfrak{m}$ *munie d'un sous-graphe* $\mathfrak{g}$*. Les arêtes appartenant à* $\mathfrak{g}$ *sont en ligne pleine, et les autres arêtes en pointillé. (b) Le couple dual. (c) La quadrangulation associée à* $\mathfrak{m}$ *par la bijection de Tutte. (d) La* $O(n)$*-triangulation associée à* $(\mathfrak{m}, \mathfrak{g})$*.*

en particulier que le poids w_q^{cFK} est autodual. Par conséquent, la carte cFK est effectivement une spécification de la $O(n)$-triangulation à bord de longueur 2. Plus précisément,

$$F_2^{\Delta}(0, h, \sqrt{q}) = 2 \sum_{n \geq 0} z_n^{\mathrm{cFK}}(\sqrt{q}) \cdot h^{2n} \tag{I.17}$$

Ce lien a été utilisé dans plusieurs travaux [BLR17, GMS15, GS17] pour calculer des statistiques concernant les boucles d'une $O(n)$-triangulation *fully packed* via la bijection de hamburger-cheeseburger pour les cartes cFK. Ce sera intéressant de les comparer aux statistiques des boucles trouvées dans le chapitre III et [BBD16], obtenues avec une méthode qui repose sur la décomposition en gasket. Un accord entre les deux fournirait une confirmation de l'universalité des modèles de cartes décorées. Pour finir, remarquons que le lien décrit ci-dessus s'étend aux cartes décorées par une FK-percolation non autoduale définies par (I.11), dont la contrepartie sera la $O(n)$-triangulation avec brisure de symétrie de domaine définie dans [BBG12a].

Modèle d'Ising sur les sommets d'une triangulation comme un modèle $O(1)$. Pour faire un lien avec la $O(n)$-triangulation, il convient de considérer un modèle d'Ising dont les spins sont sur les sommets de la triangulation, avec une condition au bord de Dirichlet où les spins sur tous les sommets du bord sont fixés à +. On considère de telles configurations de spins sur l'ensemble C_p des triangulations à bord de périmètre p (notez que l'on n'impose plus un bord simple ici), et l'on définit le poids $w_{\nu,t}^{\mathrm{Ising},*}(\mathfrak{t}, \sigma) = \nu^{\#\,\mathrm{mono}(\mathfrak{t},\sigma)} t^{\#\,\mathrm{face}(\mathfrak{t})}$ comme pour l'Ising-triangulation avec spins sur les faces. Soit $z_{p,0}^*(\nu, t)$ la fonction de partition associée.

Une configuration de boucles sur cette Ising-triangulation est donnée par les interfaces d'Ising, tracées selon la règle locale suivante :

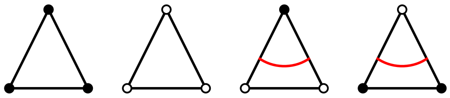

Une face dans les deux premiers cas contribue 3/2 arêtes monochromatiques au modèle d'Ising (chaque côté du triangle est compté comme 1/2 arête puisqu'une arête est partagée par deux triangles) et une face non visitée au modèle $O(n)$. Et une face dans les deux derniers cas contribue 1/2 arête monochromatique et une face visitée. On en déduit que si $\nu^{3/2}t = g$ et $\nu^{1/2}t = h$, alors on a l'égalité de poids entre le modèle d'Ising-triangulation et de $O(1)$-triangulation à un facteur $\nu^{p/2}$ près, et par conséquent

$$F_p^{\Delta}(g,h,1) = \nu^{-p/2} z^*_{p,0}(\nu,t)\,.$$

Si l'on croit à l'universalité, alors d'après (I.16) on aura $z^*_{p,0}(\nu_c^*,t_c^*) \underset{p\to\infty}{\sim} \tilde{a}_0^*\,(u_c^*)^{-p}p^{-7/3}$, où les constantes $\tilde{a}_0^*$, u_c^* ainsi que la position précise du point critique (ν_c^*,t_c^*) sont *a priori* différentes de leurs analogues pour le modèle avec les spins sur les faces, mais l'exposant de périmètre $a = 7/3$ reste le même. C'est en accord avec la valeur de a pour la $O(1)$-quadrangulation au point *critique non générique dilué* donnée par (I.13) : $\frac{7}{3} = 2+\frac{1}{\pi}\arccos(\frac{1}{2})$.

L'étape suivante naturelle sera de calculer l'exposant de périmètre pour toute valeur du couple (ν,t), et de les comparer au diagramme de phase de la $O(1)$-quadrangulation dans la Figure I.4. D'autre part, on peut étudier l'analogue de l'exposant de volume pour la $O(1)$-quadrangulation et le comparer à (I.15). Ces comparaisons peuvent être étendues aux caractéristiques plus géométriques des deux modèles. Ce sera une piste pour les travaux futurs.

Chapter II

Phase diagram of $O(n)$-decorated Boltzmann maps

This Chapter is adapted from the appendix of [Bud17].

1 Introduction

In this chapter we consider a class of random loop-decorated bipartite maps extending slightly the rigid loop-decorated quadrangulations considered by Borot, Bouttier and Guitter in [BBG12c]. Recall from Chapter I that we always consider maps that are *planar* and *rooted*. The root is represented by a distinguished *corner*. It identifies a distinguished *external face* (the other faces being internal faces), whose degree is called the *perimeter* of the map. For $p \geq 1$, we denote by $\mathcal{M}_p$ the set of bipartite maps of perimeter $2p$. A *(rigid) loop configuration* on a bipartite map is a set $\boldsymbol{\ell} = \{\ell_1, \ell_2, \ldots\}$ of disjoint undirected simple closed paths in the dual map which only visit *internal* faces of *degree four*, and with the additional constraint that when a loop visits a face, it must cross it through opposite edges. In other words, the internal faces of $\mathfrak{m}$ can only be of the following types

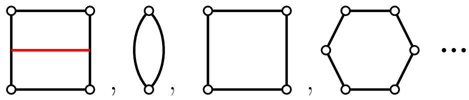

The pair $(\mathfrak{m}, \boldsymbol{\ell})$ will henceforth be called a *loop-decorated map with a boundary.* Let $\mathcal{LM}_p$ be the set of the loop-decorated maps $(\mathfrak{m}, \boldsymbol{\ell})$ with $\mathfrak{m} \in \mathcal{M}_p$.

Given a sequence $\mathbf{q} = (q_1, q_2, \dots)$ of non-negative real numbers, $h \geq 0$ and $n \geq 0$, we define the *weight* $w_{\mathbf{q},h,n}(\mathfrak{m}, \boldsymbol{\ell})$ of a loop-decorated map with a boundary $(\mathfrak{m}, \boldsymbol{\ell})$ to be

$$w_{\mathbf{q},h,n}(\mathfrak{m}, \boldsymbol{\ell}) := \left[\prod_{\ell \in \boldsymbol{\ell}} n\, h^{|\ell|}\right]\left[\prod_{f} q_{\deg(f)/2}\right], \tag{II.1}$$

where $|\ell|$ is the length of the loop ℓ, the second product is over the internal faces not visited by a loop. Then the *rigid loop model partition function* $F_p(\mathbf{q}, h, n)$ can be defined as the total weight

$$F_p(\mathbf{q}, h, n) := \sum_{(\mathfrak{m},\boldsymbol{\ell}) \in \mathcal{LM}_p} w_{\mathbf{q},h,n}(\mathfrak{m}, \boldsymbol{\ell}). \tag{II.2}$$

It is not hard to see that $F_p(\mathbf{q}, h, n) < \infty$ for all $p \geq 1$ if and only if this is true for at least one p (see discussion below (II.8)), and in that case we call the triple $(\mathbf{q}, h, n)$ *admissible.*

When $(\mathbf{q}, h, n)$ is admissible, the weights $w_{\mathbf{q},h,n}(\mathfrak{m}, \boldsymbol{\ell})$ give rise to a probability measure on $\mathcal{LM}_p$ when normalized by $1/F_p(\mathbf{q}, h, n)$. The geometric properties of the random loop-decorated map thus defined is the subject of the next chapter. This chapter concentrates on establishing analytic criteria which characterize the admissibility of the parameters $(\mathbf{q}, h, n)$ and the phase to which they belong. We will consider parameters $(\mathbf{q}, h, n)$ in the domain

$$\mathbb{D} := [0, \infty)^d \times (0, \infty) \times (0, 2)$$

where $\mathbf{q} \in [0, \infty)^d$ means that $q_k \geq 0$ for $k \leq d$ and $q_k = 0$ for $k > d$. First let us introduce the four phases of the model.

Theorem II.1 (asymptotics of $F_p(\mathbf{q}, h, n)$ [BBG12c])**.** *Assume that $(\mathbf{q}, h, n) \in \mathbb{D}$ is admissible, then*

$$F_p(\mathbf{q}, h, n) \underset{p\to\infty}{\sim} C\, \gamma^{2p}\, p^{-(\alpha+1/2)}\,. \tag{II.3}$$

where $C > 0$ and $\gamma > 0$ both depend on $(\mathbf{q}, h, n)$. Moreover, the set of admissible parameters is partitioned into four phases according to the value of the exponent α:

$$\alpha = \begin{cases} 1 & \textit{if } (\mathbf{q}, h, n) \textit{ is subcritical} \\ \frac{3}{2} - b & \textit{if } (\mathbf{q}, h, n) \textit{ is non-generic critical and dense} \\ \frac{3}{2} + b & \textit{if } (\mathbf{q}, h, n) \textit{ is non-generic critical and dilute} \\ 2 & \textit{if } (\mathbf{q}, h, n) \textit{ is generic critical} \end{cases}$$

where $b = \frac{1}{\pi}\arccos(\frac{n}{2}) \in (0, \frac{1}{2})$.

We will take the above values of α as our working definition of the phases. We will briefly mention an alternative definition of the phases related to Galton-Watson trees at the end of Section 2.3, which justifies better their names. Theorem II.1 is given in [BBG12c] in the case where $q_k = g\delta_{k,2}$ (i.e. the case of rigid loop-decorated *quadrangulation*). The derivation consists of computing explicitly the *resolvent function*

$$\mathcal{W}_{\mathbf{q},h,n}(x) = 1 + \sum_{k\geq 1} x^{-2k} F_k(\mathbf{q},h,n)$$

by solving a functional equation, which we give later as (II.4), using complex-analytic methods. However, to identify a solution of (II.4) with the resolvent function $\mathcal{W}_{\mathbf{q},h,n}$ defined above, one must first show that the triple $(\mathbf{q},h,n)$ is admissible. In [BBG12c] it was assumed that a triple $(\mathbf{q},h,n)$ is admissible if the equation (II.4) has a solution satisfying some *positivity constraint*. The main purpose of this chapter is to provide a proof to this equivalence (Proposition II.8) and its consequences on the phase diagram, which we summarize in the following proposition.

Consider the set of parameters

$$\mathcal{D} = \Big\{(\mathbf{q},h,n,\gamma) \in \mathbb{D}\times(0,\infty) \,\Big|\, \gamma \leq h^{-1/2}\Big\}$$

$\mathcal{D}$ is a closed set inside $\mathbb{D}\times(0,\infty)$. We denote by $\mathring{\mathcal{D}}$ (resp. $\partial\mathcal{D}$) its topological interior (resp. boundary), which is simply given by replacing $\leq$ in the above definition by $<$ (resp. $=$).

Proposition II.2 (Analytic description of the phases)**.** *There are explicit real-valued functions $\mathfrak{f}$, $\mathfrak{g}$, $\mathfrak{h}$ defined respectively on $\mathring{\mathcal{D}}$, $\mathbb{D}$ and $\mathcal{D}$, such that a triple $(\mathbf{q},h,n) \in \mathbb{D}$ is*

(i) subcritical if and only if $\mathfrak{f}(\mathbf{q},h,n,\gamma) > 0$ and $\mathfrak{h}(\mathbf{q},h,n,\gamma) = 1$ for some $\gamma \in (0,h^{-1/2})$.

(ii) generic critical if and only if $\mathfrak{f}(\mathbf{q},h,n,\gamma) = 0$ and $\mathfrak{h}(\mathbf{q},h,n,\gamma) = 1$ for some $\gamma \in (0,h^{-1/2})$.

(iii) non-generic critical and dense if and only if $\mathfrak{g}(\mathbf{q},h,n) > 0$ and $\mathfrak{h}\big(\mathbf{q},h,n,h^{-1/2}\big) = 1$.

(iv) non-generic critical and dilute if and only if $\mathfrak{g}(\mathbf{q},h,n) = 0$ and $\mathfrak{h}\big(\mathbf{q},h,n,h^{-1/2}\big) = 1$.

Moreover, the four phases are non-empty and form a partition of the admissible triples in $\mathbb{D}$.

These characterizations of the phases are also valid for non-decorated maps, that is, when $h = n = 0$. However in that case, the two non-generic critical phases are empty, as suggested by the appearance of $h^{-1/2}$ in their characterizations. The functions $\mathfrak{f}$, $\mathfrak{g}$ and $\mathfrak{h}$ will be defined in Section 3 as limits of the solution to the functional equation (II.4). In [BBG12c], these functions are computed explicitly and used in conjunction of Proposition II.2 to deduce the phase diagram in the case $q_k = g\delta_{k,2}$, which is given in Figure II.1. We will also use some properties of $\mathfrak{f}$ and $\mathfrak{g}$ found from their explicit expressions (Lemma II.C and the lemmas in Section 3.3).

2 Functional equation for the resolvent $\mathcal{W}_{\mathbf{q},h,n}$

For $\gamma > 0$, let $S_\gamma = \overline{\mathbb{C}} \setminus [-\gamma,\gamma]$, where $\overline{\mathbb{C}} = \mathbb{C}\cup\{\infty\}$ is the Riemann sphere. The set S_γ is topologically an open disk. We denote by $\overline{S}_\gamma$ the compactification of S_γ obtained by gluing a circle to the boundary of S_γ. The set $\overline{S}_\gamma$ is topologically a closed disk. We parametrize it

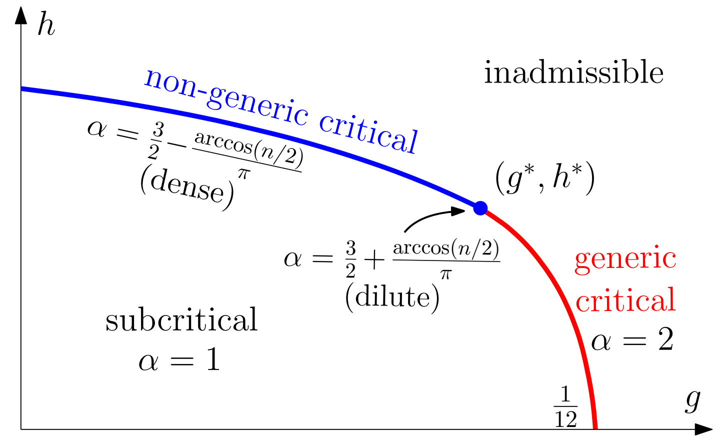

Figure II.1 – *Phase diagram of the loop-decorated quadrangulation model [BBG12c, Bud17] for a given value of $n \in (0,2)$ (the diagram is qualitatively the same for all such n). The critical phases form a line that separates the sub-critical region (below) and the inadmissible region (above).*

by $\overline{S}_\gamma = (\overline{\mathbb{C}} \setminus (-\gamma,\gamma)) \cup (\{\pm1\} \times (-\gamma,\gamma))$. Under this parametrization, we shall denote an element of $\{\pm1\} \times (-\gamma,\gamma)$ by $x \pm i0$ with $x \in (-\gamma,\gamma)$.

We say that a function $\mathcal{W} : \overline{S}_\gamma \to \mathbb{C}$ is *holomorphic on* $\overline{S}_\gamma$ if it is holomorphic on S_γ and continuous on $\overline{S}_\gamma$. Since $\overline{S}_\gamma$ is compact, a such $\mathcal{W}$ must be bounded. We define the *spectral density* associated to $\mathcal{W}$ by $\rho(x) = \frac{\mathcal{W}(\gamma x - i0) - \mathcal{W}(\gamma x + i0)}{2\pi i x}$, where $x \in [-1,1]$.[1] Since $\mathcal{W}$ is continuous on $\overline{S}_\gamma$, the spectral density ρ is always continuous on $[-1,0) \cup (0,1]$ and vanishes at $x = \pm1$. It may *a priori* have a discontinuity of type $O(x^{-1})$ at $x = 0$.

Proposition II.3 (Equation of the resolvent [BBG12c]). *If $(\mathbf{q}, h, n) \in [0,\infty)^{\mathbb{N}} \times [0,\infty) \times [0,\infty)$ is admissible, then there exists $\gamma \in (0, h^{-1/2}]$ such that the function $\mathcal{W}(x) \equiv \mathcal{W}_{\mathbf{q},h,n}(x)$ satisfies*

$$\begin{cases} \mathcal{W} \text{ is an even holomorphic function on } \overline{S}_\gamma \text{ such that for all } x \in (-\gamma,\gamma), \\ \qquad \mathcal{W}(x - i0) + \mathcal{W}(x + i0) + n\mathcal{W}\Big(\dfrac{1}{hx}\Big) = n + x^2 - \displaystyle\sum_{k=1}^{\infty} q_k x^{2k} . \end{cases} \tag{II.4}$$

Moreover, $\rho_{\mathbf{q},h,n}$ is a non-negative continuous even function on $[-1,1]$.

The rest of this section is devoted to a more or less self-contained proof of Proposition II.3. The impatient reader can skip directly to Section 3 without much loss of continuity. Most results in this section have already appeared in various places (e.g. [BBG12c, MM07, BDFG04, BM17, JS15, CK15]). However we keep a derivation of them here because it uses the same tools (namely, the gasket decomposition, the Bouttier–Di Francesco–Guitter bijection and Janson–Stefánsson's tree transform) as those in the next chapter.

2.1 Gasket decomposition

We first recall the gasket decomposition of [BBG12c]. Given a loop-decorated bipartite map $(\mathfrak{m}, \boldsymbol{\ell}) \in \mathcal{LM}_p$, let $l \geq 0$ be the number of outer-most loops in $\boldsymbol{\ell}$, i.e. loops which can be

[1] This definition differs slightly from the one in the original paper [BBG12c] of Borot, Bouttier and Guitter, and is related to theirs by $x\mathcal{W}_{\mathtt{BBG}}(x) = \mathcal{W}(x)$ and $\rho_{\mathtt{BBG}}(x) = \gamma \cdot \rho(\gamma^{-1}x)$.

reached from the boundary of $\mathfrak{m}$ without crossing any other loop. The gasket decomposition consists in erasing all the outer-most loops and all the edges crossed by these loops. This disconnects the map into $l+1$ connected components:

- The connected component containing the external face is called the *gasket* of $(\mathfrak{m}, \boldsymbol{\ell})$ and denoted $\mathcal{G}(\mathfrak{m}, \boldsymbol{\ell})$. It is a bipartite map (without loops) with a boundary of length $2p$ whose internal faces are either directly inherited from $\mathfrak{m}$, or one of the l *holes* obtained by removing the outer-most loops and their interior component. Notice that a hole may have a non-simple boundary, as in Figure II.2.
- The l remaining connected components are contained in the holes. More precisely, inside a hole of degree $2p'$, we find an element $(\mathfrak{m}', \boldsymbol{\ell}') \in \mathcal{LM}_{p'}$.

To be rigorous, we need to specify a root for each internal map $(\mathfrak{m}', \boldsymbol{\ell}')$. This can be done in a deterministic way thanks to the lack of automorphisms of rooted maps (see Section 1.3 of Chapter I). Similarly, the holes can be numbered from 1 to l in a deterministic fashion.

Therefore, given a bipartite map $\hat{\mathfrak{m}}$ of perimeter $2p$, the loop-decorated maps $(\mathfrak{m}, \boldsymbol{\ell})$ that admit $\hat{\mathfrak{m}}$ as their gasket can be recovered by gluing either a plain $2k$-gon, or a loop-decorated quadrangulation in $\mathcal{LM}_k$—wrapped in a "collar" of $2k$ quadrangles traversed by a loop—into each internal face of $\hat{\mathfrak{m}}$ degree $2k$. See Figures 3 and 4 in [BBG12c]. It follows that the total weight of loop-decorated maps in the set $\mathcal{G}^{-1}(\hat{\mathfrak{m}}) \subset \mathcal{LM}_p$ is

$$\sum_{(\mathfrak{m},\boldsymbol{\ell})\in\mathcal{G}^{-1}(\hat{\mathfrak{m}})} w_{\mathbf{q},h,n}(\mathfrak{m}, \boldsymbol{\ell}) = \prod_f \Big(q_{\frac{1}{2}\deg(f)} + n\, h^{\deg(f)} F_{\frac{1}{2}\deg(f)}(\mathbf{q}, h, n) \Big), \tag{II.5}$$

where the product is over all internal faces of $\hat{\mathfrak{m}}$. In other words, the gasket $\hat{\mathfrak{m}}$ receives the weight of a Boltzmann map (as defined in Section 2.1 of Chapter I):

$$w_{\hat{\mathbf{q}}}(\hat{\mathfrak{m}}) := \sum_{(\mathfrak{m},\boldsymbol{\ell})\in\mathcal{G}^{-1}(\hat{\mathfrak{m}})} w_{\mathbf{q},h,n}(\mathfrak{m}, \boldsymbol{\ell}) = \prod_f \hat{q}_{\frac{1}{2}\deg(f)} \tag{II.6}$$

with the *effective weight sequence* $\hat{\mathbf{q}} = (\hat{q}_1, \hat{q}_2, \dots)$ given by

$$\hat{q}_k := q_k + nh^{2k} F_k(\mathbf{q}, h, n). \tag{II.7}$$

Summing (II.5) over $\hat{\mathfrak{m}}$ gives the *fixed point equation* on the partition function $F_p(\mathbf{q}, h, n)$:

$$F_p(\hat{\mathbf{q}}) := F_p(\hat{\mathbf{q}}, 0, 0) = \sum_{\hat{\mathfrak{m}}\in\mathcal{M}_p} w_{\hat{\mathbf{q}}}(\hat{\mathfrak{m}}) = \sum_{(\mathfrak{m},\boldsymbol{\ell})\in\mathcal{LM}_p} w_{\mathbf{q},h,n}(\mathfrak{m}, \boldsymbol{\ell}) = F_p(\mathbf{q}, h, n). \tag{II.8}$$

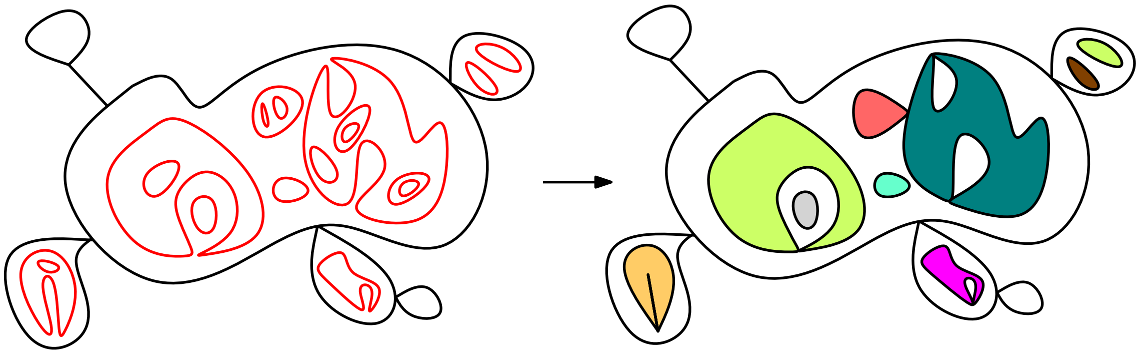

Figure II.2 – *Illustration of the gasket decomposition. Notice that after removing the outer-most loops and their interiors, the holes in the gasket may be non-simple faces. See also [BBG12c, Figure 4]*

Comparing (II.7) and (II.8), we see that for any $p, k \geq 1$, $F_k(\mathbf{q}, h, n)$ is bounded by a positive constant times $F_p(\mathbf{q}, h, n)$. Therefore the admissibility condition $F_p(\mathbf{q}, h, n) < \infty$ does not depend on p.

Equation (II.8) also shows that if a triple $(\mathbf{q}, h, n)$ is admissible for the loop-decorated Boltzmann map model, then $\hat{\mathbf{q}}$ given by (II.7) is admissible for the non-decorated Boltzmann map model. Though less obvious, the converse is also true. More precisely,

Proposition II.A ([Bud17])**.** *If $\hat{\mathbf{q}}$ is an admissible weight sequence, $h, n \geq 0$, and $\mathbf{q}$ defined by*

$$q_k = \hat{q}_k - nh^{2k} F_k(\hat{\mathbf{q}}) \tag{II.9}$$

is non-negative, then the triple $(\mathbf{q}, h, n)$ is admissible and $F_p(\mathbf{q}, h, n) = F_p(\hat{\mathbf{q}})$.

The proof consists of showing that an algorithm that constructs a loop-decorated Boltzmann map of parameter $(\mathbf{q}, h, n)$ from the law of its gasket terminates almost surely. We refer to [Bud17] for details.

In terms of the resolvent function, (II.7) and (II.8) are equivalent to

$$\mathcal{W}_{\mathbf{q},h,n}(x) = \mathcal{W}_{\hat{\mathbf{q}},0,0}(x) \qquad \text{and} \qquad \sum_{k=1}^{\infty} \hat{q}_k x^{2k} = \sum_{k=1}^{\infty} q_k x^{2k} + n\left(\mathcal{W}_{\mathbf{q},h,n}\left(\frac{1}{hx}\right) - 1\right) \tag{II.10}$$

Comparing this to (II.4), we see that Proposition II.3 is true in general if and only if it is true in the special case $h = n = 0$, that is, the case of a non-decorated (bipartite) maps.

2.2 Enumeration of non-decorated maps via the BDG bijection

As is mentioned in Chapter I, the problem of enumeration of (non-decorated) bipartite maps has been solved in many different ways. Here we will present in some detail the approach that uses the Bouttier–Di Francesco–Guitter (BDG) bijection [BDFG04] to encode the map by a labeled forest. We will come back to this bijective encoding in the next Chapter to study the nesting structure of loops in a loop-decorated bipartite map. Let us recall the necessary background of this classical bijection, and refer to [BDFG04, MM07, BM17] for details.

The BDG bijection in its simplest form deals with *pointed maps*, that is, a map with a distinguished vertex ρ. Let $\mathcal{M}_p^\bullet = \{(\hat{\mathfrak{m}}, \rho) \,|\, \hat{\mathfrak{m}} \in \mathcal{M}_p \text{ and } \rho \text{ is a vertex of } \hat{\mathfrak{m}}\}$ be the set of pointed bipartite maps of perimeter $2p$. Here we will use a slight variant [BM17, Section 3.3] of the classical BDG bijection in terms of the treatment of the root. For $(\hat{\mathfrak{m}}, \rho) \in \mathcal{M}_p^\bullet$, it constructs a labeled forest $(\mathfrak{F}, L)$ with two types of vertices $(\circ)$,$(\bullet)$ as follows.

1. Label each vertex $(\circ)$ of $\hat{\mathfrak{m}}$ by its distance to the distinguished vertex ρ. Since $\hat{\mathfrak{m}}$ is bipartite, the labels of any two adjacent vertices $(\circ)$ differ exactly by one.
2. Draw a new vertex $(\bullet)$ in each face f of $\hat{\mathfrak{m}}$, including the external face. Link the new vertex $(\bullet)$ to a vertex $(\circ)$ adjacent to f if the next vertex $(\circ)$ in the clockwise order around f has a smaller label.
3. Remove the edges of $\mathfrak{m}$ and the vertex ρ. It can be shown that the resulting graph is a tree [BDFG04]. Let v_0 be the vertex $(\bullet)$ corresponding to the external face of $\hat{\mathfrak{m}}$. By removing v_0 and its adjacent edges, we obtain a forest $\mathfrak{F}$ of cyclically ordered trees, rooted at the neighbors $(\circ)$ of v_0.

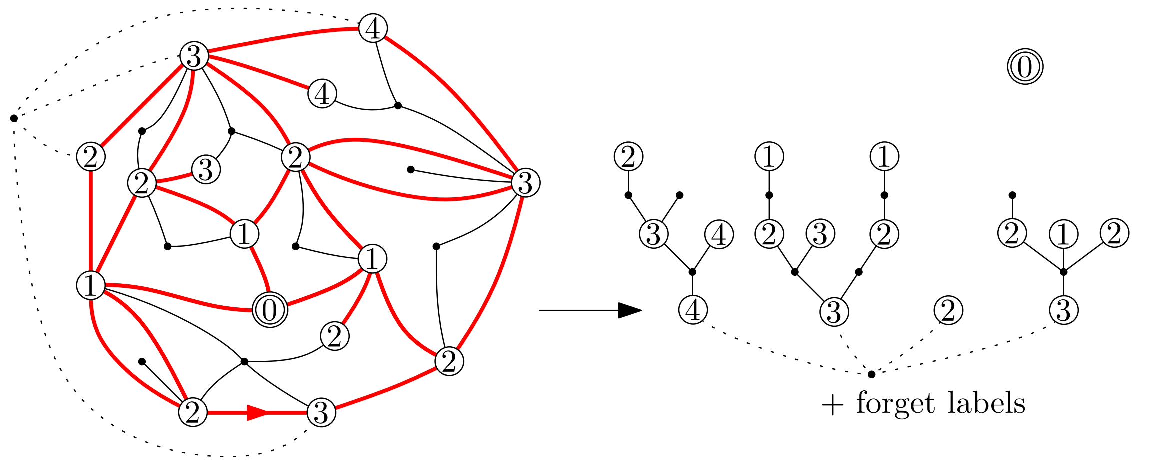

Figure II.3 – *Illustration of the construction of a forest of p mobiles from a pointed bipartite planar map with a boundary of perimeter 2p. The first mobile in the forest is not specified by the map and is chosen uniformly at random among all the mobiles.*

4. Finally, we choose one of the trees to be the first one, and subtract the labels in all trees by a constant so that the root vertex (∘) of this first tree has label zero.

With a moment of thought on the Step 2. of the above construction, one observes that

(i) The type of a vertex in $\mathfrak{F}$ is fixed by its location: the odd generations (the roots being generation 1) contain labeled vertices (∘) and the even generations contain unlabeled vertices (•).

(ii) Each internal face of degree $2k$ in $\hat{\mathfrak{m}}$ gives rise to a vertex (•) of degree k in $\mathfrak{F}$, and $\mathfrak{F}$ is composed of p trees.

(iii) Given a vertex (•) of degree k, the possible labels on its neighbors (∘) in $\mathfrak{F}$ are exactly those which, when read in the clockwise order around the vertex (•), can decrease at most by 1 at each step. And the labels of the p roots satisfy the same constraint.

A labeled forest satisfying the above conditions and having the label zero on the root of its first tree is called a *well-labeled forest of mobiles.*[2] It is clear that the steps 1.–4. do *not* construct a bijection from $(\hat{\mathfrak{m}},\rho)$ to $(\mathfrak{F},L)$, because (a) one can move the root corner of $\hat{\mathfrak{m}}$ to any of the $2p$ corners of the root face without affecting $(\mathfrak{F},L)$, and (b) Step 4. requires an arbitrary choice of the first tree among the p trees of $\mathfrak{F}$. However, the effects of these two problems almost cancel out: in fact one can modify Step 4. so that $(\hat{\mathfrak{m}},\rho)\mapsto(\mathfrak{F},L)$ becomes a 2-to-1 mapping from $\mathcal{M}_p^\bullet$ to the well-labeled forests of p mobiles. See [BM17, Section 6.1] for details and for a construction of the inverse mapping. Then it follows from the observation (ii) above that the partition function $F_p^\bullet$ of pointed bipartite Boltzmann maps is

$$F_p^\bullet(\hat{\mathbf{q}}) := \sum_{(\hat{\mathfrak{m}},\rho)\in\mathcal{M}_p^\bullet} w_{\hat{\mathbf{q}}}(\hat{\mathfrak{m}}) \;=\; 2\sum_{(\mathfrak{F},L)}\;\prod_{v\in\bullet(\mathfrak{F})}\hat{q}_{\deg(v)}\,, \tag{II.11}$$

where the last sum is on all well-labeled forests of p mobiles.

[2]It is a *well-labeled mobile* when the forest is a tree.

As mentioned in Chapter I, the labels are important for keeping track of the distances in the map $\hat{\mathfrak{m}}$. Since the distances are not our focus here, we will discard the labels. To do so, we use the fact that, given a vertex ($\bullet$) of degree k and the label of one of its neighbors ($\circ$), there are exactly $\frac{1}{2}\binom{2k}{k}$ possible labelings of the other neighbors ($\circ$) satisfying the condition (iii) above (see [MM07, Proof of Proposition 7]). Then it is not hard to see that the number of labelings that turns a forest $\mathfrak{F}$ of p trees into a forest of well-labeled mobiles is

$$\frac{1}{2}\binom{2p}{p}\prod_{v\in\bullet(\mathfrak{F})}\frac{1}{2}\binom{2\deg v}{\deg v}.$$

Multiplying the weight of a forest in (II.11) by the number of its possible labelings, we get

$$F_p^\bullet(\hat{\mathbf{q}})=\binom{2p}{p}\sum_{\mathfrak{F}\in\mathcal{T}^p}\prod_{v\in\bullet(\mathfrak{F})}\widetilde{q}_{\deg(v)}\qquad\text{where}\qquad \widetilde{q}_k=\frac{1}{2}\binom{2k}{k}\hat{q}_k\,, \tag{II.12}$$

and $\mathcal{T}^p$ is the set of forests consisting of p trees. Since the weight of a forest $\mathfrak{F}\in\mathcal{T}^p$ factorizes over its p trees, the above sum factorizes as

$$F_p^\bullet(\hat{\mathbf{q}})=\binom{2p}{p}\big(R_{\mathbf{q}}\big)^p\qquad\text{where}\qquad R_{\mathbf{q}}:=\sum_{\mathfrak{t}\in\mathcal{T}}\prod_{v\in\bullet(\mathfrak{t})}\widetilde{q}_{\deg(v)} \tag{II.13}$$

is the generating function of well-labeled mobiles.

A remarkable feature of the last identity is that the weight sequence $\hat{\mathbf{q}}$ intervene only *via* the generating function $R_{\hat{\mathbf{q}}}$, so that the dependency of $F_p^\bullet(\hat{\mathbf{q}})$ on p takes a universal form. In particular, its asymptotic $F_p^\bullet(\hat{\mathbf{q}})\sim\frac{1}{\sqrt{\pi}}(4R_{\mathbf{q}})^p\,p^{-1/2}$ always has the same exponent $1/2$. This is in contrast with the asymptotics of the non-pointed partition function $F_p(\hat{\mathbf{q}})=F_p(\mathbf{q},h,n)$ given in Theorem II.1. We postpone the task of relating $F_p(\hat{\mathbf{q}})$ to $F_p^\bullet(\hat{\mathbf{q}})$ until Section 2.4, and derive first some properties of the mobile generating function $R_{\mathbf{q}}$ using a tree transformation due to Janson and Stefánsson.

2.3 Janson and Stefánsson's tree transformation

In [JS15, Section 3], Janson and Stefánsson discovered a transformation which modify the edges of a (rooted plane) tree $\mathfrak{t}$—seen as a mobile—to form another tree so that each vertex ($\circ$) in $\mathfrak{t}$ becomes a leaf, and each vertex ($\bullet$) of degree k in $\mathfrak{t}$ becomes an internal vertex with k children. We refer to [CK15, Section 3.2] for details of this transformation. The curious reader may have a look at Figure II.4 below and try to guess how the bijection works.

In the definition (II.13) of $R_{\mathbf{q}}$, each vertex v of the tree $\mathfrak{t}$ is assigned a weight depending on its degree *and* on the parity of its generation. Namely, the weight of v is $\widetilde{q}_{\deg(v)}$ if v is in an even generation ($\bullet$), and 1 if v is in an odd generation ($\circ$). Janson and Stefánsson's transformation is useful in that it modifies the tree so that the weight of a vertex only depends on its number of children. More precisely, if we set $\widetilde{q}_0=1$, then the weight of a vertex after the transformation is always $\widetilde{q}_{\deg'(v)}$, where $\deg'(v)$ denotes the number of children of the vertex v. It follows that

$$R_{\mathbf{q}}=\sum_{\mathfrak{t}\in\mathcal{T}}w_{\hat{\mathbf{q}}}^{\mathrm{JS}}(\mathfrak{t})\qquad\text{where}\qquad w_{\hat{\mathbf{q}}}^{\mathrm{JS}}(\mathfrak{t}):=\prod_{v\in V(\mathfrak{t})}\widetilde{q}_{\deg'(v)}\,. \tag{II.14}$$

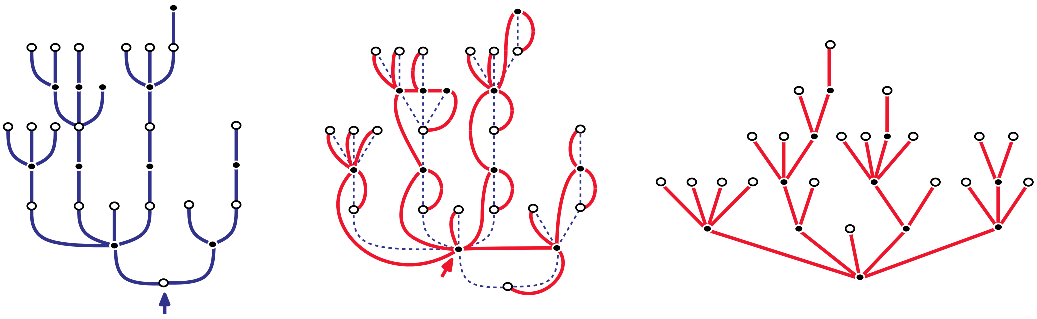

Figure II.4 – *Illustration of the Janson & Stefánsson transformation.*

where $V(\mathfrak{t})$ denotes the set of *all* vertices of $\mathfrak{t}$.

The weights $w_{\hat{\mathbf{q}}}^{\mathrm{JS}}$ define a measure of total mass $R_{\mathbf{q}}$ on the set of finite (rooted plane) trees. When $R_{\mathbf{q}} < \infty$, we can define a random tree $\mathfrak{T}^{\mathrm{JS}}$ by

$$\mathbb{P}(\mathfrak{T}^{\mathrm{JS}} = \mathfrak{t}) = \frac{1}{R_{\mathbf{q}}} w_{\hat{\mathbf{q}}}^{\mathrm{JS}}(\mathfrak{t})\,.$$

It is classical that a random tree defined by a weight like $w_{\hat{\mathbf{q}}}^{\mathrm{JS}}$ is a Galton–Watson tree. More precisely, we have the following result which combines [MM07, Proposition 1] and [JS15, Appendix] (see also [CK15, Proposition 3.6]).

Proposition II.4 (Equation for $R_{\mathbf{q}}$ [MM07, JS15]). *We have $R_{\mathbf{q}} < \infty$ if and only if for*

$$u_{\mathbf{q}}(r) := r - \sum_{k\geq 1} \widetilde{q}_k r^k\,,$$

the equation $u_{\mathbf{q}}(r) = 1$ has a positive solution. When this is the case, $R_{\mathbf{q}}$ is given by the smallest such solution, and $\mathfrak{T}^{\mathrm{JS}}$ is a Galton–Watson tree of offspring distribution

$$\mu_{\mathrm{JS}}(k) = \widetilde{q}_k R_{\mathbf{q}}^{k-1}\,, \quad k \geq 0\,. \tag{II.15}$$

Proof. Euler's relation for trees #vertices = #edges +1 implies $\sum_{v\in V(\mathfrak{t})}\big(\deg'(v) - 1\big) = -1$ in any tree $\mathfrak{t}$. For any $r > 0$, let $\mu_{\mathrm{JS}}^{(r)}(k) := \widetilde{q}_k r^{k-1}$. Then we have

$$\frac{1}{r} w_{\hat{\mathbf{q}}}^{\mathrm{JS}}(\mathfrak{t}) = \prod_{v\in V(\mathfrak{t})} \widetilde{q}_{\deg'(v)} r^{\deg'(v)-1} = \prod_{v\in V(\mathfrak{t})} \mu_{\mathrm{JS}}^{(r)}(\deg'(v)) \tag{II.16}$$

Assume that $u_{\mathbf{q}}(r) = 1$ has a positive solution and let r_0 be the smallest one. Recall that $\widetilde{q}_0 = 1$. So $u_{\mathbf{q}}(r_0) = 1$ readily implies that $\mu_{\mathrm{JS}}^{(r_0)}$ is a probability distribution on $\mathbb{Z}_{\geq 0}$. Then (II.16) implies that $r_0^{-1} w_{\hat{\mathbf{q}}}^{\mathrm{JS}}$ coincides with the law of the Galton–Watson tree of offspring distribution $\mu_{\mathrm{JS}}^{(r_0)}$ on *finite* trees. Moreover, since $u_{\mathbf{q}}(0) = 0$ and $u_{\mathbf{q}}$ is concave, the smallest positive solution r_0 is characterized by $u'_{\mathbf{q}}(r_0) > 0$, which is equivalent to

$$\sum_{k\geq 0} k\,\mu_{\mathrm{JS}}^{(r_0)}(k) \leq 1\,.$$

This implies that the above Galton–Watson tree is either subcritical or critical, thus almost surely finite. So the distribution $r_0^{-1} w_{\hat{\mathbf{q}}}^{\mathrm{JS}}$ has total mass 1 on the set of all finite trees, and it follows that $R_{\mathbf{q}} = r_0 < \infty$.

Inversely, if $R_{\mathbf{q}} < \infty$, then $R_{\mathbf{q}}^{-1} w_{\hat{\mathbf{q}}}^{\mathrm{JS}}$ defines a probability distribution on finite trees. From (II.16) it is not hard to see that the degree distribution of the root vertex of a random tree of law $R_{\mathbf{q}}^{-1} w_{\hat{\mathbf{q}}}^{\mathrm{JS}}$ is $\mu_{\mathrm{JS}}^{(R_{\mathbf{q}})}$. In particular, we have $\sum_{k\geq 0} \mu_{\mathrm{JS}}^{(R_{\mathbf{q}})}(k) = 1$, that is, $u_{\mathbf{q}}(R_{\mathbf{q}}) = 1$. $\square$

Alternative definition of the phases. The definition of *subcritical*, *generic critical* and *non-generic critical* phase is best understood through the above relation between $\hat{\mathbf{q}}$ and the off-spring distribution μ_{JS}. It is classical to call μ_{JS} *subcritical* if its mean $m = \sum k\mu_{\mathrm{JS}}(k)$ is smaller than 1, and *critical* if $m = 1$. The critical case can be further divided into *generic critical*, if the second moment $m_2 = \sum k^2 \mu_{\mathrm{JS}}(k)$ is finite, and *non-generic critical* otherwise. By extension, an admissible triple $(\mathbf{q}, h, n)$ or its effective weight sequence $\hat{\mathbf{q}}$ is *subcritical*, *generic critical* or *non-generic critical* if the corresponding μ_{JS} is so.[3]

The distinction between dense and dilute (non-generic critical) phases only appears when one looks at the 3/2-th moment of the off-spring distribution μ_{JS}. But this is less standard. In the sequel we will stick to our working definition of the phases by their values of α.

2.4 Back to the non-pointed gasket

In Section 2.2 we started considering *pointed* bipartite maps because the BDG bijection turns them into objects (well-labeled mobiles) that are simple to enumerate. To come back to the non-pointed maps—which the gasket is—we need to weight each pointed map by the inverse of its number of vertices. In Chapter III, we will carry this out directly in a probabilistic setting. But since here we focus on the enumeration, we will perform this weighting within the partition function. More precisely, let us give an additional weight u to each vertex except the distinguished one in a pointed map, so that the pointed partition function becomes

$$F_p^\bullet(\hat{\mathbf{q}}; u) := \sum_{(\hat{\mathfrak{m}},\rho)\in\mathcal{M}_p^\bullet} u^{\# V(\hat{\mathfrak{m}})-1} w_{\hat{\mathbf{q}}}(\hat{\mathfrak{m}})\,. \tag{II.17}$$

Then the non-pointed partition function will be given by $F_p(\hat{\mathbf{q}}) = \int_0^1 F_p^\bullet(\hat{\mathbf{q}}; u)\mathrm{d}u$. Via the BDG bijection and Janson & Stefánsson's transform, the vertices other than ρ in a pointed map are mapped bijectively to the leaves of the trees. Therefore the weight u in the definition (II.17) of $F_p^\bullet$ can be pushed through these mappings, so that (II.13) and (II.14) become

$$F_p^\bullet(\hat{\mathbf{q}}; u) = \binom{2p}{p} \big(R_{\mathbf{q}}(u)\big)^p \qquad \text{where} \qquad R_{\mathbf{q}}(u) := \sum_{\mathfrak{t}\in\mathcal{T}} u^{\#\,\mathrm{leaf}(\mathfrak{t})} w_{\hat{\mathbf{q}}}^{\mathrm{JS}}(\mathfrak{t})\,.$$

It follows that

$$F_p(\hat{\mathbf{q}}) = \binom{2p}{p} \int_0^1 \big(R_{\mathbf{q}}(u)\big)^p \,\mathrm{d}u \tag{II.18}$$

[3]The term *generic* is sometimes used to refer to another class of weight sequences for trees [DJW07, JS11, Kor15]. When restricted to the (admissible) critical case, they correspond to the so-called *regular critical* sequences [LG13], which is a subset of *generic critical* sequences defined above.

On the other hand, the number of leaves in a tree is related to the degrees of its internal vertices by (this can also be viewed as a consequence of Euelr's relation)

$$\#\,\mathrm{leaf} - 1 = \sum_{v \text{ internal}} \Big(\deg'(v) - 1\Big) .$$

So multiplying the weight $w^{\mathrm{JS}}_{\hat{\mathbf{q}}}$ by $u^{\#\,\mathrm{leaf}-1}$ has the same effect as multiplying the weight of each internal vertex of degree k by u^{k-1}. It follows that $u^{-1}R_{\mathbf{q}}(u) = R_{\hat{\mathbf{q}}(u)}$, where $\hat{q}_k(u) := u^{k-1}\hat{q}_k$ for $k \geq 1$. Comparing this to Proposition II.4, we see that $R_{\mathbf{q}}(u)$ is the smallest positive solution of the equation $u = u_{\mathbf{q}}(r)$ (In particular, it is finite if and only if a such solution exists). In other words, $R_{\mathbf{q}}$ is the functional inverse of $u_{\mathbf{q}}$ on the interval $u \in [0, u_c]$, where $u_c := \max_{r \geq 0} u_{\mathbf{q}}(r)$. Here the maximum is reached because, denoting by R_c the radius of convergence of $u_{\mathbf{q}}$, either $u_{\mathbf{q}}(R_c) = -\infty$, in which case the maximum is reached before R_c, or $u_{\mathbf{q}}(R_c) > -\infty$, in which case $u_{\mathbf{q}}$ is continuous on the compact interval $[0, R_c]$. Hence we have the following dichotomy: either $R_{\mathbf{q}}(u) < \infty$ for all $u \in [0,1]$ (when $u_c \geq 1$), or $R_{\mathbf{q}}(u) = \infty$ for some $u < 1$ (when $u_c < 1$). Comparing this to the expressions (II.13) and (II.18) of $F^\bullet_p(\hat{\mathbf{q}})$ and $F_p(\hat{\mathbf{q}})$, we see that:

Lemma II.5 (Same admissibility condition for non-pointed and pointed maps)**.** *For any $p \geq 1$, the following conditions are equivalent: (i) $F_p(\hat{\mathbf{q}}) < \infty$, (ii) $F^\bullet_p(\hat{\mathbf{q}}) < \infty$, (iii) $R_{\mathbf{q}} < \infty$.*

Moreover, when $R_{\mathbf{q}}$ is finite, one can perform a change of variable in (II.18) using the equation $u_{\mathbf{q}}(R_{\mathbf{q}}(u)) = u$, which yields

$$F_p(\hat{\mathbf{q}}) = \binom{2p}{p} \int_0^{R_{\mathbf{q}}} r^p \cdot u'_{\mathbf{q}}(r)\,\mathrm{d}r\,. \tag{II.19}$$

Now we are ready to prove Proposition II.3. As observed at the end of Section 2.1, the gasket decomposition allows one to reduce the problem to the case of $h = n = 0$.

Proof of Proposition II.3. Given an admissible triple $(\mathbf{q}, h, n) \in [0,\infty)^{\mathbb{N}} \times [0,\infty) \times [0,\infty)$, the effective weight sequence $\hat{\mathbf{q}}$ satisfies $R_{\mathbf{q}} < \infty$. We multiply both sides of (II.19) by x^{-2p} before summing over p. (Notice that (II.19) is also valid for $p = 0$.) Since all terms are positive, we can interchange the sum and the integral, which yields

$$\mathcal{W}_{\hat{\mathbf{q}},0,0}(x) = \int_0^{R_{\mathbf{q}}} \left(\sum_{p=0}^{\infty} \binom{2p}{p} \frac{r^p}{x^{2p}} \right) u'_{\mathbf{q}}(r)\,\mathrm{d}r = \int_0^{R_{\mathbf{q}}} \frac{u'_{\mathbf{q}}(r)}{\sqrt{1 - 4r/x^2}}\mathrm{d}r\,. \tag{II.20}$$

for all $|x| > \gamma := \sqrt{4R_{\mathbf{q}}}$. By choosing the determination of the square root with a branch cut along $\mathbb{R}_{\leq 0}$, the above integral gives the analytic continuation of $\mathcal{W}_{\hat{\mathbf{q}},0,0}$ on $S_\gamma = \overline{\mathbb{C}} \setminus [-\gamma,\gamma]$. Moreover, using the fact that $u'_{\mathbf{q}}$ is bounded by 1 on $[0, R_1]$, it is not hard to see that this analytic continuation extends continuously to $x \pm i0$ for $x \in [-\gamma,\gamma]$. Thus $\mathcal{W}_{\hat{\mathbf{q}},0,0}$ is an even holomorphic function on $\overline{S}_\gamma$.

With the determination of the square root chosen above, the denominator in (II.20) extends to $\sqrt{1 - 4r/(x \pm i0)^2} = \pm i x^{-1}\sqrt{4r - x^2}$ for $|x| < \sqrt{4r}$ (see (II.33)), it follows that for all $x \in (-\gamma,\gamma)$,

$$\frac{1}{\sqrt{1 - 4r/(x - i0)^2}} + \frac{1}{\sqrt{1 - 4r/(x + i0)^2}} = \frac{2}{\sqrt{1 - 4r/x^2}} \mathbb{1}_{\{r \leq x^2/4\}}\,. \tag{II.21}$$

Apply this relation to (II.20), then make the change of variable $r = \frac{x^2}{4}s$, we obtain:

$$\mathcal{W}_{\hat{\mathbf{q}},0,0}(x+i0)+\mathcal{W}_{\hat{\mathbf{q}},0,0}(x-i0) \;=\; 2\int_0^{\frac{x^2}{4}} \frac{u'_{\mathbf{q}}(r)\,\mathrm{d}r}{\sqrt{1-4r/x^2}} \;=\; 2\int_0^1 \frac{\mathrm{d}s}{\sqrt{1-s}}\left(\frac{x^2}{4} - \sum_{k\geq 1} k\tilde{q}_k\left(\frac{x^2 s}{4}\right)^k\right).$$

One can interchange the sum with the integral because all the terms but one have the same sign. Then it follows from the integral $\int_0^1 \frac{s^k \mathrm{d}s}{\sqrt{1-s}} = \frac{4^k}{k\binom{2k}{k}}$ and the definition (II.12) of $\tilde{q}_k$ that

$$\mathcal{W}_{\hat{\mathbf{q}},0,0}(x+i0)+\mathcal{W}_{\hat{\mathbf{q}},0,0}(x-i0) = x^2 - \sum_{k\geq 1} \hat{q}_k\, x^{2k}.$$

Combine this with the fixed point equation (II.10), we obtain Equation (II.4) for a general admissible triple $(\mathbf{q}, h, n)$.

By taking the difference instead of sum of $\mathcal{W}_{\hat{\mathbf{q}},0,0}(x \pm i0)$ in the above calculation, one obtains the following expression of the spectral density:

$$\rho_{\mathbf{q},h,n}(x) = \rho_{\hat{\mathbf{q}},0,0}(x) = \frac{1}{\pi}\int_{x^2}^1 \frac{u'_{\mathbf{q}}(R_{\mathbf{q}}s)\cdot R_{\mathbf{q}}\,\mathrm{d}s}{\sqrt{s-x^2}}.$$

Then it is clear that $\rho_{\mathbf{q},h,n}$ is continuous at $x=0$, even and non-negative on $[-1,1]$.

It remains to find the range of γ, remark that $1/\gamma$ is the radius of convergence of the power series $\mathcal{W}_{\mathbf{q},h,n}(1/x) = \sum_k F_k(\mathbf{q},h,n)x^{2k}$, so $F_k(\mathbf{q},h,n) \approx \gamma^{2k}$ up to sub-exponential factors. On the other hand, (II.19) requires that $u_{\mathbf{q}}$ has a radius of convergence at least $R_{\mathbf{q}} = \gamma^2/4$, so up to sub-exponential factors we must have $4^k\hat{q}_k \approx \tilde{q}_k \lesssim 4^k\gamma^{-2k}$. Inject the above asymptotics into $nh^{2k}F_k(\mathbf{q},h,n) \leq \hat{q}_k$, we see that $\gamma^2 h \leq 1$, that is $\gamma \in (0, h^{-1/2}]$. □

Without solving Equation (II.4), one can also prove (see [BBG12c, Section 3.2]) that $\alpha = 1$ and $\alpha = 2$ respectively in the subcritical and generic critical phase, assuming that α is defined by the asymptotic in Theorem II.1, and the phases are defined by the alternative definition given at the end of Section 2.3. However it is much harder (if possible) to derive rigorously the value of α in the non-generic phase, or to prove that the non-generic phase actually exists, without solving (II.4).[4]

In the next section, we will analyse in detail the structure of the solutions of (II.4), in which the parameter γ may or may not come from the solution of a map-enumeration problem.

3 Admissibility criteria and phase diagram

The next few propositions will consider parameters $(\mathbf{q}, h, n)$ in the space $\mathbb{D}_\infty := [0,\infty)^{\mathbb{N}} \times [0,\infty) \times [0,2)$. It extends $\mathbb{D} = [0,\infty)^d \times (0,\infty) \times (0,2)$ to include non-decorated bipartite maps with unbounded face degree, that is, the case where $h = n = 0$ and $q_k > 0$ for k arbitrarily large.

[4] Nevertheless, [BBG12c, Section 3.2 and 4.1] contains an argument which shows that in the non-generic critical case, *if* the asymptotics of $F_p(\mathbf{q},h,n)$ has the form given in Theorem II.1, then α must be either $3/2 - b$ or $3/2 + b$, with $b = \frac{1}{\pi}\arccos(\frac{n}{2})$.

Proposition II.B (Existence, uniqueness and continuity in parameters of solution of (II.4), [BBG12c])**.** *For all* $(\mathbf{q}, h, n) \in \mathbb{D}_\infty$ *and* $\gamma \in (0, h^{-1/2}]$*, the equation* (II.4) *has at most one solution, which we denote by* $\mathcal{W}^{(\gamma)}_{\mathbf{q},h,n}$*.*
If $(\mathbf{q}, h, n) \in \mathbb{D}$*, then* $\mathcal{W}^{(\gamma)}_{\mathbf{q},h,n}$ *does exist, and the associated spectral density* $\rho^{(\gamma)}_{\mathbf{q},h,n}(x)$ *is jointly continuous with respect to* $(x; \mathbf{q}, h, n, \gamma) \in [-1, 1] \times \mathcal{D}$*.*

Now we can define the functions $\mathfrak{f}$, $\mathfrak{g}$ and $\mathfrak{h}$ appeared in Proposition II.2:

$$\begin{aligned} \mathfrak{f}(\mathbf{q}, h, n, \gamma) &:= \lim_{x\to 1^-} \frac{\rho^{(\gamma)}_{\mathbf{q},h,n}(x)}{\sqrt{1-x^2}} && \text{for } (\mathbf{q}, h, n, \gamma) \in \mathring{\mathcal{D}} \\ \mathfrak{g}(\mathbf{q}, h, n) &:= \lim_{x\to 1^-} \frac{\rho^{(\gamma)}_{\mathbf{q},h,n}(x)}{(1-x^2)^{1-b}} && \text{for } (\mathbf{q}, h, n, \gamma) \in \partial\mathcal{D} \\ \mathfrak{h}(\mathbf{q}, h, n, \gamma) &:= \mathcal{W}^{(\gamma)}_{\mathbf{q},h,n}(\infty) && \text{for } (\mathbf{q}, h, n, \gamma) \in \mathcal{D} \end{aligned}$$

(Recall that $b = \frac{1}{\pi}\arccos(\frac{n}{2}) \in (0, \frac{1}{2})$, and $(\mathbf{q}, h, n, \gamma) \in \partial\mathcal{D}$ is equivalent to $(\mathbf{q}, h, n) \in \mathbb{D}$ and $\gamma = h^{-1/2}$.)

Given $(\mathbf{q}, h, n) \in \mathbb{D}$, Proposition II.B gives one unique solution $\mathcal{W}^{(\gamma)}_{\mathbf{q},h,n}$ of (II.4) for each value of $\gamma \in (0, h^{-1/2}]$. To find the solution $\mathcal{W}_{\mathbf{q},h,n}$ of that enumerates loop-decorate maps, one still needs to determine the value of γ by taking into account additional properties of the combinatorial solution. It was observed numerically in [BBG12c] that one can select at most one value of γ using the necessary conditions $\mathcal{W}^{(\gamma)}_{\mathbf{q},h,n}(\infty) = 1$ and $\rho^{(\gamma)}_{\mathbf{q},h,n}(x) \geq 0$ for all $x \in [-1, 1]$. And it was assumed implicitly that these conditions are also sufficient. In other words, if one such $\gamma \in (0, h^{-1/2}]$ exists, then $(\mathbf{q}, h, n)$ is indeed admissible and we have $\mathcal{W}_{\mathbf{q},h,n} = \mathcal{W}^{(\gamma)}_{\mathbf{q},h,n}$. In this section we prove that this is indeed the case (Proposition II.8) using the (combinatorial) admissibility condition stated in Proposition II.A.

3.1 An analytic condition for admissibility

Our approach is based on the following integral equation on the spectral density. It is basically Equation (II.4) expressed in terms of $\rho^{(\gamma)}_{\mathbf{q},h,n}$ instead of $\mathcal{W}^{(\gamma)}_{\mathbf{q},h,n}$. Its proof is purely complex-analytic and will be given in Section 4.1.

Lemma II.6 (Integral equation for $\rho^{(\gamma)}_{\mathbf{q},h,n}$)**.** *Consider* $(\mathbf{q}, h, n) \in \mathbb{D}_\infty$ *and* $\gamma \in (0, h^{-1/2}]$ *such that* (II.4) *has a solution. Let* $\tau = \gamma^2 h \in [0, 1]$*. Then for all* $x \in [-1, 1]$*,*

$$-\frac{2\pi\, \rho^{(\gamma)}_{\mathbf{q},h,n}(x)}{\sqrt{1-x^2}} = (q_1 - 1)\gamma^2 + \sum_{k=2}^{\infty} q_k \gamma^{2k} I_k(x) + n \int_{-1}^{1} \frac{\tau^2 y^2}{1 - \tau^2 x^2 y^2} \frac{\rho^{(\gamma)}_{\mathbf{q},h,n}(y)\,\mathrm{d}y}{\sqrt{1-\tau^2 y^2}}\,, \tag{II.22}$$

where $I_k(x) = \frac{1}{\pi}\int_{-1}^{1} \frac{x^{2k}-y^{2k}}{x^2-y^2} \frac{\mathrm{d}y}{\sqrt{1-y^2}}$ *is an even polynomial with positive coefficients.*

We will use the three consequences of Lemma II.6 collected in the following corollary. Define

$$\tilde{\rho}^{(\gamma)}_{\mathbf{q},h,n}(x) := \frac{\rho^{(\gamma)}_{\mathbf{q},h,n}(x)}{\sqrt{1-x^2}}\,.$$

Corollary II.7. *Consider* $(\mathbf{q}, h, n) \in \mathbb{D}_\infty$ *and* $\gamma \in (0, h^{-1/2}]$ *such that* (II.4) *has a solution.*

(i) If $\rho^{(\gamma)}_{\mathbf{q},h,n}$ is non-negative and not identically zero on $[-1,1]$, then it only vanishes at ± 1.

(ii) If $(\mathbf{q},h,n) \in \mathbb{D}$, then (II.22) defines an analytic continuation of $\tilde{\rho}^{(\gamma)}_{\mathbf{q},h,n}(x)$ on the disk $\{x \in \mathbb{C} : |x| < \tau^{-1}\}$, and the mapping $(\mathbf{q},h,n,\gamma) \mapsto \tilde{\rho}^{(\gamma)}_{\mathbf{q},h,n}$ is continuous with respect to the topology of uniform convergence on compact subsets of $\{x \in \mathbb{C} : |x| < \tau^{-1}\}$.

In particular, $\mathfrak{f}$ is well-defined and continuous on $\mathring{\mathcal{D}}$.

(iii) When $n = h = 0$, (II.22) is the explicit solution of (II.4), for which we have

$$\mathcal{W}^{(\gamma)}_{\mathbf{q},0,0}(\infty) = u_{\mathbf{q}}\Big(\frac{\gamma^2}{4}\Big) \qquad \text{and} \qquad \mathfrak{f}(\mathbf{q},0,0,\gamma) = \frac{\gamma^2}{2\pi} u'_{\mathbf{q}}\Big(\frac{\gamma^2}{4}\Big), \tag{II.23}$$

where $u_{\mathbf{q}}(r) = r - \sum_{k=1}^{\infty} \frac{1}{2}\binom{2k}{k} q_k r^k$ is the same as the function defined in Proposition II.4.

Proof. If $\rho^{(\gamma)}_{\mathbf{q},h,n}$ is non-negative and not identically zero, then right hand side of (II.22) is strictly increasing on $[0,1]$ and strictly decreasing on $[-1,0]$. Thus $\rho^{(\gamma)}_{\mathbf{q},h,n}$ cannot vanish on $(-1,1)$. On the other hand, $\mathcal{W}^{(\gamma)}_{\mathbf{q},h,n}$ is continuous at $\pm\gamma \in \overline{S}_\gamma$, so $\rho^{(\gamma)}_{\mathbf{q},h,n}(\pm 1) = 0$. This proves (i).

For (ii), we start by noticing that $y \mapsto y\,\rho^{(\gamma)}_{\mathbf{q},h,n}(y)$ is always continuous, thus bounded, on $[-1,1]$. For all $x \in \mathbb{C}$ such that $|x| < x_0 < \tau^{-1}$, we have

$$\int_{-1}^{1} \left| \frac{\partial}{\partial x} \frac{\tau^2 y^2}{1 - \tau^2 x^2 y^2} \frac{\rho^{(\gamma)}_{\mathbf{q},h,n}(y)}{\sqrt{1-\tau^2 y^2}} \right| \mathrm{d}y \;\le\; \int_{-1}^{1} \frac{2\tau^4 x_0 \,|y|^3}{(1 - \tau^2 x_0^2 y^2)^2} \frac{\left|y\,\rho^{(\gamma)}_{\mathbf{q},h,n}(y)\right|}{\sqrt{1-\tau^2 y^2}} \mathrm{d}y \;<\; \infty\,.$$

Then it follows from the dominated convergence theorem that the right hand side of (II.22) has a finite complex derivative at x (Recall that $(\mathbf{q},h,n) \in \mathbb{D}$ implies $q_k = 0$ for $k > d$). Thus it defines an analytic continuation of $\tilde{\rho}^{(\gamma)}_{\mathbf{q},h,n}$ on $\{x \in \mathbb{C} : |x| < \tau^{-1}\}$.

With a similar dominated convergence argument, we deduce from Theorem II.3 that $(x,\mathbf{q},h,n,\gamma) \mapsto \tilde{\rho}^{(\gamma)}_{\mathbf{q},h,n}(x)$ is also jointly continuous when x is in the above domain of analytic continuation. Fix $(\mathbf{q},h,n,\gamma) \in \mathcal{D}$ and $r \le \tau^{-1} - 2\epsilon$ with some $\epsilon > 0$. There exists a neighborhood V of $(\mathbf{q},h,n,\gamma)$ such that for all $(\mathbf{q}',h',n',\gamma') \in V$, we still have $r \le (\tau')^{-1} - \epsilon$ for $\tau' = (\gamma')^2 h'$. Then for any sequence of parameters $(\mathbf{q}^{(j)},h^{(j)},n^{(j)},\gamma^{(j)})_{j\ge 0}$ converging to $(\mathbf{q},h,n,\gamma)$ in V, the sequence of functions $\tilde{\rho}^{\gamma^{(j)}}_{\mathbf{q}^{(j)},h^{(j)},n^{(j)}}$ are analytic and converges pointwise to $\tilde{\rho}^{(\gamma)}_{\mathbf{q},h,n}$ on $\{x \in \mathbb{C} : |x| < r + \epsilon\}$. They are also uniformly bounded. Then it follows from the Vitali theorem (see e.g. [Hen77, p. 566]) that they converge uniformly on the closed disk $\{x \in \mathbb{C} : |x| \le r\}$. This proves that $(\mathbf{q},h,n,\gamma) \mapsto \tilde{\rho}^{(\gamma)}_{\mathbf{q},h,n}$ is continuous uniformly on all compacts of the analytic extension.

If $(\mathbf{q},h,n,\gamma) \in \mathring{\mathcal{D}}$, then τ is bounded away from 1 in some neighborhood of $(\mathbf{q},h,n,\gamma)$. So $f(\mathbf{q},h,n,\gamma) = \tilde{\rho}^{(\gamma)}_{\mathbf{q},h,n}(1)$ is well-defined and continuous with respect to its parameters.

Now let us prove (iii). When $n = h = 0$, (II.22) gives explicitly the spectral density $\rho^{(\gamma)}_{\mathbf{q},h,n}$. The resolvent can be recovered using Cauchy's integral formula: $\mathcal{W}(\gamma x) = \int_{-1}^{1} \frac{xy}{x-y} \rho(y) \mathrm{d}y$. Alternatively, one can use directly the expression (II.34) of $\mathcal{W}^{(\gamma)}_{\mathbf{q},h,n}$ in the proof of Lemma II.6.

Taking the limits $x \to \infty$ and $x \to 1$ respectively in (II.34) and in (II.22), we get

$$\mathcal{W}^{(\gamma)}_{\mathbf{q},h,n}(\infty) = \frac{1}{2}\sum_{k=1}^{\infty}(q_k - \delta_{k,1})J_k(\infty)$$
$$\text{and} \qquad \mathfrak{f}(\mathbf{q},0,0,\gamma) = -\frac{1}{2\pi}\sum_{k=1}^{\infty}(q_k - \delta_{k,1})\gamma^{2k}I_k(1)\,.$$

Then (II.23) follows from the following integral formula:

$$J_k(\infty) = -\frac{1}{\pi}\int_{-\gamma}^{\gamma}\frac{y^{2k}\mathrm{d}y}{\sqrt{\gamma^2 - y^2}} = -\frac{\gamma^{2k}}{4^k}\binom{2k}{k}$$
$$\text{and} \qquad I_k(1) = \frac{1}{\pi}\int_{-1}^{1}\frac{1-y^{2k}}{1-y^2}\frac{\mathrm{d}y}{\sqrt{1-y^2}} = \frac{2k}{4^k}\binom{2k}{k}\,. \qquad \square$$

Now we can prove the analytic condition for the admissibility of $(\mathbf{q},h,n)$ discussed at the beginning of this section is indeed necessary and sufficient.

Proposition II.8 (Admissibility condition). *$(\mathbf{q},h,n) \in \mathbb{D}_\infty$ is admissible if and only if for some $\gamma \in (0,h^{-1/2}]$, the solution of (II.4) exists and satisfies*

$$\mathcal{W}^{(\gamma)}_{\mathbf{q},h,n}(\infty) = 1 \qquad \textit{and} \qquad \rho^{(\gamma)}_{\mathbf{q},h,n}(x) \geq 0 \textit{ for all } x \in [-1,1]\,. \tag{II.24}$$

In this case, the above condition uniquely determines γ, and we have $\mathcal{W}^{(\gamma)}_{\mathbf{q},h,n} = \mathcal{W}_{\mathbf{q},h,n}$.

Proof. If $(\mathbf{q},h,n)$ is admissible, Proposition II.3 implies that (II.24) has a solution $\gamma \in (0,h^{-1/2}]$.

Inversely, assume that there exists $\gamma \in (0,h^{-1/2}]$ such that the solution of (II.4) exists and satisfies (II.24). Let $F^{(\gamma)}_k = [x^{-2k}]\mathcal{W}^{(\gamma)}_{\mathbf{q},h,n}(x)$ be the coefficients of the Taylor expansion of $\mathcal{W}^{(\gamma)}_{\mathbf{q},h,n}$ at $x = \infty$. Then (II.24) implies that $F^{(\gamma)}_0 = 1$ and for all $k \geq 1$,

$$F^{(\gamma)}_k \;=\; \frac{1}{2\pi i}\int_{\mathcal{C}} x^{2k-1}\mathcal{W}^{(\gamma)}_{\mathbf{q},h,n}(x)\mathrm{d}x \;=\; \gamma^{2k}\int_{-1}^{1}x^{2k}\rho^{(\gamma)}_{\mathbf{q},h,n}(x)\mathrm{d}x \;\geq\; 0$$

where $\mathcal{C}$ is any anti-clockwise-oriented cycle around the cut $[-\gamma,\gamma]$. Let $\hat{q}_k = q_k + n\,h^{2k}F^{(\gamma)}_k$. Since $F^{(\gamma)}_0 = 1$, we have

$$\sum_{k=0}^{\infty}\hat{q}_k x^{2k} = \sum_{k=0}^{\infty}q_k x^{2k} + n\,\mathcal{W}^{(\gamma)}_{\mathbf{q},h,n}\left(\frac{1}{hx}\right) - n\,.$$

Plug this into (II.4), we see that $\mathcal{W}^{(\gamma)}_{\mathbf{q},h,n}$ satisfies the defining equation of $\mathcal{W}^{(\gamma)}_{\hat{\mathbf{q}},0,0}$. Therefore $\mathcal{W}^{(\gamma)}_{\hat{\mathbf{q}},0,0}$ exists and $\mathcal{W}^{(\gamma)}_{\hat{\mathbf{q}},0,0} = \mathcal{W}^{(\gamma)}_{\mathbf{q},h,n}$. Then Corollary II.7(iii) reads

$$\mathcal{W}^{(\gamma)}_{\mathbf{q},h,n}(\infty) = u_{\mathbf{q}}\left(\frac{\gamma^2}{4}\right) \qquad \text{and} \qquad \mathfrak{f}(\mathbf{q},h,n,\gamma) = \frac{\gamma^2}{2\pi}u'_{\hat{\mathbf{q}}}\left(\frac{\gamma^2}{4}\right)$$

Use again (II.24), we get $u_{\mathbf{q}}(\frac{\gamma^2}{4}) = 1$ and $u'_{\hat{\mathbf{q}}}(\frac{\gamma^2}{4}) \geq 0$. Since $u_{\mathbf{q}}$ is strictly concave, this implies that $\frac{\gamma^2}{4}$ is the smallest positive solution of the equation $u_{\mathbf{q}}(r) = 1$.

By Proposition II.4, a such solution exists if and only if $(\hat{\mathbf{q}},0,0)$ is admissible (in fact this is an equivalence). So we can apply Proposition II.3 to $(\hat{\mathbf{q}},0,0)$ and conclude that there exists $\gamma' \in (0,h^{-1/2}]$ such that $\mathcal{W}^{(\gamma')}_{\hat{\mathbf{q}},0,0} = \mathcal{W}_{\hat{\mathbf{q}},0,0}$. But since $\mathcal{W}_{\hat{\mathbf{q}},0,0}(\infty)=1$ and $\rho_{\hat{\mathbf{q}},0,0}\geq 0$, $\frac{(\gamma')^2}{4}$ must also be the smallest positive solution of $u_{\mathbf{q}}(r)=1$. Thus $\gamma=\gamma'$ and $F_k^{(\gamma)} = F_k(\hat{\mathbf{q}},0,0)$. It follows that $\hat{\mathbf{q}}$ and $(\mathbf{q},h,n)$ satisfy all the conditions of Proposition II.A, therefore $(\mathbf{q},h,n)$ is admissible and $F_k(\mathbf{q},h,n) = F_k^{(\gamma)}$. It follows that $\mathcal{W}^{(\gamma)}_{\mathbf{q},h,n} = \mathcal{W}_{\mathbf{q},h,n}$, and γ is uniquely determined because $(-\gamma,\gamma)$ is the locus of discontinuity of $\mathcal{W}^{(\gamma)}_{\mathbf{q},h,n}$. $\square$

3.2 Positivity bootstrap: subcritical and generic critical case

In general it is much easier to show $\mathfrak{f}(\mathbf{q},h,n,\gamma)\geq 0$ or $\mathfrak{g}(\mathbf{q},h,n)\geq 0$ than to show $\rho^{(\gamma)}_{\mathbf{q},h,n}\geq 0$ on the whole interval $[-1,1]$. In [BBG12a, Section 4.6] it was conjectured based on numerical observation that these two conditions are actually equivalent for spectral densities of loop models on planar maps. In this subsection and the next, we show that this is indeed true for the rigid loop model on bipartite maps. The proof is based on a continuity argument that bootstrap the positivity of $\rho^{(\gamma)}_{\mathbf{q},h,n}$ near $x=1$ to its positivity on $[-1,1]$. We believe that this is the first time a such argument is applied to the enumeration problem of maps, whereas the methods in the previous sections are relatively well-known in the literature.

Recall that $\mathcal{D} = \left\{(\mathbf{q},h,n,\gamma)\in\mathbb{D}\times(0,\infty)\,\middle|\,\gamma\leq h^{-1/2}\right\}$ is a set of parameters on which $\rho^{(\gamma)}_{\mathbf{q},h,n}$ is well-defined and pointwise continuous with respect to the parameters. $\mathring{\mathcal{D}}$ and $\partial\mathcal{D}$, defined by replacing $\leq$ in the definition of $\mathcal{D}$ with $<$ and $=$, are the topological interior and boundary of $\mathcal{D}$ as a subspace of $\mathbb{D}\times(0,\infty)$.

For fixed (h,n,γ), the spectral density $\rho^{(\gamma)}_{\mathbf{q},h,n}$ is a linear function of the polynomial $n+x^2-\sum_k q_k x^{2k}$ on the right hand side of (II.4). If the polynomial had only the constant term n (which corresponds to the case $\mathbf{q}=\boldsymbol{\delta}_1$, c.f. the remark after Lemma II.13), then the solution of (II.4) would be $\mathcal{W}(x)=\frac{n}{n+2}$, which has zero spectral density. Thus $\rho^{(\gamma)}_{\mathbf{q},h,n}$ is a linear function of the coefficients $(1-q_1,-q_2,\ldots,-q_d)$ of the non-constant terms in the polynomial. In other words, we have for all $(\mathbf{q},h,n,\gamma)\in\mathcal{D}$,

$$\rho^{(\gamma)}_{\mathbf{q},h,n} = (1-q_1)\rho^{(\gamma)}_{\mathbf{0},h,n} - \sum_{k=1}^{\infty} q_k \rho^{(\gamma)}_{\boldsymbol{\delta}_1-\boldsymbol{\delta}_k,h,n}\,,$$

where $\mathbf{0}$ is the zero sequence, and $\boldsymbol{\delta}_k$ is the sequence whose k-th term is 1 and all other terms are 0. Dividing by $\sqrt{1-x^2}$ and taking the limit $x\to 1$, we get for all $(\mathbf{q},h,n,\gamma)\in\mathring{\mathcal{D}}$

$$\mathfrak{f}(\mathbf{q},h,n,\gamma) = (1-q_1)\,\mathfrak{f}(\mathbf{0},h,n,\gamma) - \sum_{k=2}^{d} q_k\,\mathfrak{f}(\boldsymbol{\delta}_1-\boldsymbol{\delta}_k,h,n,\gamma)\ .$$

Following the methods of [BBG12c], one can in principle compute each term in the above sum explicitly. The first term has a relatively simple expression whose sign can be determined. But going into the details here will lead us too far, so we will simply admit the following:

Lemma II.C. *For all $h>0$, $n\in(0,2)$ and $\gamma\in(0,h^{-1/2})$, we have $\mathfrak{f}(\mathbf{0},h,n,\gamma)>0$.*

Physically it means that a fully-packed model ($\mathbf{q}=\mathbf{0}$, i.e. every internal face is visited by a loop) is never generic critical (i.e. $\mathfrak{f}=0$). However the lemma is a bit stronger than the previous statement because it also includes non-physical values of the parameter γ.

Let us consider

$$\mathcal{A} = \left\{ (\mathbf{q}, h, n, \gamma) \in \mathring{\mathcal{D}} \,\middle|\, \mathfrak{f}(\mathbf{q}, h, n, \gamma) > 0 \right\}.$$

We denote by $\overline{\mathcal{A}}$ be the closure of $\mathcal{A}$ in $\mathcal{D}$. By continuity, we have $\mathfrak{f} \geq 0$ on $\overline{\mathcal{A}} \cap \mathring{\mathcal{D}}$. On the other hand, if $\mathfrak{f}(\mathbf{q}, h, n, \gamma) = 0$ for some $(\mathbf{q}, h, n, \gamma) \in \mathring{\mathcal{D}}$, then by contradiction there exists some $k \in \{1, \ldots, d\}$ such that $q_k > 0$ and $\mathfrak{f}(\boldsymbol{\delta}_1 - \boldsymbol{\delta}_k, h, n, \gamma) \neq 0$. (We are using Lemma II.C here.) This implies that $\mathfrak{f}$ takes both positive and negative values in a neighborhood of $(\mathbf{q}, h, n, \gamma)$, and therefore $(\mathbf{q}, h, n, \gamma) \in \overline{\mathcal{A}}$. We conclude that

$$\overline{\mathcal{A}} \cap \mathring{\mathcal{D}} = \left\{ (\mathbf{q}, h, n, \gamma) \in \mathring{\mathcal{D}} \,\middle|\, \mathfrak{f}(\mathbf{q}, h, n, \gamma) \geq 0 \right\}$$

Lemma II.9. *The set $\mathcal{A}$ is connected.*

Proof. For each $h > 0$, $n \in (0, 2)$ and $\gamma \in (0, h^{-1/2})$, the section $\{\mathbf{q} : (\mathbf{q}, h, n, \gamma) \in \mathcal{A}\}$ of $\mathcal{A}$ is a simplex in $\mathbb{R}^d$ which contains $\mathbf{0}$ by Lemma II.C. Thus every point in $\mathcal{A}$ is path-connected to a point of the form $(\mathbf{0}, h, n, \gamma)$. These points are obviously path-connected to each other. □

Lemma II.10 (Positivity bootstrap: $\gamma < h^{-1/2}$)**.** $\rho^{(\gamma)}_{\mathbf{q},h,n} \geq 0$ *for all* $(\mathbf{q}, h, n, \gamma) \in \overline{\mathcal{A}}$.

Proof. Consider $\mathcal{A}_+ = \left\{ (\mathbf{q}, h, n, \gamma) \in \mathcal{A} \,\middle|\, \rho^{(\gamma)}_{\mathbf{q},h,n}(x) \geq 0 \text{ for all } x \in [-1, 1] \right\}$. By comparing $F_k(\mathbf{q}, h, n)$ to the partition function of non-decorated maps, we see that $(\mathbf{q}, h, n)$ is admissible and subcritical when $n < 1$ and $\max(h, q_1, \ldots, q_d)$ is small enough. Then Theorem II.3 provides a γ such that $\rho^{(\gamma)}_{\mathbf{q},h,n} \geq 0$ and $\mathfrak{f}(\mathbf{q}, h, n, \gamma) > 0$. Therefore $\mathcal{A}_+ \neq \varnothing$.

Now fix $(\mathbf{q}, h, n, \gamma) \in \mathcal{A}_+$. We have $\mathfrak{f}(\mathbf{q}, h, n, \tau) = \tilde{\rho}^{(\gamma)}_{\mathbf{q},h,n}(\pm 1) > 0$ and, by Corollary II.7(i), $\tilde{\rho}^{(\gamma)}_{\mathbf{q},h,n}$ does not vanish on $(-1, 1)$. Thus $\tilde{\rho}^{(\gamma)}_{\mathbf{q},h,n}$ is bounded away from zero on the compact interval $[-1, 1]$. Then the continuity of $(\mathbf{q}, h, n, \gamma) \mapsto \rho^{(\gamma)}_{\mathbf{q},h,n}$ in Corollary II.7(ii) implies that $\rho^{(\gamma')}_{\mathbf{q}',h',n'} \geq 0$ for all $(\mathbf{q}', h', n', \gamma')$ in a neighborhood of $(\mathbf{q}, h, n, \gamma)$, that is, $\mathcal{A}_+$ is open in $\mathcal{A}$. But $\mathcal{A}_+$ is also closed in $\mathcal{A}$, because $(\mathbf{q}, h, n, \gamma) \mapsto \rho^{(\gamma)}_{\mathbf{q},h,n}(x)$ is continuous for each $x \in [-1, 1]$. Since $\mathcal{A}$ is connected, we conclude that $\mathcal{A}_+ = \mathcal{A}$, that is, $\rho^{(\gamma)}_{\mathbf{q},h,n} \geq 0$ for all $(\mathbf{q}, h, n, \gamma) \in \mathcal{A}$. By the continuity of $(x; \mathbf{q}, h, n, \gamma) \mapsto \rho^{(\gamma)}_{\mathbf{q},h,n}(x)$, the same holds for all $(\mathbf{q}, h, n, \gamma) \in \overline{\mathcal{A}}$. □

3.3 Positivity bootstrap: non-generic critical case

When $\gamma = h^{-1/2}$ (that is, when $(\mathbf{q}, h, n, \gamma) \in \partial\mathcal{D}$), the limit which defines $\mathfrak{f}$ will always be zero because $\mathfrak{g}$ is well-defined and finite (see below). However it is different from the case treated in the previous subsection because $\rho^{(\gamma)}_{\mathbf{q},h,n}$ no longer has an analytic continuation in any neighborhood of $x = 1$. Instead, we will use the function $\mathfrak{g}$ to capture the behavior of $\rho^{(\gamma)}_{\mathbf{q},h,n}$ in the vicinity of $x = 1$ and show results that are analogous to the previous subsection.

However, it seems that there is not any analogous result of Lemma II.6 which helps determine the behavior of $\rho^{(\gamma)}_{\mathbf{q},h,n}$ near $x = 1$ when $\gamma = h^{-1/2}$. Instead, we will rely on the following explicit expression of $\rho^{(\gamma)}_{\mathbf{q},h,n}$ to find its leading order asymptotics when $x \to 1^-$.

Lemma II.11 ([BBG12c] for the case $\mathbf{q} = g\boldsymbol{\delta}_2$)**.** *For* $(\mathbf{q}, h, n) \in \mathbb{D}$ *and* $\gamma = h^{-1/2}$*, we have*

$$\rho^{(\gamma)}_{\mathbf{q},h,n}(x) = \frac{1}{2\pi\sqrt{4 - n^2}} \frac{1}{x} \left(L_{\mathbf{q},h,n}(x) \left(\frac{1 - x}{1 + x} \right)^b - L_{\mathbf{q},h,n}(-x) \left(\frac{1 + x}{1 - x} \right)^b \right) \tag{II.25}$$

where $L_{\mathbf{q},h,n}(x) = P_{\mathbf{q},h,n}(x) - P_{\mathbf{q},h,n}(x^{-1})$ and $P_{\mathbf{q},h,n}$ is the polynomial with no constant term determined by

$$P_{\mathbf{q},h,n}\left(\frac{1}{x}\right) = \sum_{k=1}^{d}(q_k - \delta_{k,1})\gamma^{2k}\frac{1}{x^{2k}}\left(\frac{1+x}{1-x}\right)^b + O(1) \qquad \textit{as } x \to 0\,. \tag{II.26}$$

In other words, $P_{\mathbf{q},h,n}(1/x)$ is the singular part in the Laurent series expansion of the above function at $x = 0$.

We will detail the calculation that derives the above result in the next section. It follows step by step the derivation for the case $\mathbf{q} = g\boldsymbol{\delta}_2$ in [BBG12c].

The expression of $\rho^{(\gamma)}_{\mathbf{q},h,n}(x)$ can be easily expanded at $x = 1$, which gives

$$\rho^{(\gamma)}_{\mathbf{q},h,n}(x) = -\frac{2^b P'_{\mathbf{q},h,n}(-1)}{\pi\sqrt{4-n^2}}(1-x)^{1-b} - \frac{2^{-b}P'_{\mathbf{q},h,n}(1)}{\pi\sqrt{4-n^2}}(1-x)^{1+b} + O((1-x)^{2-b}) \tag{II.27}$$

It follows that $\mathfrak{g}$ is well-defined on $\mathbb{D}$ and we have

$$\mathfrak{g}(\mathbf{q},h,n) = -\frac{2^{2b}P'_{\mathbf{q},h,n}(-1)}{2\pi\sqrt{4-n^2}}\,. \tag{II.28}$$

The polynomial $P'_{\mathbf{q},h,n}$ can be decomposed as

$$P'_{\mathbf{q},h,n}(x) = (1-q_1)\gamma^2\, P'_1(x) - \sum_{k=2}^{d} q_k\gamma^{2k}\, P'_k(x)\,, \tag{II.29}$$

where P_k is the polynomial without constant term determined by

$$P_k\left(\frac{1}{x}\right) = \frac{1}{x^{2k}}\left(\frac{1+x}{1-x}\right)^b + O(1) \tag{II.30}$$

It is not hard to see that the coefficients of P_k are polynomials of b. Therefore $P_{\mathbf{q},h,n}$ and $\mathfrak{g}(\mathbf{q},h,n)$ are continuous functions of $(\mathbf{q},h,n) \in \mathbb{D}$. For example, we deduce from $x^{-2}\left(\frac{1+x}{1-x}\right)^b = x^{-2} + 2b\,x^{-1} + O(1)$ that $P_1(x) = x^2 + 2bx$. Therefore $P'_1(-1) = -2(1-b) < 0$. Then it follows from (II.28) and (II.29) that

Lemma II.12. $\mathfrak{g}(\mathbf{0},h,n) > 0$ *for all $h > 0$, $n \in (0,2)$.*

Similarly to Lemma II.C, physically this means that a fully-packed model cannot be non-generic critical and dilute.

As we will see in Lemma II.D, the phase of an admissible triple $(\mathbf{q},h,n)$ is determined by the leading asymptotics of $\rho_{\mathbf{q},h,n}(x)$ when $x \to 1^-$. From (II.27), it is clear that the leading asymptotics of $\rho^{(\gamma)}_{\mathbf{q},h,n}(x)$ when $x \to 1^-$ is of order $(1-x)^{1-b}$ if $P'_{\mathbf{q},h,n}(-1) \neq 0$, and is of order $(1-x)^{1+b}$ if $P'_{\mathbf{q},h,n}(-1) = 0$ and $P'_{\mathbf{q},h,n}(1) \neq 0$. The following lemma asserts that these are the only cases (except for a trivial case) for non-negative weight sequence $\mathbf{q}$. The proof is purely algebraic and is left to the end of Section 4.

Lemma II.13 (There are only two non-generic critical phases)**.** *For all $(\mathbf{q},h,n) \in \mathbb{D}$, the values $P'_{\mathbf{q},h,n}(1)$ and $P'_{\mathbf{q},h,n}(-1)$ both vanish only when $\mathbf{q} = \boldsymbol{\delta}_1$.*

Remark. When $\mathbf{q} = \boldsymbol{\delta}_1$, each digon (i.e. face of degree two) is given a weight 1. Since one can replace an edge by arbitrarily many digons without changing the perimeter of a map, this implies that the total weight of bipartite maps in $\mathcal{M}_p$ is infinite. Thus the triple $(\mathbf{q}, h, n)$ is never admissible when $\mathbf{q} = \boldsymbol{\delta}_1$.

Now we complete the characterization of the phase diagram following the same scheme as in the sub- or generic critical case. Consider the set

$$\mathcal{B} = \left\{(\mathbf{q}, h, n, \gamma) \in \partial\mathcal{D} \,\middle|\, \mathfrak{g}(\mathbf{q}, h, n) > 0\right\}$$

We denote by $\overline{\mathcal{B}}$ the closure of $\mathcal{B}$ in $\partial\mathcal{D}$. Thanks to the positivity of $\mathfrak{g}(\mathbf{0}, h, n)$, we can use the exact same arguments as in the previous section to show that $\mathcal{B}$ is connected, and

$$\overline{\mathcal{B}} = \left\{(\mathbf{q}, h, n, \gamma) \in \partial\mathcal{D} \,\middle|\, \mathfrak{g}(\mathbf{q}, h, n) \geq 0\right\}.$$

Lemma II.14 (Positivity bootstrap: $\gamma = h^{-1/2}$)**.** *$\rho^{(\gamma)}_{\mathbf{q},h,n} \geq 0$ for all $(\mathbf{q}, h, n, \gamma) \in \overline{\mathcal{B}}$.*

Proof. As in the proof of Lemma II.10, since $\mathcal{B}$ is connected, it suffices to show that $\mathcal{B}_+ = \left\{(\mathbf{q}, h, n, \gamma) \in \mathcal{B} \,\middle|\, \rho^{(\gamma)}_{\mathbf{q},h,n}(x) \geq 0 \text{ for all } x \in [-1, 1]\right\}$ is non-empty and both closed and open in $\mathcal{B}$. By Lemma II.C and II.12, the quadruple $(\mathbf{0}, h, n, h^{-1/2})$ is both in $\overline{\mathcal{A}}$ and $\mathcal{B}$ for all $h > 0$ and $n \in (0, 2)$. Then Lemma II.10 implies that it is also in $\mathcal{B}_+$. Thus $\mathcal{B}_+ \neq \varnothing$.

As in Lemma II.10, $\mathcal{B}_+$ is closed in $\mathcal{B}$ thanks to the continuity of $(\mathbf{q}, h, n, \gamma) \mapsto \rho^{(\gamma)}_{\mathbf{q},h,n}(x)$ for each fixed x. To prove that $\mathcal{B}_+$ is also open, let us consider

$$\check{\rho}^{(\gamma)}_{\mathbf{q},h,n}(x) := \frac{1}{(1 - x^2)^{1-b}} \rho^{(\gamma)}_{\mathbf{q},h,n}(x)$$

for $(\mathbf{q}, h, n, \gamma) \in \partial\mathcal{D}$. This function is well-defined and continuous on $[-1, 1]$. Since $1 - x^2$ is bounded away from zero on $[-1/2, 1/2]$, Corollary II.7(ii) implies that $(\mathbf{q}, h, n, \gamma) \mapsto \check{\rho}^{(\gamma)}_{\mathbf{q},h,n}$ is continuous for the uniform norm for functions on $[-1/2, 1/2]$. On the other hand, it is not hard to see from the explicit expression (II.25) of $\rho^{(\gamma)}_{\mathbf{q},h,n}$ that $(\mathbf{q}, h, n, \gamma) \mapsto \check{\rho}^{(\gamma)}_{\mathbf{q},h,n}$ is also continuous for the uniform norm for functions on $[-1, -1/2]$ and $[1/2, 1]$. We conclude that $(\mathbf{q}, h, n, \gamma) \mapsto \check{\rho}^{(\gamma)}_{\mathbf{q},h,n}$ is continuous for the uniform norm for functions on $[-1, 1]$. Then the same argument as in Lemma II.10 shows that $\mathcal{B}_+$ is open in $\mathcal{B}$. □

3.4 Proof of Proposition II.2

Let us recapitulate the relations between the sets of parameters that we have seen so far. To keep the notation simple, we will write, for example, $\{(\mathbf{q}, h, n, \gamma) \in \mathcal{D} \,|\, \mathfrak{h}(\mathbf{q}, h, n, \gamma) = 1\}$ as $\{\mathfrak{h} = 1\}$. In other words, the sets considered are subsets of $\mathcal{D}$. Moreover, when the defining condition of a set involves the function $\mathfrak{f}$ (resp. $\mathfrak{g}$), it is implicitly a subset of the domain of definition $\mathring{\mathcal{D}}$ (resp. $\partial\mathcal{D}$)[5].

First, the definition of $\mathfrak{f}$ and $\mathfrak{g}$ trivially implies

$$\{\rho \geq 0\} \;\subseteq\; \{\mathfrak{f} \geq 0\} \sqcup \{\mathfrak{g} \geq 0\} \tag{II.31}$$

[5]Although the limit which defines $\mathfrak{f}$ exists and is zero on $\partial\mathcal{D}$, we consider $\mathfrak{f}$ to be defined only on $\mathring{\mathcal{D}}$.

where $\sqcup$ represents the disjoint union. Using the linearity of $\mathfrak{f}$ and $\mathfrak{g}$ with respect to the weight sequence $\mathbf{q}$ and their positivity when $\mathbf{q}=\mathbf{0}$ (Lemma II.C and II.12), we have shown that

$$\overline{\mathcal{A}} \cap \mathring{\mathcal{D}} \;=\; \{\mathfrak{f} \geq 0\} \qquad \text{and} \qquad \overline{\mathcal{B}} \;=\; \{\mathfrak{g} \geq 0\}$$

And finally the positivity bootstrap (Lemma II.10 and II.14) give

$$\overline{\mathcal{A}} \cup \overline{\mathcal{B}} \;\subseteq\; \{\rho \geq 0\}$$

The last three displays combine to $\overline{\mathcal{A}} \cup \overline{\mathcal{B}} \subseteq \{\rho \geq 0\} \subseteq (\overline{\mathcal{A}} \cap \mathring{\mathcal{D}}) \sqcup \overline{\mathcal{B}}$, which implies that the inclusion (II.31) must be an equality. By Proposition II.8, a triple $(\mathbf{q}, h, n) \in \mathbb{D}$ is admissible if and only if there is some γ such that $(\mathbf{q}, h, n, \gamma) \in \{\rho \geq 0\} \cap \{\mathfrak{h} = 1\}$. Then it follows from the decomposition $\{\rho \geq 0\} = \{\mathfrak{f} > 0\} \sqcup \{\mathfrak{f} = 0\} \sqcup \{\mathfrak{g} > 0\} \sqcup \{\mathfrak{g} = 0\}$ that the four conditions in Proposition II.2 indeed describe a partition of the set of admissible parameters.

On $\{\mathfrak{g} > 0\}$ and $\{\mathfrak{g} = 0\}$, we have seen above Lemma II.13 that when $x \to 1^-$, the spectral density $\rho^{(\gamma)}_{\mathbf{q},h,n}(x)$ is respectively of order $(1-x)^{1-b}$ and $(1-x)^{1+b}$ respectively. On $\{\mathfrak{f} > 0\}$ and $\{\mathfrak{f} = 0\}$, since $\tau = \gamma^2 h < 1$, Corollary II.7(ii) ensures that $\tilde{\rho}^{(\gamma)}_{\mathbf{q},h,n}(x) = (1-x^2)^{-1/2} \rho^{(\gamma)}_{\mathbf{q},h,n}(x)$ is analytic at $x = 1$. Therefore $\rho^{(\gamma)}_{\mathbf{q},h,n}(x)$ is of order $(1-x)^{1/2}$ when $\mathfrak{f}(\mathbf{q}, h, n, \gamma) = \tilde{\rho}^{(\gamma)}_{\mathbf{q},h,n}(1) > 0$, and of order $O((1-x)^{3/2})$ when $\mathfrak{f} = 0$. Moreover, it is clear from (II.22) that the derivative of $\tilde{\rho}^{(\gamma)}_{\mathbf{q},h,n}$ at $x = 1$ is strictly positive. So $\rho^{(\gamma)}_{\mathbf{q},h,n}(x)$ is exactly of order $(1-x)^{3/2}$ when $\mathfrak{f} = 0$. To summarize, for all $(\mathbf{q}, h, n, \gamma) \in \{\mathfrak{f} \geq 0\} \sqcup \{\mathfrak{g} \geq 0\}$, the spectral density has an asymptotics of the form

$$\rho^{(\gamma)}_{\mathbf{q},h,n}(x) \underset{x \to 1^-}{\sim} C\,(1-x)^{\beta} \tag{II.32}$$

with a constant $C > 0$ depends on $(\mathbf{q}, h, n, \gamma)$, and

$$\beta = \begin{cases} 1/2 & \text{if} \quad (\mathbf{q}, h, n, \gamma) \in \{\mathfrak{f} > 0\}, \\ 1-b & \text{if} \quad (\mathbf{q}, h, n, \gamma) \in \{\mathfrak{g} > 0\}, \\ 1+b & \text{if} \quad (\mathbf{q}, h, n, \gamma) \in \{\mathfrak{g} = 0\}, \\ 3/2 & \text{if} \quad (\mathbf{q}, h, n, \gamma) \in \{\mathfrak{f} = 0\}. \end{cases}$$

The asymptotics of the coefficients $F^{(\gamma)}_p(\mathbf{q}, h, n) := [x^{-2p}] \mathcal{W}^{(\gamma)}_{\mathbf{q},h,n}(x)$ can be deduced using the following lemma, which is a simple application of Cauchy's integral formula and Laplace's method. Its proof is left to the reader.

Lemma II.D. *We have $F^{(\gamma)}_p(\mathbf{q}, h, n) = \gamma^{2p} \int_{-1}^{1} x^{2p} \rho^{(\gamma)}_{\mathbf{q},h,n}(x) \mathrm{d}x$. Consequently, if $\rho^{(\gamma)}_{\mathbf{q},h,n}$ satisfies (II.32), then $F^{(\gamma)}_p(\mathbf{q}, h, n) \sim C'\,\gamma^{2p}\,p^{-(\alpha+1/2)}$ for $\alpha = \beta + 1/2$.*

This shows that the four conditions in Proposition II.2 indeed implies that $F_p(\mathbf{q}, h, n) \sim C\,\gamma^{2p}\,p^{-(\alpha+1/2)}$ with the value of α given in Theorem II.1 as our working definition of the phases. This completes the proof of Proposition II.2 (and proves Theorem II.1 too).

4 Proofs of technical lemmas

4.1 Integral equation for the spectral density (Lemma II.6)

Let $\mathcal{C}_0$ be the circle of radius $h^{-1/2}$ oriented anti-clockwise. Recall that we consider the determination of square root such that $\mathrm{Re}(\sqrt{y}) > 0$ for all $y \in \mathbb{C} \setminus (-\infty, 0]$. Then we have

$$y\sqrt{1-\frac{\gamma^2}{y^2}} \;=\; i\,\mathrm{sgn}(\mathrm{Im}\, y)\sqrt{\gamma^2-y^2} \tag{II.33}$$

whenever $y \in \mathbb{C}\setminus\mathbb{R}$. First we show that (II.4) implies the following equation for all $x \in \mathbb{C}\setminus\mathbb{R}$.

$$-2\,\mathcal{W}(x) = -nJ_0(x) + \sum_{k=1}^{\infty}(q_k - \delta_{k,1})J_k(x) + \frac{n}{2\pi i}\oint_{\mathcal{C}_0} K(x,y)\,\mathcal{W}(y)\mathrm{d}y \tag{II.34}$$

where $J_k(x) = \frac{x^2}{\pi}\sqrt{1-\frac{\gamma^2}{x^2}}\int_{-\gamma}^{\gamma}\frac{y^{2k}}{y^2-x^2}\frac{\mathrm{d}y}{\sqrt{\gamma^2-y^2}}$ and $K(x,y) = \frac{h^2 y}{1-h^2x^2y^2}\frac{x^2\sqrt{1-\gamma^2/x^2}}{\sqrt{1-\gamma^2h^2y^2}}$.

We start by expanding the definition of $K(x,y)$ and making the change of variable $y \to \frac{1}{hy}$ in the integral on the right hand side. This gives

$$n\oint_{\mathcal{C}_0} K(x,y)\,\mathcal{W}(y)\mathrm{d}y \;=\; n\,x^2\sqrt{1-\frac{\gamma^2}{x^2}}\oint_{\mathcal{C}_0}\frac{1}{y^2-x^2}\frac{\mathcal{W}(\frac{1}{hy})\,\mathrm{d}y}{y\sqrt{1-\frac{\gamma^2}{y^2}}}\,.$$

The function $y \mapsto \frac{1}{y^2-x^2}\frac{\mathcal{W}(1/(hy))}{y\sqrt{1-\gamma^2/y^2}}$ is meromorphic on $\mathbb{C}\setminus\left\{y\in\mathbb{R} :\ |y|\leq\gamma \text{ or } |y|\geq\frac{1}{h\gamma}\right\}$ and, thanks to the parity of $\mathcal{W}$, it has two simple poles of opposite residues at $y = \pm x$. Therefore we can deform $\mathcal{C}_0$ to the cut $[-\gamma,\gamma] \pm i0$ and use (II.33) and (II.4) to obtain

$$\begin{aligned}
& n\oint_{\mathcal{C}_0} K(x,y)\mathcal{W}(y)\mathrm{d}y \\
&= n\,x^2\sqrt{1-\frac{\gamma^2}{x^2}}\int_{-\gamma}^{\gamma}\frac{1}{y^2-x^2}\frac{2i\,\mathcal{W}(\frac{1}{hy})\,\mathrm{d}y}{\sqrt{\gamma^2-y^2}} \\
&= x^2\sqrt{1-\frac{\gamma^2}{x^2}}\int_{-\gamma}^{\gamma}\frac{1}{y^2-x^2}\frac{2i\,\mathrm{d}y}{\sqrt{\gamma^2-y^2}}\Big(n - \sum_{k=1}^{\infty}(q_k-\delta_{k,1})y^{2k} - \mathcal{W}(y-i0) - \mathcal{W}(y+i0)\Big) \\
&= 2\pi i\left(nJ_0(x) - \sum_{k=1}^{\infty}(q_k-\delta_{k,1})J_k(x) - \frac{x^2}{\pi}\sqrt{1-\frac{\gamma^2}{x^2}}\,\mathcal{I}(x)\right)\,.
\end{aligned} \tag{II.35}$$

where $\mathcal{I}(x) := \int_{-\gamma}^{\gamma}\frac{\mathcal{W}(y-i0)+\mathcal{W}(y+i0)}{y^2-x^2}\frac{\mathrm{d}y}{\sqrt{\gamma^2-y^2}}$ can be viewed as the integral of $F(y) = \frac{1}{y^2-x^2}\frac{\mathcal{W}(y)}{\sqrt{\gamma^2-y^2}}$ on the union of $[-\gamma,\gamma]-i0$ and $[-\gamma,\gamma]+i0$. Since F is a meromorphic function on $\mathbb{C}\setminus\mathbb{R}$ with two simple poles at $\pm x$, we can make the deformation of the integration contour in Figure II.5 to obtain

$$\mathcal{I}(x) \;=\; \left(\int_{\mathcal{C}_+}+\int_{\mathcal{C}_-}\right)F(y)\,\mathrm{d}y + 2\pi i\,\mathrm{sgn}(\mathrm{Im}\,x)\left(\operatorname*{Res}_{y\to x} - \operatorname*{Res}_{y\to -x}\right)F(y)\,.$$

$\sqrt{\gamma^2-y^2}$ changes sign when y crosses the real axis at a point $|y| > \gamma$. Therefore for all

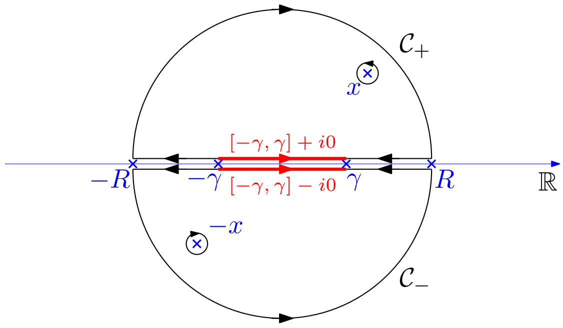

Figure II.5 – *Deformation of the contour of integration of the function* $F(y) = \frac{1}{y^2-x^2}\frac{\mathcal{W}(y)}{\sqrt{\gamma^2-y^2}}$.

$y \in \mathbb{R}\setminus[-\gamma,\gamma]$, we have $F(y+i0)+F(y-i0)=0$ and thus the integrals on the straight line parts of $\mathcal{C}_+$ and $\mathcal{C}_-$ cancel each other. Then from $F(y)=O(|y|^{-2})$ as $|y|\to\infty$ we deduce that $\lim_{R\to\infty}\left(\int_{\mathcal{C}_+}+\int_{\mathcal{C}_-}\right)F(y)\mathrm{d}y = 0$. As $\mathcal{W}$ is even, we have $-\operatorname{Res}_{y\to -x}F(y) = \operatorname{Res}_{y\to x}F(y) = \frac{1}{2x}\frac{\mathcal{W}(x)}{\sqrt{\gamma^2-x^2}}$ and therefore

$$\mathcal{I}(x) = 2\pi i\,\mathrm{sgn}(\mathrm{Im}\,x)\,\frac{1}{x}\frac{\mathcal{W}(x)}{\sqrt{\gamma^2-x^2}} = -\frac{2\pi\,\mathcal{W}(x)}{x^2\sqrt{1-\frac{\gamma^2}{x^2}}}\,.$$

Combining the above equality with (II.35), we obtain (II.34).

Now let us come back to Lemma II.6. It is easy to see that I_k is an even polynomial of degree $2k-2$ with positive coefficients:

$$I_k(x) \;=\; \frac{1}{\pi}\int_{-1}^{1}\frac{y^{2k}-x^{2k}}{y^2-x^2}\frac{\mathrm{d}y}{\sqrt{1-y^2}} \;=\; \sum_{j=0}^{k-1}\frac{x^{2j}}{\pi}\int_{-1}^{1}\frac{y^{2(k-1-j)}}{\sqrt{1-y^2}}\mathrm{d}y\,.$$

The definitions of I_k and J_k readily imply that $\gamma^{-2k}J_k(\gamma x)-x^{2k}J_0(\gamma x) = x^2\sqrt{1-\frac{1}{x^2}}I_k(x)$. It is a simple exercise that $J_0(x)=-1$. Therefore the discontinuity of J_k and $x\mapsto K(\gamma x,y)$ both come exclusively from the factor $x^2\sqrt{1-\frac{1}{x^2}}$. By (II.33) we have for $x\in(-1,1)$,

$$\frac{1}{2\pi i x}\left(x^2\sqrt{1-\tfrac{1}{(x-i0)^2}}-x^2\sqrt{1-\tfrac{1}{(x+i0)^2}}\right) \;=\; -\frac{1}{\pi}\sqrt{1-x^2}\,.$$

It follows that

$$\frac{J_k(\gamma x-i0)-J_k(\gamma x+i0)}{2\pi i x} \;=\; -\frac{1}{\pi}\gamma^{2k}\sqrt{1-x^2}\,I_k(x)\,,$$

and

$$\frac{K(\gamma x-i0,\gamma y)-K(\gamma x+i0,\gamma y)}{2\pi i x} \;=\; -\frac{1}{\pi}\frac{\tau^2 y}{1-\tau^2x^2y^2}\frac{\sqrt{1-x^2}}{\sqrt{1-\tau^2y^2}}\cdot\frac{1}{\gamma}\,,$$

where $\tau=\gamma^2 h$. Notice that $I_0=0$ and $I_1=1$. Taking the spectral density on both sides of (II.34) gives

$$-\frac{2\pi\,\rho(x)}{\sqrt{1-x^2}} \;=\; (q_1-1)\gamma^2+\sum_{k=2}^{\infty}q_k\gamma^{2k}I_k(x)+\frac{n}{2\pi i}\int_{\gamma^{-1}\mathcal{C}_0}\frac{\tau^2 y}{1-\tau^2x^2y^2}\frac{\mathcal{W}(\gamma y)\,\mathrm{d}y}{\sqrt{1-\tau^2y^2}}\,.$$

Deform the contour $\gamma^{-1}\mathcal{C}_0$ to the cut $[-1,1]\pm i0$ in the above display and we obtain (II.22).

4.2 Resolvent in non-generic critical phase (Lemma II.11)

We fix a set of parameter $(\mathbf{q}, h, n, \gamma)$ and drop them from the notation. Recall the equation of the resolvent:

$$\begin{cases} \mathcal{W} \text{ is an even holomorphic function on } \overline{S}_\gamma \text{ such that for all } x \in (-\gamma, \gamma), \\ \qquad \mathcal{W}(x - i0) + \mathcal{W}(x + i0) + n\mathcal{W}\Big(\dfrac{1}{hx}\Big) = n + x^2 - \displaystyle\sum_{k=1}^{d} q_k x^{2k}\,. \end{cases} \tag{II.36}$$

By linearity, we write the solution in the form of $\mathcal{W} = \mathcal{W}_{\mathtt{part}} + \mathcal{W}_{\mathtt{hom}}$, where $\mathcal{W}_{\mathtt{part}}$ is meromorphic on $\mathbb{C}$ and satisfies the above equation, and $\mathcal{W}_{\mathtt{hom}}$ is meromorphic on $\overline{S}_\gamma$ and satisfies the homogenous equation

$$\mathcal{W}_{\mathtt{hom}}(x - i0) + \mathcal{W}_{\mathtt{hom}}(x + i0) + n\mathcal{W}_{\mathtt{hom}}\Big(\frac{1}{hx}\Big) = 0 \qquad \text{for all } x \in (-\gamma, \gamma)\,. \tag{II.37}$$

It is not hard to see that $\mathcal{W}_{\mathtt{part}}$ can be found among the even Laurent polynomials. Write $\mathcal{W}_{\mathtt{part}}(x) = c + \sum_{k=1}^{d}\big(a_k x^{2k} + \frac{b_k}{(hx)^{2k}}\big)$, then we have $(2+n)c = n$ and for all $k = 1, \dots, d$,

$$2\Big(a_k x^{2k} + \frac{b_k}{(hx)^{2k}}\Big) + n\Big(\frac{a_k}{(hx)^{2k}} + b_k x^{2k}\Big) = (\delta_{k,1} - q_k)x^{2k}$$

so that

$$\begin{bmatrix} 2 & n \\ n & 2 \end{bmatrix} \begin{bmatrix} a_k \\ b_k \end{bmatrix} = \begin{bmatrix} \delta_{k,1} - q_k \\ 0 \end{bmatrix}.$$

Inverting the matrix, we get $a_k = \frac{2}{4-n^2}(\delta_{k,1} - q_k)$, $b_k = \frac{-n}{4-n^2}(\delta_{k,1} - q_k)$ and $c = \frac{n(2-n)}{4-n^2}$.

In the non-generic critical case, $\gamma = h^{-1/2}$, so the particular solution can be written as

$$\mathcal{W}_{\mathtt{part}}(\gamma x) = \frac{1}{4-n^2}\Big(-2Q(x) + nQ\Big(\frac{1}{x}\Big) + n(2-n)\Big)$$

where $Q(x) = \sum_{k=1}^{d}(q_k - \delta_{k,1})\gamma^{2k}x^{2k}$. Following [BBG12c], we look for $\mathcal{W}_{\mathtt{hom}}$ in the form of

$$\mathcal{W}_{\mathtt{hom}}(\gamma x) = \frac{1}{4-n^2}\bigg(L(x)\Big(\frac{x-1}{x+1}\Big)^b + L(-x)\Big(\frac{x+1}{x-1}\Big)^b\bigg), \tag{II.38}$$

where $L(x)$ is a Laurent polynomial. Notice that $x \mapsto \big(\frac{x-1}{x+1}\big)^b$ is a holomorphic function on S_γ taking real values on $\mathbb{R} \setminus [-\gamma, \gamma]$. By looking separately at the norm and the argument, it is not hard to see that for all $x \in (-\gamma, \gamma)$,

$$\Big(\frac{x + i0 - 1}{x + i0 + 1}\Big)^b = \Big(\frac{1-x}{1+x}\Big)^b e^{i\pi b} \qquad \text{and} \qquad \Big(\frac{x - i0 - 1}{x - i0 + 1}\Big)^b = \Big(\frac{1-x}{1+x}\Big)^b e^{-i\pi b}\,. \tag{II.39}$$

Moreover, $\big(\frac{x+1}{x-1}\big)^b = \big(\frac{(-x)-1}{(-x)+1}\big)^b$, so

$$\Big(\frac{x + i0 + 1}{x + i0 - 1}\Big)^b = \Big(\frac{1+x}{1-x}\Big)^b e^{-i\pi b} \qquad \text{and} \qquad \Big(\frac{x - i0 + 1}{x - i0 - 1}\Big)^b = \Big(\frac{1+x}{1-x}\Big)^b e^{i\pi b}\,. \tag{II.40}$$

Combine (II.39) and (II.40) with $\left(\frac{x^{-1}\pm 1}{x^{-1}\mp 1}\right)^b = \left(\frac{1\pm x}{1\mp x}\right)^b$, it follows that (II.37) is equivalent to

$$\Big(2\cos(\pi b)L(x) + nL(x^{-1})\Big)\left(\frac{1-x}{1+x}\right)^b + \Big(2\cos(\pi b)L(-x) + nL(-x^{-1})\Big)\left(\frac{1+x}{1-x}\right)^b = 0$$

We see that (II.38) indeed gives a solution of (II.37) provided that $2\cos(\pi b) = n$ and $L(x) + L(x^{-1}) = 0$.[6] The second condition is equivalent to saying that the Laurent polynomial L is of the form $L(x) = P(x) - P(x^{-1})$, where P is a polynomial without constant term.

It remains to choose P so that $\mathcal{W} = \mathcal{W}_{\mathtt{part}} + \mathcal{W}_{\mathtt{hom}}$ is holomorphic on $\overline{S}_\gamma$. In other words, the poles of $\mathcal{W}_{\mathtt{part}}$ and $\mathcal{W}_{\mathtt{hom}}$ at $x = 0$ and $x = \infty$ cancel out. Since $\mathcal{W}$ satisfies (II.4), it suffices to check that the poles at $x = 0$ cancel out. This amounts to that

$$\begin{aligned}&\mathcal{W}_{\mathtt{part}}(\gamma x) + \mathcal{W}_{\mathtt{hom}}(\gamma x + i0)\\ &= \frac{1}{4-n^2}\left(n\,Q\Big(\frac{1}{x}\Big) - P\Big(\frac{1}{x}\Big)\left(\frac{1-x}{1+x}\right)^b e^{i\pi b} - P\Big(-\frac{1}{x}\Big)\left(\frac{1+x}{1-x}\right)^b e^{-i\pi b}\right) + O(1)\end{aligned}$$

is bounded as $x \to 0$. That is, $n\,Q(x) = R(x)e^{i\pi b} + R(-x)e^{-i\pi b}$ for a polynomial R such that

$$P\Big(\frac{1}{x}\Big)\left(\frac{1-x}{1+x}\right)^b = R\Big(\frac{1}{x}\Big) + O(1)\,.$$

Since Q is even, R must be even too. It follows that $R(x) = Q(x)$, and therefore

$$P\Big(\frac{1}{x}\Big) = Q\Big(\frac{1}{x}\Big)\left(\frac{1+x}{1-x}\right)^b + O(1) \qquad \text{as } x \to 0\,.$$

This is the expression of $P_{\mathbf{q},h,n}$ given in (II.26).

To compute the spectral density, notice that $\mathcal{W}_{\mathtt{part}}$ has no discontinuity on $(-\gamma, \gamma)$ (except the pole at 0). Thus $\rho(x) = \frac{\mathcal{W}_{\mathtt{hom}}(\gamma x - i0) - \mathcal{W}_{\mathtt{hom}}(\gamma x + i0)}{2\pi i x}$. Use again (II.39) and (II.40), we get

$$\begin{aligned}\rho(x) &= \frac{1}{2\pi i x}\frac{e^{i\pi b} - e^{-i\pi b}}{4-n^2}\left(L(x)\left(\frac{1-x}{1+x}\right)^b - L(-x)\left(\frac{1+x}{1-x}\right)^b\right)\\ &= \frac{1}{2\pi x}\frac{2\sin(\pi b)}{4-n^2}\left(L(x)\left(\frac{1-x}{1+x}\right)^b - L(-x)\left(\frac{1+x}{1-x}\right)^b\right)\end{aligned}$$

which is the same as (II.25) because $\sin(\pi b) = \sqrt{1 - n^2/4}$.

4.3 There are only two non-generic critical phases (Lemma II.13)

We have seen that $P_1(x) = x^2 + 2bx$. Thus $P_1'(-1) = -2(1-b)$ and $P_1'(1) = 2(1+b)$ are both non-zero. Then the decomposition (II.29) of $P_{\mathbf{q},h,n}$ shows that $P'_{\mathbf{q},h,n}(1) = P'_{\mathbf{q},h,n}(-1) = 0$ is equivalent to

$$(1-q_1)\gamma^2 = \sum_{k=2}^{d} q_k \gamma^{2k}\frac{P_k'(1)}{P_1'(1)} = \sum_{k=2}^{d} q_k\gamma^{2k}\frac{P_k'(-1)}{P_1'(-1)}\,.$$

[6] The other obvious choice $2\cos(\pi b) = -n$ and $L(x) = L(x^{-1})$ will merely lead to another parametrization of the same solution.

which implies

$$\sum_{k=2}^{d} q_k \gamma^{2k} \left(\frac{P_k'(1)}{P_1'(1)} - \frac{P_k'(-1)}{P_1'(-1)} \right) = 0\,. \tag{II.41}$$

Since $q_k \geq 0$, to prove Lemma II.13 it suffices to show that the coefficients of $q_k \gamma^{2k}$ in the above sum are all positive.

Let H_k be the polynomial such that $P_k'(1) = H_k(b)$. From the definition (II.30) of P_k it is easy to see that $P_k'(-1) = -H_k(-b)$. Therefore the coefficients in (II.41) can be written as $\frac{H_k(b)}{2(1+b)} - \frac{H_k(-b)}{2(1-b)}$. They will be all positive provided the following lemma is true for $k \geq 2$.

Lemma II.15. *H_k is an odd polynomial with positive coefficients with respect to the variable $1+b$.*

Proof. By the definition (II.30) of P_k,

$$\begin{aligned} P_k\left(\frac{1}{x}\right) &= \frac{1}{x^{2k}} \frac{1-x}{1+x} \exp\left((1+b) \log\left(\frac{1+x}{1-x}\right) \right) + O(1) \\ &= \frac{1}{x^{2k}} \frac{1-x}{1+x} \sum_{m=0}^{2k-1} \frac{(1+b)^m}{m!} \left(\log\left(\frac{1+x}{1-x}\right)\right)^m + O(1)\,, \\ \text{so} \qquad -\frac{1}{x^{2k}} P_k'\left(\frac{1}{x}\right) &= \sum_{m=0}^{2k-1} \frac{B^m}{m!} \frac{\mathrm{d}}{\mathrm{d}x} \left[\frac{1}{x^{2k}} \frac{1-x}{1+x} \left(\log\left(\frac{1+x}{1-x}\right)\right)^m + O(1) \right]\,. \end{aligned}$$

Write $H_k(b) = \sum_m \frac{h_{m,k}}{m!}(1+b)^m$ and $\left(\log\left(\frac{1+x}{1-x}\right)\right)^m = \sum_n a_{n,m} x^n$, then the last line implies

$$h_{m,k} = \sum_{l+n<2k} (2k-n-l)\, c_l\, a_{n,m}$$

where $(c_l)_{l\geq 0}$ is defined by $\frac{1-x}{1+x} = \sum_l c_l x^l$. Or explicitly, $c_0 = 1$ and $c_l = 2(-1)^l$ for all $l \geq 1$. Using the fact that $\sum_{l=0}^{K} (K-l) c_l = 0$ if K is even and 1 if K is odd, we get

$$h_{m,k} = \sum_{n=0}^{2k-1} \left(\sum_{l=0}^{2k-n} (2k-n-l) c_l \right) a_{n,m} = \sum_{n=1}^{k} a_{2n-1,m}$$

Since $\log\left(\frac{1+x}{1-x}\right) = \sum_n \frac{x^{2n+1}}{2n+1}$, the coefficient $a_{2n-1,m}$ is always non-negative, and vanishes if and only if m is even. So $h_{m,k}$ is also non-negative, and vanishes if and only if m is even. $\square$

Chapter III

Perimeter cascade in a critical $O(n)$-Boltzmann quadrangulation

This Chapter is adapted from joint work with Nicolas Curien and Pascal Maillard [CCM17] (preprint).

1 Introduction

This chapter builds on the previous one and concentrates on the special case of critical Boltzmann quadrangulations decorated by an $O(n)$ loop model. We have seen that the $O(n)$-decorated random quadrangulation has a non-generic critical phase where the exponent α in the asymptotic (III.3) of its partition function takes a value strictly between 1 and 2, the two values that correspond to a subcritical and critical non-decorated Boltzmann map, respectively. In this chapter we analyze in detail the nested sequence of the perimeters of the loops and show that it converges towards an explicit multiplicative cascade related to a

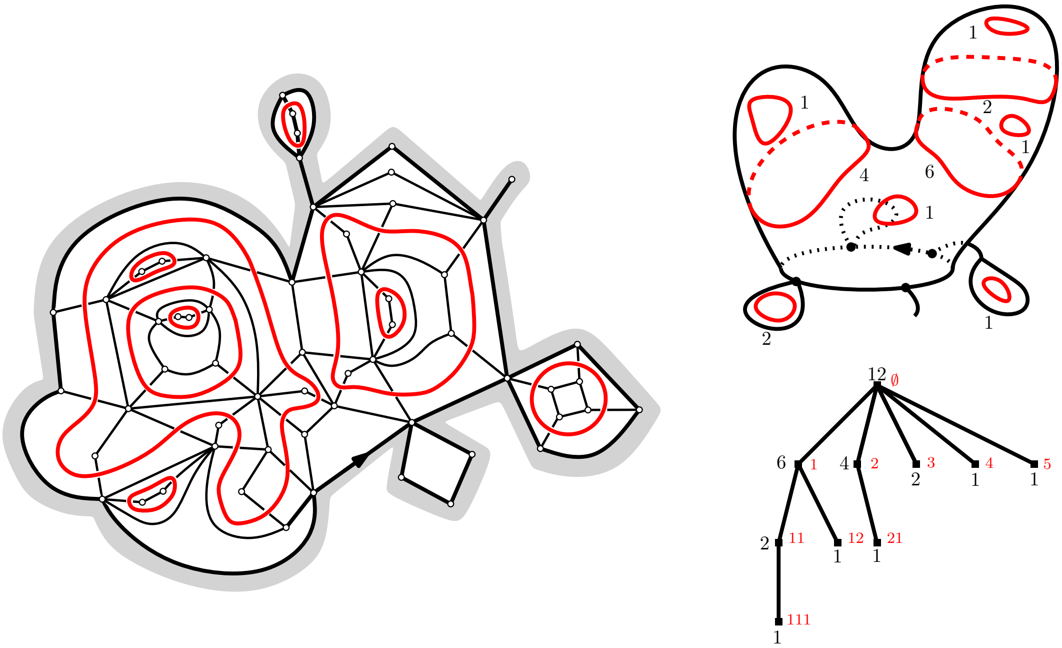

Figure III.1 – *Left: a loop-decorated quadrangulation with a boundary of perimeter* 24*. Top right: the topological representation of the quadrangulation as a "cactus" which highlights the nesting of the loops. Bottom right: the nesting tree labeled by the half-perimeters of the loops.*

stable Lévy process with index α. To properly state our results, let us first recall the setup and main result of Chapter II.

Definition of the model. We work with the specification of the model in Chapter II when $q_k = g\delta_{k,2}$. More precisely, recall that all maps are assumed *planar* and *rooted* by a distinguished *corner*. This corner identifies a distinguished *external face*, whose degree is called the *perimeter* of the map. A *quadrangulation with a boundary* is a map $\mathfrak{q}$ whose internal faces all have degree four. A *(rigid) loop configuration* on $\mathfrak{q}$ is a set $\boldsymbol{\ell} = \{\ell_1, \ell_2, \ldots\}$ of disjoint undirected simple closed paths in the dual of $\mathfrak{q}$ which do not visit the external face, and with the additional constraint that when a loop visits a face of $\mathfrak{q}$, it must cross it through opposite edges. In other words, the internal faces of $\mathfrak{q}$ can only be of the following two types

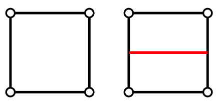,

see Figure III.1. We call the pair $(\mathfrak{q}, \boldsymbol{\ell})$ a *loop-decorated quandrangulation with a boundary*, and denote by $\mathcal{LQ}_p$ the set of all loop-decorated quadrangulations with a boundary of perimeter $2p$.

Given $n \in (0,2)$, $g \geq 0$ and $h \geq 0$, we specify the measure $w_{\mathbf{q},h,n}$ of the previous chapter to the case $q_k = g\delta_{k,2}$ so that it becomes concentrated on $\cup_{p\geq 1}\mathcal{LQ}_p$. Explicitly,

$$w_{g,h,n}(\mathfrak{q}, \boldsymbol{\ell}) = g^{|\mathfrak{q}|-|\boldsymbol{\ell}|} h^{|\boldsymbol{\ell}|} n^{\#\boldsymbol{\ell}} \tag{III.1}$$

where $|\mathfrak{q}|$ is the number of internal faces of $\mathfrak{q}$, $|\boldsymbol{\ell}|$ is the total length of the loops in $\boldsymbol{\ell}$ and $\#\boldsymbol{\ell}$ is the number of loops in $\boldsymbol{\ell}$. For example, the weight of the quadrangulation presented in Figure III.1 is $g^8h^{38}n^9$. We can normalize this measure and define a probability measure on $\mathcal{LQ}_p$ for each $p \geq 1$ by

$$\mathbb{P}^{(p)}_{g,h,n}(\cdot) = \frac{w_{g,h,n}(\cdot)}{F_p(g,h,n)} \qquad \text{where} \qquad F_p(g,h,n) = \sum_{(\mathfrak{q},\boldsymbol{\ell})\in\mathcal{LQ}_p} w_{g,h,n}(\mathfrak{q},\boldsymbol{\ell}), \tag{III.2}$$

provided that the set of parameters (g,h,n) is *admissible*, that is, $F_p(g,h,n)$ is finite (it is not hard to see that the finiteness does not depend on the value of $p \geq 1$).

As seen in the previous chapter, the set of admissible parameters can be partitioned into phases according to the value of the exponent α in the following asymptotics:

$$F_p(g,h,n) \underset{p\to\infty}{\sim} C\,\kappa^p\,p^{-\alpha-1/2}, \tag{III.3}$$

where $C > 0, \kappa > 0$, and α may take the values $\alpha = 1$ (*subcritical*), $\alpha = 2$ (*generic critical*) or

$$\alpha = \frac{3}{2} \pm \frac{1}{\pi}\arccos(n/2) \quad \in (1,2)\setminus\{3/2\} \tag{III.4}$$

(*non-generic critical*). For large p, the geometry of a random map distributed according to $\mathbb{P}^{(p)}_{g,h,n}$ depends heavily on the value of α.

In the subcritical phase, which includes the subcritical (non-decorated) Boltzmann quadrangulations (i.e. $h = 0$ and $g < g_c := 1/12$, see Section 2.4 of Chapter I), the random maps distributed according to $\mathbb{P}^{(p)}_{g,h,n}$ are tree-like for large p and are expected to converge in the scaling limit towards Aldous' CRT [Bet15b]. In the generic critical phase, which includes the critical Boltzmann quadrangulations (i.e. $h = 0$ and $g = g_c$), they are believed to converge towards the Brownian disk [BM17]. In the non-generic critical phase however, the geometry of these maps remains elusive and the only available information we have is on their *gasket* [LGM11] (see Section 2.1 for the definition). The case $\alpha = \frac{3}{2} - \frac{1}{\pi}\arccos(n/2) \in (1, \frac{3}{2})$ is called the *dense* case because in a suitable scaling limit, the loops are believed to touch themselves and each other, whereas in the *dilute* case $\alpha = \frac{3}{2} + \frac{1}{\pi}\arccos(n/2) \in (\frac{3}{2}, 2)$ they are believed to be simple and not to touch each other almost surely.

> *We assume we are given a non-generic critical set of parameters (g,h,n) with $n \in (0,2)$ and $g,h \geq 0$ so that (III.3) holds for a value of $\alpha \in (1,3/2)\cup(3/2,2)$ that is fixed in the rest of this chapter. We shall sometimes drop the implicit dependence on (g,h,n) in what follows.*

Discrete and continuous cascades. We are interested in the perimeters and the nesting structure of the loops in a random loop-decorated quadrangulation distributed according to $\mathbb{P}^{(p)}_{g,h,n}$ as $p \to \infty$. If $(\mathfrak{q},\boldsymbol{\ell})$ is a loop-decorated quadrangulation with a boundary of perimeter $2p$, we can associate with it a random labeled tree as follows. We start with the so-called Ulam tree[1]

$$\mathcal{U} = \bigcup_{k\geq 0}(\mathbb{N}^*)^k.$$

where a sequence $u = (u_1,\ldots,u_k) \in (\mathbb{N}^*)^k$ represents a vertex in the k-th generation of the tree. Its l-th child is $(u_1,\ldots,u_k,l)$. In particular $(\mathbb{N}^*)^0 = \{\varnothing\}$, where $\varnothing$ is the empty

[1] Here and throughout we use the French notation $\mathbb{N} = \{0,1,2,\ldots\}$ and $\mathbb{N}^* = \mathbb{N}\backslash\{0\}$.

sequence representing the root. If $u, v \in \mathcal{U}$ we write uv for the concatenation of u and v, and we denote by $|u|$ the length of u. We assign each loop $\ell \in \boldsymbol{\ell}$ to a vertex of $\mathcal{U}$ in the following fashion: First, the root vertex $\varnothing$ is associated with an imaginary loop of length $2p$ surrounding the boundary of $\mathfrak{q}$. Next we assign to the children $1, 2, 3, \cdots$ of $\varnothing$ the outermost loops of $(\mathfrak{q}, \boldsymbol{\ell})$—i.e. those loops which can be reached from the boundary of $\mathfrak{q}$ without crossing any other loop—ranked by decreasing perimeter (if there is a tie we break it using a deterministic rule). We then continue genealogically inside each of these loops in the most obvious way, see Figure III.1. Although $\mathcal{U}$ is an infinite (even non locally finite) tree, the set of vertices attached to a loop of $\boldsymbol{\ell}$ is a finite subtree of $\mathcal{U}$. Once this is done, we define the labeling

$$\chi : u \in \mathcal{U} \mapsto \chi(u) \in \mathbb{N}$$

which is the half-perimeter of the loop associated to u in $(\mathfrak{q}, \boldsymbol{\ell})$ or 0 if there are no such loop.

We now introduce the limiting continuous multiplicative cascade. Given a distribution ν on $(\mathbb{R}_+)^{\mathbb{N}^*}$, let $\{(\xi_i^{(u)})_{i\geq 1} : u \in \mathcal{U}\}$ be an i.i.d. family of (infinite) random vectors of law ν. The multiplicative cascade with offspring distribution ν is then the random process $(Z(u))_{u\in\mathcal{U}}$ indexed by the Ulam tree such that $Z(\varnothing) = 1$ and such that for any $u \in \mathcal{U}$ and any $i \in \mathbb{N}^*$ we have $Z(ui) = Z(u) \cdot \xi_i^{(u)}$. We will apply this to a particular law ν: Let $(\zeta_t)_{t\geq 0}$ be an α-stable Lévy process with no negative jumps started at 0; in other words for some constant $C > 0$ we have $\mathbb{E}[\exp(-\lambda\zeta_t)] = \exp(Ct\lambda^\alpha)$ for all $\lambda > 0$. Let τ denote the hitting time of -1 of this process. Notice that $\tau < \infty$ a.s. because ζ does not drift to infinity, and we have $\zeta_\tau = -1$ since ζ has no negative jumps. We write $(\boldsymbol{\Delta\zeta})_\tau^\downarrow$ for the infinite vector consisting of the sizes of the jumps of ζ before time τ, ranked in decreasing order. Then we define a probability distribution ν_α on $(\mathbb{R}_+)^{\mathbb{N}^*}$ by

$$\int \mathrm{d}\nu_\alpha(\mathbf{x}) F(\mathbf{x}) = \frac{\mathbb{E}\left[\frac{1}{\tau} F((\boldsymbol{\Delta\zeta})_\tau^\downarrow)\right]}{\mathbb{E}\left[\frac{1}{\tau}\right]}.$$

By the scaling property of stable Lévy processes, the above definition of ν_α does not depend on the constant $C > 0$ appearing in the normalization of ζ.

We also define the function $\phi_\alpha(\theta) := \mathbb{E}\left[\sum_{i\geq 1} (Z_\alpha(i))^\theta\right]$, which we call the *Biggins transform* of the multiplicative cascade Z_α after the seminal work of Biggins. We can now state our main result:

Theorem III.1 (Convergence of the perimeter cascade)**.** *Let $\chi^{(p)}$ be the random labeling obtained on the Ulam tree when the underlying loop-decorated quadrangulation is distributed according to $\mathbb{P}^{(p)}_{g,h,n}$. Then we have the following convergence in distribution*

$$\frac{1}{p}\Big(\chi^{(p)}(u)\Big)_{u\in\mathcal{U}} \xrightarrow[p\to\infty]{(d)} \Big(Z_\alpha(u)\Big)_{u\in\mathcal{U}}$$

in $\ell^\infty(\mathcal{U})$, where Z_α is the multiplicative cascade with offspring distribution ν_α. In addition, the Biggins transform of the multiplicative cascade Z_α is explicit and equals

$$\phi_\alpha(\theta) = \frac{\sin(\pi(2-\alpha))}{\sin(\pi(\theta-\alpha))} \quad \text{for } \theta \in (\alpha, \alpha+1) \quad \text{and} \quad \phi_\alpha(\theta) = \infty \text{ otherwise.}$$

Remark III.2. Here $\ell^\infty(\mathcal{U})$ is defined as usual as the set of bounded functions on the countable set $\mathcal{U}$, endowed with the supremum norm. The above convergence is stronger than the convergence of finite dimensional marginals, i.e. the weak convergence under the product topology of $\mathbb{R}^{\mathcal{U}}$. For example, finite dimensional convergence does not exclude the possibility that the laws of $p^{-1}\chi^{(p)}(u)$ and of $Z_\alpha(u)$ are significantly different for some $u = u(p)$ that escapes from any finite subset of $\mathcal{U}$ as $p \to \infty$.

Properties of the multiplicative cascade Z_α. In Section 4 we establish some interesting properties of the multiplicative cascade Z_α. First, in Section 4.1, we define the family of additive martingales, an important observable of the multiplicative cascade. We also calculate the rate function of the multiplicative cascade, i.e. the Legendre–Fenchel transform of $\log \phi_\alpha$. In Section 4.2, we study the *Malthusian martingale*

$$\sum_{|u|=n} (Z_\alpha(u))^{\min(2,2\alpha-1)} .$$

We show that it is uniformly integrable and identify the law of its limit which is found to be equal to (in the dilute phase $\alpha > 3/2$) or related to (in the dense phase $\alpha < 3/2$) an inverse Gamma law with explicit parameters. As explained there, this strongly supports the fact (and even gives a path for the proof) that the renormalized volume of a critical $O(n)$-decorated map with a boundary also converges towards this law. Finally, in Section 4.3, we establish L^p-convergence of the additive martingales, for suitable p. This ensures that the multiplicative cascade Z_α displays no pathological behavior.

We now outline the proof of Theorem III.1, which comes in three parts:

Convergence of finite dimensional marginals. We have seen in Chapter II that a loop-decorated quadrangulation $(\mathfrak{q}, \boldsymbol{\ell})$ distributed according to $\mathbb{P}^{(p)}_{g,h,n}$ can be split into its gasket—the part of $\mathfrak{q}$ outside the outer-most loops of $\boldsymbol{\ell}$—and a number of smaller loop-decorated quadrangulations which, conditionally on the gasket, are independent and follow the same type of distribution as $(\mathfrak{q}, \boldsymbol{\ell})$. This settles the Markovian branching structure of the perimeter process $\chi^{(p)}$, thus reducing the problem of convergence of its finite dimensional marginals essentially to the convergence of its first generation (Proposition III.4).

Moreover, the gasket is a bipartite Boltzmann map with a boundary where each face of degree $2k$ receives a weight $\hat{q}_k$ (which is a simple function of $F_k(g, h, n)$, see (III.6)). In the previous chapter we have computed the partition function of this random map (more precisely, the pointed version of it, see below) by transforming it into a Galton–Watson forest using (a variant of) the classical Bouttier–Di Francesco–Guitter bijection [BDFG04] and a bijection of Janson & Stefánsson [JS15]. Under our assumption, the resulting forest consists of p i.i.d. Galton-Watson trees with a critical offspring distribution in the domain of attraction of the spectrally positive α-stable distribution. In this coding, the loops of the first generation are transformed into the (large) faces of the gasket and then into the (large) jumps of the Łukasiewicz path encoding the Galton-Watson forest. The latter naturally converges to the jumps of an α-stable Lévy process, which explains the appearance of the process $(\boldsymbol{\Delta\zeta})^{\downarrow}_{\tau}$ in the definition of ν_α. The above chain of transformations is summarized in a diagram at the beginning of Section 2.

One technical issue in this program is that the Bouttier–Di Francesco–Guitter bijection works particularly well with *pointed* maps, i.e. maps with a distinguished vertex. For this reason we start by applying the bijections to the pointed gasket, and only remove the distinguished point afterwards. This amounts to biasing the pointed gasket by the inverse of its number of vertices, which in the continuous setting give rise to the bias τ^{-1} in the definition of the measure ν_α.

A formula for left-continuous random walks. As we saw in Theorem III.1, the multiplicative cascade Z_α has an explicit and rather simple Biggins transform. This formula is obtained through a new simple identity about the (biased) first moment of some additive functionals of left-continuous random walks. This identity may have further applications and so we present it here: Let S be a left-continuous random walk on $\mathbb{Z}$ started from 0, i.e. $S_n = X_1 + \cdots + X_n$, where $(X_i)_{i\geq 1}$ are i.i.d. random variables on $\{-1, 0, 1, \cdots\}$. We denote by T_p the hitting time of $-p \in \mathbb{Z}$ by S.

Theorem III.3. *Suppose that S does not drift to ∞ i.e. that $T_1 < \infty$ almost surely. Then for any positive measurable function $f : \mathbb{Z} \to \mathbb{R}$ and any $p \geq 2$ we have*

$$\mathbb{E}\left[\frac{1}{T_p - 1}\sum_{i=1}^{T_p} f(X_i)\right] = \mathbb{E}\left[f(X_1)\frac{p}{p + X_1}\right].$$

From finite dimensional to $\ell^\infty(\mathcal{U})$ convergence. We now explain how we strengthen the finite-dimensional convergence of $p^{-1}\chi^{(p)}$ towards Z_α to $\ell^\infty(\mathcal{U})$ convergence. One essentially needs that, with high probability, $p^{-1}\chi^{(p)}$ is arbitrarily small outside a finite subset of $\mathcal{U}$, uniformly in p.

We first concentrate on the first k generations of the tree $\mathcal{U}$. Using the identity in Theorem III.3, we compute $\mathbb{E}\Big[\sum_{|u|=k}\left(p^{-1}\chi^{(p)}(u)\right)^\theta\Big]$, the discrete analogue of Biggins transform, and show that it converges to the k-th power of the continuous Biggins transform given in Theorem III.1 (Lemma III.21). This yields a moment estimate on the sizes of all the loops up to generation k, which implies the ℓ^∞ convergence on the first k generations (Proposition III.20). In order to strenghten this to $\ell^\infty(\mathcal{U})$ convergence, we rely on a geometric estimate on random planar maps: if we denote by $\overline{V}(p)$ the expected volume (i.e. number of vertices) of a random loop-decorated quadrangulation under the distribution $\mathbb{P}^{(p)}_{g,h,n}$, then using the Markovian structure of the gasket decomposition it is easy to check that

$$\sum_{|u|=k}\overline{V}(\chi^{(p)}(u)) \quad \text{is a supermartingale indexed by } k \geq 0,$$

which gives a uniform control over all generations. This additional ingredient together with recent estimates on $\overline{V}(p)$ due to Budd [Bud17] are at the core of our proof of the ℓ^∞ convergence.

Related works. Understanding the geometry of planar maps decorated with a statistical physics model in one of the major goals in today's theory of random planar maps (see [She16b, GMS15, GS17, GS15, BLR17, Che17, GKMW16] for recent progresses on the geometry of general random planar maps decorated by a Fortuin-Kasteleyn model). Our interest in the nested cascades in $O(n)$ model on random quadrangulations was triggered by the recent work of Borot, Bouttier and Duplantier [BBD16]. They study (in the case of triangulations) in great detail the number of loops separating the boundary from a typical point; in our context, this roughly speaking consists in estimating the length of a typical branch of the tree coded by the cascade $(\chi^{(p)})$. Our perspective here is different since we study the full nested tree (rather than one branch) in a scaling limit point of view (rather than in the discrete setting). In Appendix A we provide more details of the relation between the two approaches. We also give an alternative explanation of the relation with the statistics of the number of loops surrounding a small Euclidean ball in a conformal loop ensemble.

This work obviously builds upon [BBG12c] where the gasket decomposition was introduced and used to study the phase diagram in Figure II.1. Our study of the gasket in the non-generic critical case also borrows a lot from [LGM11] and indeed the law ν_α can be interpreted as the sizes of large faces in what would be a "stable map with a boundary". See also [BC17] for a geometric study of the duals of the above planar maps.

It was recently shown by Gwynne and Sun [GS15] that random planar maps decorated with a Fortuin–Kasteleyn statistical mechanics model (which naturally defines an ensemble of loops) converge in the so-called peanosphere topology to the Liouville quantum sphere introduced by Duplantier, Miller and Sheffield [DMS14], together with an independent conformal loop ensemble. This topology allows in particular to measure the lengths of the loops in the "quantum metric", as well as the "quantum volume" of their interior. A well-known conjecture stipulates that the $O(n)$-decorated quadrangulations considered in this paper converge to the Liouville quantum disk with parameter $\gamma = \sqrt{\min(\kappa, 16/\kappa)}$, also introduced in [DMS14], together with an independent CLE_κ in the disk. Here, $\kappa \in (8/3, 8)$ is related to our parameter α by

$$\alpha - \frac{3}{2} = 4/\kappa - 1, \tag{III.5}$$

so that $\kappa \in (8/3, 8) \setminus \{4\}$. In fact, our Theorem III.1 has an analogue in the continuum, which we formulate as follows:

Consider a Liouville quantum disk with parameter $\gamma = \sqrt{\min(\kappa, 16/\kappa)}$ conditioned on having quantum boundary length 1 and an independent CLE_κ in the disk, with $\kappa \in (8/3, 8) \setminus \{4\}$. Then the nesting cascade of the quantum lengths of the CLE loops has the same law as the multiplicative cascade Z_α introduced in this article where α is given by (III.5).

In fact, recent work of Miller, Sheffield and Werner [MSW17] together with a different representation of the reproduction law ν_α which can be derived from [BBCK16] yields this statement.

2 Convergence of the first generation

The goal of this section is to prove the convergence of the first generation of $\chi^{(p)}$, as stated in the following proposition:

Proposition III.4. *For any $\varphi : \ell^\infty(\mathbb{N}^*) \to \mathbb{R}$ bounded and continuous, we have*

$$\mathbb{E}\left[\varphi\left(p^{-1}\chi^{(p)}(i) : i \geq 1\right)\right] \underset{p\to\infty}{\longrightarrow} \mathbb{E}[\varphi\left(Z_\alpha(i) : i \geq 1\right)].$$

We will follow the scheme outlined in the introduction, which is summarized in the following diagram.

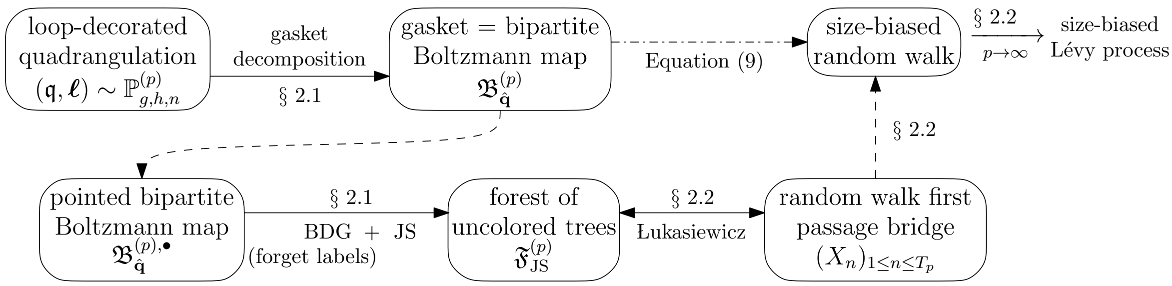

Figure III.2 – *A solid arrow $A \to B$ indicates a transformation that encodes A by B. A dashed arrow $A \dashrightarrow B$ indicates that the random object B is obtained by size-biasing the law of A. Equation (III.8) is obtained by composing all these transformations and size-biasing relations. Using it, we deduce Proposition III.4 from the classical convergence of random walks to Lévy processes.*

2.1 Coding the gasket by size-biased Galton–Watson trees

This section recalls the coding of the gasket by gasket decomposition, the BDG and JS bijections from Section 2, and summarizes their effect from a probabilistic perspective.

The gasket decomposition Recall that the gasket of a loop-decorated random quadrangulation under $\mathbb{P}^{(p)}_{g,h,n}$ is a $\hat{\mathbf{q}}$-*Boltzmann map*, denoted $\mathfrak{B}^{(p)}_{\hat{\mathbf{q}}}$, whose distribution is defined on the set of bipartite maps of perimeter $2p$ by normalizing the weights

$$w_{\hat{\mathbf{q}}}(\mathfrak{m}) = \prod_f \hat{q}_{\frac{1}{2}\deg(f)}$$

where the product runs on the internal faces of $\mathfrak{m}$, and the weight sequence $\hat{\mathbf{q}} = (\hat{q}_k)_{k\geq 1}$ is related to the $O(n)$ model by

$$\hat{q}_k = g\delta_{k,2} + nh^{2k}F_k(g,h,n). \tag{III.6}$$

Moreover, the gasket decomposition has the following Markov property: conditionally on the sizes $(2p_1, \ldots, 2p_l)$ in the *holes* of the gasket, the loop-decorated maps inside the holes are mutually independent, and follow the distributions $\mathbb{P}^{(p_i)}_{g,h,n}$ for $i = 1, \ldots, l$.

Coding of the pointed gasket Recall that a *pointed map* is a map given together with a distinguished vertex ρ. We denote by $\mathfrak{B}^{(p),\bullet}_{\hat{\mathbf{q}}}$ the *pointed* $\hat{\mathbf{q}}$-*Boltzmann map* whose distribution is defined on the set of pointed bipartite maps of perimeter $2p$ by normalizing the weights $w_{\hat{\mathbf{q}}}(\mathfrak{m}, \rho) := w_{\hat{\mathbf{q}}}(\mathfrak{m})$. As seen in Section 2.2 and 2.3, the Bouttier–Di Francesco–Guitter (BDG) bijection and Janson–Stefánsson's (JS) transform encode each pointed bipartite map $(\mathfrak{m}, \rho)$ of perimeter $2p$ by a forest $\mathfrak{F}$ of p rooted plan trees such that

- Each face of degree $2k$ $(k \geq 1)$ in $\mathfrak{m}$ becomes an internal vertex with k children in $\mathfrak{F}$.
- Each vertex of $\mathfrak{m}$ except ρ becomes a leaf of $\mathfrak{F}$.

Moreover, the partition function of $\mathfrak{B}^{(p),\bullet}_{\hat{\mathbf{q}}}$ is given by $F^\bullet_p(\hat{\mathbf{q}}) = \binom{2p}{p}(R_{\mathbf{q}})^p$, where $R_{\mathbf{q}}$ is the partition function of a Galton–Watson tree with the offspring distribution μ_{JS} given in Proposition II.4. It follows that the image of $\mathfrak{B}^{(p),\bullet}_{\hat{\mathbf{q}}}$ by the BDG bijection and JS's transform is a forest of p i.i.d. Galton–Watson tree of offspring distribution μ_{JS}, which we denote by $\mathfrak{F}_{\mathrm{JS}}^{(p)}$. The fact that the weight sequence $\hat{\mathbf{q}}$ comes from an $O(n)$-decorated Boltzmann quadrangulation would constrain the possible tail of the offspring distribution μ_{JS}. More precisely,

Lemma III.A (Tail of μ_{JS}. [BBG12c]). *Assume that $\hat{\mathbf{q}}$ is defined by an admissible triple (g,h,n) as in (III.6), then μ_{JS} has a polynomial tail if and only if (g,h,n) is non-generic critical. In this case, μ_{JS} is critical (i.e. $\sum_{k\geq 0} k\mu_{\mathrm{JS}}(k)=1$) and has the tail*

$$\mu_{\mathrm{JS}}(k) \underset{k\to\infty}{\sim} Ck^{-\alpha-1}$$

where $\alpha \in (1,2)\setminus\{3/2\}$ is given in (III.4).

Back to the non-pointed gasket To come back to the non-pointed map $\mathfrak{B}_{\hat{\mathbf{q}}}^{(p)}$, we need to bias the law of the pointed map $\mathfrak{B}_{\hat{\mathbf{q}}}^{(p),\bullet}$ by the inverse of its number of vertices. Let $\mathsf{Deg}_f^{\downarrow}$ (resp. $\mathsf{Deg}_{\mathtt{out}}^{\downarrow}$) denote the sequence of degrees of faces (resp. numbers of children) in a bipartite map (resp. forest), ranked in the decreasing order and padded into an infinite sequence with zeros. Then according to the two properties of the BDG-JS bijection listed in the previous paragraph, for any positive measurable function $\varphi : \mathbb{N}^{\mathbb{N}^*} \to \mathbb{R}$ we have

$$\begin{aligned}\mathbb{E}\left[\varphi\left(\frac{1}{2}\mathsf{Deg}_f^{\downarrow}(\mathfrak{B}_{\hat{\mathbf{q}}}^{(p)})\right)\right] &= \frac{1}{\mathbb{E}[1/\,\#\,\mathrm{vertex}(\mathfrak{B}_{\hat{\mathbf{q}}}^{(p),\bullet})]}\mathbb{E}\left[\frac{\varphi\left(\frac{1}{2}\mathsf{Deg}_f^{\downarrow}(\mathfrak{B}_{\hat{\mathbf{q}}}^{(p),\bullet})\right)}{\#\,\mathrm{vertex}(\mathfrak{B}_{\hat{\mathbf{q}}}^{(p),\bullet})}\right] \\ &= \frac{1}{\mathbb{E}[1/\,(1+\#\,\mathrm{leaf}(\mathfrak{F}_{\mathrm{JS}}^{(p)}))]}\mathbb{E}\left[\frac{\varphi\left(\mathsf{Deg}_{\mathtt{out}}^{\downarrow}(\mathfrak{F}_{\mathrm{JS}}^{(p)})\right)}{1+\#\,\mathrm{leaf}(\mathfrak{F}_{\mathrm{JS}}^{(p)})}\right].\end{aligned} \tag{III.7}$$

2.2 Scaling limit of the face degrees in the gasket

The discussion in the previous section is valid for Boltzmann maps with a general (admissible) weight sequence, and we now consider a weight sequence $\hat{\mathbf{q}}$ that is derived from a critical non-generic set of parameters (g,h,n) with exponent $\alpha\in(1,2)$ and prove Proposition III.4 (but the results are valid for any critical non-generic weight sequence $\hat{\mathbf{q}}$ as those considered in [LGM11], [BC17], [Cur17, Section 5.1.3]).

Random walk coding We use the well-known random walk coding of forests to study the right-hand side of (III.7). Let $S_n = X_1+\cdots+X_n$ be a random walk where $(X_n)_{n\geq 1}$ is an i.i.d. sequence with distribution $\mathbb{P}(X_1+1=k)=\mu_{\mathrm{JS}}(k)$ for $k\geq 0$. Define the first passage time of $(S_n)_{n\geq 0}$ to the level $-p$

$$T_p = \inf\{n\geq 0 \,|\, S_n=-p\}\,,$$

and let $L_p = \sum_{i=1}^{T_p} \mathbb{1}_{\{X_i=-1\}}$ be the number of negative steps of the walk up to T_p. Let $\boldsymbol{\mathcal{X}}^{(p)}$ be the sequence $(X_n+1)_{1\leq n\leq T_p}$ ranked in decreasing order and padded with zeros. The classical coding of forests by their Łukasiewicz paths shows that the sequence $\boldsymbol{\mathcal{X}}^{(p)}$ has the same law as $\mathsf{Deg}_{\mathtt{out}}^{\downarrow}(\mathfrak{F}_{\mathrm{JS}}^{(p)})$ and that jointly we have $\#\,\mathrm{Leaf}(\mathfrak{F}_{\mathrm{JS}}^{(p)}) = L_p$ in distribution.

Therefore (III.7) can be continued into

$$\begin{aligned}\mathbb{E}\left[\varphi\left(\frac{1}{2}\mathsf{Deg}_f^{\downarrow}(\mathfrak{B}_{\hat{\mathbf{q}}}^{(p)})\right)\right] &= \frac{1}{\mathbb{E}[1/\left(1+\#\,\mathrm{leaf}(\mathfrak{F}_{\mathrm{JS}}^{(p)})\right)]}\mathbb{E}\left[\frac{\varphi\left(\mathsf{Deg}_{\mathsf{out}}^{\downarrow}(\mathfrak{F}_{\mathrm{JS}}^{(p)})\right)}{1+\#\,\mathrm{leaf}(\mathfrak{F}_{\mathrm{JS}}^{(p)})}\right] \\ &= \frac{1}{\mathbb{E}[1/(1+L_p)]}\mathbb{E}\left[\frac{\varphi\left(\boldsymbol{\mathcal{X}}^{(p)}\right)}{1+L_p}\right]. \end{aligned} \tag{III.8}$$

By definition, the first generation of $\chi^{(p)}$ is the sequence of half-degrees of the *holes* in the gasket, sorted in the decreasing order and padded with zeros. Recall that the faces of the gasket are either holes or regular faces of degree 4. Therefore, if $\hat{\mathbf{q}}$ is the weight sequence given by (III.6), then the first generation of $\chi^{(p)}$ differs from $\frac{1}{2}\mathsf{Deg}_f^{\downarrow}(\mathfrak{B}_{\hat{\mathbf{q}}}^{(p)})$ at most by 2 in the $\ell^\infty(\mathbb{N}^*)$ norm. From the last display and the fact that $L_p \geq p$ it follows that, for any bounded continuous function $\varphi : \ell^\infty(\mathbb{N}^*) \to \mathbb{R}$, we have

$$\mathbb{E}\left[\varphi\left(p^{-1}\chi^{(p)}(i) : i \geq 1\right)\right] = \frac{1}{\mathbb{E}[1/L_p]}\mathbb{E}\left[\frac{\varphi\left(p^{-1}\cdot\boldsymbol{\mathcal{X}}^{(p)}\right)}{L_p}\right] + o(1). \tag{III.9}$$

as $p \to \infty$. With all the reductions we have been through we are now in position to prove Proposition III.4.

Proof of Proposition III.4. Recall from Lemma III.A that the step distribution of the walk S is centered and in the domain of attraction of the totally asymmetric stable law of parameter α. Recall also the notation from the Introduction and in particular that ζ is a standard α-stable Lévy process with no negative jumps. We can suppose that ζ has been normalized so that by a classical invariance principle we have

$$\left(\frac{1}{n}S_{[tn^\alpha]}\right)_{t\geq 0} \xrightarrow[n\to\infty]{(d)} (\zeta_t)_{t\geq 0}$$

for the Skorokhod topology. With standard arguments, one can show that the above convergence in distribution holds jointly with (using the notation of the Introduction)

$$p^{-\alpha}T_p \xrightarrow[p\to\infty]{(d)} \tau \qquad \text{and} \qquad \frac{1}{p}\boldsymbol{\mathcal{X}}^{(p)} \xrightarrow[p\to\infty]{(d)} (\boldsymbol{\Delta\zeta})^{\downarrow} \tag{III.10}$$

where the second convergence takes place in the $\ell^\infty(\mathbb{N}^*)$ topology. We now give a lemma controlling L_p via T_p in a precise manner:

Lemma III.5. *There is $c > 0$ depending only on the weight sequence $\hat{\mathbf{q}}$, such that for all $\varepsilon > 0$ and $p \geq 1$,*

$$\mathbb{P}(T_p \leq \varepsilon\, p^\alpha) \leq \mathbb{P}(L_p \leq \varepsilon\, p^\alpha) \leq \exp\left(-\,c\,\varepsilon^{-\frac{1}{\alpha-1}}\right) \tag{III.11}$$

$$\mathbb{P}\left(\left|\frac{L_p}{T_p} - \mu_{\mathrm{JS}}(0)\right| \geq p^{-\alpha/4}\right) \leq c^{-1}p^{\alpha/2}\exp(-c\sqrt{p}) \tag{III.12}$$

and for all $K \geq \dfrac{2}{\mu_{\mathrm{JS}}(0)}$,

$$\mathbb{P}\left(\frac{T_p}{L_p} \geq K\right) \leq c^{-1}\exp(-c\,Kp). \tag{III.13}$$

We finish the proof of Proposition III.4 given Lemma III.5. Equation (III.12) implies that L_p/T_p converges to $\mu_{\mathrm{JS}}(0)$ in probability, thus in distribution jointly with (III.10). Hence we have

$$\mu_{\mathrm{JS}}(0)\cdot\frac{p^\alpha}{L_p}\,\varphi\Big(p^{-1}\boldsymbol{\mathcal{X}}^{(p)}\Big)\quad\xrightarrow[p\to\infty]{(d)}\quad\frac{1}{\tau}\,\varphi\Big((\boldsymbol{\Delta\zeta})^{\downarrow}\Big).$$

On the other hand, (III.11) implies that the sequence $(p^\alpha L_p^{-1})_{p\geq 1}$ is uniformly integrable. Therefore we can take expectations in the last convergence in distribution and it follows that

$$\begin{aligned}\frac{\mathbb{E}\left[L_p^{-1}\varphi\Big(p^{-1}\boldsymbol{\mathcal{X}}^{(p)}\Big)\right]}{\mathbb{E}[L_p^{-1}]} &= \frac{\mu_{\mathrm{JS}}(0)\cdot\mathbb{E}\left[p^\alpha L_p^{-1}\varphi\Big(p^{-1}\boldsymbol{\mathcal{X}}^{(p)}\Big)\right]}{\mu_{\mathrm{JS}}(0)\cdot\mathbb{E}[p^\alpha L_p^{-1}]}\\ &\xrightarrow[p\to\infty]{}\frac{\mathbb{E}\left[\tau^{-1}\varphi\Big((\boldsymbol{\Delta\zeta})^{\downarrow}\Big)\right]}{\mathbb{E}[\tau^{-1}]}=\mathbb{E}[\varphi(Z_\alpha(i):i\geq 1)].\end{aligned}$$

With (III.8) this finishes the proof of the proposition. □

Proof of Lemma III.5. The first inequality in (III.11) follows from $L_p\leq T_p$. For the second inequality, consider for $\lambda>0$ the non-negative martingale

$$M_n=\exp\Big(-\lambda S_n-\Psi(\lambda)\sum_{i=1}^{n}\mathbb{1}_{\{X_i=-1\}}\Big)$$

where $\Psi(\lambda)$ is defined by the equation $\mathbb{E}\left[\exp(-\lambda X_1-\Psi(\lambda)\mathbb{1}_{\{X_1=-1\}})\right]=1$, or explicitly by

$$\Psi(\lambda)=-\log\Big(1-\frac{\mathbb{E}[e^{-\lambda X_1}]-1}{e^\lambda\mathbb{P}(X_1=-1)}\Big).$$

By Fatou's lemma, $\mathbb{E}[M_{T_p}]=\mathbb{E}[\exp(\lambda p-\Psi(\lambda)L_p)]\leq 1$. Notice that since $\mathbb{E}[e^{-\lambda X_1}]\geq e^{-\lambda\mathbb{E}[X_1]}=1$, we always have $\Psi(\lambda)\geq 0$ as soon as $\lambda>0$. We can thus apply the Chernoff bound and get

$$\mathbb{P}(L_p\leq\varepsilon p^\alpha)\ \leq\ \mathbb{E}\Big[\exp\Big(\varepsilon p^\alpha\Psi(\lambda)-\Psi(\lambda)L_p\Big)\Big]\ \leq\ \exp\Big(\varepsilon p^\alpha\Psi(\lambda)-\lambda p\Big).\tag{III.14}$$

From our standing assumptions, we know that X_1 has the power law tail behavior $\mathbb{P}(X_1\geq x)\sim Cx^{-\alpha}$ $(x\to\infty)$ and so by standard Abelian theorems its Laplace transform witnesses the following asymptotic:

$$\mathbb{E}[e^{-\lambda X_1}]=1+C'\lambda^\alpha+o(\lambda^\alpha).$$

It follows that $\Psi(\lambda)\sim C''\lambda^\alpha$ as $\lambda\to 0$. On the other hand, it is easy to see that $\Psi(\lambda)\sim\lambda$ when $\lambda\to\infty$. Therefore there exists a constant c' such that $\Psi(\lambda)\leq c'\,\lambda^\alpha$ for all $\lambda>0$. Then (III.11) follows from (III.14) by taking $\lambda=c''(\varepsilon^{\frac{1}{\alpha-1}}p)^{-1}$ with $c''>0$ sufficiently small.

For (III.12), observe that for all $\beta > 0$ and $\theta \in (0, \alpha)$,

$$\begin{aligned}
\mathbb{P}\Big(\Big| \frac{L_p}{T_p} - \mu_{\mathrm{JS}}(0) \Big| \geq p^{-\beta\alpha} \Big) &= \sum_{n=1}^{\infty} \mathbb{P}\Big(\Big| \frac{1}{n} \sum_{i=1}^{n} \mathbb{1}_{\{X_i=-1\}} - \mu_{\mathrm{JS}}(0) \Big| \geq p^{-\beta\alpha} \text{ and } T_p = n \Big) \\
&\leq \mathbb{P}(T_p < p^{\theta}) + \sum_{n=p^{\theta}}^{\infty} \mathbb{P}\Big(\Big| \frac{1}{n} \sum_{i=1}^{n} \mathbb{1}_{\{X_i=-1\}} - \mu_{\mathrm{JS}}(0) \Big| \geq p^{-\beta\alpha} \Big) \\
&\underset{(*)}{\leq} \exp\Big(- c\, p^{\frac{\alpha-\theta}{\alpha-1}} \Big) + \sum_{n=p^{\theta}}^{\infty} 2 \exp(-\tilde{c}\, n\, p^{-2\beta\alpha}) \\
&\leq \exp\Big(- c\, p^{\frac{\alpha-\theta}{\alpha-1}} \Big) + 2\, \tilde{c}^{-1} p^{2\beta\alpha} \exp(-\tilde{c}\, p^{\theta-2\beta\alpha}).
\end{aligned}$$

where for $(*)$ we used (III.11) with $\varepsilon = p^{\theta-\alpha}$ and the standard Chernoff bound for i.i.d. Bernoulli random variables. The constant $\tilde{c}$ depends only on μ_0. We obtain (III.12) by taking $\beta = 1/4$ and optimizing over θ.

For (III.13), we start by observing that $L_p \geq p$, therefore $T_p \geq pK$ on the event $\{T_p/L_p \geq K\}$. Then using the same arguments as for (III.12), we get for all $K \geq 2/\mu_{\mathrm{JS}}(0)$,

$$\begin{aligned}
\mathbb{P}\Big(\frac{T_p}{L_p} \geq K \Big) &= \sum_{n=pK}^{\infty} \mathbb{P}\Big(\frac{1}{n} \sum_{i=1}^{n} \mathbb{1}_{\{X_i=-1\}} \geq K^{-1} \text{ and } T_p = n \Big) \\
&\leq \sum_{n=pK}^{\infty} \exp\Big(-\tilde{c}\, (\mu_{\mathrm{JS}}(0) - K^{-1})\, n \Big) \;\leq\; \frac{\exp\Big(-\frac{1}{2} \tilde{c}\, \mu_{\mathrm{JS}}(0)\, K p \Big)}{1 - \exp\Big(-\frac{1}{2} \tilde{c}\, \mu_{\mathrm{JS}}(0) \Big)}. \qquad \square
\end{aligned}$$

3 A formula for left-continuous random walks

In this section, we prove Theorem III.3 and an analogue of it for spectrally positive Lévy processes.

3.1 Proof of Theorem III.3

Throughout the section, we denote by $S_n = X_1 + \cdots + X_n$ a left-continuous random walk on $\mathbb{Z}$ (that is, $(X_i)_{i\geq 1}$ are i.i.d. with $X_i \geq -1$) and by T_p the hitting time of $-p \in \mathbb{Z}$ by $S = (S_n)_{n\geq 0}$. In particular we have $S_{T_p} = -p$. The proof of Theorem III.3 will make a heavy use of Kemperman's formula:

$$\text{For all } n \geq 1 \text{ and } p \geq 1, \qquad \mathbb{P}(T_p = n) = \frac{p}{n}\, \mathbb{P}(S_n = -p).$$

See e.g. [Pit06, Section 6.1] (where there the notation S_n stands for our $S_n - n$). More precisely it follows from [Pit06, Lemma 6.1] that if $n \geq 1$ and $p \geq 1$, then for any positive measurable function $F(x_1, \ldots, x_n)$ which is invariant under cyclic permutation of its arguments, we have the extended Kemperman's formula:

$$\mathbb{E}[F(X_1, \cdots, X_n) \mathbb{1}_{\{T_p = n\}}] = \frac{p}{n} \mathbb{E}[F(X_1, \cdots, X_n) \mathbb{1}_{\{S_n = -p\}}].$$

Proof of Theorem III.3. Let $n \geq 2$, we have

$$\begin{aligned}
A_n &:= \mathbb{E}\left[\sum_{i=1}^{n} f(X_i)\mathbb{1}_{\{T_p=n\}}\right] \\
&= \frac{p}{n}\,\mathbb{E}\left[\sum_{i=1}^{n} f(X_i)\mathbb{1}_{\{S_n=-p\}}\right] && \text{by extended Kemperman's formula} \\
&= p\,\mathbb{E}\left[f(X_1)\mathbb{1}_{\{S_n=-p\}}\right] && \text{by cyclic symmetry} \\
&= p\,\mathbb{E}\left[f(X_1)\mathbb{P}(S_{n-1}=-p-X_1 \,|\, X_1)\right] && \text{by Markov property} \\
&= \mathbb{E}\left[f(X_1)\frac{p}{p+X_1}(n-1)\mathbb{P}(T_{p+X_1}=n-1 \,|\, X_1)\right] && \text{by Kemperman's formula.}
\end{aligned}$$

Since $p \geq 2$, we have $T_p \geq 2$ and $T_{p+x} \geq 1$ almost surely, for every $x \in \{-1, 0, 1, \ldots\}$. Hence,

$$\begin{aligned}
\mathbb{E}\left[\frac{1}{T_p-1}\sum_{i=1}^{T_p} f(X_i)\right] = \sum_{n=2}^{\infty}\frac{A_n}{n-1} &= \mathbb{E}\left[f(X_1)\frac{p}{p+X_1}\sum_{n=2}^{\infty}\mathbb{P}(T_{p+X_1}=n-1 \,|\, X_1)\right] \\
&= \mathbb{E}\left[f(X_1)\frac{p}{p+X_1}\right],
\end{aligned}$$

where in the penultimate line we used the fact that $T_p < \infty$ almost surely to deduce that the sum inside the expectation is equal to 1. This completes the proof of the theorem. □

The theorem has the following generalization, whose proof is an easy extension of the above proof and left to the reader.

Proposition III.6. *Suppose that $(S_n)_{n\geq 0}$ does not drift to $+\infty$. Let $m \in \mathbb{N}$, $f : \mathbb{Z}^m \to \mathbb{R}_+$ and $g : \bigcup_{j=1}^{\infty} \mathbb{Z}^j \to \mathbb{R}_+$ be symmetric measurable functions. Then for any $p \geq 1$ we have*

$$\begin{aligned}
&\mathbb{E}\left[\frac{\mathbb{1}_{\{T_p>m\}}}{(T_p-1)\cdots(T_p-m)}\sum_{(i_1,\ldots,i_p)\in\mathcal{A}^m_{T_p}} f(X_{i_1},\cdots,X_{i_m})g((X_j)_{j\notin\{i_1,\ldots,i_p\},j\leq T_p})\right] \\
&\qquad = \mathbb{E}\left[f(X_1,\cdots,X_m)\frac{p\,\mathbb{1}_{\{T_p>m\}}}{p+X_1+\cdots+X_m}\mathbb{E}[g((X_j)_{j\leq T_{p+X_1+\cdots+X_p}})]\right]
\end{aligned}$$

where $\mathcal{A}^m_{T_p}$ is the set of all ordered m-tuples of distinct elements (m-arrangements) from $\{1,\cdots,T_p\}$.

3.2 Passing to the limit: An analogous formula for Lévy processes

Let now $(\eta_t)_{t\geq 0}$ be a Lévy process with no negative jumps started from $\eta_0 = 0$. Denote by $\pi(\mathrm{d}x)$ its Lévy measure (supported on $\mathbb{R}_+$) and by τ the hitting time of -1. We are interested in the mean intensity measure of the jumps $\Delta\eta_t := \eta_t - \eta_{t-}$ of η up to time τ.

Proposition III.7. *Suppose that $\tau < \infty$ almost surely. Let $f : \mathbb{R}_+^* \to \mathbb{R}$ be non-negative, measurable and such that $f(0) = 0$. Then we have*

$$\mathbb{E}\left[\frac{1}{\tau}\sum_{t\leq\tau} f(\Delta\eta_t)\right] = \int f(x)\frac{1}{1+x}\pi(\mathrm{d}x).$$

Remark III.8. Notice that, somehow surprisingly, the drift and the Brownian component of the Lévy process do not appear explicitly in the result (as long as the Lévy process does not drift to ∞). However, they do affect the distribution of τ and of the jumps until time τ.

Also note that Proposition III.7 admits an obvious extension analogously to Proposition III.6.

Proof. We could of course adapt the proof of Theorem III.3 to the current setting (in the spirit of [BCP03]) however, we find it shorter to simply argue by approximation. Let $S_k^{(n)} = X_1^{(n)} + \cdots + X_k^{(n)}$ be a sequence of left-continuous random walks and $(a_n)_{n\geq 0}$ a sequence of positive integers, such that we have

$$\left(a_n^{-1} S_{\lfloor nt \rfloor}^{(n)}\right)_{t\geq 0} \quad \xrightarrow[n\to\infty]{(d)} \quad (\eta_t)_{t\geq 0} \tag{III.15}$$

in distribution in the Skorokhod topology. In particular this means that $n\mathbb{P}(X_1^{(n)} \geq xa_n) \to \pi((x,\infty))$ for all x which is not an atom of π. Note also that it is always possible to perform such an approximation in such a way that the walk $S^{(n)}$ does not drift towards ∞. For any continuous function f on $\mathbb{R}_+^*$ with compact support, we then have (where the equality $(*)$ is justified just below)

$$\mathbb{E}\left[\frac{1}{\tau}\sum_{t\leq\tau} f(\Delta\eta_t)\right] \underset{(*)}{=} \lim_{n\to\infty} \mathbb{E}\left[\frac{n}{T_{a_n}}\sum_{i=1}^{T_{a_n}} f\left(a_n^{-1}X_i^{(n)}\right)\right]$$
$$\underset{\text{Thm.}III.3}{=} \lim_{n\to\infty} n\mathbb{E}\left[f(a_n^{-1}X_1)\frac{a_n}{a_n+X_1}\right] = \int f(x)\frac{1}{1+x}\pi(\mathrm{d}x).$$

The statement then follows by a monotone class argument. In order to justify $(*)$ one can first invoke the Skorokhod embedding theorem and assume that (III.15) holds almost surely. It then follows from standard arguments that $\frac{n}{T_{a_n}}\sum_{i=1}^{T_{a_n}} f\left(a_n^{-1}X_i^{(n)}\right) \to \frac{1}{\tau}\sum_{t\leq\tau} f(\Delta\eta_t)$ in distribution as $n\to\infty$. It thus remains to prove uniform integrability in order to allow convergence of the expectations. Without loss of generality, we can assume that f is supported in $[1,\infty)$ and bounded by 1, that is, $f \leq \mathbb{1}_{\{x\geq 1\}}$. Define $N_k^{(n)} = \#\left\{1\leq i\leq k : X_i^{(n)} \geq a_n\right\}$, then we can write

$$\mathbb{E}\left[\left(\frac{n}{T_{a_n}}\sum_{i=1}^{T_{a_n}} f\left(a_n^{-1}X_i^{(n)}\right)\right)^2\right] \leq \mathbb{E}\left[\left(\frac{n}{T_{a_n}}N_{T_{a_n}}^{(n)}\right)^2\right] \leq \mathbb{E}\left[\left(\frac{n}{T_{a_n}}N_n^{(n)}\right)^2 \mathbb{1}_{\{T_{a_n}\leq n\}}\right] + \mathbb{E}\left[\left(\sup_{k\geq n}\frac{n}{k}N_k^{(n)}\right)^2\right]$$

Since $\mathbb{P}(X_1^{(n)} \geq a_n)$ is of order $1/n$, we can choose λ large enough so that $\mathbb{P}(X_1^{(n)} \geq a_n) \leq 1-\exp(-\lambda/n)$ for all n. Then the process $(N_k^{(n)})_{k\geq 1}$ is stochastically bounded by $(Y_{k/n})_{k\geq 1}$, where Y is a standard Poisson process of intensity λ. Easy estimates show that $\mathbb{E}\left[(\sup_{t\geq 1} t^{-1}Y_t)^2\right] < \infty$, which gives a uniform bound to the second term on the right-hand side of the last display. For the first term, we apply Cauchy-Schwarz inequality to get that

$$\mathbb{E}\left[\left(\frac{n}{T_{a_n}}N_n^{(n)}\right)^2 \mathbb{1}_{\{T_{a_n}\leq n\}}\right] \leq \left(\mathbb{E}[Y_1^4]\cdot\mathbb{E}\left[\left(\frac{n}{T_{a_n}}\right)^4 \mathbb{1}_{\{T_{a_n}\leq n\}}\right]\right)^{1/2}.$$

Using estimates similar to those of Lemma III.5 we deduce that $\mathbb{E}\left[(n/T_{a_n})^4\mathbb{1}_{\{T_{a_n}\leq n\}}\right]$ is bounded uniformly in n. Gathering the estimates we deduce that $\mathbb{E}\left[\left(\frac{n}{T_{a_n}}\sum_{i=1}^{T_{a_n}} f\left(a_n^{-1}X_i^{(n)}\right)\right)^2\right]$ is bounded uniformly in n. This gives the desired uniform integrability. □

4 Properties of the limiting multiplicative cascade

In this section, we examine in detail the multiplicative cascade Z_α defined in the introduction. The most important quantity of a multiplicative cascade, which determines much of its asymptotic behavior, is the Biggins transform. We calculate this transform in Section 4.1, relying on the formula for Lévy processes proved in the previous section (Proposition III.7). This allows to define additive martingales which we make explicit. We also calculate the Legendre–Fenchel transform of the (log-)Biggins transform, which describes the asymptotic growth of the multiplicative cascade. In Section 4.2, we show that the Malthusian martingale of the multiplicative cascade is uniformly integrable and calculate the law of its limit. We conjecture this law to be the asymptotic law of the renormalized volume of the $O(n)$-decorated quadrangulations considered in this paper. Finally, in Section 4.3, we study L^p-convergence of the additive martingales.

4.1 The Biggins transform and additive martingales

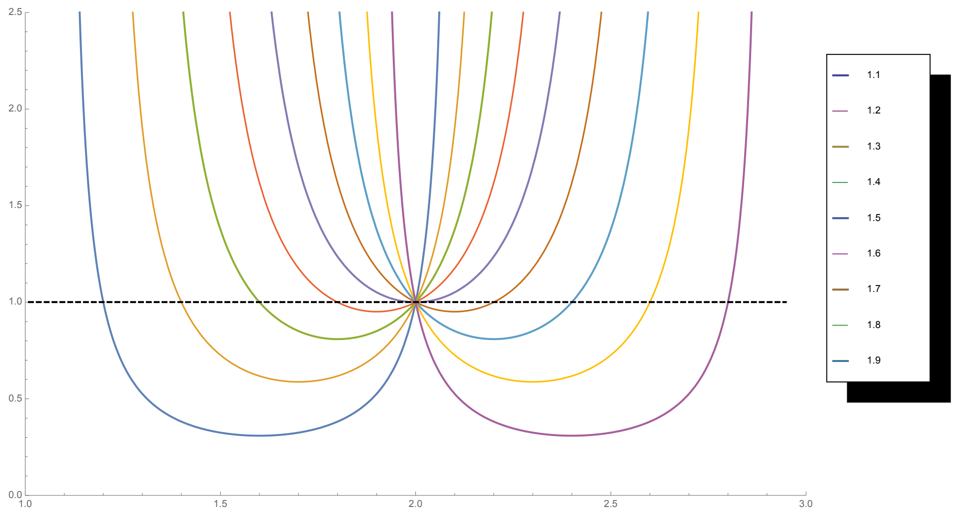

Figure III.3 – *The various functions $\phi_\alpha(\theta)$ for $\alpha = 1.1, 1.2, \ldots, 1.9$, and the line $y = 1$ (dashed).*

In this section we prove the formula for the Biggins transform of the measure ν_α (see Figure III.3 for a plot for different values of α):

$$\phi_\alpha(\theta) = \mathbb{E}\left[\sum_{i=1}^{\infty} \Big(Z_\alpha(i)\Big)^\theta\right] = \frac{\sin(\pi(2-\alpha))}{\sin(\pi(\theta-\alpha))} \quad \text{for } \theta \in (\alpha, \alpha+1). \tag{III.16}$$

Proof of (III.16). We use Proposition III.7 when $\eta = \zeta$ is a spectrally positive α-stable Lévy process for $\alpha \in (1,2)$. In this case recall that we have $\mathbb{E}[e^{-\lambda\zeta}] = \exp(C\lambda^\alpha)$ and the Lévy measure of ζ is equal to

$$\pi(\mathrm{d}x) = \frac{C}{\Gamma(-\alpha)} \frac{\mathrm{d}x}{x^{\alpha+1}} \mathbf{1}_{(x>0)}.$$

Applying the above-mentioned proposition we deduce that

$$\mathbb{E}\left[\frac{1}{\tau}\sum_{t\leq\tau}(\Delta\zeta_t)^\theta\right] = \int \frac{x^\theta}{1+x}\pi(\mathrm{d}x) = \frac{C}{\Gamma(-\alpha)}\int_0^\infty \frac{x^{\theta-\alpha-1}}{x+1}\mathrm{d}x = \begin{cases} \frac{C\pi}{\Gamma(-\alpha)\sin(\pi(\theta-\alpha))} & \text{if } \theta\in(\alpha,\alpha+1) \\ +\infty & \text{otherwise.}\end{cases}$$

For the last equality, see e.g. [EMOT54, 6.2(3)]. Moreover, it is classical (see e.g. [Ber96, Chapter VII, Theorem 1]) that for $\lambda \geq 0$ we have $\mathbb{E}[e^{-\lambda\tau}] = e^{-(\lambda/C)^{1/\alpha}}$ and so

$$\mathbb{E}[1/\tau] = \mathbb{E}\left[\int_0^\infty e^{-\lambda\tau}\,d\lambda\right] = \int_0^\infty e^{-(\lambda/C)^{1/\alpha}}\,\mathrm{d}\lambda = C\,\Gamma(1+\alpha). \tag{III.17}$$

Combining the last two displays with Euler's reflection formula we indeed compute the Biggins transform of the measure ν_α as promised

$$\frac{\mathbb{E}\left[\frac{1}{\tau}\sum_{t\leq\tau}(\Delta\zeta_t)^\theta\right]}{\mathbb{E}[1/\tau]} = \begin{cases} \frac{\sin(\pi(2-\alpha))}{\sin(\pi(\theta-\alpha))} & \text{if } \theta\in(\alpha,\alpha+1) \\ +\infty & \text{otherwise.}\end{cases}$$

We see that the above result does not depend on the normalizing constant C appearing in the definition of ζ. As we already remarked in the introduction, this can more directly be seen using a scaling argument to show that the law of ν_α is independent of C. □

Additive martingales. Consider the following family of processes, indexed by $\theta \in (\alpha, \alpha+1)$,

$$W_n(\alpha,\theta) = \phi_\alpha(\theta)^{-n}\sum_{u:|u|=n} Z_\alpha(u)^\theta. \tag{III.18}$$

It is well-known and easy to show that each of these processes is a non-negative martingale with respect to the σ-field $\mathcal{F}_n = \sigma(Z_\alpha(u), |u| \leq n)$. Since for each $n \in \mathbb{N}$, $W_n(\alpha,\theta)$ is an additive functional of $(Z_\alpha(u))_{|u|=n}$, they are also called *(the) additive martingales* of the multiplicative cascade Z_α. Of special importance is the so-called *Malthusian martingale* corresponding to the *Malthusian parameter* θ_α which is the smaller solution of the equation $\phi_\alpha(\theta) = 1$. (Since $\theta \mapsto \phi_\alpha(\theta)$ is strictly convex, there are at most two solutions.) One easily checks that for $\alpha \in (1,2)\setminus\{3/2\}$, there are exactly two solutions to this equation, namely 2 and $2\alpha-1$, and so the Malthusian parameter equals

$$\theta_\alpha = \min(2, 2\alpha-1) = \begin{cases} 2 & \text{if } \alpha > 3/2 \quad \text{(dilute case)} \\ 2\alpha-1 & \text{if } \alpha < 3/2 \quad \text{(dense case)}\end{cases}. \tag{III.19}$$

Remark III.9. In particular we deduce that for $\theta \in ((2\alpha-1)\wedge 2, (2\alpha-1)\vee 2)$, which is a non-empty interval as soon as $\alpha \neq 3/2$, the multiplicative cascade Z_α satisfies

$$\mathbb{E}\left[\sum_{u\in\mathcal{U}}(Z_\alpha(u))^\theta\right] = \sum_{k=0}^\infty(\phi_\alpha(\theta))^k < \infty.$$

In particular Z_α belongs to $\ell^\theta(\mathcal{U})$ almost surely.

In Section 4.2, we prove that the Malthusian martingale is uniformly integrable and identify the law of the limit. In Section 4.3, we provide moment bounds on $W_1(\alpha,\theta)$, which allow to prove convergence in L^p of $W_n(\alpha,\theta)$ for suitable p and θ.

Remark III.10. In the critical case $\alpha = 3/2$—which we do not consider in this paper—the equation $\phi_{3/2}(\theta) = 1$ has only one solution $\theta = 2$. It is well-known that in this case, the martingale $W_n(\alpha, 2)$ converges to 0 almost surely, but one can still get a non-trivial limit either by considering the so-called *derivative martingale* [Kyp98] or by renormalizing the martingale $W_n(\alpha, 2)$ appropriately [AS11], the two approaches leading to the same result.

For completeness, we note that the Legendre–Fenchel transform of $\log \phi_\alpha$ can also be explicitly evaluated (we leave the calculation to the reader). This allows to determine the asymptotic growth of the multiplicative cascade, see Biggins [Big79] for further details.

Proposition III.11. *Denote by* arccot *the branch of the arccotangent taking values in* $(0, \pi)$*. For* $x \in \mathbb{R}$*,*

$$(\log \phi_\alpha)^*(x) := \sup_{\theta \in \mathbb{R}} \{\theta x - \log \phi_\alpha(\theta)\} = \alpha x + \tfrac{x}{\pi}\mathrm{arccot}(-\tfrac{x}{\pi}) - \tfrac{1}{2}\log(1 + \tfrac{x^2}{\pi^2}) - \log \sin(\pi(2-\alpha)). \tag{III.20}$$

This function is strictly increasing and its (unique) root is negative if $\alpha \neq 3/2$ *and* 0 *if* $\alpha = 3/2$*.*

4.2 The volume of the map: the law of the Malthusian martingale limit

Recall the definition of the modified Bessel function of the third kind K_ν (also called Macdonald function), see e.g. [EMOT53, Section 7.2.2]:

$$\begin{aligned} K_\nu(z) &= \frac{\pi}{2\sin(\pi\nu)}(I_{-\nu}(z) - I_\nu(z)) \\ &= \frac{\Gamma(\nu)\Gamma(1-\nu)}{2} \sum_{n=0} \frac{1}{n!}\left[\frac{(z/2)^{2n-\nu}}{\Gamma(n-\nu+1)} - \frac{(z/2)^{2n+\nu}}{\Gamma(n+\nu+1)}\right]. \end{aligned} \tag{III.21}$$

Recall that $\alpha \in (1,2) \setminus \{3/2\}$ throughout the paper. Define for every $\theta > 0$,

$$\psi_{\alpha,\theta}(x) = \frac{2}{\Gamma(\alpha - 1/2)} x^{(\alpha-1/2)/\theta} K_{\alpha-1/2}(2x^{1/\theta}).$$

Then $\psi_{\alpha,\theta}(0) = 1$ for all α and θ, by (III.21). Note that $\psi_{\alpha,\theta}(x) = \psi_{\alpha,\theta'}(x^{\theta'/\theta})$ for every $\theta', \theta > 0$. Also recall the formula [EMOT53, 7.12.23]

$$\psi_{\alpha,\theta}(x) = \psi_{\alpha,2}(x^{2/\theta}) = \frac{1}{\Gamma(\alpha - 1/2)} \int_0^\infty e^{-x^{2/\theta}y - 1/y} y^{-(\alpha+1/2)}\, dy. \tag{III.22}$$

In particular, $\psi_{\alpha,2}$ is the Laplace transform of the inverse-Gamma distribution with parameters $\alpha - 1/2$ and 1. The following theorem identifies the law of the Malthusian martingale limit in terms of the function $\psi_{\alpha,\theta}$:

Theorem III.12 (Distributions of the Mathusian martingales)**.**

- *$\alpha > 3/2$ (dilute case): The martingale $(W_n(\alpha, 2))_{n\geq 0}$ is uniformly integrable and its limit has Laplace transform $x \mapsto \psi_{\alpha,2}((\alpha - 3/2)x)$, i.e. it follows the inverse-Gamma distribution with parameters $\alpha - 1/2$ and $\alpha - 3/2$.*

- $\alpha < 3/2$ *(dense case): The martingale* $(W_n(\alpha, 2\alpha-1))_{n\geq 0}$ *is uniformly integrable and its limit has Laplace transform* $x \mapsto \psi_{\alpha,2\alpha-1}(\frac{\Gamma(\alpha+1/2)}{\Gamma(3/2-\alpha)}x)$.

Remark III.13. The above martingale limit should be interpreted as the scaling limit (in distribution) of the volume (i.e. the number of vertices) of the loop-decorated map. This interpretation is supported by the following observations:

(i) If $\mathfrak{m}$ is a random map and $\mathfrak{m}^\bullet$ is its pointed version, then the expected volume of $\mathfrak{m}$ is the ratio between the partition function of $\mathfrak{m}^\bullet$ and the partition function of $\mathfrak{m}$. Using this one can show that the expected volume of $(\mathfrak{q}, \boldsymbol{\ell})$ under $\mathbb{P}^{(p)}_{g,h,n}$ scales like p^{θ_α} when $p \to \infty$ (see Theorem III.B), whereas the expected volume of the gasket scales like p^α. Since $\theta_\alpha > \alpha$, this suggests that the volume of $(\mathfrak{q}, \boldsymbol{\ell})$ and the volume inside the outer-most loops of $(\mathfrak{q}, \boldsymbol{\ell})$ have the same scaling limit. By induction, one can further restrict to the volume inside the loops of n-th generation without changing the limit.

(ii) According to the asymptotics of the expected volume started in the previous point, conditionally on $\chi^{(p)}(u)$, the volume inside the loop corresponding to $u \in \mathcal{U}$ has an expectation proportional to $\chi^{(p)}(u)^{\theta_\alpha}$ when $p \to \infty$. So

$$W_n(\alpha, \theta_\alpha) \;=\; \sum_{u:|u|=n} Z_\alpha(u)^{\theta_\alpha} \;\approx\; \frac{1}{p^{\theta_\alpha}} \sum_{u:|u|=n} \chi^{(p)}(u)^{\theta_\alpha}$$

is approximately the (rescaled) expected volume inside the n-th-generation loops.

In the dense case, the Laplace transform $\psi_{\alpha,2\alpha-1}$ implicitly appeared in the physics literature in the same context as this paper [KS92, Equation (2.5)] (we are grateful to Timothy Budd for showing this to us, this helped us find the right law!). Note that Theorem III.12 shows in particular that if $\alpha \in (1, 3/2)$, the function $\psi_{\alpha,2\alpha-1}$ is the Laplace transform of a probability distribution, which is not obvious *a priori* and for which we do not have a direct proof. In particular, we do not have an explicit expression of its density. Note however that this probability distribution is related to the Laplace transform of the inverse-Gamma distribution of parameter $\alpha - 1/2$ by the subordination relation

$$\psi_{\alpha,2}(x) = \psi_{\alpha,2\alpha-1}(x^{\alpha-1/2}).$$

Remark III.14. In order to show uniform integrability of additive martingales, one usually uses a famous result of Biggins, later improved by Lyons [Lyo97], which states that the martingale $W_n(\alpha,\theta)$ is uniformly integrable if

$$\theta(\log\phi_\alpha)'(\theta) < \log\phi_\alpha(\theta) \quad \text{and} \quad \mathbb{E}[W_1(\alpha,\theta)\log_+(W_1(\alpha,\theta))] < \infty,$$

where $\log_+(x) = \max(\log(x), 0)$. Otherwise, $W_n(\alpha,\theta)$ converges almost surely to 0. Our proof of uniform integrability bypasses this result.

The main part of the proof of Theorem III.12 is the following Lemma III.15, which identifies the function $\psi_{\alpha,\theta}$ as the solution to a certain functional equation. Together with a general result on multiplicative cascades (Proposition III.16 below), this will readily imply the theorem.

Lemma III.15. *For every* $\alpha \in (1,2)$, $\theta > 0$, *the function* $\psi_{\alpha,\theta}$ *satisfies the equation*

$$\psi_{\alpha,\theta}(x) = \mathbb{E}\left[\prod_{i=1}^{\infty} \psi_{\alpha,\theta}(xZ_\alpha(i)^\theta)\right], \; x > 0, \quad \psi(0) = 1. \tag{III.23}$$

Proof. It is enough to prove the formula for $\theta = 1$, by the relation $\psi_{\alpha,\theta}(x) = \psi_{\alpha,1}(x^{1/\theta})$, $x > 0$. We therefore assume $\theta = 1$ from now on and write $\psi := \psi_{\alpha,1}$.

We start by expressing the right-hand side of (III.23) in terms of the jumps of an α-stable Lévy process: Let $(\zeta_t)_{t\geq 0}$ be an α-stable Lévy process with no negative jumps started at 0, more precisely we assume that its cumulant is given by

$$\log \mathbb{E}[e^{-\lambda\zeta_1}] = \int_0^\infty (e^{-\lambda x} - 1 + \lambda x)\frac{1}{x^{\alpha+1}}\,dx. \tag{III.24}$$

Let τ denote the hitting time of -1 of ζ. Then (III.23) reads,

$$\psi(x) = c_\alpha \mathbb{E}\left[\frac{1}{\tau}\prod_{t<\tau}\psi(x\Delta\zeta_t)\right], \quad c_\alpha := \left(\mathbb{E}\left[\frac{1}{\tau}\right]\right)^{-1}, \tag{III.25}$$

where the product is over all jump times t less than τ. By (III.17) and Euler's reflection formula,

$$c_\alpha = -\frac{\sin(\pi\alpha)}{\pi} = \frac{\sin(\pi(\alpha-1))}{\pi}. \tag{III.26}$$

Now derive (III.25) with respect to x, which gives by the product formula,

$$\psi'(x) = c_\alpha \mathbb{E}\left[\frac{1}{\tau}\sum_{t<\tau}(\Delta\zeta_t)\psi'(x\Delta\zeta_t)\prod_{s<\tau,\, s\neq t}\psi(x\Delta\zeta_t)\right].$$

We the extension of Proposition III.7 mentioned after its statement, we calculate this as follows:

$$\psi'(x) = c_\alpha\int_0^\infty \frac{dy}{y^{\alpha+1}}y\psi'(xy)\frac{1}{1+y}\mathbb{E}\left[\prod_{t<\tau}\psi(x\Delta\zeta_t)\right]^{1+y}. \tag{III.27}$$

In order to calculate the expectation on the right-hand side of (III.27), we use the fact that the functional $(\prod_{t<\tau}\psi(\lambda\Delta\zeta_t))$ induces a change of measure of the Lévy process ζ, which turns it into a non-conservative Lévy process, i.e. a Lévy process with killing. More precisely, define the subprobability measure $\mathbb{P}_{\psi,x}$ by

$$\mathbb{E}_{\psi,x}[H_t] = \mathbb{E}\left[H_t\prod_{s<t}\psi(x\Delta\zeta_s)\right],$$

for every $\sigma((\zeta_s)_{0\leq s\leq t})$-measurable bounded r.v. H_t. It is a standard fact that under $\mathbb{P}_{\psi,x}$, the process ζ is again a Lévy process with cumulant $\kappa_{\psi,x}$ given by

$$\kappa_{\psi,x}(\lambda) = \int_0^\infty (e^{-\lambda y}\psi(xy) - 1 + \lambda y)\frac{1}{y^{\alpha+1}}\,dy. \tag{III.28}$$

It follows from the definition of $\kappa_{\psi,x}$ that it is a continuous, strictly increasing function on $[0,\infty)$. We may thus define its inverse $\kappa_{\psi,x}^{-1}$ on $[\kappa_{\psi,x}(0),\infty)$ (note that $\kappa_{\psi,x}(0) \leq 0$, so in particular, $\kappa_{\psi,x}^{-1}(0)$ is well defined). The following is well-known:

$$\mathbb{E}\left[\prod_{t<\tau}\psi(x\Delta\zeta_t)\right] = \mathbb{E}_{\psi,x}[1] = e^{-\kappa_{\psi,x}^{-1}(0)}. \tag{III.29}$$

It turns out that $\kappa_{\psi,x}^{-1}(0) = 2x$, or, equivalently, $\kappa_{\psi,x}(2x) = 0$, as can be easily checked by elementary computations, using the formula (III.22) (or by a computer algebra software). Together with (III.29), Equation (III.27) then becomes,

$$\psi'(x) = c_\alpha \int_0^\infty \frac{dy}{y^\alpha} \psi'(xy) \frac{1}{1+y} e^{-2x(1+y)}.$$

Changing variables $y \mapsto y/x$ in the integral, this equation becomes,

$$\psi'(x) = c_\alpha e^{-2x} x^\alpha \int_0^\infty \frac{dy}{y^\alpha} \psi'(y) \frac{1}{x+y} e^{-2y}. \tag{III.30}$$

Now recall that $\psi(x) = C_\alpha x^{\alpha-1/2} K_{\alpha-1/2}(2x)$ for some $C_\alpha > 0$. Then by [EMOT53, 7.11(21)] we have $\psi'(x) = -2C_\alpha x^{\alpha-1/2} K_{\alpha-3/2}(2x)$. Using this identity, (III.30) is equivalent to

$$e^{2x} \frac{K_{\alpha-3/2}(2x)}{\sqrt{x}} = c_\alpha \int_0^\infty \frac{1}{x+y} e^{-2y} \frac{K_{\alpha-3/2}(2y)}{\sqrt{y}}\, dy,$$

or, equivalently,

$$\frac{e^{x/2} K_{\alpha-3/2}(x/2)}{\sqrt{x}} = c_\alpha \int_0^\infty \frac{1}{x+y} e^{-y} \frac{e^{y/2} K_{\alpha-3/2}(y/2)}{\sqrt{y}}\, dy. \tag{III.31}$$

Recall $c_\alpha = \sin(\pi(\alpha-1))/\pi = \sin(\pi((\alpha-3/2)+1/2))/\pi$. Equation (III.31) is then a special case of a known formula for Whittaker functions, see e.g. [CPV+08, p335] or [OLBC10, 13.16.6]. This finishes the proof of (III.23). □

The following proposition is a general result on multiplicative cascades, for which we provide a proof for completeness. Although results of this flavor are omnipresent in the literature and its proof idea, using multiplicative martingales, is by now standard, we could not find a suitable reference in the literature working under our minimal assumptions.

Proposition III.16. *Let $(Z_u)_u$ be a multiplicative cascade with $Z_\emptyset = 1$. Suppose that $\mathbb{E}[\sum_{i=1}^\infty Z_i] = 1$. Furthermore, suppose there exists a measurable function $\phi : \mathbb{R}_+ \to [0,1]$ satisfying $\phi(0) = 1$, $1 - \phi(x) \sim x$ as $x \to 0$, and*

$$\forall x \geq 0 : \phi(x) = \mathbb{E}\left[\prod_{i=1}^\infty \phi(xZ_i)\right].$$

Then the martingale $W_n = \sum_{|u|=n} Z_u$ is uniformly integrable and its limiting random variable has Laplace transform ϕ.

Proof. We first note that $(W_n)_{n\geq 0}$ is a non-negative martingale and thus converges a.s. to a limit W_∞. It is easy to show that this implies that $\max_{|u|=n} Z_u \to 0$ a.s., as $n \to \infty$.

Now introduce for every $x \geq 0$ the process $M_n(x) = \prod_{|u|=n} \phi(xZ_u)$, $n \geq 0$. It is well-known and easy to show that for every $x \geq 0$, $(M_n(x))_{n\geq 0}$ is a martingale, called a *multiplicative martingale* associated to the multiplicative cascade $(Z_u)_u$. It takes values in $[0,1]$ and therefore converges a.s. and in L^1 to a limit $M_\infty(x)$. Furthermore, since $1 - \phi(x) \sim x$ as $x \to 0$ by assumption and $\max_{|u|=n} Z_u \to 0$ a.s., as $n \to \infty$,

$$\log M_\infty(x) = \lim_{n\to\infty} \sum_{|u|=n} \log \phi(xZ_u) = \lim_{n\to\infty} \sum_{|u|=n} (-xZ_u) = -xW_\infty.$$

This shows that for every $x \geq 0$,

$$\phi(x) = M_0(x) = \mathbb{E}[M_\infty(x)] = \mathbb{E}[e^{-xW_\infty}],$$

Hence, ϕ is the Laplace transform of W_∞. Moreover, since $1 - \phi(x) \sim x$ as $x \to 0$, the r.v. W_∞ has unit expectation. Scheffé's lemma then gives that W_n converges in L^1 to W_∞, hence the martingale $(W_n)_{n\geq 0}$ is uniformly integrable. □

Proof of Theorem III.12. By Lemma III.15 and Proposition III.16, it suffices to show that $1-\psi_{\alpha,2}(x) \sim x/(\alpha-3/2)$ as $x \to 0$ (if $\alpha > 3/2$), and $1-\psi_{\alpha,2\alpha-1}(x) \sim (\Gamma(3/2-\alpha)/\Gamma(\alpha+1/2))x$ as $x \to 0$ (if $\alpha < 3/2$). But this is an easy consequence of (III.21), noting that the second-order term as $z \to 0$ is the $n = 1$ term of the first sum if $\alpha > 3/2$ ($\nu > 1$), whereas it is the $n = 0$ term of the second sum if $\alpha < 3/2$ ($\nu < 1$). □

4.3 L^p-convergence of the additive martingales

The additive martingales introduced in Section 4.1 are important observables of the multiplicative cascade Z_α and it is vital to know that they do not display pathological behavior. This is ensured by the following proposition:

Proposition III.17. *Let $p > 1$ and $\theta \in (\alpha, \alpha + 1)$ be such that $\log \phi_\alpha(p\theta) < p \log \phi_\alpha(\theta)$. Then the martingale $(W_n(\alpha, \theta))_{n\geq 0}$ converges in L^p.*

The proposition will follow from classical results once the following lemma is established:

Lemma III.18. *Let $\theta \in (\alpha, \alpha + 1)$. Then,*

$$\mathbb{E}\left[(W_1(\alpha, \theta))^p\right] < \infty \qquad \textit{for every } p < (\alpha + 1)/\theta.$$

Proof of Proposition III.17. Let p and θ as in the statement of the proposition. A classical result by Biggins [Big92, Theorem 1] then gives the required convergence, provided $\mathbb{E}\left[(W_1(\alpha, \theta))^p\right] < \infty$. But by the hypothesis on p and θ, we necessarily have $p\theta < \alpha + 1$, since $\phi_\alpha(\lambda) = +\infty$ for $\lambda \geq \alpha + 1$. Lemma III.18 then implies the result. □

Proof of Lemma III.18. Throughout the proof, we denote by C and C_ε arbitrary positive, finite constants, whose values may change from line to line. They may depend on α and the constant C_ε may furthermore depend on $\varepsilon > 0$ introduced later. Recall the definition of the multiplicative cascade in terms of a spectrally positive α-stable Lévy process ζ. It is well-known that τ, the hitting time of -1 by ζ, is a positive $1/\alpha$-stable random variable. We collect some well-known estimates on its density, see e.g. [Zol86, Chapter 2.5]:

$$\mathbb{P}(\tau \in dt) \sim Ct^{-1/\alpha-1}, \quad t \to \infty \tag{III.32}$$

$$\mathbb{P}(\tau \in dt) = \exp(-(1 + o(1))t^{-1/\alpha-1}), \quad t \to 0. \tag{III.33}$$

We now bound the tail of $W_1(\alpha, \theta)$. Let $x \mapsto t_x$, $\mathbb{R}_+ \to \mathbb{R}_+$ be an arbitrary function for the moment, whose value we will choose later on. Then, for all $x \geq 0$,

$$\begin{aligned}\mathbb{P}(W_1(\alpha, \theta) > x) &= C\mathbb{E}\left[\frac{1}{\tau}\mathbf{1}_{\sum_{s\leq\tau}(\Delta\zeta_s)^\theta > x}\right] \\ &= C\mathbb{E}\left[\frac{1}{\tau}\mathbf{1}_{\sum_{s\leq\tau}(\Delta\zeta_s)^\theta > x, \tau > t_x}\right] + C\mathbb{E}\left[\frac{1}{\tau}\mathbf{1}_{\sum_{s\leq\tau}(\Delta\zeta_s)^\theta > x, \tau \leq t_x}\right].\end{aligned} \tag{III.34}$$

By (III.32), we bound the first summand on the right-hand side of (III.34) for large x by

$$\mathbb{E}\left[\frac{1}{\tau}\mathbf{1}_{\sum_{s\le\tau}(\Delta\zeta_s)^\theta>x,\,\tau>t_x}\right] \le \mathbb{E}\left[\frac{1}{\tau}\mathbf{1}_{\tau>t_x}\right] \le C(t_x)^{-(1/\alpha+1)}. \tag{III.35}$$

As for the second summand, we use Hölder's inequality to get for every $\varepsilon>0$,

$$\mathbb{E}\left[\frac{1}{\tau}\mathbf{1}_{\sum_{s\le\tau}(\Delta\zeta_s)^\theta>x,\,\tau\le t_x}\right] \le \mathbb{E}\left[\frac{1}{\tau^{1/\varepsilon}}\right]^{\varepsilon}\mathbb{P}\left(\sum_{s\le\tau}(\Delta\zeta_s)^\theta>x,\,\tau\le t_x\right)^{1-\varepsilon}. \tag{III.36}$$

By (III.33),

$$\mathbb{E}\left[\frac{1}{\tau^{1/\varepsilon}}\right]^{\varepsilon}\le C_\varepsilon. \tag{III.37}$$

We continue with bounding the probability on the right-hand side in (III.36). Since ζ is α-stable, there is a constant $\rho\in(0,1)$, such that $\mathbb{P}(\zeta_s\le 0)=\rho$ for all $s\ge 0$. Applying this with the Markov property at time τ, we get

$$\begin{aligned}
&\rho\mathbb{P}\left(\sum_{s\le\tau}(\Delta\zeta_s)^\theta>x,\,\tau\le t_x\right)\\
&=\mathbb{P}\left(\sum_{s\le t_x}(\Delta\zeta_s)^\theta>x,\,\tau\le t_x,\,\zeta_{t_x}\le -1\right)\\
&\le \mathbb{P}\left(\sum_{s\le t_x}(\Delta\zeta_s)^\theta>x,\,\max_{s\le\tau}(\Delta\zeta_s)^\theta\le\delta x\right)+\mathbb{P}\left(\max_{s\le t_x}(\Delta\zeta_s)^\theta>\delta x,\,\zeta_{t_x}\le -1\right),
\end{aligned}$$

where δ is some small positive constant. Classical large-deviation estimates for sums of iid heavy-tailed random variables [Nag79] yield that the first term on the right-hand side is for large x smaller than any fixed polynomial in x as long as $t_x\le x^{\alpha/\theta-\varepsilon}$ and δ is sufficiently small. As for the second term on the right-hand side, denote by $\widetilde{\zeta}$ a process defined as ζ, except that all the jumps greater than $(\delta x)^{1/\theta}$ are suppressed. Then, by independence of the large and small jumps,

$$\mathbb{P}\left(\max_{s\le t_x}(\Delta\zeta_s)^\theta>\delta x,\,\zeta_{t_x}\le -1\right)\le\mathbb{P}(-\widetilde{\zeta}_{t_x}\ge(\delta x)^{1/\theta}).$$

One easily checks that as $x\to\infty$, $|\mathbb{E}[\widetilde{\zeta}_{t_x}]|\sim t_xC(\delta x)^{-(\alpha-1)/\theta}=o(\delta x)^{1/\theta})$ as long as $t_x=o(x^{\alpha/\theta})$. Hence, the event in the above probability is a large deviation event. By the finiteness of the moment generating function of $-\widetilde{\zeta}$ for positive values of the argument, the Chernoff bound easily implies that the probability $\mathbb{P}(-\widetilde{\zeta}_{t_x}\ge(\delta x)^{1/\theta})$ decays streched exponentially in x, as long as $t_x\le x^{\alpha/\theta-\varepsilon}$.

Summarizing the previous arguments, the probability

$$\mathbb{P}\left(\sum_{s\le\tau}(\Delta\zeta_s)^\theta>x,\,\tau\le t_x\right)$$

decreases superpolynomially in x as long as $t_x\le x^{\alpha/\theta-\varepsilon}$. Together with (III.34), (III.35), (III.36) and (III.37), we have for every $\varepsilon>0$, for large x,

$$\mathbb{P}(W_1(\alpha,\theta)>x)\le C_\varepsilon(t_x)^{-(1/\alpha+1)},$$

as long as $t_x\le x^{\alpha/\theta-\varepsilon}$. Choosing t_x to be equal to this bound, this gives for every $\varepsilon>0$, for large x, $\mathbb{P}(W_1(\alpha,\theta)>x)\le C_\varepsilon x^{-(1+\alpha)/\theta+\varepsilon}$. This readily implies the statement of the lemma. $\square$

5 Convergence towards the continuous multiplicative cascade

In this section we prove our main result Theorem III.1. We do it step by step in order to emphasize the different requirements for the different types of convergence.

5.1 Finite dimensional convergence

Proposition III.19 (Finite dimensional convergence)**.** *With the notation of Theorem III.1 we have the following convergence in distribution in the sense of finite-dimensional marginals*

$$(p^{-1}\chi^{(p)}(u) : u \in \mathcal{U}) \quad \xrightarrow[p\to\infty]{(d)} \quad (Z_\alpha(u) : u \in \mathcal{U}).$$

Proof. This is a more or less straightforward corollary of the convergence of the first generation (Proposition III.4) together with the Markov property in the gasket decomposition. Recall the notation of the introduction and in particular $\chi^{(p)}(\varnothing) = p$, recall also that $(\xi_i^{(u)} : i \geq 1)_{u\in\mathcal{U}}$ are independent random variables distributed according to ν_α and indexed by $\mathcal{U}$. Fix $k_0 \geq 1$. It follows from Proposition III.4 that we have

$$\left(\frac{\chi^{(p)}(i)}{\chi^{(p)}(\varnothing)}\right)_{1\leq i\leq k_0} \xrightarrow[p\to\infty]{(d)} \left(\xi_i^{(u)}\right)_{1\leq i\leq k_0}.$$

Now, it follows from the gasket decomposition that conditionally on the perimeters $(\chi^{(p)}(i) : 1 \leq i \leq k_0)$ of the first generation of the loops, the loop-decorated quadrangulations filling in the first k_0 holes (ranked in decreasing order of their perimeters) in the gasket are independent and distributed according to $\mathbb{P}_{g,h,n}^{\chi^{(p)}(i)}$. Since we have $\chi^{(p)}(k_0) \to \infty$ in probability (indeed $\frac{1}{p}\chi^{(p)}(k_0) \to Z_\alpha(k_0)$ in distribution and $Z_\alpha(k_0) > 0$ almost surely) we can then apply Proposition III.4 once more to these second generation quadrangulations to deduce that

$$\left(\frac{\chi^{(p)}(ij)}{\chi^{(p)}(i)}\right)_{1\leq j\leq k_0} \xrightarrow[p\to\infty]{(d)} \left(\xi_j^{(i)}\right)_{1\leq j\leq k_0},$$

and these convergences in law hold jointly for all $i \in \varnothing \cup \{1, 2, ..., k_0\}$. Iterating the above argument we get that for any finite subtree $\mathfrak{t} \subset \mathcal{U}$ containing the root and for any vertex $u, ui \in \mathfrak{t}$ we have the joint convergences $\chi^{(p)}(ui)/\chi^{(p)}(u) \to \xi_i^{(u)}$ in distribution. This implies the finite dimensional convergence. □

5.2 ℓ^∞ convergence generation by generation

In this subsection we strengthen Proposition III.19 into a convergence in ℓ^∞ for any finite number of generations. Indeed, the convergence of Proposition III.19 does not prevent $\chi^{(p)}$ from having $\chi^{(p)}(u) \asymp p$ at some vertex $u \to \infty$ (i.e. u leaves any fixed finite subset of $\mathcal{U}$) as $p \to \infty$. The following statement shows that this is impossible if the height of u stays bounded. For any $k \geq 1$ let $\mathcal{U}_k$ be subtree of the first k generations in $\mathcal{U}$.

Proposition III.20. *For any $k \geq 1$ we have the following convergence in distribution in $\ell^\theta(\mathcal{U}_k)$ for all $\theta > \alpha$*

$$(p^{-1}\chi^{(p)}(u) : u \in \mathcal{U}_k) \quad \xrightarrow[p\to\infty]{(d)} \quad (Z_\alpha(u) : u \in \mathcal{U}_k).$$

As it will turn out, the last proposition is a consequence of the finite-dimensional convergence (Proposition III.19) together with a convergence in mean of the sum of powers in the cascade. More precisely we will use:

Lemma III.21. *For any $\theta \in (\alpha, \alpha+1)$ and for any $k \geq 1$ we have*

$$\mathbb{E}\left[\sum_{u \in \mathcal{U}:|u|=k} \Big(p^{-1}\chi^{(p)}(u)\Big)^{\theta}\right] \xrightarrow[p\to\infty]{} \mathbb{E}\left[\sum_{u \in \mathcal{U}:|u|=k} \Big(Z_\alpha(u)\Big)^{\theta}\right] = \phi_\alpha(\theta)^k.$$

Proof. We prove the convergence by induction on $k \geq 1$. Using the notation of Section 2.2 and in particular (III.8) as well as (III.9) we have

$$\mathbb{E}\left[\sum_{|u|=k} (p^{-1}\chi^{(p)}(u))^{\theta}\right] \leq \frac{1}{\mathbb{E}[1/L_p]}\mathbb{E}\left[\frac{1}{L_p}\sum_{1\leq i\leq T_p}\left(\frac{X_i+1}{p}\right)^{\theta}\right] + O(p^{-1}).$$

The inequality comes from the fact that some faces (of degree four) of the gasket are not holes surrounded by a loop and the $O(p^{-1})$ from the approximation $L_p \approx L_p + 1$ (Recall that $p \leq L_p \leq T_p$). By Fatou's lemma the right-hand side in Lemma III.21 is less than the liminf of the left-hand side. Therefore it suffices to prove that the right-hand side in the last display converges towards $\phi_\alpha(\theta)$. This will be shown using Theorem III.3 and the approximation

$$\mu_{\mathrm{JS}}(0)\frac{1}{L_p}\sum_{i=1}^{T_p}\left(\frac{X_i+1}{p}\right)^{\theta} \approx U_p^{(\theta)} := \frac{1}{T_p}\sum_{i=1}^{T_p}\left(\frac{X_i+1}{p}\right)^{\theta}. \tag{III.38}$$

Indeed since $T_p \geq p$, by Theorem III.3 we can write

$$\mathbb{E}[U_p^{(\theta)}] = \mathbb{E}\left[\frac{1}{T_p-1}\sum_{i=1}^{T_p}\left(\frac{X_i+1}{p}\right)^{\theta}\right]\cdot(1+O(p^{-1})) = \mathbb{E}\left[\left(\frac{X_1+1}{p}\right)^{\theta}\frac{p}{p+X_1}\right]\cdot(1+O(p^{-1})).$$

Recall that $p^\alpha\,\mathbb{P}(X_1 \geq xp) \to \pi([x,\infty))$ where $\pi(\mathrm{d}x) = Cx^{-\alpha-1}/\Gamma(-\alpha)\mathbb{1}_{\{x>0\}}$ is the Lévy measure of the α-stable Lévy process ζ. As in the proof of Proposition III.7, we can use dominate convergence to get that

$$p^\alpha \cdot \mathbb{E}[U_p^{(\theta)}] \xrightarrow{p} \int \frac{x^\theta}{1+x}\pi(\mathrm{d}x) = \mathbb{E}\left[\frac{1}{\tau}\sum_{t\leq\tau}(\Delta\zeta_t)^\theta\right].$$

We have already seen in the proof of Theorem III.4 that $p^\alpha\cdot\mathbb{E}[\mu_{\mathrm{JS}}(0)/L_p] \to \mathbb{E}[1/\tau]$. Provided that the approximation (III.38) holds in expectation with an error of order $o(p^{-\alpha})$, we can gather the pieces and indeed deduce the desired convergence for $k=1$ by the calculation done in Section 4.1.

To justify (III.38), for our fixed $\theta \in (\alpha, \alpha+1)$, let $\gamma, \gamma' > 1$ be such that $\gamma\theta < \alpha+1$ and $\frac{1}{\gamma}+\frac{1}{\gamma'} = 1$, then

$$\begin{aligned}
\left|\mathbb{E}\left[\mu_{\mathrm{JS}}(0)\cdot\frac{T_p}{L_p}U_p^{(\theta)}\right] - \mathbb{E}\left[U_p^{(\theta)}\right]\right| &\leq \mathbb{E}\left[\left|\mu_{\mathrm{JS}}(0)\frac{T_p}{L_p}-1\right|\cdot U_p^{(\theta)}\right] \\
&\leq \mathbb{E}\left[\left|\mu_{\mathrm{JS}}(0)\frac{T_p}{L_p}-1\right|^{\gamma'}\right]^{\frac{1}{\gamma'}}\cdot\mathbb{E}\left[(U_p^{(\theta)})^{\gamma}\right]^{\frac{1}{\gamma}} \quad \text{(Hölder's inequality)} \\
&\leq \mathbb{E}\left[\left|\mu_{\mathrm{JS}}(0)\frac{T_p}{L_p}-1\right|^{\gamma'}\right]^{\frac{1}{\gamma'}}\cdot\mathbb{E}\left[U_p^{(\gamma\theta)}\right]^{\frac{1}{\gamma}} \quad \text{(Jensen's inequality)}
\end{aligned}$$

The large deviation bound (III.12) and (III.13) imply that $\mathbb{E}\left[|\mu_{\mathrm{JS}}(0)T_p/L_p - 1|^{\gamma'}\right]$ tends to 0 faster than $p^{-\alpha\gamma'/4}$ as $p \to \infty$. On the other hand, the above calculation shows that $\mathbb{E}[U_p^{(\gamma\theta)}]$ is of order $p^{-\alpha}$. Hence the right-hand side of the last display is of order $o(p^{-\alpha/4-\alpha/\gamma})$. By choosing γ close enough to 1 this can be made smaller than $p^{-\alpha}$. This justifies our approximation (III.38).

Now assume that the convergence of the lemma takes place up to the k-th generation and write

$$G_k(p) = \mathbb{E}\left[\sum_{|u|=k} \left(p^{-1}\chi^{(p)}(u)\right)^{\theta}\right],$$

to simplify notation. Then there exists a constant $C = C(k,\theta)$ such that $G_k(p) \le C$ for all $p \ge 1$, and for any $\varepsilon > 0$ there exists p_0 such that for all $p \ge p_0$,

$$G_k(p) \le \phi_\alpha(\theta)^k + \varepsilon.$$

Using the Markov property of the gasket decomposition at the first generation we get with the above two inequalities, for all $p \ge 1$,

$$\begin{aligned} G_{k+1}(p) &= \mathbb{E}\left[\sum_{i=1}^{\infty} \left(\frac{\chi^{(p)}(i)}{p}\right)^{\theta} G_k(\chi^{(p)}(i))\right] \\ &\le \left(\phi_\alpha(\theta)^k + \varepsilon\right) \mathbb{E}\left[\sum_{i=1}^{\infty} \left(\frac{\chi^{(p)}(i)}{p}\right)^{\theta} \mathbb{1}_{\{\chi^{(p)}(i) \ge p_0\}}\right] + C\mathbb{E}\left[\sum_{i=1}^{\infty} \left(\frac{\chi^{(p)}(i)}{p}\right)^{\theta} \mathbb{1}_{\{\chi^{(p)}(i) < p_0\}}\right] \end{aligned}$$

By the $k = 1$ case, the first term on the right-hand side is bounded using

$$\mathbb{E}\left[\sum_{i=1}^{\infty} \left(\frac{\chi^{(p)}(i)}{p}\right)^{\theta} \mathbb{1}_{\{\chi^{(p)}(i) \ge p_0\}}\right] \le \mathbb{E}\left[\sum_{i=1}^{\infty} \left(\frac{\chi^{(p)}(i)}{p}\right)^{\theta}\right] \quad \xrightarrow[p\to\infty]{} \quad \phi_\alpha(\theta).$$

As for the second term, fix $\theta' \in (\alpha, \theta)$ then for $p \ge p_0$ we can write

$$\mathbb{E}\left[\sum_{i=1}^{\infty} \left(\frac{\chi^{(p)}(i)}{p}\right)^{\theta} \mathbb{1}_{\{\chi^{(p)}(i) < p_0\}}\right] \le \left(\frac{p_0}{p}\right)^{\theta-\theta'} \mathbb{E}\left[\sum_{i=1}^{\infty} \left(\frac{\chi^{(p)}(i)}{p}\right)^{\theta'}\right] \quad \xrightarrow[p\to\infty]{} \quad 0,$$

by the $k = 1$ case proven above (with θ replaced by θ'). Taking the limits $p \to \infty$ and then $\varepsilon \to 0$, we get the upper bound

$$\limsup_{p\to\infty} G_{k+1}(p) \;\le\; \phi_\alpha(\theta)^{k+1},$$

whereas the lower bound $\liminf_{p\to\infty} G_{k+1}(p) \;\ge\; \phi_\alpha(\theta)^{k+1}$ is trivial from the finite-dimensional convergence together with Fatou's lemma. □

Proof of Proposition III.20. Since the identity function $\iota : \ell^{\theta}(\mathcal{U}_k) \to \ell^{\theta'}(\mathcal{U}_k)$ is continuous for all $\theta \le \theta'$, it suffices to prove the convergence in distribution for all θ close enough to α. Fix $\theta \in (\alpha, \alpha+1)$ and $k \ge 1$. Since $\mathbb{E}\left[\sum_{u\in\mathcal{U}_k} (Z_\alpha(u))^{\theta}\right] = 1 + \phi_\alpha(\theta) + \cdots + \phi_\alpha(\theta)^k < \infty$, for any $\varepsilon > 0$ there is a finite subset $V \subset \mathcal{U}_k$ such that

$$\mathbb{E}\left[\sum_{u\in\mathcal{U}_k\setminus V} (Z_\alpha(u))^{\theta}\right] < \varepsilon^{\theta}.$$

According to the convergence in Lemma III.21, we have

$$\limsup_{p\to\infty} \mathbb{E}\left[\sum_{u\in\mathcal{U}_k\setminus V} \left(p^{-1}\chi^{(p)}(u)\right)^{\theta}\right] \le \varepsilon^{\theta}. \tag{III.39}$$

Now if $f : \ell^{\theta}(\mathcal{U}_k) \to \mathbb{R}_+$ is a bounded K-Lipschitz function we have

$$\Big|\mathbb{E}\left[f(Z_\alpha)\right] - \mathbb{E}\left[f(Z_\alpha \mathbb{1}_V)\right]\Big| \le K\cdot\mathbb{E}\left[\Big|Z_\alpha - Z_\alpha\mathbb{1}_V\Big|_\theta\right] \underset{\text{Hölder}}{\le} K\cdot\left(\mathbb{E}\left[\sum_{u\in\mathcal{U}_k\setminus V}(Z_\alpha(u))^{\theta}\right]\right)^{1/\theta} \le K\cdot\varepsilon\,,$$

and similarly $\mathbb{E}[f(p^{-1}\chi^{(p)})] \approx \mathbb{E}[f(p^{-1}\chi^{(p)}\mathbb{1}_V)]$ up to an error of order ε as $p\to\infty$. From the finite-dimensional convergence (Proposition III.19) we deduce that $\mathbb{E}\left[f(p^{-1}\chi^{(p)}\mathbb{1}_V)\right] \to \mathbb{E}\left[f(Z_\alpha\mathbb{1}_V)\right]$ as $p\to\infty$. Put all together this shows $\mathbb{E}\left[f(p^{-1}\chi^{(p)})\right] \to \mathbb{E}\left[f(Z_\alpha)\right]$ as $p\to\infty$ and proves the desired convergence in distribution. ☐

5.3 ℓ^∞ convergence

As we already notice, Proposition III.20 implies the convergence of $p^{-1}\chi^{(p)} \longrightarrow Z_\alpha$ in $\ell^\infty(\mathcal{U}_k)$. However, it does not yet yield the full convergence in $\ell^\infty(\mathcal{U})$ and the missing estimate is of the form: for any $\varepsilon > 0$, there exists an integer k such that

$$\limsup_{p\to\infty} \mathbb{P}\left(\exists\, u \in \mathcal{U}\setminus\mathcal{U}_k \,:\, \chi^{(p)}(u) \ge \varepsilon p\right) \le \varepsilon. \tag{III.40}$$

In other words, the labels beyond generation k are uniformly small when k is large. Notice that if we had replaced $p^{-1}\chi^{(p)}$ by the limiting cascade Z_α, the estimate would be immediate: by the remark after (III.19), the process (Z_α) almost surely belongs to $\ell^\theta(\mathcal{U})$ for a certain $\theta > 0$. Our way to prove (III.40) is similar as in the continuous case and we want to find a supermartingale of the form

$$\left(\sum_{|u|=k} f\left(\chi^{(p)}(u)\right)\right)_{k\ge 0}$$

where f is an increasing function. The underlying quadrangulation model provides us naturally one such supermartingale: for $p \ge 1$, let $\overline{V}(p)$ be the expected volume (i.e. number of vertices) of a random loop-decorated quadrangulation of distribution $\mathbb{P}^{(p)}_{g,h,n}$. Then the gasket decomposition (Section 2.1) immediately shows that we have the strict inequality for all p:

$$\mathbb{E}\left[\sum_{i=1}^{\infty} \overline{V}\left(\chi^{(p)}(i)\right)\right] < \overline{V}(p). \tag{III.41}$$

In particular, $(\sum_{|u|=k}\overline{V}(\chi^{(p)}(u)),\, k\ge 0)$ is indeed a supermartingale for the discrete cascade. Timothy Budd recently proved the following asymptotics of $\overline{V}(p)$:

Theorem III.B ([Bud17])**.** *Recall that* $\theta_\alpha = \max(2\alpha-1, 2)$*. Then we have* $\overline{V}(p) \underset{p\to\infty}{\sim} Cp^{\theta_\alpha}$ *for some* $C > 0$ *which depends only on the parameters of the model.*

With this estimate, one can proceed to the proof of Theorem III.1.

Proof of the $\ell^\infty(\mathcal{U})$ convergence. Recall that we assume $n < 2$, so that $\alpha \neq \frac{3}{2}$ and $\inf \phi_\alpha < 1$. Choose θ such that $\phi_\alpha(\theta) < 1$. Then by Lemma III.21, there exist finite constants C, p_0 and $c < 1$ such that

$$\mathbb{E}\left[\sum_{i=1}^{\infty}\left(p^{-1}\chi^{(p)}(i)\right)^{\theta}\right] \leq \begin{cases} C & \text{for all } p \geq 1 \\ c & \text{for all } p \geq p_0 \end{cases} \tag{III.42}$$

This inequality indicates that the θ-moment decreases exponentially as long as the labels do not drop below p_0 too often. To make this idea precise, for $u \in \mathcal{U}$ let $N_0(u)$ be the number of ancestors of u which have a label smaller than p_0. The following lemma controls the size of $\chi^{(p)}(u)$ depending on whether $N_0(u)$ is smaller or greater than a threshold m.

Lemma III.22. *(i) For all $k \geq m \geq 0$ we have*

$$\mathbb{E}\left[\sum_{u\in\mathcal{U}:|u|=k}\left(\frac{\chi^{(p)}(u)}{p}\right)^{\theta}\mathbb{1}_{\{N_0(u)\leq m\}}\right] \leq C^m c^{k-m}. \tag{III.43}$$

(ii) Consider the set of vertices $L_m = \inf\{u \in \mathcal{U} : N_0(u) \geq m\}$ where the infimum of a subset $U \subset \mathcal{U}$ is defined by $\inf U = \{u \in U : u$ has no ancestor in $U\}$. Then there exists $\tilde{c} < 1$ such that for all p and m,

$$\mathbb{E}\left[\sum_{u\in L_m}\overline{V}\left(\chi^{(p)}(u)\right)\right] \leq \tilde{c}^{m-1}\overline{V}(p) \tag{III.44}$$

By Markov's inequality, (III.43) and (III.44) imply respectively

$$\mathbb{P}\left(\exists\, u \in \mathcal{U}\setminus\mathcal{U}_k : N_0(u) \leq m \text{ and } \chi^{(p)}(u) \geq \varepsilon p\right) \leq \varepsilon^{-\theta}\sum_{l>k} C^m c^{l-m} = \varepsilon^{-\theta}\left(\frac{C}{c}\right)^m \frac{c^{k+1}}{1-c}$$

and $$\mathbb{P}\left(\exists\, u \in \mathcal{U} : N_0(p) > m \text{ and } \chi^{(p)}(u) \geq \varepsilon p\right) \leq \tilde{c}^m \frac{\overline{V}(p)}{\overline{V}(\varepsilon p)}$$

Take the sum of the two inequalities and use the asymptotics of $\overline{V}$ in Theorem III.B to show that

$$\limsup_{p\to\infty}\mathbb{P}\left(\exists\, u \in \mathcal{U}\setminus\mathcal{U}_k \,:\, \chi^{(p)}(u) \geq \varepsilon p\right) \leq \varepsilon^{-\theta}\left(\frac{C}{c}\right)^m \frac{c^{k+1}}{1-c} + \tilde{c}^m\varepsilon^{-\theta_\alpha}.$$

The right-hand side tends to zero when $k, m \to \infty$ under the constraint $\frac{k}{m} \geq \frac{\log C - \log c}{-\log c} + \varepsilon$. This proves the bound (III.40) and the $\ell^\infty(\mathcal{U})$ convergence in Theorem III.1 modulo Lemma III.22. □

Proof of Lemma III.22. We prove the bound (III.43) by induction on k. We write

$$M_{k,m}(p) = \mathbb{E}\left[\sum_{u\in\mathcal{U}:|u|=k}\left(\frac{\chi^{(p)}(u)}{p}\right)^{\theta}\mathbb{1}_{\{N_0(u)\leq m\}}\right]$$

to simplify notation. In the case $k = 1$ (and $m \in \{0, 1\}$) the only ancestor of the first generation is the root and the estimate follows from (III.42). If $k \geq 1$ then we distinguish according to:

- If $p \geq p_0$, then for all $i \geq 1$ and $u \in \mathcal{U}$, we have $N_0(iu) = N_0^{(i)}(u)$, where $N_0^{(i)}$ is a copy of the function N_0 defined on the sub-tree rooted at the vertex i. It follows that

$$\begin{aligned}
M_{k+1,m}(p) &= \mathbb{E}\left[\sum_{i=1}^{\infty}\left(\frac{\chi^{(p)}(i)}{p}\right)^{\theta} \sum_{u\in\mathcal{U}:|u|=k}\left(\frac{\chi^{(p)}(iu)}{\chi^{(p)}(i)}\right)^{\theta} \mathbb{1}_{\left\{N_0^{(i)}(u)\leq m\right\}}\right] \\
&= \mathbb{E}\left[\sum_{i=1}^{\infty}\left(\frac{\chi^{(p)}(i)}{p}\right)^{\theta} M_{k,m}\left(\chi^{(p)}(i)\right)\right] \qquad \text{(Markov property of the cascade)} \\
&\leq C^m c^{k-m}\, \mathbb{E}\left[\sum_{i=1}^{\infty}\left(p^{-1}\chi^{(p)}(i)\right)^{\theta}\right] \qquad \text{(induction hypothesis)} \\
&\leq C^m c^{k+1-m}.
\end{aligned}$$

- If $p < p_0$, then we have $N_0(iu) = N_0^{(i)}(u) + 1$ and hence for $m \geq 1$,

$$\begin{aligned}
M_{k+1,m}(p) &= \mathbb{E}\left[\sum_{i=1}^{\infty}\left(\frac{\chi^{(p)}(i)}{p}\right)^{\theta} M_{k,m-1}\left(\chi^{(p)}(i)\right)\right] \\
&\leq C^{m-1}c^{k-(m-1)}\, \mathbb{E}\left[\sum_{i=1}^{\infty}\left(p^{-1}\chi^{(p)}(i)\right)^{\theta}\right] \leq C^m c^{k+1-m}.
\end{aligned}$$

  For $m = 0$, we have $M_{k+1,0}(p) = 0$ since $p < p_0$. This completes the induction.

Let us move to the second point of the lemma. To show (III.44), first remark that (III.41) implies the existence of a constant $\tilde{c} < 1$ such that

$$\mathbb{E}\left[\sum_{i=1}^{\infty}\overline{V}\left(\chi^{(p)}(i)\right)\right] \leq \tilde{c}\,\overline{V}(p) \tag{III.45}$$

for all $p \leq p_0$. To simplify notation, we will write $\hat{V}(U) = \mathbb{E}\left[\sum_{u\in U}\overline{V}(\chi^{(p)}(u))\right]$ for any subset $U \subset \mathcal{U}$.

For $k \geq 1$, let $L_k = \inf\{u \in \mathcal{U} : N_0(u) \geq k\}$ and $L_k^+ = \{ui : u \in L_k,\ i \in \mathbb{N}^*\}$ (L_k^+ is the set of children of L_k). From the definition of $N_0(.)$ it is not hard to see that $\chi^{(p)}(u) \leq p_0$ for all $u \in L_k$. The random sets L_k, L_k^+ are so-called *optional lines* for the filtration generated by the process $\chi^{(p)}$ (see e.g. [BK04]) and we have

$$\{\varnothing\} = L_0 \prec L_0^+ \preceq L_1 \prec L_1^+ \preceq L_2 \prec L_2^+ \preceq L_3 \prec \cdots$$

where we used the partial order on the subsets of $\mathcal{U}$ defined by $U \preceq \tilde{U}$ if each vertex $u \in \tilde{U}$ either is in U or has an ancestor in U. On the one hand, by general theory on optional lines, if $L \preceq L'$ are two optional lines then $\hat{V}(L) \geq \hat{V}(L')$. On the other hand, since $\chi^{(p)}(u) \leq p_0$ for all $u \in L_k$ we can use (III.45) to deduce that

$$\hat{V}(L_k^+) = \mathbb{E}\left[\sum_{u\in L_k}\overline{V}\left(\chi^{(p)}(u)\right)\cdot\mathbb{E}\left[\sum_{i=1}^{\infty}\frac{\overline{V}\left(\chi^{(q)}(i)\right)}{\overline{V}(q)}\right]_{q=\chi^{(p)}(u)}\right] \leq \tilde{c}\,\hat{V}(L_k).$$

Gathering the two inequalities we indeed deduce that $L_{m+1} \leq \tilde{c}^m\hat{V}(L_0) = \tilde{c}^m\overline{V}(p)$, as desired. ☐

A Relation with other nesting statistics

In this section, we outline the relation of our work to the recent work by Borot, Bouttier and Duplantier [BBD16] about the number of loops surrounding a typical vertex in a $O(n)$-decorated random planar map and to analogous quantities in conformal loop ensembles.

Number of loops surrounding a typical vertex in the $O(n)$-decorated quadrangulation. We consider a random *pointed* quadrangulation of (large) perimeter p decorated with an $O(n)$ loop model, as defined in the introduction of the main text. Borot, Bouttier and Duplantier [BBD16] have studied the large deviations of the number of loops surrounding the marked vertex, by methods from analytic combinatorics. With our notation, their result reads as follows:

Theorem III.C ([BBD16], Theorem 2.2)**.** *Let N denote the number of loops surrounding the marked vertex. Then, for all $x > 0$, as $p \to \infty$,*

$$\frac{1}{\log p} \log \mathbb{P}(N = \lfloor x \log p \rfloor) \longrightarrow -\frac{1}{\pi} J(\pi x),$$

$$\textit{where} \quad J(x) = x \log\left(\frac{2}{n}\frac{x}{\sqrt{1+x^2}}\right) + \operatorname{arccot}(x) - \arccos(\tfrac{n}{2}).$$

In fact, the result in [BBD16] is more precise in that the authors actually give an asymptotic equivalent for $\mathbb{P}(N = \lfloor x \log p \rfloor)$. Also note that there is a mistake in the definition of the function J in [BBD16] (the first x factor is missing).

We now sketch how we can heuristically recover this result from the continuous multiplicative cascade Z_α of Theorem III.1. Let $\delta > 0$ be a small constant. We define $\mathcal{L}_\delta$ to be the set of those vertices u in the Ulam tree for which $Z_\alpha(u) < \delta$ and $Z_\alpha(v) \geq \delta$ for every ancestor v of u. ($\mathcal{L}_\delta$ is an optional line, see the proof of Lemma III.22.) In the discrete setting, these vertices correspond to loops in a $O(n)$-decorated quadrangulation of perimeter p whose perimeter is smaller than δp, but the loops surrounding them have perimeter larger than δp.

Similarly to the definition of the martingale $W_n(\alpha, \theta)$ in (III.18) we now define

$$W^\delta(\alpha, \theta) = \sum_{u \in \mathcal{L}_\delta} Z_\alpha(u)^\theta \phi_\alpha(\theta)^{-|u|},$$

where as usual, $|u|$ denotes the generation of a vertex u in the Ulam tree. One can then show (for example with the methods from [BK04]) that $\mathbb{E}[W^\delta(\alpha, \theta)] = 1$ for every $\theta \in (\alpha, \operatorname{argmin}_\theta \phi_\alpha(\theta)) = (\alpha, \alpha + 1/2)$.

As a consequence, we have for such θ,

$$1 = \mathbb{E}[W^\delta(\alpha, \theta)] = \mathbb{E}\left[\sum_{u \in \mathcal{L}} Z_\alpha(u)^\theta \phi_\alpha(\theta)^{-|u|}\right] \approx \delta^\theta \mathbb{E}\left[\sum_{u \in \mathcal{L}_\delta} \phi_\alpha(\theta)^{-|u|}\right].$$

Now, as said before, every $u \in \mathcal{L}_\delta$ roughly corresponds to a loop in the $O(n)$ model of perimeter δp and $|u|$ is then the number of loops surrounding it. Assuming we could take $\delta = \frac{1}{p}$ this suggests that

$$\mathbb{E}[\sum_v \phi_\alpha(\theta)^{-N(v)}] \approx p^\theta, \quad \theta \in (\alpha, \alpha + 1/2), \tag{III.46}$$

where the sum is on the vertices of the loop-decorated quadrangulation and $N(v)$ is the number of loops separating the vertex v from the outerface.

We now write (III.46) in a different form in order to link it to Theorem III.C. First recall from Section 4.2 (or Theorem III.B) that the volume of the $O(n)$-decorated quandrangulation scales as p^{θ_0}, where $\theta_0 = \min(2, 2\alpha - 1)$. Equation (III.46) is then equivalent to

$$\mathbb{E}[\phi_\alpha(\theta)^{-N}] \approx p^{\theta-\theta_0}, \quad \theta \in (\alpha, \alpha + 1/2),$$

where N, as in Theorem III.C, is now the number of loops surrounding the marked vertex in a *pointed* $O(n)$-decorated quadrangulation. This allows to express the moment generating function of N by

$$\mathbb{E}[e^{\lambda N}] \approx p^{\kappa_\alpha(\lambda)}, \tag{III.47}$$

where $\kappa_\alpha(\lambda) = \phi_\alpha^{-1}(e^{-\lambda}) - \theta_0$, with ϕ_α^{-1} the inverse of the restriction of ϕ_α to $(\alpha, \alpha+1/2)$ and $\lambda < -\log \min_\theta \phi_\alpha(\theta)$. Now, (III.4) gives $\sin(\pi(2-\alpha)) = n/2$ and $\theta_0 - \alpha = \pi^{-1} \arcsin(n/2)$, so that we can express κ_α by

$$\kappa_\alpha(\lambda) = \frac{1}{\pi}\Big(\arcsin(\tfrac{n}{2}e^\lambda) - \arcsin(\tfrac{n}{2})\Big) = \frac{1}{\pi}\Big(\arccos(\tfrac{n}{2}) - \arccos(\tfrac{n}{2}e^\lambda)\Big), \quad \lambda < \log(\tfrac{2}{n}), \tag{III.48}$$

and $\kappa_\alpha(\lambda) = +\infty$ for $\lambda > \log(\frac{2}{n})$, by convexity.

Equation (III.47) now suggests that for every $x > 0$, as $p \to \infty$,

$$\frac{1}{\log p} \log \mathbb{P}(N = \lfloor x \log p \rfloor) \longrightarrow -\kappa_\alpha^*(x),$$

where $\kappa_\alpha^*(x) = \sup_{\lambda\in\mathbb{R}}\{\lambda x - \kappa_\alpha(x)\}$ is the Legendre–Fenchel transform of the function κ_α. Using the explicit expression in (III.48), a simple calculation shows:

$$\kappa_\alpha^*(x) = \frac{1}{\pi} J(\pi x), \quad x > 0,$$

where J is the function from Theorem III.C. This establishes (again, heuristically) that theorem.

Number of loops in a conformal loop ensemble surrounding a small Euclidean ball. We now show how one can heuristically relate (III.46) to a similar statement for the number of loops in a conformal loop ensemble in the unit disk surrounding a small Euclidean ball, thereby recovering (again heuristically) a result by Miller, Watson and Wilson [MWW16]. The argument is similar to the one by Borot, Bouttier and Duplantier [BBD16], but may be easier to understand since we avoid here the use of Legendre–Fenchel transforms. Recall from the introduction that it is conjectured that in a $O(n)$-decorated quadrangulation with boundary, the volume measure together with the loops converges in some sense to the so-called Liouville quantum disk (with parameter $\gamma = \sqrt{\kappa}$) together with an independent CLE_κ in the disk, where κ is related to our parameter α by $\alpha - \frac{3}{2} = 4/\kappa - 1$ (see (III.5)). For simplicity, we restrict ourselves to the dilute case ($\alpha > 3/2$, or $8/3 < \kappa < 4$). The result from [MWW16] is the following: Let $\widetilde{N}_r$ denote the number of CLE_κ loops surrounding a fixed Euclidean ball of radius $r \ll 1$. Then [MWW16],

$$\mathbb{E}[\psi_\kappa(\theta)^{-\widetilde{N}_r}] \approx r^{-\theta}, \tag{III.49}$$

where

$$\psi_\kappa(\theta) = \frac{-\cos(4\pi/\kappa)}{\cos(\pi\sqrt{(1-4/\kappa)^2 - 8\theta/\kappa})} = \frac{\cos(\pi(\alpha-3/2))}{\cos(\pi\sqrt{(\alpha-3/2)^2 - \theta(2\alpha-1)})}. \tag{III.50}$$

This function appeared already in [SSW09]. Note that we can express it as

$$\psi_\kappa(\theta) = \phi_\alpha\left(1 + \frac{4}{\kappa} - \sqrt{(1-4/\kappa)^2 - 8\theta/\kappa}\right), \tag{III.51}$$

where ϕ_α is the Biggins transform of the multiplicative cascade Z_α.

Here is an explanation for the relation (III.51): Denote by μ_κ the Liouville quantum gravity measure in the disk. We can then discretize the disk into blocks of μ_κ-mass approximately δ^2, for example by a dyadic decomposition as in [DS11]. Such a block is then the analogue of a vertex of the $O(n)$-decorated quadrangulation of perimeter p, with $\delta = 1/p$ (recall that in the dilute phase, the volume scales like the perimeter squared).

For each $c > 0$, denote by $\nu_{\delta,\delta^{1/c}}$ the number of blocks of diameter approximately $\delta^{1/c}$. It is implicit in [DS11] that

$$\nu_{\delta,\delta^{1/c}} \approx \delta^{-2+\frac{2}{c\kappa}(c-(1-\kappa/4))^2}. \tag{III.52}$$

For each block b, denote by $\widetilde{N}(b)$ the number of CLE loops surrounding the block. Equations (III.49) and (III.52) suggest that

$$\begin{aligned}\mathbb{E}[\sum_b \psi_\kappa(\theta)^{-\widetilde{N}(b)}] &\approx \sup_{c>0} \nu_{\delta,\delta^{1/2c}} \times \mathbb{E}[\psi_\kappa(\theta)^{-\widetilde{N}_{\delta^{1/c}}}] \\ &\approx \sup_{c>0} \delta^{-2+\frac{2}{c\kappa}(c-(1-\kappa/4))^2 - \frac{\theta}{c}}.\end{aligned}$$

A simple calculation shows that

$$\inf_{c>0} \frac{2}{c\kappa}(c-(1-\kappa/4))^2 - \frac{\theta}{c} = 1 - \frac{4}{\kappa} + \sqrt{(1-4/\kappa)^2 - 8\theta/\kappa},$$

for θ small enough. This gives

$$\mathbb{E}[\sum_b \psi_\kappa(\theta)^{-\widetilde{N}(b)}] \approx \delta^{-1-\frac{4}{\kappa}+\sqrt{(1-4/\kappa)^2-8\theta/\kappa}}. \tag{III.53}$$

On the other hand, by (III.46) we expect that

$$\mathbb{E}[\sum_b \phi_\kappa(\widetilde{\theta})^{-\widetilde{N}(b)}] \approx \delta^{-\widetilde{\theta}}, \tag{III.54}$$

for $\widetilde{\theta} \in (\alpha, \alpha+1/2)$. Comparing (III.53) and (III.54) suggests that $\psi_\kappa(\theta) = \phi_\alpha(\widetilde{\theta})$ if θ and $\widetilde{\theta}$ are related through

$$\widetilde{\theta} = 1 + \frac{4}{\kappa} - \sqrt{(1-4/\kappa)^2 - 8\theta/\kappa}.$$

This readily implies (III.51).

Chapter IV

Local limit of the critical-FK random map

This Chapter is adapted from [Che17].

1 Introduction

In this chapter we investigate the critical Fortuin-Kasteleyn (cFK) random map model. For each $q \in [0, \infty]$ and integer $n \geq 1$, this model chooses a planar map of n edges with a probability proportional to the partition function of critical q-Potts model on that map. Sheffield introduced the hamburger-cheeseburger bijection which maps the cFK random maps to a family of random words, and remarked that one can construct infinite cFK random maps using this bijection. We make this idea precise by a detailed proof of the local convergence. When $q = 1$, this provides an alternative construction of the UIPQ. In addition, we show that the limit is almost surely one-ended and recurrent for the simple random walk for any q, and mutually singular in distribution for different values of q.

Firest let use recall some basic defintions.

Subgraph-rooted maps and their dual. Recall from Chapter I that all maps that we consider are assumed to be *planar*. Self-loops and multiple edges are allowed in the underlying graph. A map is a *triangulation* (resp. a *quadrangulation*) if all of its faces are of degree three (resp. four). The *dual map* $\mathfrak{m}^\dagger$ of a planar map $\mathfrak{m}$ is obtained by putting one dual vertex in each face of $\mathfrak{m}$, and for each edge $\mathbf{e}$ of $\mathfrak{m}$, drawing one dual edge $\mathbf{e}^\dagger$ that links the two dual vertices in the two faces adjacent to $\mathbf{e}$.

A *rooted* map is a map with a distinguished corner $\mathbf{r}$. We call *root edge* the distinguished oriented edge on the left of $\mathbf{r}$, and *root vertex* (resp. *root face*) the vertex (resp. face) incident to $\mathbf{r}$. Rooting a map on a corner (instead of the more traditional choice of rooting on an oriented edge) allows a canonical choice of the root for the dual map: the dual root is obtained by exchanging the root face and the root vertex. A *subgraph* $\mathfrak{g}$ of a planar map $\mathfrak{m}$ is a graph consisting of a subset of the edges of $\mathfrak{m}$ and of all its vertices. Given a subgraph $\mathfrak{g}$ of a map $\mathfrak{m}$, the *dual subgraph*, denoted by $\mathfrak{g}^\dagger$, is the subgraph of $\mathfrak{m}^\dagger$ consisting of all the edges that do *not* intersect $\mathfrak{g}$. Following the terminology in [Ber07], we call *subgraph-rooted map* a rooted planar map with a distinguished subgraph. Figure IV.1(a) gives an example of a subgraph-rooted map with its dual.

Local limit. For subgraph-rooted maps, the local distance is defined by

$$d_{\mathtt{loc}}((\mathfrak{m},\mathfrak{g}),(\mathfrak{m}',\mathfrak{g}')) = \inf\left\{2^{-R}\,\middle|\, R\in\mathbb{N},\, B_R(\mathfrak{m},\mathfrak{g}) = B_R(\mathfrak{m}',\mathfrak{g}')\right\} \tag{IV.1}$$

where $B_R(\mathfrak{m},\mathfrak{g})$, the ball of radius R in $(\mathfrak{m},\mathfrak{g})$, is the subgraph-rooted map consisting of all vertices of $\mathfrak{m}$ at graph distance at most R from the root vertex and the edges between them. An edge of $B_R(\mathfrak{m},\mathfrak{g})$ belongs to the distinguished subgraph of $B_R(\mathfrak{m},\mathfrak{g})$ if and only if it is in $\mathfrak{g}$. The space of all finite subgraph-rooted maps is not complete with respect to $d_{\mathtt{loc}}$ and we denote by $\mathcal{M}$ its Cauchy completion. We call *infinite subgraph-rooted map* the elements of $\mathcal{M}$ which are not finite subgraph-rooted map. Note that with this definition all infinite maps are *locally finite*, that is, every vertex is of finite degree.

The study of infinite random maps goes back to the works of Angel, Benjamini and Schramm on the Uniform Infinite Planar Triangulation (UIPT) [BS01, AS03] obtained as the local limit of uniform triangulations of size tending to infinity. Since then variants of this theorem have been proved for different classes of maps [CD06, Kri06, Mén10, CMM13, BS14]. A common point of the these infinite random lattices is that they are constructed from the uniform distribution on some finite sets of planar maps. In this work, we consider a different type of distribution.

cFK random map. For $n\geq 1$ we write $\mathcal{M}_n$ for the set of all subgraph-rooted maps with n edges. Recall that in a dual subgraph-rooted maps, the distinguished subgraph $\mathfrak{g}$ and its dual subgraph $\mathfrak{g}^\dagger$ do not intersect. Therefore we can draw a set of loops tracing the boundary between them, as in Figure IV.1(b). Let $\ell(\mathfrak{m},\mathfrak{g})$ be the *number of loops separating* $\mathfrak{g}$ *and* $\mathfrak{g}^\dagger$. For each $q>0$, let $\mathbb{Q}_n^{(q)}$ be the probability distribution on $\mathcal{M}_n$ defined by

$$\mathbb{Q}_n^{(q)}(\mathfrak{m},\mathfrak{g}) \;\propto\; q^{\frac{1}{2}\ell(\mathfrak{m},\mathfrak{g})} \tag{IV.2}$$

By taking appropriate limits, we can define $\mathbb{Q}_n^{(q)}$ for $q\in\{0,\infty\}$. A *critical Fortuin-Kasteleyn (cFK) random map* of size n and of parameter q is a random variable of law $\mathbb{Q}_n^{(q)}$ (see Equation (IV.5) below for the connection with the Fortuin-Kasteleyn random cluster model). From the definition of the loop number ℓ, it is easily seen that the law $\mathbb{Q}_n^{(q)}$ is self-dual (which is why we call it critical):

$$\mathbb{Q}_n^{(q)}(\mathfrak{m},\mathfrak{g}) = \mathbb{Q}_n^{(q)}(\mathfrak{m}^\dagger,\mathfrak{g}^\dagger) \tag{IV.3}$$

Our main result is:

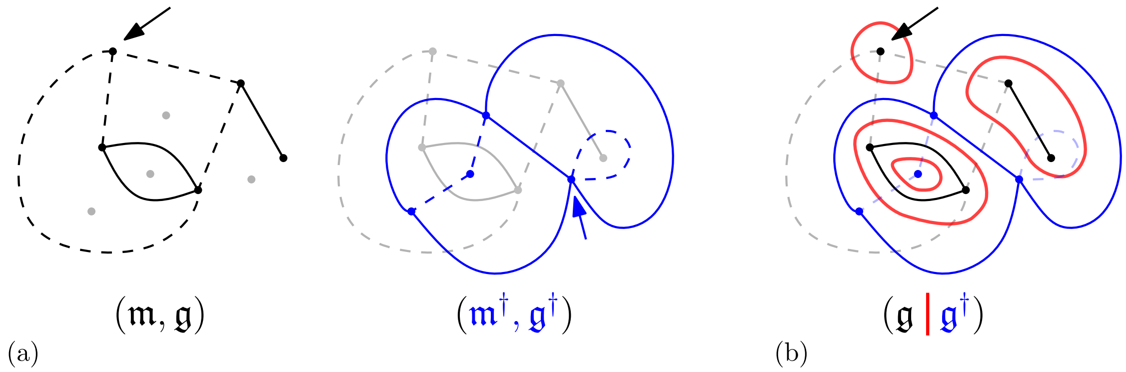

Figure IV.1 – *(a) A subgraph-rooted map and its dual. Edges of the distinguished subgraph are drawn in solid line, and the other edges in dashed line. The root corner is indicated by an arrow. (b) Loops separating the distinguished subgraph and its dual subgraph.*

Theorem IV.1. *For each $q \in [0, \infty]$, we have $\mathbb{Q}_n^{(q)} \xrightarrow[n\to\infty]{} \mathbb{Q}_\infty^{(q)}$ in distribution with respect to the metric $d_{\mathtt{loc}}$. Moreover, if $(\mathfrak{m}, \mathfrak{g})$ has law $\mathbb{Q}_\infty^{(q)}$, then*

- $(\mathfrak{m}, \mathfrak{g}) = (\mathfrak{m}^\dagger, \mathfrak{g}^\dagger)$ *in distribution,*
- *the map $\mathfrak{m}$ is almost surely one-ended and recurrent for the simple random walk,*
- *the laws of $\mathfrak{m}$ for different values of q are mutually singular.*

Background The FK percolation was first proposed under the name *random cluster model* in the pioneering work of Fortuin and Kasteleyn [FK72] as a unified reformulation of the percolation, the Ising/Potts model and the uniform spanning tree. The FK percolation on deterministic lattices exhibits rich critical behaviors, namely they are believed (and now partially proved) to give rise to a continuum of universality classes depending on the value of q, see e.g. [Wu82, Gri06]. The famous KPZ formula [KPZ88, DS11] provides an equation relating critical exponents of a statistical physics model on random lattices, and their regular-lattice counterpart. This provides one motivation to study FK percolation on random maps. Another motivation comes from the theory of Liouville quantum gravity, see [Pol81, ADJ97].

So far two classes of methods have been developed to prove local convergence of finite random maps. The first one, initially used in [AS03] is based on precise asymptotic enumeration formulas for certain classes of maps. Although enumeration results about (a generalization of) cFK decorated maps have been obtained using combinatorial techniques [Kos89, EK95, BBM11, GJSZJ12, BBG12c, BBG12b, BBG12a], we are not going to follow this approach here. Instead, we will first transform our finite map model through a bijection into simpler objects. The archetype of such bijection is the famous Cori-Vauquelin-Schaeffer bijection and its generalizations [Sch98, BDFG04]. Then we take local limits of these simpler objects and construct the limit of the maps directly from the latter. This technique has been used e.g. in [CD06, CMM13, BS14]. In this work the role of the Schaeffer bijection will be played by Sheffield's hamburger-cheeseburger bijection [She16b] which maps a cFK random map to a *random word* in a measure-preserving way. We will then construct the local limit of cFK random maps by showing that the random word converges locally to a limit, and that the hamburger-cheeseburger bijection has an almost surely continuous extension for that limit.

The cFK random maps have also been the subject of the recent works [BLR17] and [GMS15, GS17, GS15]. These works focused on finer properties of the infinite cFK random map such as exact scaling exponents or scaling limit of the model. In particular, the scaling exponents associated with the length and the enclosed area of a loop in the infinite cFK random map were derived independently. The main purpose of the present paper is to prove the local convergence of finite cFK maps to the infinite cFK map. We offer a detailed proof and construct explicitly the infinite-volume version of the hamburger-cheeseburger bijection. The one-endedness and recurrence of the infinite cFK random map are obtained as a by-product of this bijection. The fact that the joint law of $(\mathfrak{m}, \mathfrak{g})$ is mutually singular for different q follows from the various scaling exponents computed in [BLR17] and [GMS15]. By replacing the law of $(\mathfrak{m}, \mathfrak{g})$ by its marginal in $\mathfrak{m}$, we improve slightly the result. Our proof is based on an ergodicity result of the cFK random maps, which is of independent interest (See Appendix A).

The rest of this chapter is organized as follows. In Section 2 we discuss the law of the cFK random map in more details and examine three interesting special cases. In Section 3 we first define the random word model underlying the hamburger-cheeseburger bijection. Then we show that the model has an explicit local limit, and we prove some properties of the limit. In Section 4 we construct the hamburger-cheeseburger bijection and prove Theorem IV.1 by translating the properties of the infinite random word in terms of the maps.

2 More on cFK random map

Let $(\mathfrak{m}, \mathfrak{g})$ be a subgraph-rooted map and denote by $c(\mathfrak{g})$ the number of connected components in $\mathfrak{g}$. Recalling the definition of $\ell(\mathfrak{m}, \mathfrak{g})$ given in the introduction, it is not difficult to see that $\ell(\mathfrak{m}, \mathfrak{g}) = c(\mathfrak{g}) + c(\mathfrak{g}^\dagger) - 1$. However $c(\mathfrak{g}^\dagger)$ is nothing but the number of faces of $\mathfrak{g}$, therefore by Euler's relation we have

$$\ell(\mathfrak{m}, \mathfrak{g}) = e(\mathfrak{g}) + 2c(\mathfrak{g}) - v(\mathfrak{m}), \tag{IV.4}$$

where $e(\mathfrak{g})$ is the number of edges $\mathfrak{g}$, and $v(\mathfrak{m})$ is the number of vertices in $\mathfrak{m}$. This gives the following expression of the first marginal of $\mathbb{Q}_n^{(q)}$: for rooted map $\mathfrak{m}$ with n edges, we have

$$\mathbb{Q}_n^{(q)}(\mathfrak{m}) \propto q^{-\frac{1}{2}v(\mathfrak{m})} \sum_{\mathfrak{g} \subset \mathfrak{m}} \sqrt{q}^{e(\mathfrak{g})} q^{c(\mathfrak{g})}. \tag{IV.5}$$

The sum on the right-hand side over all the subgraphs of $\mathfrak{m}$ is precisely the partition function of the Fortuin-Kasteleyn random cluster model or, equivalenty, of the Potts model on the map $\mathfrak{m}$ (The two partition functions are equal. See e.g. [Gri06, Section 1.4]. See also [BBG12a, Section 2.1] for a review of their connection with loop models on planar lattices). For this reason, the cFK random map is used as a model of quantum gravity theory in which the geometry of the space interacts with the matter (spins in the Potts model). Note that the "temperature" in the Potts model and the prefactor $q^{-\frac{1}{2}v(\mathfrak{m})}$ in (IV.5) are tuned to ensure self-duality, which is crucial for our result to hold.

Three values of the parameter q deserve special attention, since the cFK random map has nice combinatorial interpretations in these cases.

$\mathbf{q} = \mathbf{0}$: $\mathbb{Q}_n^{(0)}$ is the uniform measure on the elements of $\mathcal{M}_n$ which minimize the number of loops ℓ. The minimum is $\ell_{\mathtt{min}} = 1$ and it is achieved if and only if the subgraph $\mathfrak{g}$ is a spanning tree of $\mathfrak{m}$. Therefore under $\mathbb{Q}_n^{(0)}$, the map $\mathfrak{m}$ is chosen with probability proportional to the number of its spanning trees, and conditionally on $\mathfrak{m}$, $\mathfrak{g}$ is a uniform spanning tree of $\mathfrak{m}$.

At the limit, the marginal law of $\mathfrak{g}$ under $\mathbb{Q}_\infty^{(0)}$ will be that of a critical geometric Galton-Walton tree conditioned to survive. This will be clear once we defined the hamburger-cheeseburger bijection. In fact when $q = 0$, the hamburger-cheeseburger bijection is reduced to a bijection between tree-rooted maps and excursions of simple random walk on $\mathbb{Z}^2$ introduced earlier by Bernardi [Ber07].

$\mathbf{q} = \mathbf{1}$: $\mathbb{Q}_n^{(1)}$ is the uniform measure on $\mathcal{M}_n$. Since each planar map with n edges has 2^n subgraphs, $\mathfrak{m}$ is a uniform planar map chosen among the maps with n edges. Thus in the case $q = 1$, Theorem IV.1 can be seen as a construction of the Uniform Infinite Planar Map or of the Uniform Infinite Planar Quadrangulation via Tutte's bijection. It is a curious fact that with this approach, one has to first decorate a uniform planar map with a random subgraph in order to show the local convergence of the map. As we will see later, the couple $(\mathfrak{m}, \mathfrak{g})$ is encoded by the hamburger-cheeseburger bijection in an entangled way.

$\mathbf{q} = \infty$: Similarly to the case $q = 0$, the probability $\mathbb{Q}_n^{(\infty)}$ is the uniform measure on the elements of $\mathcal{M}_n$ which *maximize* ℓ. To see what are these elements, remark that each connected component of $\mathfrak{g}$ contains at least one vertex, therefore

$$c(\mathfrak{g}) \leq v(\mathfrak{m}) \tag{IV.6}$$

And, at least one edge must be removed from $\mathfrak{m}$ to create a new connected component, so

$$c(\mathfrak{g}) \leq c(\mathfrak{m}) + e(\mathfrak{m}) - e(\mathfrak{g}) = n + 1 - e(\mathfrak{g}) \tag{IV.7}$$

Summing the two relations, we see that the maximal number of loops is $\ell_{\mathtt{max}} = n + 1$ and it is achieved if and only if each connected component of $\mathfrak{g}$ contains exactly one vertex (i.e. all edges of $\mathfrak{g}$ are self-loops) *and* that the complementary subgraph $\mathfrak{m} \setminus \mathfrak{g}$ is a tree. Figure IV.2(a) gives an example of such couple $(\mathfrak{m}, \mathfrak{g})$.

This model of loop-decorated tree is in bijection with bond percolation of parameter $1/2$ on a uniform random plane tree with n edges, as we now explain. For a couple $(\mathfrak{m}, \mathfrak{g})$ satisfying the above conditions, consider a self-loop $\mathbf{e}$ in $\mathfrak{g}$. This self-loop separates the rest of the map $\mathfrak{m}$ into two parts which share only the vertex of $\mathbf{e}$. We divide this vertex in two, and replace the self-loop $\mathbf{e}$ by an edge joining the two child vertices. The new edge is always considered part of $\mathfrak{g}$. By repeating this operation for all self-loops in the subgraph $\mathfrak{g}$ in an arbitrary order, we transform the map $\mathfrak{m}$ into a rooted plane tree, see Figure IV.2. This gives a bijection from the support of $\mathbb{Q}_n^{(\infty)}$ to the set of rooted plane tree of n edges with a distinguished subgraph. The latter object converges locally to a critical geometric Galton-Watson tree conditioned to survive, in which each edge belongs to the distinguished subgraph with probability $1/2$ independently from other edges. Using the inverse of the bijection above (which is almost surely continuous at the limit), we can explicit the law $\mathbb{Q}_\infty^{(\infty)}$. In particular, it is easily seen that $\mathfrak{m}$ is almost surely a one-ended tree plus finitely many self-loops at each vertex. Therefore it is one-ended and recurrent.

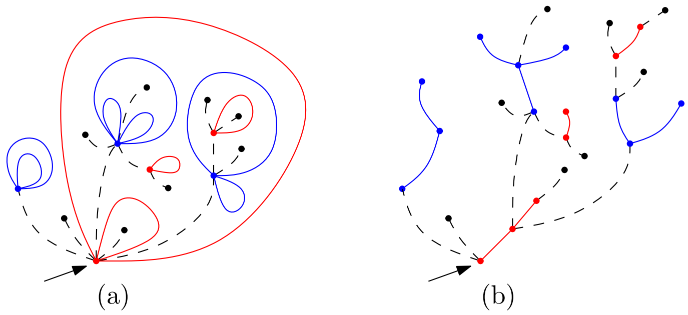

Figure IV.2 – *(a) A subgraph-rooted map which maximizes the number of loops ℓ. Colors are used only to illutrate the bijection. (b) The percolation configuration on a rooted tree associated to this map by the bijection. The divided vertices, as well as the replaced edges, are drawn in the same color before and after the bijection.*

3 Local limit of random words

In this section we define the random word model underlying the hamburger-cheeseburger bijection, and establish its local limit.

We consider words on the alphabet $\Theta = \{\mathtt{a}, \mathtt{b}, \mathtt{A}, \mathtt{B}, \mathtt{F}\}$. Formally, a *word* w is a mapping from an interval I of integers to Θ. We write $w \in \Theta^I$ and we call I the *domain* of w. Let $\mathcal{W}$ be the space of all words, that is,

$$\mathcal{W} = \bigcup_I \Theta^I \tag{IV.8}$$

where I runs over all subintervals of $\mathbb{Z}$. Note that a word can be finite, semi-infinite or bi-infinite. We denote by $\emptyset$ the *empty word*. Given a word w of domain I and $k \in I$, we denote by w_k the letter of index k in w. More generally, if J is an (integer or real) interval, we denote by w_J the *restriction* of the word w to $I \cap J$. For example, if $w = \mathtt{bAbaFABa} \in \Theta^{\{0,\dots,7\}}$, then $w_{[2,6)} = \mathtt{baFA} \in \Theta^{\{2,3,4,5\}}$. We endow $\mathcal{W}$ with the local distance

$$D_{\mathtt{loc}}(w, w') = \inf\left\{2^{-R} \,\middle|\, R \in \mathbb{N},\, w_{[-R,R)} = w'_{[-R,R)}\right\} \tag{IV.9}$$

Note that the equality $w_{[-R,R)} = w'_{[-R,R)}$ implies that $I \cap [-R, R) = I' \cap [-R, R)$, where I (resp. I') is the domain of the word w (resp. w'). It is easily seen that $(\mathcal{W}, D_{\mathtt{loc}})$ is a compact metric space.

3.1 Reduction of words

Now we define the reduction operation on the words. For each word w, this operation specifies a pairing between letters in the word called *matching*, and returns two shorter words $\overline{w}^{\lambda}$ and $\overline{w}^{\Lambda}$.

We follow the exposition given in [She16b]. The letters $\mathtt{a}, \mathtt{b}, \mathtt{A}, \mathtt{B}, \mathtt{F}$ are interpreted as, respectively, a hamburger, a cheeseburger, a hamburger order, a cheeseburger order and a *flexible* order. They obey the following order fulfillment relation: a hamburger order $\mathtt{A}$ can only be fulfilled by a hamburger $\mathtt{a}$, a cheeseburger order $\mathtt{B}$ by a cheeseburger $\mathtt{b}$, while a flexible order F can be fulfilled either by a hamburger a or by a cheeseburger b. We write $\lambda = \{\texttt{a}, \texttt{b}\}$ and $\Lambda = \{\texttt{A}, \texttt{B}, \texttt{F}\}$ for the set of lowercase letters (burgers) and uppercase letters (orders).

Finite case. A finite word $w \in \Theta^I$ can be seen from left to right as a sequence of events that happen in a restaurant with time indexed by I. Namely, at each time $k \in I$, either a burger is produced, or an order is placed. The restaurant puts all its burgers on a stack S, and takes note of unfulfilled orders in a list L. Both S and L start as the empty string. When a burger is produced, it is appended at the end of the stack. When an order arrives, we check if it can be fulfilled by one of the burgers in the stack. If so, we take the *last* such burger in the stack and fulfills the order. (That is, the stack is last-in-first-out.) Otherwise, the order goes to the end of the list L. Figure IV.3 illustrates this dynamics with an example.

w_k		a	a	B	b	A	F	B	F	a
S	$\emptyset$	a	aa	aa	aab	ab	a	a	$\emptyset$	a
L	$\emptyset$	$\emptyset$	$\emptyset$	B	B	B	B	BB	BB	BB

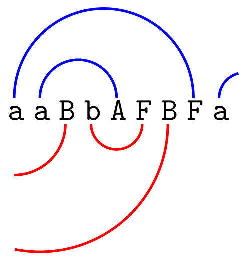

Figure IV.3 – *The reduction procedure of a word and the associated arch diagram*

We encode the *matching* of w by a function $\phi_w : I \to I \cup \{-\infty, \infty\}$. If the burger produced at time j is consumed by an order placed at time k, then the letters w_j and w_k are said to be *matched*, and we set $\phi_w(j) = k$ and $\phi_w(k) = j$. On the other hand, if a letter w_k corresponds to a unfulfilled order or a leftover burger, then it is *unmatched*, and we set $\phi_w(k) = \infty$ if it is a burger ($w_k \in \lambda$) and $\phi_w(k) = -\infty$ if it is an order ($w_k \in \Lambda$).

Moreover, let us denote by $\overline{w}^\Lambda$ (resp. $\overline{w}^\lambda$) the state of the list L (resp. the stack S) at the end of the above order-fulfillment algorithm. Together they give the reduced form of the word w.

Definition IV.2 (reduced word)**.** The reduced word associated to a finite word w is the concatenation $\overline{w} = \overline{w}^\Lambda \overline{w}^\lambda$. That is, it is the list of unmatched uppercase letters in w, followed by the list of unmatched lowercase letters in w.

The matching and the reduced word can be represented as an arch diagram as follows. For each letter w_j in the word w, draw a vertex in the complex plane at position j. For each pair of matched letters w_j and w_k, draw a semi-circular arch that links the corresponding pair of vertices. This arch is drawn in the upper half plane if it is incident to an a-vertex, and in the lower half plane if it is incident to a b-vertex. For an unmatched letter w_j, we draw an open arch from j tending to the left if $\phi_w(j) = -\infty$, or to the right if $\phi_w(j) = \infty$. See Figure IV.3.

It should be clear from the definition of matching operation that the arches in this diagram do not intersect each other. We shall come back to this diagram in Section 4 to construct the hamburger-cheeseburger bijection.

Infinite case. Remark that a hamburger produced at time j is consumed by a hamburger order at time $k > j$ if and only if 1) all the hamburgers produced during the interval $[j+1, k-1]$ are consumed strictly before time k, and 2) all the hamburger or flexible orders placed during $[j+1, k-1]$ are fulfilled by a burger produced strictly after time j. In terms of the reduced word, this means that two letters $w_j = \mathtt{a}$ and $w_k = \mathtt{A}$ are matched if and only if $\overline{w_{(j,k)}}$ does not contain any $\mathtt{a}$, $\mathtt{A}$ or $\mathtt{F}$. This can be generalized to any pair of burger/order.

Proposition IV.3 ([She16b]). *For $j < k$, assume that $w_j \in \lambda$ and $w_k \in \Lambda$ can be matched. Then they are matched in w if and only if $\overline{w_{(j,k)}}$ does not contain any letter that can be matched to either w_j or w_k.*

This shows that the matching rule is entirely determined by the reduction operator. More importantly, we see that the matching rule is *local*, that is, whether $\phi_w(j) = k$ or not only depends on $w_{[j,k]}$. From this we deduce that the reduction operator is compatible with string concatenation, that is, $\overline{uv} = \overline{u\overline{v}} = \overline{\overline{u}v}$ for any pair of finite words u, v.

This locality property allows us to define ϕ_w for infinite words w. Then, we can also read $\overline{w}^\lambda$ (resp. $\overline{w}^\Lambda$) from ϕ_w as the (possibly infinite) sequence of unmatched lowercase (resp. uppercase) letters. However $\overline{w}$ is not defined in general, since the concatenation $\overline{w}^\Lambda\overline{w}^\lambda$ does not always make sense.

Random word model and local limit. For each $p \in [0,1]$, let $\theta^{(p)}$ be the probability measure on Θ such that

$$\theta^{(p)}(\mathtt{a}) = \theta^{(p)}(\mathtt{b}) = \frac{1}{4} \qquad \theta^{(p)}(\mathtt{A}) = \theta^{(p)}(\mathtt{B}) = \frac{1-p}{4} \qquad \theta^{(p)}(\mathtt{F}) = \frac{p}{2}$$

Here p should be interpreted as the proportion of flexible orders among all the orders. Remark that, regardless of the value of p, the distribution is symmetric when exchanging $\mathtt{a}$ with $\mathtt{b}$ and $\mathtt{A}$ with $\mathtt{B}$. As we will see in Section 4, this corresponds to the self-duality of cFK random maps.

For $n \geq 1$, let $I_k = \{-k, \dots, 2n-1-k\}$, and set

$$\mathcal{W}_n = \bigcup_{0 \leq k < 2n} \left\{ w \in \Theta^{I_k} \,\middle|\, \overline{w} = \emptyset \right\} \tag{IV.10}$$

For $p \in [0,1]$, let $\mathbb{P}_n^{(p)}$ be the probability measure on $\mathcal{W}_n$ proportional to the direct product of $\theta^{(p)}$, that is, for all $w \in \mathcal{W}_n$,

$$\mathbb{P}_n^{(p)}(w) \propto \prod_j \theta^{(p)}(w_j) \tag{IV.11}$$

where the product is taken over the domain of w. In addition, let $\mathbb{P}_\infty^{(p)} = {\theta^{(p)}}^{\otimes \mathbb{Z}}$ be the product measure on bi-infinite words. Our proof of Theorem IV.1 relies mainly on the following proposition, stated by Sheffield in an informal way in [She16b].

Proposition IV.4. *For all $p \in [0,1]$, we have $\mathbb{P}_n^{(p)} \to \mathbb{P}_\infty^{(p)}$ in law for $D_{\mathtt{loc}}$ as $n \to \infty$.*

3.2 Proof of Proposition IV.4

We follow the approach proposed by Sheffield in [She16b, Section 4.2]. Let $W^{(p)}$ be a random word of law $\mathbb{P}_\infty^{(p)}$, so that $W_{[0,n)}^{(p)}$ is a word of length n with i.i.d. letters. By compactness of

$(\mathcal{W}, D_{\texttt{loc}})$, it suffices to show that for any ball $B_{\texttt{loc}}$ in this space, we have $\mathbb{P}_n^{(p)}(B_{\texttt{loc}}) \longrightarrow \mathbb{P}_\infty^{(p)}(B_{\texttt{loc}})$. Note that $D_{\texttt{loc}}$ is an ultrametric and the ball $B_{\texttt{loc}}(w, 2^{-R})$ of radius 2^{-R} around w is the set of words which are identical to w when restricted to $[-R, R)$. In the rest of the proof, we fix an integer $R \geq 1$ and a word $w \in \Theta^{[-R,R)\cap\mathbb{Z}}$. Recall that $W^{(p)}$ has law $\mathbb{P}_\infty^{(p)}$. In the following we omit the parameter p from the superscripts to keep simple notations.

Recall that the space $\mathcal{W}_n$ is made up of $2n$ copies of the set $\{w \in \Theta^{2n} \,|\, \overline{w} = \emptyset\}$ differing from each other by translation of the indices. Therefore $\mathbb{P}_n$ can be seen as the conditional law of $W_{[-K,2n-K)}$ on the event $\{\overline{W_{[-K,2n-K)}} = \emptyset\}$, where K is a uniform random variable on $\{0, \dots, 2n-1\}$ independent from W. Moreover, for the word $W_{[-K,2n-K)}$ to have w as its restriction to $[-R, R)$, one must have $R \leq K \leq 2n - R$. Hence,

$$\begin{aligned}
\mathbb{P}_n\left(B_{\texttt{loc}}(w, 2^{-R})\right) &= \mathbb{P}\left(R \leq K \leq 2n - R \text{ and } W_{[-R,R)} = w \,\middle|\, \overline{W_{[-K,2n-K)}} = \emptyset\right) \\
&= \frac{1}{2n}\sum_{k=R}^{2n-R} \mathbb{P}\left(W_{[-R,R)} = w \,\middle|\, \overline{W_{[-k,2n-k)}} = \emptyset\right) \\
&= \frac{1}{2n}\sum_{k=0}^{2n-2R} \mathbb{P}\left(W_{[k,k+2R)} \simeq w \,\middle|\, \overline{W_{[0,2n)}} = \emptyset\right) \\
&= \mathbb{E}\left[\frac{1}{2n}\sum_{k=0}^{2n-2R} \mathbb{1}_{\left\{W_{[k,k+2R)}\simeq w\right\}} \,\middle|\, \overline{W_{[0,2n)}} = \emptyset\right]
\end{aligned}$$

where in the last two steps, we denote by $u \simeq v$ the fact that two words are equal up to an overall translation of indices. On the other hand, set

$$\pi_w = \mathbb{P}(B_{\texttt{loc}}(w, 2^{-R})) = \prod_{k=-R}^{R-1} \theta(w_k) \tag{IV.12}$$

By translation invariance of W we have

$$\mathbb{E}\left[\frac{1}{2n}\sum_{k=0}^{2n-2R} \mathbb{1}_{\left\{W_{[k,k+2R)}\simeq w\right\}}\right] = \frac{2n-2R+1}{2n}\pi_w \tag{IV.13}$$

In fact, up to boundary terms of the order $O(R/n)$, the quantity inside the expectation is the empirical measure of the Markov chain $(W_{[k,k+2R)})_{k\geq 0}$ taken at the state w. This is an irreducible Markov chain on the finite state space Θ^{2R}. Sanov's theorem (see e.g. [DZ10, Theorem 3.1.2]) gives the following large deviation estimate. For any $\epsilon > 0$, there are constants $A_\epsilon, C_\epsilon > 0$ depending only on ϵ and on the transition matrix of $(W_{[k,k+2R)})_{k\geq 0}$, such that

$$\mathbb{P}\left(\left|\frac{1}{2n}\sum_{k=0}^{2n-2R} \mathbb{1}_{\left\{W_{[k,k+2R)}\simeq w\right\}} - \pi_w\right| > \epsilon\right) \leq A_\epsilon e^{-C_\epsilon n} \tag{IV.14}$$

for all $n \geq 1$. Since $\left|\frac{1}{2n}\sum_{k=0}^{2n-2R} \mathbb{1}_{\{W_{[k,k+2R)}\simeq w\}} - \pi_w\right|$ is bounded by 1, we have

$$\begin{aligned}
\left|\mathbb{P}_n\left(B_{\mathtt{loc}}(w,2^{-R})\right) - \pi_w\right| &\leq \mathbb{E}\left[\left|\frac{1}{2n}\sum_{k=0}^{2n-2R} \mathbb{1}_{\{W_{[k,k+2R)}\simeq w\}} - \pi_w\right| \,\middle|\, \overline{W_{[0,2n)}} = \emptyset\right] \\
&\leq \epsilon + \mathbb{P}\left(\left|\frac{1}{2n}\sum_{k=0}^{2n-2R} \mathbb{1}_{\{W_{[k,k+2R)}\simeq w\}} - \pi_w\right| > \epsilon \,\middle|\, \overline{W_{[0,2n)}} = \emptyset\right) \\
&\leq \epsilon + \frac{1}{\mathbb{P}\left(\overline{W_{[0,2n)}} = \emptyset\right)} \cdot \mathbb{P}\left(\left|\frac{1}{2n}\sum_{k=0}^{2n-2R} \mathbb{1}_{\{W_{[k,k+2R)}\simeq w\}} - \pi_w\right| > \epsilon\right) \\
&\leq \epsilon + \frac{A_\epsilon e^{-C_\epsilon n}}{\mathbb{P}\left(\overline{W_{[0,2n)}} = \emptyset\right)}
\end{aligned}$$

According to [She16b, Eq. (28)], [1]

$$\lim_{n\to\infty} \frac{1}{n} \log \mathbb{P}\left(\overline{W_{[0,2n)}} = \emptyset\right) = 0$$

Therefore the second term converges to zero as $n \to \infty$. Since ϵ can be taken arbitrarily close to zero, this shows that $\mathbb{P}_n\left(B_{\mathtt{loc}}(w,2^{-R})\right) \to \pi_w$ as $n \to \infty$.

3.3 Some properties of the limiting random word

In this section we show two properties of the infinite random word $W^{(p)}$ which will be the word-counterpart of Theorem IV.1. Both properties are true for general $p \in [0,1]$. However we will only write proofs for $p < 1$, since the case $p = 1$ corresponds to cFK random maps with parameter $q = \infty$, for which the local limit is explicit. (The proofs for $p = 1$ are actually easier, but they require different arguments.)

Proposition IV.5 (Sheffield [She16b]). *For all $p \in [0,1]$, almost surely,*

(i) $\overline{W^{(p)}} = \emptyset$*, that is, every letter in* $W^{(p)}$ *is matched.*

(ii) For all $k \in \mathbb{Z}$, $\overline{W^{(p)}_{(-\infty,k)}}^{\lambda}$ *contains infinitely many* $\mathtt{a}$ *and infinitely many* $\mathtt{b}$.

Proof. The first assertion is proved as Proposition 2.2 in [She16b]. For the second assertion, recall that $\overline{W^{(p)}_{(-\infty,k)}}^{\lambda}$ represents a left-infinite stack of burgers. Now assume for some $k \in \mathbb{Z}$, it contains only N letters $\mathtt{a}$ with positive probability. Then, with probability $\left(\frac{1-p}{4}\right)^{N+1}$ and independently of $W^{(p)}_{(-\infty,k)}$, all the $N+1$ letters in $W^{(p)}_{[k,k+N]}$ are $\mathtt{A}$. This will leave the $\mathtt{A}$ at position $k+N$ unmatched in W, which happens with zero probability according to the first assertion. This gives a contradiction when $p < 1$. □

[1] It has been shown in [GMS15] that $\mathbb{P}\left(\overline{W_{[0,2n)}} = \emptyset\right)$ decays as a power of n, with the exact exponent as a function of p. But we do not need this fact here.

For each random word $W^{(p)}$, consider a random walk Z on $\mathbb{Z}^2$ starting from the origin: $Z_0 = (0,0)$, and for all $k \in \mathbb{Z}$,

$$Z_{k+1} - Z_k = \begin{cases} (1,0) & \text{if } W_k^{(p)} = \mathtt{a} \\ (-1,0) & \text{if } W_k^{(p)} \text{ is matched to an } \mathtt{a} \\ (0,1) & \text{if } W_k^{(p)} = \mathtt{b} \\ (0,-1) & \text{if } W_k^{(p)} \text{ is matched to a } \mathtt{b} \end{cases} \tag{IV.15}$$

By Proposition IV.5, Z_k is almost surely well-defined for all $k \in \mathbb{Z}$. A lot of information about the random word W can be read from Z. The main result of [She16b] shows that under diffusive rescaling, Z converges to a Brownian motion in $\mathbb{R}^2$ with a diffusivity matrix that depends on p, demonstrating a phase transition at $p = 1/2$.

Let $(X,Y) = Z$. Then X represents the net hamburger count and Y the net cheeseburger count. Set $i_0 = \sup\{i < 0 \,|\, X_i = -1\}$ and $j_0 = \inf\{j > 0 \,|\, X_j = -1\}$. Let N_0 be the number of times that X visits the state 0 between time i_0 and j_0. We shall see in Section 4.2 that N_0 is exactly the degree of root vertex in the infinite cFK-random map. Below we prove that the distribution of N_0 has an exponential tail, that is, there exists constants A and $c > 0$ such that $\mathbb{P}(N_0 \geq x) \leq Ae^{-cx}$ for all $x \geq 0$.

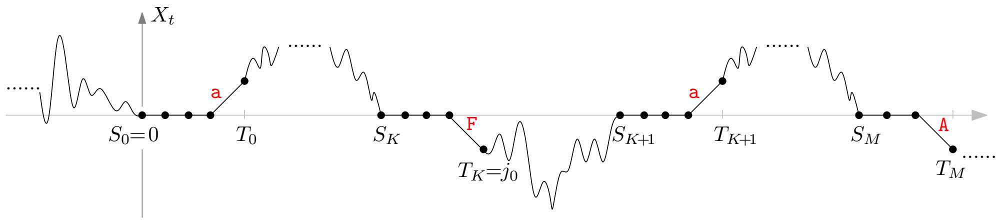

Figure IV.4 – *The decomposition of* N_0^+ *into intervals* $[S_k, T_k]$.

Proposition IV.6. *N_0 has an exponential tail distribution for all $p \in [0,1]$.*

Proof. First let us consider N_0^+, the number of times that X visits the state 0 between time 0 and j_0. Remark that at positive time, the process X is adapted to the natural filtration $(\mathcal{F}_k)_{k\geq 0}$, where $\mathcal{F}_k$ is the σ-algebra generated by $W_{[0,k)}$. Define two sequences of $\mathcal{F}$-stopping times $(S_m)_{m\geq 0}$ and $(T_m)_{m\geq 0}$ by $S_0 = 0$, and that for all $m \geq 0$,

$$\begin{aligned} T_m &= \inf\{k > S_m \,|\, X_k \neq 0\} \\ S_{m+1} &= \inf\{k > T_m \,|\, X_k = 0\} \end{aligned}$$

The sequence S (resp. T) marks the times that X arrives at (resp. departs from) the state 0. Therefore the total number of visits of the state 0 between time 0 and T_m is $\sum_{i=0}^{m}(T_i - S_i)$, see Figure IV.4.

By construction, j_0 is the smallest T_m such that $X_{T_m} = -1$. On the other hand, we have $X_{T_m} \in \{-1,+1\}$ for all m and

$$\begin{aligned} X_{T_m} = +1 \quad &\Leftrightarrow \quad W_{T_m} = \mathtt{a} \\ X_{T_m} = -1 \quad &\Leftrightarrow \quad W_{T_m} = \mathtt{A} \text{ or } W_{T_m} \text{ is an } \mathtt{F} \text{ matched to an } \mathtt{a} \end{aligned}$$

Consider the stopping time

$$M = \inf\{m \geq 0 \,|\, W_{T_m} = \mathtt{A}\} \tag{IV.16}$$

Then we have $j_0 \leq T_M$, and therefore

$$N_0^+ \leq \sum_{m=0}^{M} (T_m - S_m) \tag{IV.17}$$

On the other hand, M is the smallest m such that, starting from time S_m, an $\mathtt{A}$ comes before an $\mathtt{a}$. Therefore M is a geometric random variable of mean $\frac{1-p}{p}$.

Assume $p < 1$ so that M is almost surely finite. Fix an integer $m \geq 0$. By the strong Markov property, conditionally to $\{M = m\}$, the sequence $(T_i - S_i, i = 0 \ldots m-1)$ is i.i.d., and each term in the sequence has the same law as the first arrival time of $\mathtt{a}$ in the sequence $(W_k)_{k\geq 0}$ conditioned not to contain $\mathtt{A}$. In other words, conditionally to $\{M = m\}$, $(T_i - S_i, i = 0 \ldots m-1)$ is an i.i.d. sequence of geometric random variables of mean $\frac{1}{2+p}$. Similarly, conditionally to $\{M = m\}$, $T_m - S_m$ is a geometric random variable of mean $\frac{1-p}{2+p}$ independent from the sequence $(T_i - S_i, i = 0 \ldots m-1)$. Then, a direct computation shows that the exponential moment $\mathbb{E}[e^{\lambda N_0^+}]$ is finite for some $\gamma > 0$. And by Markov's inequality, the distribution of N_0^+ has an exponential tail when $p < 1$.

Now we claim that conditionally to the value of N_0, the variable N_0^+ is uniform on $\{1, \ldots, N_0\}$ which implies that N_0 also has an exponential tail distribution. To see why the conditional law is uniform, consider N_0 and N_0^+ for finite words defined in the same way as for the infinite word $W_\infty^{(p)}$. Note that for a finite word w the process X does not necessarily hit -1 at negative (resp. positive) times. In this case we just replace i_0 (resp. j_0) by the infimum (resp. supremum) of the domain of w. Then, $w \mapsto (N_0, N_0^+)$ is a $D_{\mathtt{loc}}$-continuous function defined on the union of $\cup_{n\geq 0}\mathcal{W}_n$ and the support of $W_\infty^{(p)}$. Therefore for any integers $k \leq m$,

$$\mathbb{P}_n^{(p)}(N_0 = m, N_0^+ = k) \xrightarrow[n\to\infty]{} \mathbb{P}_\infty^{(p)}(N_0 = m, N_0^+ = k) \tag{IV.18}$$

But, given the sequence of letters in a word, the law $\mathbb{P}_n^{(p)}$ chooses the letter of index 0 uniformly at random among all the letters. A simple counting shows that for all $1 \leq k, k' \leq m$, we have $\mathbb{P}_n^{(p)}(N_0 = m, N_0^+ = k) = \mathbb{P}_n^{(p)}(N_0 = m, N_0^+ = k')$. Letting $n \to \infty$ shows that the conditional law of N_0^+ given N_0 is uniform under $\mathbb{P}_\infty^{(p)}$. □

4 The hamburger-cheeseburger bijection

4.1 Construction

In this section we present (a slight variant of) the hamburger-cheeseburger bijection of Sheffield. We refer to [She16b] for the proof of bijectivity and for historical notes.

We define the hamburger-cheeseburger bijection $\widetilde{\Psi}$ on a subset of the space $\mathcal{W}$, and it takes values in the space $\widetilde{\mathcal{M}}$ of *doubly-rooted planar maps with a distinguished subgraph*, that is, planar maps with two distinguished corners and one distinguished subgraph. We can write this space as

$$\widetilde{\mathcal{M}} = \{(\mathfrak{m}, \mathfrak{g}, \mathbf{s}) \,|\, (\mathfrak{m}, \mathfrak{g}) \in \mathcal{M} \text{ and } \mathbf{s} \text{ is a corner of } \mathfrak{m}\} \tag{IV.19}$$

Note that the second root $\mathbf{s}$ may be equal to or different from the root of $\mathfrak{m}$. We define in the same way $\widetilde{\mathcal{M}}_n$, the doubly-rooted version of the space $\mathcal{M}_n$. Its cardinal is $2n$ times that of $\mathcal{M}_n$.

We start by constructing $\widetilde{\Psi} : \mathcal{W}_n \to \widetilde{\mathcal{M}}_n$ in three steps. The first step transforms a word in $\mathcal{W}_n$ into a decorated planar map called *arch graph*. The second and the third step apply graph duality and local transformations to the arch graph to get a *tree-rooted map*, and then *a subgraph-rooted map* in $\widetilde{\mathcal{M}}_n$.

Step 1: from words to arch graphs. Fix a word $w \in \mathcal{W}_n$. Recall from Section 3 the construction of the non-crossing arch diagram associated to w. In particular since $\overline{w} = \emptyset$, there is no half-arch. We link neighboring vertices by unit segments $[j-1, j]$ and link the first vertex to the last vertex by an edge that wires around the whole picture on either side of the real axis, without intersecting any other edges. This defines a planar map $\mathfrak{A}$ of $2n$ vertices and $2n$ edges. In $\mathfrak{A}$ we distinguish edges coming from arches and the other edges. The latter forms a simple loop passing through all the vertices.

We further decorate $\mathfrak{A}$ with additional pieces of information. Recall that the word w is indexed by an interval of the form $I_k = \{-k, \dots, 2n-1-k\}$ where $0 \le k < 2n$. We will mark the oriented edge $\mathbf{r}$ from the vertex 0 to the vertex -1, and the oriented edge $\mathbf{s}$ from the first vertex $(-k)$ to the last vertex $(2n-1-k)$. If $k = 0$, then $\mathbf{r}$ and $\mathbf{s}$ coincide. Furthermore, we mark each arch incident to an `F`-vertex by a star $*$. (See Figure IV.5) We call the decorated planar map A the *arch graph* of w. One can check that it completely determines the underlying word w.

Step 2: from arch graphs to tree-rooted maps. We now consider the dual map $\mathbf{\Delta}$ of the arch graph $\mathfrak{A}$. Let $\mathfrak{q}$ be the subgraph of $\mathbf{\Delta}$ consisting of edges whose dual edge is on the loop in $\mathfrak{A}$. We denote by $\mathbf{\Delta} \setminus \mathfrak{q}$ the set of remaining edges of $\mathbf{\Delta}$ (that is, the edges intersecting one of the arches).

Proposition IV.7. *The map $\mathbf{\Delta}$ is a triangulation, the map $\mathfrak{q}$ is a quadrangulation with n faces and $\mathbf{\Delta} \setminus \mathfrak{q}$ consists of two trees.* □

We denote by $\mathfrak{t}$ and $\mathfrak{t}^\dagger$ the two trees in $\mathbf{\Delta} \setminus \mathfrak{q}$, with $\mathfrak{t}$ corresponding to faces of the arch graph in the upper half plane. Then $\mathfrak{q}, \mathfrak{t}$ and $\mathfrak{t}^\dagger$ form a partition of edges in the triangulation $\mathbf{\Delta}$. Note that $\mathfrak{t}$ and $\mathfrak{t}^\dagger$ give the (unique) bipartition of vertices of $\mathfrak{q}$. Let $\mathfrak{m}$ be the planar map associated to $\mathfrak{q}$ by Tutte's bijection, such that $\mathfrak{m}$ has the same vertex set as $\mathfrak{t}$. (The latter prescription allows us to bypass the root, and define Tutte's bijection from unrooted quadrangulations to unrooted maps.) We thus obtain a couple $(\mathfrak{m}, \mathfrak{t})$ in which $\mathfrak{m}$ is a map with n edges and $\mathfrak{t}$ a spanning tree of $\mathfrak{m}$. Remark that $\mathfrak{t}^\dagger$ is the dual spanning tree of $\mathfrak{t}$ in the dual map $\mathfrak{m}^\dagger$. This relates the duality of maps with the duality on words which consists of exchanging `a` with `b` and `A` with `B`.

Figure IV.5(a) summarizes the mapping from words to tree-rooted maps (Step 1 and 2) with an example. Note that we have omitted the two roots and the stars on the arch graph in the above discussion. But since graph duality and Tutte's bijection provide canonical bijections between edges, the roots and stars can be simply transferred from the arches in $\mathfrak{A}$ to the edges in $\mathfrak{m}$. With the roots and stars taken into account, it is clear that $w \mapsto (\mathfrak{m}, \mathfrak{t})$ is a bijection from $\mathcal{W}_n$ onto its image.

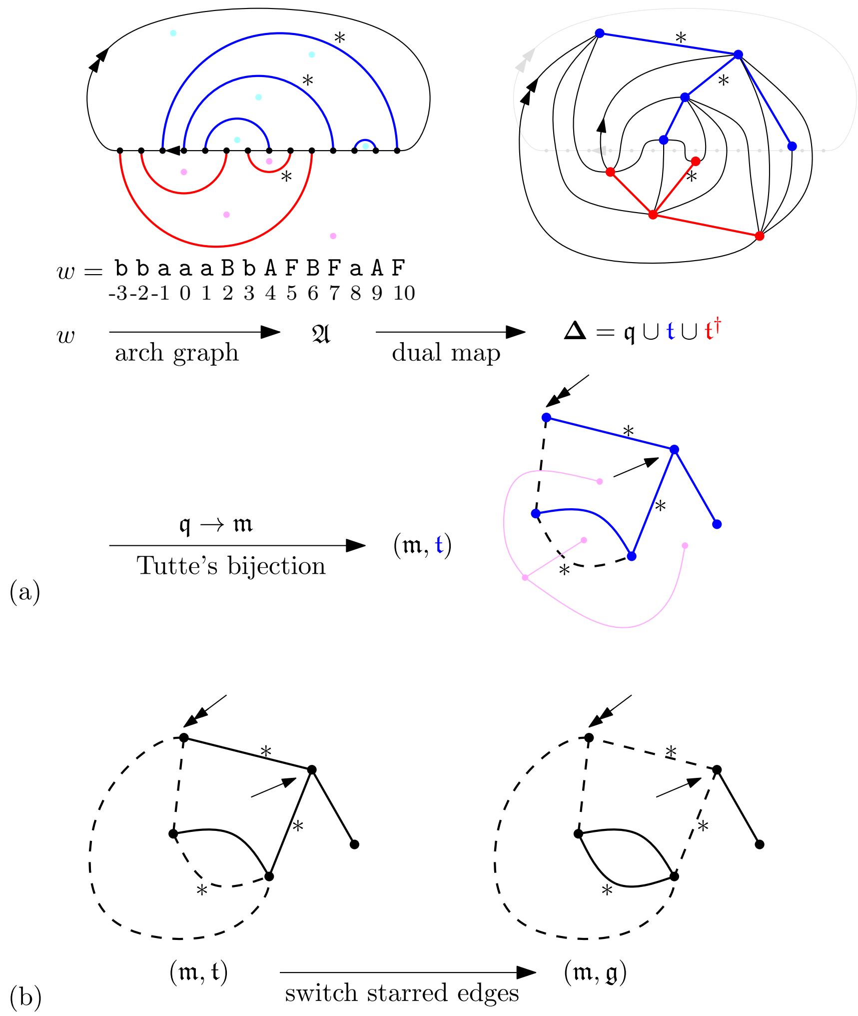

Figure IV.5 – *Construction of the hamburger-cheeseburger bijection. (a) From word to tree-rooted map. (b) From tree-rooted map to subgraph-rooted map.*

Step 3: from tree-rooted maps to subgraph-rooted maps. Now we "switch the status" of every starred edge in $\mathfrak{m}$ relative to the spanning tree $\mathfrak{t}$. That is, if a starred edge is not in $\mathfrak{t}$, we add it to $\mathfrak{t}$; if it is already in $\mathfrak{t}$, we remove it from $\mathfrak{t}$. Let $\mathfrak{g}$ be the resulting subgraph. See Figure IV.5(b) for an example.

Recall that there are two marked corners $\mathbf{r}$ and $\mathbf{s}$ in the map $\mathfrak{m}$. By an abuse of notation, from now on we denote by $\mathfrak{m}$ the *rooted* map with root corner $\mathbf{r}$. Then, the hamburger-cheeseburger bijection is defined by $\widetilde{\Psi}(w) = (\mathfrak{m}, \mathfrak{g}, \mathbf{s})$. Let $\Psi(w) = (\mathfrak{m}, \mathfrak{g})$ be its projection obtained by forgetting the second root corner. We denote by $(\#\mathtt{F})w$ the number of letters $\mathtt{F}$ in w, and by ℓ the number of loops associated to the corresponding subgraph-rooted map $(\mathfrak{m}, \mathfrak{g})$.

Theorem IV.8 (Sheffield [She16b]). *The mapping $\widetilde{\Psi} : \mathcal{W}_n \to \widetilde{\mathcal{M}}_n$ is a bijection such that $\ell = 1 + (\#\mathtt{F})w$ for all $w \in \mathcal{W}_n$. And $\mathbb{Q}_n^{(q)}$ is the image measure of $\mathbb{P}_n^{(p)}$ by Ψ whenever*

$$p = \frac{\sqrt{q}}{2 + \sqrt{q}}.$$

Proof. The proof of this can be found in [She16b]. However we include a proof of the second fact to enlighten the relation $p = \frac{\sqrt{p}}{2+\sqrt{q}}$. For $w \in \mathcal{W}_n$, since $\overline{w} = \emptyset$, we have $(\#\mathtt{a})w + (\#\mathtt{b})w = (\#\mathtt{A})w + (\#\mathtt{B})w + (\#\mathtt{F})w = n$. Therefore, when $p = \frac{\sqrt{q}}{2+\sqrt{q}}$,

$$\begin{aligned}\mathbb{P}_n^{(p)}(w) &\propto \left(\frac{1}{4}\right)^{(\#\mathtt{a})w+(\#\mathtt{b})w}\left(\frac{1-p}{4}\right)^{(\#\mathtt{A})w+(\#\mathtt{B})w}\left(\frac{p}{2}\right)^{(\#\mathtt{F})w}\\ &= \left(\frac{1}{4}\right)^{n}\left(\frac{1-p}{4}\right)^{n-(\#\mathtt{F})w}\left(\frac{p}{2}\right)^{(\#\mathtt{F})w} \propto \left(\frac{2p}{1-p}\right)^{(\#\mathtt{F})w} = \sqrt{q}^{\ell-1}\end{aligned}$$

After normalization, this shows that $\mathbb{Q}_n^{(q)}$ is the image measure of $\mathbb{P}_n^{(p)}$ by Ψ. □

Proposition IV.9. *We can extend the mapping Ψ to $\mathcal{W} \to \mathfrak{m}$ so that it is $\mathbb{P}_\infty^{(p)}$-almost surely continuous with respect to $D_{\mathtt{loc}}$ and $d_{\mathtt{loc}}$, for all $p \in [0,1]$.*

Proof. Observe that if we do not care about the location of the second root $\mathbf{s}$, then the word w used in the construction of Ψ does not have to be finite. Set

$$\mathcal{W}_\infty = \left\{ w \in \Theta^{\mathbb{Z}} \;\middle|\; \begin{array}{c}\overline{w} = \emptyset \text{ and for all } k \in \mathbb{Z}, \overline{w_{(-\infty,k)}}^{\lambda} \text{ contains}\\ \text{infinitely many } \mathtt{a} \text{ and infinitely many } \mathtt{b}\end{array} \right\} \tag{IV.20}$$

We claim that indeed, for each $w \in \mathcal{W}_\infty$, Step 1, 2 and 3 of the construction define a (locally finite) infinite subgraph-rooted map: as in the case of finite words, the condition $\overline{w} = \emptyset$ ensures that the arch graph $\mathfrak{A}$ of w is a well-defined infinite planar map (that is, all the arches are closed). To see that its dual map $\boldsymbol{\Delta}$ is a locally finite, infinite triangulation, we only need to check that each face of $\mathfrak{A}$ has finite degree. Observe that a letter $\mathtt{a}$ in w appears in $\overline{w_{(-\infty,k)}}^{\lambda}$ if and only if it is on the left of w_k, and that its partner is on the right of w_k. This corresponds to an arch passing above the vertex k. Therefore, the remaining condition in the definition of $\mathcal{W}_\infty$ says that there are infinitely many arches which pass above and below each vertex of $\mathfrak{A}$. This guarantees that $\mathfrak{A}$ has no unbounded face. The rest of the construction consists of local operations only. So the resulting subgraph-rooted map $(\mathfrak{m}, \mathfrak{g}) = \Psi(w)$ is a locally finite subgraph-rooted map.

Also, by Proposition IV.5, we have $\mathbb{P}_\infty^{(p)}(\mathcal{W}_\infty) = 1$. It remains to see that (the extension) of Ψ is continuous on $\mathcal{W}' = \bigcup_n \mathcal{W}_n \cup \mathcal{W}_\infty$. Let $w^{(n)}, w \in \mathcal{W}'$ so that $w^{(n)} \to w$ for $D_{\mathtt{loc}}$. If w is finite, there is nothing to prove. Otherwise, let $(\mathfrak{m}, \mathfrak{g}) = \Psi(w)$ and consider a ball B of finite radius r around the root in the map $\mathfrak{m}$. By locality of the mapping $\boldsymbol{\Delta} \rightsquigarrow \mathfrak{m}$, the ball B can be determined by a ball B' of finite radius r' (which may depend on $\mathfrak{m}$) in $\boldsymbol{\Delta}$. But each triangle in $\boldsymbol{\Delta}$ corresponds to a letter in the word, so there exists r'' (which may depend on $\mathfrak{m}$) such that if $w^{(n)}_{[-r'',r'']} = w_{[-r'',r'']}$ then the balls of radius r' in $\boldsymbol{\Delta}$ coincide. This proves that Ψ is continuous on $\mathcal{W}_\infty$. □

4.2 Proof of Theorem IV.1

Combining Proposition IV.4, Theorem IV.8 and Proposition IV.9 yields the convergence statement of the theorem. The self-duality of the infinite cFK random map follows from the finite self-duality. It remains to show that the infinite cFK random maps are almost surely one-ended and recurrent for all q, and that their laws are mutually singular for different values of q.

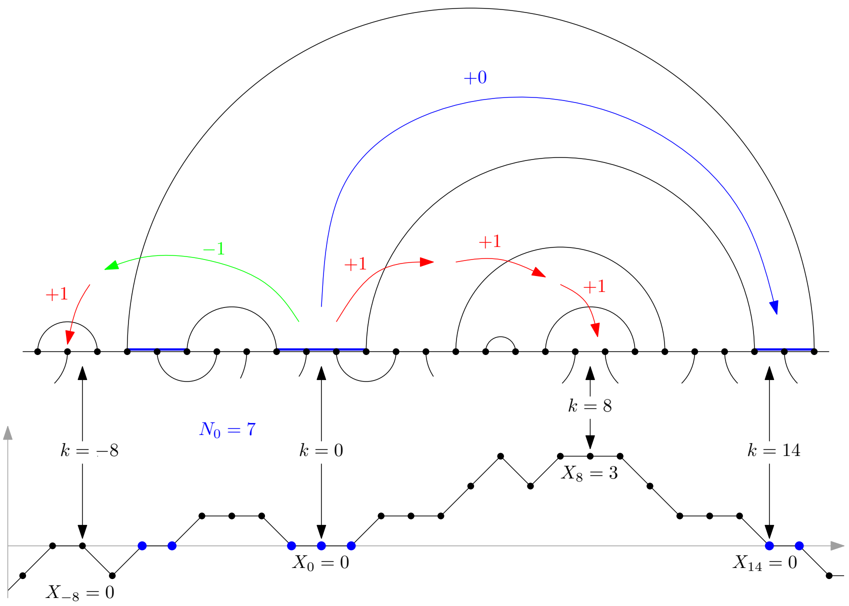

Figure IV.6 – *An example of an infinite arch graph, and the associated process $(X_k)_{k\in\mathbb{Z}}$. We shifted the arch graph horizontally by $1/2$ relative to the graph of X, since the time k for the process X naturally corresponds to the interval $[k-1,k]$ in the arch graph.*

One-endedness. Recall that a graph $\mathfrak{g} = (V, E)$ is said to be one-ended if for any finite subset of vertices U, $V \setminus U$ has exactly one infinite connected component. We will prove that for a word $w \in \mathcal{W}_\infty$, $\Psi(w)$ is one-ended. Let $\mathfrak{A}$ (resp. $\mathbf{\Delta}$) be the arch graph (resp. triangulation) associated to w, and let $(\mathfrak{m}, \mathfrak{g}) = \Psi(w)$. By the second condition in the definition of $\mathcal{W}_\infty$ (see (IV.20)), there exist arches that connect vertices on the left of w_{-R} to vertices on the right of w_R for any finite number R. Therefore the arch graph $\mathfrak{A}$ is one-ended. It is then an easy exercise to deduce from this that the triangulation $\mathbf{\Delta}$ and then the map $\mathfrak{m}$ are also one-ended.

Recurrence. To prove the recurrence of $\mathfrak{m}$ we use the general criterion established by Gurel-Gurevich and Nachmias [GGN13]. Notice first that under $\mathbb{Q}_n^{(q)}$, the random maps are *uniformly rooted*, that is, conditionally on the map, the root vertex ρ is chosen with probability proportional to its degree. By [GGN13] it thus suffices to check that the distribution of $\deg(\rho)$ has an exponential tail. For this we claim that the variable N_0 studied in Lemma IV.6 exactly corresponds to the degree of the root in an infinite cFK random map. From the construction of the hamburger-cheeseburger bijection, we see that the vertices of the map $\mathfrak{m}$ corresponds to the faces of the arch graph *in the upper half plane*. In particular, the root vertex ρ corresponds to the face *above* the interval $[-1, 0]$, and $\deg(\rho)$ is the number of unit intervals on the real axis which are also on the boundary of this face. On the other hand, X_k is the *net number* of arches that one *enters* to get from the face above $[-1, 0]$ to the face above $[k-1, k]$, see Figure IV.6. So N_0 exactly counts the above number of intervals.

Mutual singularity. The basic idea is to construct a measurable function f on infinite rooted planar maps such that $f(\mathfrak{m})$ is almost surely constant for each $q \in [0, \infty]$, and that

$f(\mathfrak{m}) = f(q)$ is an injective function of q. One such function can be defined as follows. Consider the simple random walk on the map $\mathfrak{m}$. We regard it as a sequence of oriented edges $(\vec{E}_k, k \geq 0)$ such that $\vec{E}_0$ is the root edge (i.e. the edge on the left of the root corner), and such that $\vec{E}_{k+1}$ starts at the vertex where $\vec{E}_k$ ends. An oriented edge $\vec{e}$ is *pending* if the starting point of $\vec{e}$ has degree 1. Let

$$f(\mathfrak{m}) = \lim_{n\to\infty} \frac{1}{n} \sum_{k=0}^{n-1} \mathbb{1}_{\left\{\vec{E}_k \text{ is pending}\right\}}$$

From the ergodicity result in the appendix and Birkhoff's ergodic theorem, it follows that $f(\mathfrak{m}) = \mathbb{Q}(\vec{E}_0 \text{ is pending})$ almost surely. Recall that $\vec{E}_0$ is the root edge of $\mathfrak{m}$. A moment of look at Figure IV.5 shows that $\vec{E}_0$ is a pending edge in $(\mathfrak{m}, \mathfrak{g}) = \Phi(w)$ if and only if $w_{-1} = \mathtt{a}$ and $w_0 \in \{\mathtt{A}, \mathtt{F}\}$. Therefore,

$$\begin{aligned}\mathbb{Q}(\vec{E}_0 \text{ is pending}) &= \mathbb{P}(w_{-1} = \mathtt{a} \text{ and } w_0 \in \{\mathtt{A}, \mathtt{F}\}) \\ &= \theta(\mathtt{a})\big(\theta(\mathtt{A}) + \theta(\mathtt{F})\big) = \frac{1+p}{16} = \frac{1}{16}\left(1 + \frac{\sqrt{q}}{2+\sqrt{q}}\right)\end{aligned}$$

We see that $f(q) = f(\mathfrak{m})$ is injective in q.

A Ergodicity of cFK random maps

Here we use the framework set up by Benjamini and Curien in [BC12] and we follow the exposition in [Cur16, Section 3.1]. Consider the space $\vec{\mathcal{M}}$ of all locally finite rooted maps endowed with a path $\vec{e} = (\vec{e}_n)_{n\geq 0}$ starting from the root edge. Let $\vec{d}_{\mathtt{loc}}$ be the natural local distance on $\vec{\mathcal{M}}$

$$\vec{d}_{\mathtt{loc}}((\mathfrak{m}, \vec{e}), (\mathfrak{m}', \vec{e}')) = \inf\left\{2^{-R} \,\middle|\, B_R(\mathfrak{m}) = B_R(\mathfrak{m}') \text{ and } \vec{e}_k = \vec{e}'_k \text{ for } 0 \leq k \leq R\right\}$$

and consider the associated Borel σ-algebra. If $\mathfrak{m}$ is a rooted map, let $Q_\mathfrak{m}$ be the law of the simple random walk starting from the root edge of $\mathfrak{m}$. We denote by $\mathbb{Q} \otimes Q$ the probability measure

$$\mathbb{Q} \otimes Q(A) = \int Q_\mathfrak{m}(A_\mathfrak{m})\, \mathbb{Q}(d\mathfrak{m})$$

on $\vec{\mathcal{M}}$, where $A_\mathfrak{m} = \{(\vec{e}_n)_{n\geq 0} \,|\, (\mathfrak{m}, (\vec{e}_n)_{n\geq 0}) \in A\}$. To simplify notation, we will write $Q_\mathfrak{m}(A)$ instead of $Q_\mathfrak{m}(A_\mathfrak{m})$ in the sequel.

If $\vec{e}$ is an oriented edge of $\mathfrak{m}$, we write $\mathfrak{m}|_{\vec{e}}$ for the map obtained by re-rooting $\mathfrak{m}$ at $\vec{e}$. Observe that if $(\mathfrak{m}, (\vec{E}_n)_{n\geq 0})$ is a random variable of law $\mathbb{Q} \otimes Q$, then

$$\mathfrak{m} = \mathfrak{m}|_{\vec{E}_1}$$

in distribution. (Remark that the left-hand-side is the same as $\mathfrak{m}|_{\vec{E}_0}$.) This is a consequence of the fact that $\mathfrak{m}$ is the local limit of a sequence of uniformly rooted finite maps. It follows that the shift operator

$$\tau : (\mathfrak{m}, (\vec{e}_n)_{n\geq 0}) \mapsto (\mathfrak{m}|_{\vec{e}_1}, (\vec{e}_{n+1})_{n\geq 0})$$

preserves the measure $\mathbb{Q} \otimes Q$.

Proposition IV.10. *The shift operator τ is ergodic for $\mathbb{Q} \otimes Q$.*

Proof. Let A be a τ-invariant event for $\mathbb{Q} \otimes Q$, that is, $\mathbb{Q} \otimes Q(A \Delta \tau^{-1}(A)) = 0$, where Δ denotes the symmetric difference: $A \Delta B = (A \setminus B) \cup (B \setminus A)$. We do the proof in three steps:

(a) $\mathbb{Q}$-almost surely, $Q_{\mathfrak{m}}(A) \in \{0, 1\}$.

Recall that the simple random walk on $\mathfrak{m}$ is $\mathbb{Q}$-almost surely recurrent. Therefore, it can be decomposed into an i.i.d. sequence of excursions from the root edge. An event invariant by τ is also invariant by the shift operator associated to this i.i.d. sequence. Thus (a) follows from Kolmogorov's zero-one law.

(b) $\mathbb{Q}$-almost surely, the value of $Q_{\mathfrak{m}}(A)$ is invariant under any re-rooting of the map $\mathfrak{m}$.

First let us fix a rooted map $\mathfrak{m}$. Let x be the vertex to which the root edge points. Denote by d the degree of x, and $\vec{\rho}_1, \dots, \vec{\rho}_d$ the d oriented edges that point away from x. We deduce from the Markov property of the simple random walk that

$$\begin{aligned} Q_{\mathfrak{m}}(\tau^{-1}A) &= Q_{\mathfrak{m}}\Big\{ (\vec{e}_n)_{n\geq 0} \;\Big|\; (\mathfrak{m}|_{\vec{e}_1}, (\vec{e}_{n+1})_{n\geq 0}) \in A \Big\} \\ &= \sum_{k=1}^{d} Q_{\mathfrak{m}}\Big\{ (\vec{e}_n)_{n\geq 0} \;\Big|\; (\mathfrak{m}|_{\vec{e}_1}, (\vec{e}_{n+1})_{n\geq 0}) \in A \text{ and } \vec{e}_1 = \vec{\rho}_k \Big\} \\ &= \sum_{k=1}^{d} \frac{1}{d} Q_{\mathfrak{m}|_{\vec{\rho}_k}}\Big\{ (\vec{e}_n)_{n\geq 0} \;\Big|\; (\mathfrak{m}|_{\vec{\rho}_k}, (\vec{e}_n)_{n\geq 0}) \in A \Big\} \;=\; \frac{1}{d}\sum_{k=1}^{d} Q_{\mathfrak{m}|_{\vec{\rho}_k}}(A) \end{aligned}$$

From

$$\int \Big| Q_{\mathfrak{m}}(A) - Q_{\mathfrak{m}}(\tau^{-1}A) \Big| \, \mathbb{Q}(\mathrm{d}\mathfrak{m}) \leq \mathbb{Q} \otimes Q(A \Delta \tau^{-1} A) = 0$$

we deduce that $\mathbb{Q}$-almost surely,

$$Q_{\mathfrak{m}}(A) = \frac{1}{d} \sum_{k=1}^{d} Q_{\mathfrak{m}|_{\vec{\rho}_k}}(A)$$

But according to (a), $Q_{\mathfrak{m}}(A)$ and $Q_{\mathfrak{m}|_{\vec{\rho}_k}}(A)$ ($k = 1, \dots, d$) are either 0 or 1. Thus $\mathbb{Q}$-almost surely, $Q_{\mathfrak{m}}(A) = 1$ if and only if for all $k = 1, \dots, d$, $Q_{\mathfrak{m}|_{\vec{\rho}_k}}(A) = 1$. In other words, the value of $Q_{\mathfrak{m}}(A)$ is unchanged when re-rooting at a neighbor of the root edge. But since the maps are connected, we obtain (b) by iterating the above argument.

(c) If an event $\hat{A}$ on the space of (locally finite) rooted maps is $\mathbb{Q}$-almost surely invariant under re-rooting, then $\mathbb{Q}(\hat{A}) \in \{0, 1\}$.

Consider the measure-preserving mapping $\hat{\Phi} : w \mapsto \mathfrak{m}$, where $(\mathfrak{m}, \mathfrak{g}) = \Phi(w)$ for some subgraph $\mathfrak{g}$. Via this mapping, a translation of indices in a word w give rise to a re-rooting of the corresponding map $\mathfrak{m}$. Therefore if an event $\hat{A}$ is $\mathbb{Q}$-almost surely invariant under re-rooting, then $\hat{\Phi}^{-1}\hat{A}$ is $\mathbb{P}$-almost surely invariant under translation of the indices. But, under $\mathbb{P}$ the letters of w are i.i.d. random variables, so we have $\mathbb{Q}(\hat{A}) = \mathbb{P}(\hat{\Phi}^{-1}\hat{A}) \in \{0, 1\}$.

Finally, considering $\hat{A} = \{\mathfrak{m} : Q_{\mathfrak{m}}(A) = 1\}$ shows that $\mathbb{Q} \otimes Q(A) \in \{0, 1\}$, as desired. $\square$

Remark. Only the step (c) of the proof uses specific features of the cFK random maps, namely, their representation by an i.i.d. sequence of letters. For any infinite random map whose law is stationary under τ, the proof of (a) and (b) goes through provided that the random map is almost surely recurrent. (Note that the proof of (b) depends on (a).) The case of almost surely transient random maps was treated in [Cur16, Proposition 10]. There, (a) was proved under the following reversibility condition: if $\overleftarrow{e}$ is the root edge of $\mathfrak{m}$, oriented in the opposite direction, then

$$\mathfrak{m} = \mathfrak{m}|_{\overleftarrow{e}}$$

in distribution. And (b) was replaced by the following variant, which follows directly from the transience of the map.

(b') Almost surely, $Q_{\mathfrak{m}}(A)$ is unchanged by any finite modification of the map $\mathfrak{m}$.

Chapter V

Critical Ising model on infinite random triangulation of the half plane

This Chapter is adapted from joint work with Joonas Turunen [CT17] (in progress).

1 Introduction

In this chapter we consider a Boltzmann random triangulation of polygon coupled to an Ising model on its faces with a Dobrushin boundary condition having p spin + and q spin −. A critical point of this model has been identified in [BBM11]. In this work we concentrate on the behavior of the model at this critical point. First we simplify the method of elimination of the so-called *catalytic variable* used in [BBM11] and compute the partition function of the model for arbitrary (p, q). In particular, the perimeter exponent is shown to be $7/3$ instead of the $5/2$ for critical uniform triangulations. Then we use the peeling exploration to study the interface between the two boundary components. We found that in the limit $p, q \to \infty$, this interface touches the boundary of the triangulation only finitely often almost surely. Scaling limits of the perimeter process associated to the peeling exploration are also obtained.

The critical Ising model is one of the simplest combinatorial structures that, when coupled to a random planar map, have a non-trivial impact on the geometry of the latter. The systematic study of the Ising model on random lattices was pioneered by Boulatov and Kazakov back in the eighties [Kaz86, BK87]. Using relations to the two-matrix model, they computed the partition function of the Ising model on random triangulations and quadrangulations in the thermodynamic limit, identifying its phase transitions and computing the associated critical exponents. This approach was later refined and generalized to deal with Ising models on more general maps as well as the Potts model [EO05, EB99]. A more mathematical derivation of the partition function on the discrete level was later given by Bernardi, Bousquet-Mélou and Schaeffer in [BMS02, BBM11]. In these works, the partition function is shown to be algebraic and admitting a rational parametrization. Our work complements the ones in [BK87, BBM11] by dealing with Ising-decorated triangulations with a large boundary and a Dobrushin boundary condition. In addition, we use the peeling process to derive the scaling limits of quantities which describes the interface geometry of the Ising configuration.

Let us define our conventions and terminology before stating the main results.

Planar maps. We refer to [Mie14, Cur17] for self-contained introductions to random planar maps. Here we consider planar maps in which loops and multiple edges are allowed. A map is *rooted* when it has a distinguished corner. This corner determines a distinguished vertex ρ, called the *origin*, and a distinguished face f_e, called the *external face*. The other faces are called *internal faces*. We denote by $\mathcal{F}(\mathfrak{m})$ the set of internal faces of a map $\mathfrak{m}$.

In the following, all maps are assumed planar and rooted.

A map is a *triangulation of the ℓ-gon* ($\ell \geq 1$) if the internal faces all have degree three, and the contour of its external face is a simple closed path (i.e. it visits each vertex at most once) of length ℓ. The number ℓ is called the *perimeter* of the triangulation, and an edge (resp. vertex) adjacent to the external face is called a *boundary edge* (resp. *boundary vertex*).

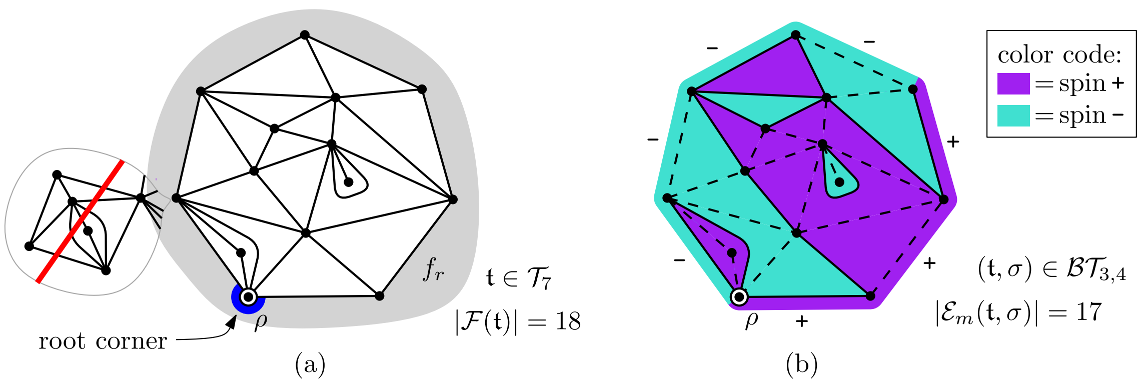

Figure V.1 – *(a) a triangulation* $\mathfrak{t}$ *of the 7-gon with 18 internal faces. The boundary will no longer be simple if one attaches to* $\mathfrak{t}$ *the map inside the bubble to its left. (b) a bicolored triangulation of the* $(3, 4)$*-gon with 17 monochromatic edges (in dashed lines).*

Figure V.1(a) gives an example of a triangulation of the 7-gon. By convention, the edge map — the map containing only one edge and no internal face — is a triangulation of the 2-gon.

Bicolored triangulations of the (p,q)-gon. We consider the Ising model with spins on the internal faces of a triangulation of polygon. The triangulation together with an Ising spin configuration on it is represented by a couple $(\mathfrak{t},\sigma)$ where $\sigma \in \{+,-\}^{\mathcal{F}(\mathfrak{t})}$. An edge e of $\mathfrak{t}$ is said to be *monochromatic* if the spins on both sides of e are the same. When e is a boundary edge, this definition requires a boundary condition which specifies a spin outside each boundary edge. By an abuse of notation, we consider the information about the boundary condition to be contained in the coloring σ, and denote by $\mathcal{E}_m(\mathfrak{t},\sigma)$ the set of monochromatic edges in $(\mathfrak{t},\sigma)$.

> *In this work, we concentrate on the* Dobrushin boundary conditions *which assign a sequence of spins of the form* $+\cdots+-\cdots-$ *to the boundary edges in the counter-clockwise order starting from the origin.*

Let p and q be respectively the numbers of $+$ and of $-$ in this sequence. Then $(\mathfrak{t},\sigma)$ is called a *bicolored triangulation of the (p,q)-gon*. Figure V.1(b) gives an example in the case $p=3$ and $q=4$. We denote by $\mathcal{BT}_{p,q}$ the set of all bicolored triangulation of the (p,q)-gon.

We enumerate the elements of $\mathcal{BT}_{p,q}$ by the generating function

$$z_{p,q}(\nu,t) \;=\; \sum_{(\mathfrak{t},\sigma)\in\mathcal{BT}_{p,q}} \nu^{|\mathcal{E}_m(\mathfrak{t},\sigma)|}\, t^{|\mathcal{F}(\mathfrak{t})|}$$

where $\nu>0$ is related to the coupling constant of the Ising model, and t is a parameter that controls the volume of the triangulation. When $q=0$ and p is small, the above generating function has already been computed by Bernardi and Bousquet-Mélou in [BBM11]. (More precisely, they computed the generating function of a model that is dual to ours. See Section 3.2 for more details.) Part of their result can be translated in our setting as follows.

Proposition V.A ([BBM11, Section 12.2])**.** *For $\nu\ge 1$, the coefficient of t^n in $z_{1,0}$ satisfies*

$$[t^n]z_{1,0}(\nu,t) \underset{n\to\infty}{\sim} \begin{cases} \kappa\;\tau^{-n}\,n^{-5/2} & \text{if } \nu\neq\nu_c \\ \kappa_c\,t_c^{-n}\,n^{-7/3} & \text{if } \nu=\nu_c \end{cases}$$

where $\nu_c = 1+2\sqrt{7}$ and $t_c = \frac{\sqrt{10}}{8(7+\sqrt{7})^{3/2}}$, and κ,τ are continuous functions of ν such that $\kappa(\nu_c)=\kappa_c$ and $\tau(\nu_c)=t_c$. In particular, $z_{1,0}(\nu,\tau(\nu))<\infty$ for all $\nu\ge 1$.

This suggests that $\nu_c = 1+2\sqrt{7}$ is the unique value of ν at which the asymptotic behavior of the Ising-decorated random triangulation escapes from the universality class of the Brownian map (corresponding to $\nu=1$). In this work we will concentrate on this critical value of the parameter, and leave the general case to an upcoming work. In all that follows, we fix $(\nu,t)=(\nu_c,t_c)$ and write $z_{p,q}=z_{p,q}(\nu_c,t_c)$.

Theorem V.1 (Asymptotics of $z_{p,q}$)**.** *The generating function $Z(u,v)=\sum_{p,q\ge 0} z_{p,q}u^p v^q$ can be computed explicitly and is algebraic. The asymptotics of its coefficients is given by*

$$z_{p,q} \underset{q\to\infty}{\sim} \frac{a_p}{\Gamma(-4/3)}u_c^{-q}q^{-7/3}$$

$$a_p \underset{p\to\infty}{\sim} \frac{b}{\Gamma(-1/3)}u_c^{-p}p^{-4/3}$$

where $u_c = \frac{6}{5}(7+\sqrt{7})t_c$ and $b = -\frac{27}{20}(\frac{3}{2})^{2/3}$, and the sequence $(a_p)_{p\geq 0}$ is given by its the generating function $A(u) = \sum_{p\geq 0} a_p u^p$, which has the following rational parametrization:

$$\begin{cases} u = \hat{u}(H) := u_c\Big(1 - \dfrac{2}{3}(1-H)^3 - \dfrac{1}{3}(1-H)^4\Big) \\ A = \hat{A}(H) := \dfrac{1}{10}\left(\dfrac{3}{2}\right)^{7/3} \dfrac{3H^2 - 8H + 9}{(H^2 - 3H + 3)^2} \end{cases}$$

where $u = 0$ and $u = u_c$ correspond to $H = 0$ and $H = 1$ respectively.

Remark. It might be surprising at first glance that the exponents in the asymptotics of $z_{p,q}$ and of a_p are different. We will see that this difference $1 = 7/3 - 4/3$ sets the speed at which the size of the main interface between the + and - clusters increases with the boundary length. More precisely, Theorem V.2 suggests that when $q = \infty$ and p is large, the interface has a length of order p^1, where the exponent 1 comes directly from the difference above. See Section 5 for more discussion on this interpretation in terms of the interface length.

Boltzmann Ising-triangulation and peeling along the interface. Now let us state the consequences of Theorem V.1 on the interface geometry of random Ising-decorated triangulations. Thanks to the finiteness of $z_{p,q}$, we can define a probability measure on $\mathcal{BT}_{p,q}$ by

$$\mathbb{P}_{p,q}(\mathfrak{t}, \sigma) \;=\; \frac{1}{z_{p,q}}\, \nu_c^{|\mathcal{E}_m(\mathfrak{t},\sigma)|}\, t_c^{|\mathcal{F}(\mathfrak{t})|}\,.$$

Under $\mathbb{P}_{p,q}$, the law of the spin configuration σ conditionally on $\mathfrak{t}$ is given by the classical Ising model on $\mathfrak{t}$. And when $\nu = 1$, the triangulation $\mathfrak{t}$ follows the distribution of a Boltzmann triangulation of the $(p+q)$-gon as introduced in [AS03], with a weight $2t_c$ per internal face. For these reasons we call $\mathbb{P}_{p,q}$ the law of a (critical) *Boltzmann Ising-triangulation of the (p,q)-gon*.

We define an *interface* in a bicolored triangulation to be a non-self-intersecting (but not necessarily simple) path formed by non-monochromatic edges. Assume that the boundary of $(\mathfrak{t}, \sigma)$ is not monochromatic, then there are exactly two boundary vertices at the junction of the + and - boundary components. One of them is the origin ρ. We call $\rho^\dagger$ the other one. We denote by $\mathcal{I}$ the *right-most interface from ρ to $\rho^\dagger$*, as shown in Figure V.2(a).[1]

We consider a peeling process that explores $\mathcal{I}$ by revealing one triangle adjacent to $\mathcal{I}$ at each step. We will represent this process by a sequence of symbols $(\mathtt{S}_n)_{n\geq 1}$ taking values in the set

$$\mathcal{S} = \{\mathtt{C}^+, \mathtt{C}^-\} \cup \{\mathtt{L}_k^+, \mathtt{L}_k^-, \mathtt{R}_k^+, \mathtt{R}_k^- : k \geq 0\}\,.$$

Roughly speaking, the symbols $\mathtt{C}^+, \mathtt{C}^-$ indicate that the newly revealed face points towards the interior of the unexplored region, while $\mathtt{L}_k^+, \mathtt{L}_k^-, \mathtt{R}_k^+, \mathtt{R}_k^-$ indicate that the newly revealed face comes back to the boundary of the unexplored region, swallowing a sub-triangulation of perimeter $k+1$. We refer to Figure V.3 for the geometric pictures corresponding to each peeling event and to Section 2.2 for the detailed definition of the whole process $(\mathtt{S}_n)_{n\geq 1}$ (including its termination time).

[1]The non-monochromatic edges in $(\mathfrak{t}, \sigma)$ form a subgraph of $\mathfrak{t}$ which has even degree at every vertex except for ρ and $\rho^\dagger$. Therefore ρ and $\rho^\dagger$ must belong to the same connected component of this subgraph.

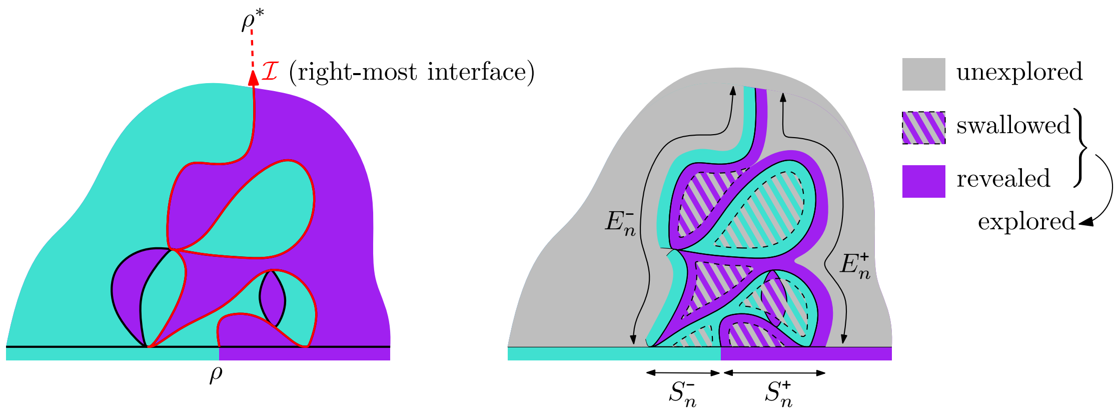

(a) (b)

Figure V.2 – *(a) The right-most interface from ρ to ρ^* in a bicolored triangulation. For clarity, only the non-monochromatic edges connected to ρ are drawn. (b) An illustration of the peeling process that explores the right-most interface $\mathcal{I}$. Notice that one can read the perimeter variation (X_n, Y_n) from the local configuration: $X_n = E_n^+ - S_n^+$ and $Y_n = E_n^- - S_n^-$.*

We would like to understand the behavior of the peeling processes $(\mathtt{S}_n)_{n\geq 0}$ in the limit of large perimeter. The regime where p and q go to infinity at comparable speeds is probably the most natural and interesting one. But currently we do not yet know how to extract the asymptotics of $z_{p,q}$ from its generating function in this regime. Instead, we will look into the regime where q goes to infinity before p. Let us call $\mathtt{P}_{p,q}$ the law of the peeling process $(\mathtt{S}_n)_{n\geq 0}$ under $\mathbb{P}_{p,q}$. In Section 4.1 we will prove that this law converges weakly as follows (Proposition V.5): $\mathtt{P}_{p,q} \xrightarrow[q\to\infty]{} \mathtt{P}_{p,\infty} \xrightarrow[p\to\infty]{} \mathtt{P}_{\infty,\infty}$, where $\mathtt{P}_{p,\infty}$ and $\mathtt{P}_{\infty,\infty}$ are probability distributions. Geometrically, this is equivalent to the local convergence in distribution of the *explored region* in Figure V.2(b), that is, the set of triangles which are either adjacent to the interface $\mathcal{I}$, or swallowed by the set of triangles adjacent to $\mathcal{I}$. More details about this geometric interpretation will be given in Section 5.

Scaling limits of the perimeter processes in infinite triangulations. We denote by (P_n, Q_n) the boundary condition of the unexplored region after n peeling steps, and by (X_n, Y_n) their variations, that is, $X_n = P_n - P_0$ and $Y_n = Q_n - Q_0$. Geometrically, X_n (resp. Y_n) is the number of edges on the + side (resp. - side) of $\mathcal{I}$ discovered by the peeling process up to time n, minus the number of + boundary edges (resp. - boundary edges) "swallowed" by the peeling process. See Figure V.2(b). Consequently, (X_n, Y_n) only depends on the configuration of the triangles along the interface $\mathcal{I}$ explored up to time n.

More precisely, it will be clear from the definition of the peeling process that (X_n, Y_n) is a deterministic function of the peeling events $(\mathtt{S}_k)_{1\leq k\leq n}$, with a functional relation independent of the initial condition (p, q). This allows us to define the law of the process $(X_n, Y_n)_{n\geq 0}$ under $\mathtt{P}_{\infty,\infty}$ even if $P_n = Q_n = \infty$ almost surely in this case.

Theorem V.2 (Scaling limit of $(X_n, Y_n)_{n\geq 0}$). *Under $\mathtt{P}_{\infty,\infty}$, the process $(X_n, Y_n)_{n\geq 0}$ is a random walk on $\mathbb{Z}^2$ starting from $(0,0)$. Its two components have the same positive drift: $\mathtt{E}_{\infty,\infty}[X_1] = \mathtt{E}_{\infty,\infty}[Y_1] = \mu := \frac{1}{4\sqrt{7}}$. Moreover, the fluctuation of $(X_n, Y_n)_{n\geq 0}$ around its mean* *has the following limit in distribution with respect to the Skorokhod topology:*

$$\frac{1}{n^{3/4}}\Big(X_{\lfloor nt\rfloor} - \mu nt, Y_{\lfloor nt\rfloor} - \mu nt\Big)_{t\geq 0} \xrightarrow[n\to\infty]{} \Big(\mathcal{X}_t, \mathcal{Y}_t\Big)_{t\geq 0},$$

where $\mathcal{X}$ and $\mathcal{Y}$ are two independent spectrally-negative $\frac{4}{3}$-stable processes of Lévy measure $\frac{c_x}{|x|^{7/3}}\mathbb{1}_{\{x<0\}}\mathrm{d}x$ and $\frac{c_y}{|y|^{7/3}}\mathbb{1}_{\{y<0\}}\mathrm{d}y$, for some explicit constants $c_x > c_y > 0$.

An important point in Theorem V.2 is that μ, the common drift of $(X_n)_{n\geq 0}$ and $(Y_n)_{n\geq 0}$, is strictly positive. This means that under $\mathtt{P}_{\infty,\infty}$, the peeling process discovers more and more edges on both sides of the interface $\mathcal{I}$ and comes back to the boundary only finitely many times. This is in contrast with the behavior of the percolation interface on uniform random maps of the half plane with the same boundary condition, which comes back to the boundary infinitely often.

Notice that there is an asymmetry between the fluctuations of the processes $(X_n)_{n\geq 0}$ and $(Y_n)_{n\geq 0}$. This is not surprising because they are defined by the peeling process that explores the *right-most* interface. Nevertheless, this asymmetry is *not* related to the fact that we have taken first the limit $q\to\infty$ and then the limit $p\to\infty$. In fact, with Theorem V.1 one can check that taking the limit $p\to\infty$ and then the limit $q\to\infty$ yields the same distribution $\mathtt{P}_{\infty,\infty}$. We conjecture that this limit actually arises when $p,q\to\infty$ at any relative speed.

Conjecture. $\mathtt{P}_{p,q} \longrightarrow \mathtt{P}_{\infty,\infty}$ weakly whenever $p,q\to\infty$.

Proving this conjecture would require one to control on the asymptotics of $(z_{p,q})_{p,q\geq 0}$ when both p and q vary, which we do not know how to do currently. What we could have done here is to strengthen the convergence of the measure $\mathtt{P}_{p,q}$ on the peeling events $(\mathtt{S}_n)_{n\geq 1}$ to the convergence of the underlying bicolored triangulation $(\mathtt{t},\sigma)$ with respect to the local distance, namely, there exist probability measures on infinite bicolored triangulations, such that $\mathbb{P}_{p,q} \xrightarrow[q\to\infty]{} \mathbb{P}_{p,\infty} \xrightarrow[p\to\infty]{} \mathbb{P}_{\infty,\infty}$ weakly with respect to the local topology.

However, including the full proof of the local convergence would almost double the length of this chapter. Instead we will only give a glimpse of it by showing an important intermediate result on the behavior of the perimeter process $(P_n)_{n\geq 0}$ under $\mathtt{P}_{p,\infty}$:

Theorem V.3 (Scaling limit of $(P_n)_{n\geq 0}$)**.** *Under $\mathtt{P}_{p,\infty}$, the process $(P_n)_{n\geq 0}$ is a Markov chain on $\mathbb{Z}_{\geq 0}$ which starts from p and is killed at zero almost surely in finite time. It has the following limit in distribution with respect to the Skorokhod topology:*

$$\frac{1}{p}(P_{\lfloor pt\rfloor})_{t\geq 0} \xrightarrow[p\to\infty]{} (\mathcal{D}_t)_{t\geq 0},$$

where $(\mathcal{D}_t)_{t\geq 0}$ is the deterministic drift process $(1+\mu t)_{t\geq 0}$ that jumps to zero and gets killed at a random time ζ whose law is

$$\mathbb{P}(\zeta > t) = (1+\mu t)^{-4/3}.$$

Geometrically, the large negative jump of $(P_n)_{n\geq 0}$ correspond to the first time that the peeling process hits a boundary vertex close to $\rho^\dagger$, swallowing most of the + boundary edges and all the + edges along the interface $\mathcal{I}$ discovered thus far. Thus the theorem should be interpreted as follows: for large p, the total length of the interface $\mathcal{I}$ under $\mathtt{P}_{p,\infty}$ is almost surely finite and roughly ζp. More discussion on the length of the interface is in Section 5.

The rest of the chapter is organized as follows.

First we derive Tutte's equation satisfied by the generating function $Z(u, v)$ by considering a one-step peeling operation (Section 2.1). We iterate this operation to define the peeling exploration of the right-most interface $\mathcal{I}$, and the associated perimeter processes (Section 2.2). In our case, Tutte's equation is an algebraic equation with two "catalytic" variables. We exploit the particularities of the Ising model to eliminate one catalytic variable by extracting coefficient (Section 3.1). Then we use the connection between our model and a model studied in [BBM11] to import their solutions of the partition functions $z_{1,0}$ and $z_{3,0}$ (Section 3.2). These solutions can also be obtained independently using a trick whose idea originates from Tutte (Appendix A.1). Injecting the solution of $z_{1,0}$ and $z_{3,0}$ into the equation with one catalytic variable, we can solve it and deduce an explicit rational parametrization of $Z(u, v)$ (Section 3.3). From this parametrization we deduce the asymptotics in Theorem V.1 using techniques presented in Appendix A.2.

Then we turn to the probabilistic part of this chapter and compute the distributional limit of the peeling process as $q \to \infty$ and then $p \to \infty$ (Section 4.1). Theorem V.2 follows from standard invariance principles about heavy-tailed random walks and some computations (Section 4.2). The proof of Theorem V.3 (Section 4.3) is much more involved and requires a technical lemma (Lemma V.10), whose proof is postponed to Appendix A.3. We finish with discussions about the geometric interpretations of our results (Section 5).

2 Tutte's equation and peeling along the interface

Recall that we have fixed the critical parameters (ν_c, t_c) and defined $Z(u, v) = \sum_{p,q \geq 0} z_{p,q} u^p v^q$ with $z_{0,0} = 1$ and $z_{p,q} = z_{p,q}(\nu_c, t_c)$ for $p + q \geq 1$. But many of the discussions below will be valid for any $\nu, t > 0$ such that $z_{p,q}(\nu, t) < \infty$. In this case we will write (ν, t) instead of (ν_c, t_c).

The primary goal of this section is to derive a recurrence relation for the double sequence $(z_{p,q})_{p,q \geq 0}$, and then a functional equation — the so-called Tutte's equation (a.k.a. loop equation, or Schwinger-Dyson equation) — for its generating function. The basic idea, which goes back to Tutte [Tut62b], is to consider the removal of one face on the boundary,

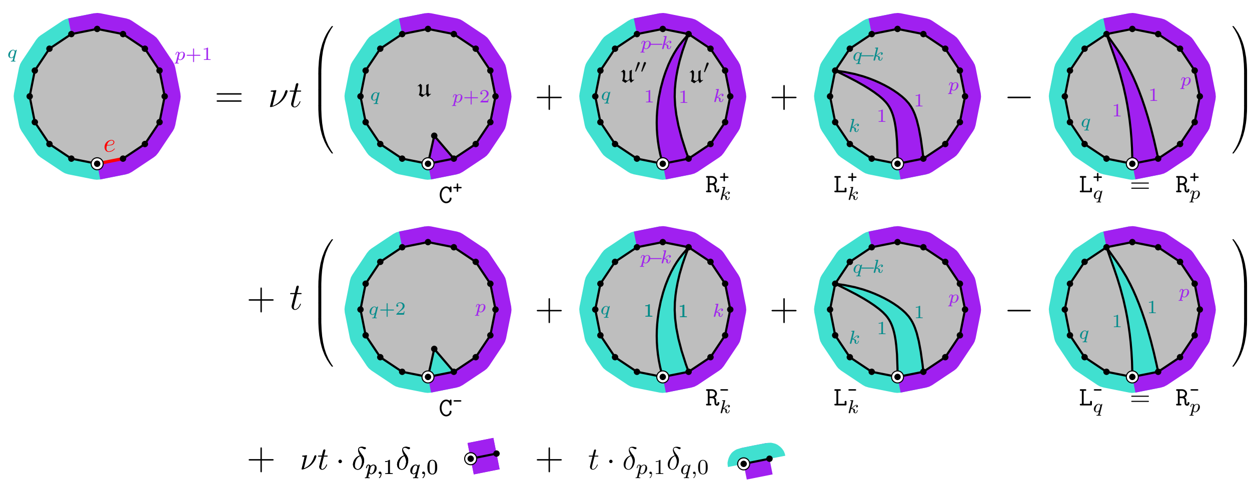

Figure V.3 – *A graphical representation of the derivation of Tutte's equation.*

which relates one bicolored triangulation of polygon to other ones with fewer faces. We will present a probabilistic derivation of Tutte's equation. This is a bit more cumbersome than a direct combinatorial derivation, but will shed light on the relation between Tutte's equation and the peeling process, which we define in the second half of this section.

2.1 Derivation of Tutte's equation

Let $p, q \geq 0$ so that the bicolored triangulation $(\mathfrak{t}, \sigma) \in \mathcal{BT}_{p+1,q}$ has at least one boundary edge with spin $\texttt{+}$. We remove the boundary edge e immediately on the right of the origin (which has spin $\texttt{+}$), and reveals the internal face f adjacent to it. It is possible that f does not exist if $(p+1, q) = (2, 0)$ or $(1, 1)$. In this case $\mathfrak{t}$ is the edge map and $(\mathfrak{t}, \sigma)$ has a weight ν or 1. When f does exist, let $* \in \{\texttt{+}, \texttt{-}\}$ be its spin and v be the vertex at the corner of f not adjacent to e. There are three possibilities for the position of v.

Event $\texttt{C}^*$: v is not on the boundary of $\mathfrak{t}$;
Event $\texttt{R}_k^*$: v is at a distance k to the right of e on the boundary of $\mathfrak{t}$; $(0 \leq k \leq p)$
Event $\texttt{L}_k^*$: v is at a distance k to the left of e on the boundary of $\mathfrak{t}$. $(0 \leq k \leq q)$

These events, as well as the discussion below, are illustrated in Figure V.3.

When the event $\texttt{C}^*$ occurs, the unexplored part of $(\mathfrak{t}, \sigma)$, denoted $\mathfrak{u}$, is again a bicolored triangulation of polygon. If $* = \texttt{+}$, then $\mathfrak{u}$ has the boundary condition $\texttt{+}^{p+2}\texttt{-}^q$ and the numbers of monochromatic edges and of internal faces in $\mathfrak{u}$ are respectively $|\mathcal{E}_m(\mathfrak{t}, \sigma)| - 1$ and $|\mathcal{F}(\mathfrak{t})| - 1$. It follows that for all $(\mathfrak{t}_0, \sigma_0) \in \mathcal{BT}_{p+2,q}$,

$$\mathbb{P}_{p+1,q}(\texttt{C}^{\texttt{+}} \text{ and } \mathfrak{u} = (\mathfrak{t}_0, \sigma_0)) = \frac{1}{z_{p+1,q}} \nu^{|\mathcal{E}_m(\mathfrak{t}_0,\sigma_0)|+1} t^{|\mathcal{F}(\mathfrak{t}_0)|+1} = \nu t \frac{z_{p+2,q}}{z_{p+1,q}} \cdot \frac{\nu^{|\mathcal{E}_m(\mathfrak{t}_0,\sigma_0)|} t^{|\mathcal{F}(\mathfrak{t}_0)|}}{z_{p+2,q}}.$$

In other words, $\mathbb{P}_{p+1,q}(\texttt{C}^{\texttt{+}}) = \nu t \frac{z_{p+2,q}}{z_{p+1,q}}$ and conditionally on $\texttt{C}^{\texttt{+}}$, the law of $\mathfrak{u}$ is $\mathbb{P}_{p+2,q}$. Similarly when $* = \texttt{-}$, we have $\mathbb{P}_{p+1,q}(\texttt{C}^{\texttt{-}}) = t \frac{z_{p,q+2}}{z_{p+1,q}}$ and conditionally on $\texttt{C}^{\texttt{-}}$, the law of $\mathfrak{u}$ is $\mathbb{P}_{p,q+2}$.

When the event $\texttt{R}_k^{\texttt{+}}$ occurs for some $0 \leq k \leq p$, the vertex v is on the part of boundary of $(\mathfrak{t}, \sigma)$ with $\texttt{+}$ spin, and the unexplored part is made of two bicolored triangulations of polygons joint together at the vertex v. We denote by $\mathfrak{u}'$ the right one and by $\mathfrak{u}''$ the left one. Then $\mathfrak{u}'$ has the boundary condition $\texttt{+}^{k+1}$ and $\mathfrak{u}''$ the boundary condition $\texttt{+}^{p+1-k}\texttt{-}^q$. Again one can relate the numbers of monochromatic edges and of internal faces in $\mathfrak{u}' \cup \mathfrak{u}''$ to $\mathcal{E}_m(\mathfrak{t}, \sigma)$ and $\mathcal{F}(\mathfrak{t})$. It then follows that for all $(\mathfrak{t}', \sigma') \in \mathcal{BT}_{k+1,0}$ and $(\mathfrak{t}'', \sigma'') \in \mathcal{BT}_{p+1-k,q}$,

$$\begin{aligned}\mathbb{P}_{p+1,q}\Big(\texttt{R}_k^{\texttt{+}},\ \mathfrak{u}' = (\mathfrak{t}', \sigma') \text{ and } \mathfrak{u}'' = (\mathfrak{t}'', \sigma'')\Big) &= \frac{1}{z_{p+1,q}} \nu^{|\mathcal{E}_m(\mathfrak{t}',\sigma')|+|\mathcal{E}_m(\mathfrak{t}'',\sigma'')|+1} t^{|\mathcal{F}(\mathfrak{t}')|+|\mathcal{F}(\mathfrak{t}'')|+1} \\ &= \nu t \frac{z_{k+1,0}\, z_{p+1-k,q}}{z_{p+1,q}} \cdot \frac{\nu^{|\mathcal{E}_m(\mathfrak{t}',\sigma')|} t^{|\mathcal{F}(\mathfrak{t}')|}}{z_{k+1,0}} \cdot \frac{\nu^{|\mathcal{E}_m(\mathfrak{t}'',\sigma'')|} t^{|\mathcal{F}(\mathfrak{t}'')|}}{z_{p+1-k,q}}\end{aligned}$$

In other words, $\mathbb{P}_{p+1,q}(\texttt{R}_k^{\texttt{+}}) = \nu t \frac{z_{k+1,0}\, z_{p+1-k,q}}{z_{p+1,q}}$ and conditionally on $\texttt{R}_k^{\texttt{+}}$, the maps $\mathfrak{u}'$ and $\mathfrak{u}''$ are independent and follow respectively the laws $\mathbb{P}_{k+1,0}$ and $\mathbb{P}_{p+1-k,q}$.

Similarly, one can work out the probabilities that the events $\texttt{R}_k^{\texttt{-}}$ $(0 \leq k \leq p)$ or $\texttt{L}_k^{\pm}$ $(0 \leq k \leq q)$ occur:

$$\mathbb{P}_{p+1,q}(\texttt{R}_k^{\texttt{-}}) = t \frac{z_{k,1}\, z_{p-k,q+1}}{z_{p+1,q}} \qquad \mathbb{P}_{p+1,q}(\texttt{L}_k^{\texttt{+}}) = \nu t \frac{z_{p+1,q-k}\, z_{1,k}}{z_{p+1,q}} \qquad \mathbb{P}_{p+1,q}(\texttt{L}_k^{\texttt{-}}) = t \frac{z_{p,q-k+1}\, z_{0,k+1}}{z_{p+1,q}}.$$

In each case, the unexplored part consists of two bicolored triangulations of polygons which are conditionally independent and follow the law of Boltzmann Ising-triangulations of appropriate Dobrushin boundary condition (See Figure V.3). Tutte's equation simply expresses the fact that the probabilities of the events $\mathtt{C}^+, \mathtt{C}^-, \mathtt{L}_k^+, \mathtt{L}_k^-, \mathtt{R}_k^+, \mathtt{R}_k^-$ under $\mathbb{P}_{p+1,q}$ sum to 1:

$$\begin{aligned} 1 \;=\; & \mathbb{P}_{p+1,q}(\mathtt{C}^+) + \sum_{k=0}^{p} \mathbb{P}_{p+1,q}(\mathtt{R}_k^+) + \sum_{k=0}^{q} \mathbb{P}_{p+1,q}(\mathtt{L}_k^+) - \mathbb{P}_{p+1,q}(\mathtt{L}_q^+) + \frac{\nu}{z_{2,0}}\delta_{p,1}\,\delta_{q,0} \\ & + \mathbb{P}_{p+1,q}(\mathtt{C}^-) + \sum_{k=0}^{p} \mathbb{P}_{p+1,q}(\mathtt{R}_k^-) + \sum_{k=0}^{q} \mathbb{P}_{p+1,q}(\mathtt{L}_k^-) - \mathbb{P}_{p+1,q}(\mathtt{L}_q^-) + \frac{1}{z_{1,1}}\delta_{p,0}\,\delta_{q,1}\,. \end{aligned}$$

In each line on the right hand side of this equation, the last term corresponds to the case where $\mathtt{t}$ is the edge map, which does not belong to any of the events. The negative term is needed to compensate for the fact that $\mathtt{R}_p^*$ and $\mathtt{L}_q^*$ actually represent the same event. Multiplying both sides by $z_{p+1,q}$ yields the following recurrence relation, valid for all $p, q \geq 0$.

$$\begin{aligned} z_{p+1,q} = \nu\, t\Big(& z_{p+2,q} + \sum_{p_1+p_2=p} z_{p_1+1,0}\, z_{p_2+1,q} + \sum_{q_1+q_2=q} z_{1,q_1}\, z_{p+1,q_2} - z_{p+1,0}\, z_{1,q}\Big) + \nu\,\delta_{p,1}\,\delta_{q,0} \\ + t\Big(& z_{p,q+2} + \sum_{q_1+q_2=q} z_{0,q_1+1}\, z_{p,q_2+1} + \sum_{p_1+p_2=p} z_{p_1,1}\, z_{p_2,q+1} - z_{p,1}\, z_{0,q+1}\Big) + \delta_{p,0}\,\delta_{q,1}\,, \end{aligned}$$

where p_1, p_2, q_1, q_2 are summed over non-negative values. Summing the last display over $p, q \geq 0$, we get Tutte's equation satisfied by $Z(u, v)$. By exchanging u and v we obtain another functional equation of Z. The two equations can be written compactly as the following linear system.

$$\begin{bmatrix} \Delta_u Z \\ \Delta_v Z \end{bmatrix} = \begin{bmatrix} \nu & 1 \\ 1 & \nu \end{bmatrix} \begin{bmatrix} t\Big(\Delta_u^2 Z + \big(\Delta_u Z_0(u) + Z_1(v)\big)\Delta_u Z - \Delta_u Z_0(u) Z_1(v)\Big) + u \\ t\Big(\Delta_v^2 Z + \big(\Delta_v Z_0(v) + Z_1(u)\big)\Delta_v Z - \Delta_v Z_0(v) Z_1(u)\Big) + v \end{bmatrix} \tag{V.1}$$

where we write $Z = Z(u, v)$ and $Z_k(u) = [v^k]Z(u, v)$ for short, and $\Delta_x f(x) = \frac{f(x)-f(0)}{x}$ denotes the discrete derivative with respect to the variable $x \in \{u, v\}$. Geometrically, the second equation describes the removal of a boundary edge with spin $\mathtt{-}$ next to the origin. This linear system will be the starting point of the asymptotic analysis of the double sequence $(z_{p,q})_{p,q\geq 0}$ in Section 3. But let us first turn our attention to the geometric implications of the above derivation of Tutte's equation and define the peeling process mentioned in the introduction.

2.2 Peeling exploration of the right-most interface

The peeling process along the right-most interface $\mathcal{I}$ is defined by iterating the face-revealing operation used in the derivation of Tutte's equation. Formally, a peeling process is a decreasing sequence $(\mathfrak{u}_n)_{n\geq 0}$ of sub-triangulations of $(\mathtt{t}, \sigma)$ delimited by closed simple paths. Each term $\mathfrak{u}_n$ is called the *unexplored map at time n*. Since it is delimited by a simple path, it is itself a bicolored triangulation of polygon. By convention, we include the edge map as a possible unexplored map. In the literature, the peeling process is often defined as a sequence of *explored maps*, that is, the complement of the unexplored maps. For our purposes the two definitions are equivalent because for a given bicolored map $(\mathfrak{t},\sigma)$, an unexplored map and its complement contain the same information.

We have already seen in Figure V.3 how revealing an internal face on the boundary splits $(\mathfrak{t},\sigma)$ into *one or two* unexplored regions delimited by closed simple paths. Thus the only missing ingredient for us to iterate this operation is a rule that, in the cases where two unexplored regions appear (i.e. when the peeling event is $\mathtt{L}_k^{\pm}$ or $\mathtt{R}_k^{\pm}$), chooses one of them to be the next unexplored map. At first glance, the natural choice would be to keep the unexplored region containing $\rho^\dagger$, the end point of the interface $\mathcal{I}$. However, this choice does not fit well with the limit $q\to\infty$, $p\to\infty$ that we would like to take. Instead, we will keep the unexplored region with greater number of $\mathtt{-}$ boundary edges (in case of a tie, choose the region on the right).

We apply this selection rule inductively to construct the peeling process. We start with $\mathfrak{u}_0=(\mathfrak{t},\sigma)$. Let ρ_n be the vertex at the junction between the $\mathtt{+}$ and $\mathtt{-}$ boundary components of $\mathfrak{u}_n$ ($\rho_0=\rho$), then $\mathfrak{u}_{n+1}$ is obtained by revealing the internal face of $\mathfrak{u}_n$ adjacent to the boundary edge of spin $\mathtt{+}$ next to ρ_n and, if necessary, choose one of the two unexplored regions according to the rule in the previous paragraph. This defines the peeling process $(\mathfrak{u}_n)_{n\geq 0}$ up to the first time T_0 that $\mathfrak{u}_n$ has no more $\mathtt{+}$ boundary edge or becomes the edge map. By induction, $\mathfrak{u}_n$ has a non-monochromatic Dobrushin boundary condition for all $n\leq T_0$. As mentioned in the introduction, (P_n,Q_n) denotes the boundary condition of $\mathfrak{u}_n$ and $(X_n,Y_n)=(P_n-P_0,Q_n-Q_0)$. Let $\mathtt{S}_n$ be the peeling event that occurred when constructing $\mathfrak{u}_n$ from $\mathfrak{u}_{n-1}$, taking values in the set of symbols $\mathcal{S}=\{\mathtt{C}^+,\mathtt{C}^-\}\cup\{\mathtt{L}_k^+,\mathtt{L}_k^-,\mathtt{R}_k^+,\mathtt{R}_k^-:k\geq 0\}$. The above quantities are all deterministic functions of the bicolored triangulation $(\mathfrak{t},\sigma)$. We view them as random variables defined on the sample space $\Omega=\bigcup_{p,q}\mathcal{BT}_{p,q}$. According to the discussion in the derivation of Tutte's equation, under the probability $\mathbb{P}_{p,q}$ and conditionally on (P_n,Q_n), the unexplored map $\mathfrak{u}_n$ is a Boltzmann Ising-triangulation of the (P_n,Q_n)-gon. We call this the *spatial Markov property* of $\mathbb{P}_{p,q}$. In particular, the conditional law of $\mathtt{S}_{n+1}$ is determined by (P_n,Q_n) in the same way as the law of $\mathtt{S}_1$ is determined by (p,q), as summarized in Table V.1.

On the other hand, the peeling event $\mathtt{S}_{n+1}$ determines the increment $(P_{n+1}-P_n,Q_{n+1}-Q_n)$ in the same way as $\mathtt{S}_1$ determines (X_1,Y_1). By induction, the value of (X_n,Y_n) is fixed by the sequence of peeling events $(\mathtt{S}_k)_{1\leq k\leq n}$. Combining this with the spatial Markov property, we see that $(P_n,Q_n)_{n\geq 0}$ is a Markov chain under $(\mathbb{P}_{p,q})_{p,q\geq 0}$ (killed at T_0). The transition probabilities of this Markov chain can be deduced from Table V.1.

3 Solution of Tutte's equation

Inverting the matrix on the right hand side of (V.1), we obtain the following system of equations:

$$(\nu^2-1)^{-1}(\nu\Delta_u Z-\Delta_v Z)=u+t\Big(\Delta_u^2 Z+\Big(\Delta_u Z_0(u)+Z_1(v)\Big)\Delta_u Z-\Delta_u Z_0(u)Z_1(v)\Big) \tag{V.2}$$

$$(\nu^2-1)^{-1}(\nu\Delta_v Z-\Delta_u Z)=v+t\Big(\Delta_v^2 Z+\Big(\Delta_v Z_0(v)+Z_1(u)\Big)\Delta_v Z-\Delta_v Z_0(v)Z_1(u)\Big) \tag{V.3}$$

Remark that both equations are affine in Z. Solving the first one gives the following expression of Z as a rational function of the univariate series Z_0 and Z_1:

$$Z(u,v)=Z_0(v)+\frac{u(Z_0(v)-Z_0(u))+(\nu^2-1)v(u^2-tZ_0(u)Z_1(v))}{\nu v-u-(\nu^2-1)tv\Big(\frac{Z_0(u)}{u}+Z_1(v)\Big)}\,. \tag{V.4}$$

$\mathtt{s}$	$\mathbb{P}_{p+1,q}(\mathtt{S}_1 = \mathtt{s})$	(X_1, Y_1)	$\mathtt{s}$	$\mathbb{P}_{p+1,q}(\mathtt{S}_1 = \mathtt{s})$	(X_1, Y_1)	
$\mathtt{C}^+$	$\nu_c t_c \frac{z_{p+2,q}}{z_{p+1,q}}$	$(1,0)$	$\mathtt{C}^-$	$t_c \frac{z_{p,q+2}}{z_{p+1,q}}$	$(-1,2)$	
$\mathtt{L}^+_k$	$\nu_c t_c \frac{z_{p+1,q-k}\, z_{1,k}}{z_{p+1,q}}$	$(0,-k)$	$\mathtt{L}^-_k$	$t_c \frac{z_{p,q-k+1}\, z_{0,k+1}}{z_{p+1,q}}$	$(-1,-k+1)$	$(0 \le k \le \frac{q}{2})$
$\mathtt{R}^+_k$	$\nu_c t_c \frac{z_{k+1,0}\, z_{p-k+1,q}}{z_{p+1,q}}$	$(-k,0)$	$\mathtt{R}^-_k$	$t_c \frac{z_{k,1}\, z_{p-k,q+1}}{z_{p+1,q}}$	$(-k-1,1)$	$(0 \le k \le p)$
$\mathtt{R}^+_{p+k}$	$\nu_c t_c \frac{z_{p+1,k}\, z_{1,q-k}}{z_{p+1,q}}$	$(-p,-k)$	$\mathtt{R}^-_{p+k}$	$t_c \frac{z_{p,k+1}\, z_{0,q-k+1}}{z_{p+1,q}}$	$(-p-1,-k+1)$	$(0 < k < \frac{q}{2})$

Table V.1 – Law of the first peeling event $\mathtt{S}_1$ under $\mathbb{P}_{p+1,q}$ and the corresponding (X_1, Y_1).

3.1 Elimination of the first catalytic variable

It turns out one can obtain a closed functional equation for $Z_0(u)$ by coefficient extraction. More precisely, by extracting the coefficients of v^0 and v^1 in (V.2) and (V.3), seen as formal power series in v, we get four algebraic equations between $Z_i(u)$ $(i = 0, 1, 2, 3)$ and u, with coefficients in $\mathbb{C}[\nu][[t]]$:

$$(\nu^2-1)^{-1}(\nu\Delta Z_0 - Z_1) = t\left(\Delta^2 Z_0 + (\Delta Z_0)^2\right) + u \tag{V.5}$$
$$(\nu^2-1)^{-1}(\nu\Delta Z_1 - Z_2) = t\left(\Delta^2 Z_1 + \Delta Z_0 \Delta Z_1 + z_1 \Delta Z_1\right) \tag{V.6}$$
$$(\nu^2-1)^{-1}(\nu Z_1 - \Delta Z_0) = t\left(Z_2 + Z_1^2\right) \tag{V.7}$$
$$(\nu^2-1)^{-1}(\nu Z_2 - \Delta Z_1) = t\Big(Z_3 + Z_1 Z_2 + z_1 Z_2\Big) + 1 \tag{V.8}$$

where we write $\Delta Z_i = \Delta_u Z_i(u)$ and $z_i = z_{i,0} = z_{0,i}$ for short. Notice that only (V.8) contains the unknown Z_3, so it can be discarded without loss. On the other hand, the three remaining equations are linear in (Z_1, Z_2). Thus we can easily eliminate these two unknowns to obtain a polynomial equation on $Z_0(u)$ of the form: (See [CAS] for details of the elimination)

$$\hat{\mathcal{P}}(Z_0(u), u, z_1, z_{1,1}; \nu, t) = 0 \tag{V.9}$$

This is not yet a closed functional equation for $Z_0(u)$ because it involves the series $z_{1,1}$ which is *a priori* not related to $Z_0(u)$. (It comes from the term $\Delta_u^2 Z_1(u) = \frac{Z_1(u) - z_1 - u z_{1,1}}{u^2}$ in (V.6).) To relate them, we can view the above equation as a formal power series in u, and extract its coefficients. The first two non-zero coefficients yield two equations relating relating $z_{1,1}$ to z_i $(i = 1, 2, 3)$ and which are linear in $(z_{1,1}, z_2)$. Solving them gives

$$z_{1,1} = (\nu^2-1)(2t\, z_1^3 - t\, z_3 - 1) - (3\nu - 2) z_1^2 + \frac{\nu z_1}{(\nu+1)t} \tag{V.10}$$

Plugging this into $\hat{\mathcal{P}} = 0$ yields a closed functional equation (with one catalytic variable) satisfied by $Z_0(u)$. This equation can be written as

$$Z_0(u) = 1 + \nu u^2 + t\, \mathcal{R}(Z_0(u), u, z_1, z_3; \nu, t) \tag{V.11}$$

where the rational function $\mathcal{R} = \mathcal{R}(y, u, z_1, z_3; \nu, t)$ is given by (See [CAS])

$$\begin{aligned}\mathcal{R} = {} & (\nu^2-1)^2 t^2 \Big((y-1) \left(\frac{y}{u}\right)^3 - z_1 \left(\frac{y}{u}\right)^2 - \frac{1+y-2y^2+z_1 u}{t} + 2z_1^3 - z_3 \Big) \\ & - (\nu^2-1) t \Big(2\nu(y-1)\left(\frac{y}{u}\right)^2 - (\nu+1) z_1 \frac{y}{u} + 3(\nu-1) z_1^2 \Big) \\ & + \nu(\nu+1)(y-1)\frac{y}{u} - \nu(\nu^2-1)u(2y-1) + \nu(\nu-3)z_1 + (\nu^2-1)^2 u^3 .\end{aligned} \tag{V.12}$$

Notice that $\mathcal{R}(Z_0(u), u, z_1, z_3; \nu, t)$ is a formal power series of t with coefficients in $\mathbb{C}(\nu, u)$. Therefore (V.11) determines $Z_0(u)$ order by order as a formal power series in t. According to the general theory on polynomial equations with one catalytic variable [BMJ06, Theorem 3], the generating function $Z_0(u)$ is algebraic.[2] The same holds for $Z_1(u)$ and $Z(u, v)$, since according to (V.5) and (V.4), they are rational functions of $Z_0(u)$ and of its coefficients.

3.2 Connection with previous work and solution for z_i

In principle, we could apply the general strategy developed in [BMJ06] to eliminate the catalytic variable u from (V.11) and obtain an explicit algebraic equation relating z_1 (resp. z_3) and t. However, in practice this gives an equation of exceedingly high degree. Instead, we need to exploit specific features of (V.11) to eliminate u while keeping the degree low. We will explain how this can be done in Appendix A.1. Here we forego the procedure of eliminating the catalytic variable u and jump directly to the solution of $z_i(\nu, t)$ $(i = 1, 2, 3)$ by importing the corresponding results from [BBM11].

In [BBM11], the quantity $2Q_i(2, \nu, t)$ is the generating series of vertex-bicolored triangulations with a general (i.e. not necessarily simple) boundary of length i and free boundary condition. The parameter t counts the number of edges, and ν the number of monochromatic edges. To avoid confusion, we replace the symbols ν and t of [BBM11] by ν^* and t^* in the following.

Let $\check{z}_i(\nu, t)$ be the generating series of face-bicolored triangulations with a general boundary of length i and monochromatic boundary condition. By using the Kramers-Wannier duality between the low-temperature expansion and high-temperature expansion of the Ising partition function (see e.g. [BDC16, Section 1.2]), one can show that if (ν^*, t^*) and (ν, t) satisfy

$$(\nu^* - 1)(\nu - 1) = 2 \qquad \text{and} \qquad 2(t^*)^3 = (\nu - 1)^3 t^2$$

then for all $i \geq 1$,

$$(t^*)^i Q_i(2, \nu^*, t^*) = (\nu - 1)^i t^i \check{z}_i(\nu, t). \tag{V.13}$$

On the other hand, $\check{z}_i(\nu, t)$ is nothing but the version of $z_i(\nu, t)$ where we remove the constraint of simple boundary. Let $\check{Z}_0(u) \equiv \check{Z}_0(\nu, t; u) = 1 + \sum_{i \geq 1} \check{z}_i(\nu, t) u^i$. By decomposing a general boundary triangulation into its "simple boundary core" and general boundary

[2] To apply literally [BMJ06, Theorem 3] to (V.11), we must be able to write $\mathcal{R}$ as a polynomial function of the discrete derivatives $\Delta^i Z_0(u)$ $(i \geq 0)$ and the parameters u, t, which is not obvious here. However, it is clear that the coefficients z_1, z_2, z_3 can be written as polynomials of u and $\Delta^i Z_0(u)$ $(i \geq 0)$. So we can multiply both sides of (V.11) by u^3, and view it as a functional equation for the unknown $\mathcal{Z}_0(u) = u^3 Z_0(u)$. Then $u^3 \mathcal{R}$ is clearly a polynomial function of u, t and $\Delta^i Z_0(u) = \Delta^{i+3} \mathcal{Z}_0(u)$ $(i \geq 0)$. Therefore [BMJ06, Theorem 3] applies.

triangulations attached to the core, we see that $\check{Z}_0(u) = Z_0(u\check{Z}_0(u))$. Extracting the first coefficients of u, we get

$$z_1 = \check{z}_1 \qquad z_2 = \check{z}_2 + z_1^2 \qquad \text{and} \qquad z_3 = \check{z}_3 - 3z_1\check{z}_2 + 2z_1^3 \tag{V.14}$$

Using (V.13) and (V.14), we can easily translate the results in [BBM11, Thm. 23] to get the following rational parametrizations of $z_i(\nu, t)$ $(i = 1, 3)$:

$$\begin{cases} t^2 &= \dfrac{(\nu-S)\,(S+\nu-2)}{32(\nu^2-1)^3S^2}\,(4S^3-S^2-2S+\nu^2-2\nu), \\ t^3z_1 &= \dfrac{(\nu-S)^2(S+\nu-2)}{64(\nu^2-1)^4S^2}(3S^3-\nu S^2-\nu S+\nu^2-2\nu), \\ t^9z_3 &= \dfrac{(\nu-S)^5(S+\nu-2)^5}{2^{22}(\nu^2-1)^{12}S^8}\cdot\Big(160S^{10}-128S^9-16(2\nu^2-4\nu+3)S^8 \\ &\;+\; 32(2\nu^2-4\nu+3)S^7-7(16\nu^2-32\nu+27)S^6-2(32\nu^2-64\nu+57)S^5 \\ &\;+\; (32\nu^4-128\nu^3+183\nu^2-110\nu+20)S^4-4(7\nu^2-14\nu-2)S^3 \\ &\;+\; \nu(\nu-2)(9\nu^2-18\nu-20)S^2+14\nu^2(\nu-2)^2S-3\nu^3(\nu-2)^3\Big). \end{cases} \tag{V.15}$$

These rational parametrizations will be checked in Appendix A.1. The singularity analysis of these series can also be imported from [BBM11, Claim 24], which gives Proposition V.A. One can also give a proof to this theorem using the tools provided in Appendix A.2.

3.3 Singularity analysis at the critical temperature

To get $Z_0(\nu, t; u)$, the generating function for Ising triangulations with a monochromatic boundary of arbitrary length, we plug the rational parametrization (V.15) into Equation (V.11). This gives us an equation of the form $\mathcal{E}(Z_0, u; \nu, S) = 0$ where $\mathcal{E}$ is a polynomial of four variables. Under the change of variables $\tilde{u} = tu$ and $\tilde{y} = \frac{t}{u}Z_0(u)$, we obtain an equation of degree 5 in its main variables $\tilde{u}$ and $\tilde{y}$ (but of degree 21 overall, see [CAS]).

It is well known that a complex algebraic curve has a rational parametrization if and only if it has genus zero [SWPD08]. Both the genus of the curve and its rational parametrization, when exists, can be computed algorithmically, and these functions are implemented in the algcurves package of Maple. It turns out that the genus of the curve $\mathcal{E}(Z_0, u) = 0$ is zero, thus a rational parametrization exists. However, the equation is too complicated for Maple to compute a rational parametrization in its full generality in reasonable time. The computation simplifies considerably in the critical case $(\nu, t) = (\nu_c, t_c)$, where t_c corresponds to $S_c = 3$ in (V.15). In this case, we found the following parametrization of $Z_0(u)$ and the corresponding parametrization of $Z_1(u)$ deduced from (V.6).

$$\begin{cases} u = \hat{u}(H) &:= \dfrac{u_c}{3}H\Big(10-12H+6H^2-H^3\Big) \\ Z_0 = \hat{Z}_0(H) &:= \dfrac{1}{10}\Big(1-(1-\sqrt{7})H+3H^2-H^3\Big)\Big(10-12H+6H^2-H^3\Big) \\ Z_1 = \hat{Z}_1(H) &:= \dfrac{3}{10\,u_c}\Big(\sqrt{7}-1+H-\dfrac{3(4-3H+H^2)}{10-12H+6H^2-H^3}\Big) \end{cases} \tag{V.16}$$

where $u = 0$ is parametrized by $H = 0$ and $u_c = \frac{6}{5}(7+\sqrt{7})t_c$, as mentioned in Theorem V.1. By making the substitution $(u, Z_0(u), Z_1(u)) \leftarrow (\hat{u}(H), \hat{Z}_0(H), \hat{Z}_1(H))$ and

$(v, Z_0(v), Z_1(v)) \leftarrow (\hat{u}(K), \hat{Z}_0(K), \hat{Z}_1(K))$ in (V.4), one obtains a rational parametrization of $Z(u,v)$ of the form

$$u = \hat{u}(H), \quad v = \hat{u}(K) \qquad \text{and} \qquad Z = \hat{Z}(H,K) \tag{V.17}$$

where $\hat{Z}(H,K)$ is the quotient of two symmetric polynomials of degree 10 and 4 respectively. Its expression is given in [CAS].

Next, we would like to apply the standard transfer theorem of analytic combinatorics [FS09, Corollary VI.1] to extract asymptotics of the coefficients of $Z(u,v)$. The idea is to use the rational parametrization to write that $Z(u,v) = \hat{Z}(\hat{u}^{-1}(u), \hat{u}^{-1}(v))$ in some neighborhood of the origin, and to extend this relation to the dominant singularity for one of the variables. The main difficulty here is, given a rational parametrization of $v \mapsto Z(u,v)$, to localize rigorously its dominant singularity (or singularities), and to show that it has an analytic continuation on a Δ-domain at this singularity. We will present a method that solves this problem in a generic setting in Appendix A.2. For the sake of continuity of exposition, we first summarize the properties of $Z(u,v)$ and $A(u)$ obtained with this method in the following lemma, and leave its proof to Appendix A.2.

For $x > 0$, let D_x (resp. $\overline{D}_x$) be the open (resp. closed) disk of radius x centered at 0. For $x, \epsilon > 0$, the *slit disk at x of margin ϵ* is defined as $D_x^{|\epsilon} = D_{x+\epsilon} \backslash [x, x+\epsilon]$. Notice that a slit disk at x contains a Δ-domain at x.

Lemma V.4. *(i) $\sum_{p,q\geq 0} z_{p,q} u^p v^q$ is absolutely convergent if and only if $(u,v) \in (\overline{D}_{u_c})^2$.*

(ii) There is a neighborhood V of $H = 0$ such that $\hat{u}|_V$ is a conformal bijection onto a slit disk at u_c and $\hat{u}(H) \to u_c$ as H tends to 1 in V.

(iii) For each $u \in \overline{D}_{u_c}$, the function $v \mapsto Z(u,v)$ has its dominant singularity at u_c and has an analytic continuation on a slit disk at u_c (whose margin depends on u).

(iv) Similarly, the function $A(u)$ defined by the rational parametrization in Theorem V.1 has its dominant singularity at u_c and has an analytic continuation on a slit disk at u_c.

Now let us carry out the singularity analysis of $Z(u,v)$ and finish the proof of Theorem V.1. By Lemma V.4(ii), the asymptotic expansion of $v \mapsto Z(u,v)$ at its dominant singularity u_c is determined by the behavior of its parametrization in a neighborhood of $K = 1$. One can check that the first and second derivatives of $K \mapsto \hat{Z}(H,K)$ *both vanish* at $K = 1$. Therefore the function has the Taylor expansion

$$\hat{Z}(H,K) \;=\; \hat{Z}(H,1) - \frac{\partial_K^3 \hat{Z}(H,1)}{6}(1-K)^3 + \frac{\partial_K^4 \hat{Z}(H,1)}{24}(1-K)^4 + O((1-K)^5)\,.$$

On the other hand, we can rewrite the equation $v = \hat{u}(K)$ as $(1-K)^3 = \frac{3}{2}\left(1-\frac{v}{u_c}\right) - \frac{1}{2}(1-K)^4$. In particular, we have $1-K \sim (\frac{3}{2})^{1/3}(1-\frac{u}{u_c})^{1/3}$ as $K \to 1$. Plug this into the Taylor expansion of $K \mapsto \hat{Z}(H,K)$, we obtain the following asymptotic expansion of $v \mapsto Z(u,v)$ at $v = u_c$:

$$Z(u,v) = Z(u,u_c) - \partial_v Z(u,u_c)(u_c - v) + A(u)\left(1 - \frac{v}{u_c}\right)^{4/3} + O\!\left(\left(1-\frac{v}{u_c}\right)^{5/3}\right),$$

where $A(u)$ is given by the rational parametrization $u = \hat{u}(H)$ and

$$A = \hat{A}(H) \;:=\; \left(\frac{3}{2}\right)^{4/3}\left(\frac{\partial_K^4 \hat{Z}(H,1)}{24} + \frac{\partial_K^3 \hat{Z}(H,1)}{12}\right) = \frac{1}{10}\left(\frac{3}{2}\right)^{7/3} \frac{9 - 8H + 3H^2}{(3 - 3H + H^2)^2}\,. \tag{V.18}$$

Thanks to Lemma V.4(iii), the transfer theorem [FS09, Corollary VI.1] applies to $v \mapsto Z(u,v)$, which implies that for all $u \in \overline{D}_{u_c}$,

$$Z_q(u) = [v^q]Z(u,v) \underset{q\to\infty}{\sim} \frac{A(u)}{\Gamma(-4/3)} u_c^{-q} q^{-7/3} . \tag{V.19}$$

It follows that

$$\frac{Z_q(u)}{Z_q(u_c)} \xrightarrow[q\to\infty]{} \frac{A(u)}{A(u_c)} .$$

This can be interpreted as the pointwise convergence of the generating functions of the discrete probability distribution $\left(\frac{z_{p,q}}{Z_q(u_c)}\right)_{p\geq 0}$ to the generating function of the sequence $\left(\frac{a_p}{A(u_c)}\right)_{p\geq 0}$. According to the general continuity theorem [FS09, Theorem IX.1], this implies the convergence of the sequences term by term:

$$\frac{z_{p,q}}{Z_q(u_c)} \xrightarrow[q\to\infty]{} \frac{a_p}{A(u_c)} .$$

for all $p \geq 0$. (In fact [FS09, Theorem IX.1] also assumes the limit sequence to be a probability distribution *a priori*, but a careful reading of the proof shows that this assumption is not necessary.) Compare the last display with (V.19), we obtain the asymptotics of $(z_{p,q})_{q\geq 0}$ stated in Theorem V.1.

This asymptotics implies in particular that $a_p \geq 0$ for all $p \geq 0$. This positivity property is in fact used in the proof of Lemma V.4(iv) in Appendix A.2. But there is no viscous circle in the proof since we have used only the assertions (i)-(iii) of Lemma V.4 to deduce the asymptotics of $(z_{p,q})_{q\geq 0}$. Now we repeat the same steps to find the asymptotics of $(a_p)_{p\geq 0}$. Contrary to $K \mapsto \hat{Z}(H,K)$, the first derivative of $H \mapsto \hat{A}(H)$ does not vanish at $H = 1$. This leads to an exponent $1/3$ instead of $4/3$ for the leading order singularity of $A(u)$ at u_c:

$$A(u) = A(u_c) + b\left(1 - \frac{u}{u_c}\right)^{1/3} + O\left(\left(1 - \frac{u}{u_c}\right)^{2/3}\right)$$

where $b = -(\frac{3}{2})^{1/3}\hat{A}'(1) = -\frac{27}{20}(\frac{3}{2})^{2/3}$. We apply the transfer theorem again to obtain the asymptotics of $(a_p)_{p\geq 0}$. This completes the proof of Theorem V.1.

4 Limits of the peeling processes

Let us recall that the peeling process of a bicolored triangulation $(\mathfrak{t},\sigma)$ is a decreasing sequence of unexplored maps $(\mathfrak{u}_n)_{n\geq 0}$. This sequence is uniquely determined by the boundary condition of $\mathfrak{u}_0$ and a sequence of peeling events $(\mathtt{S}_n)_{n\geq 1}$, where $\mathtt{S}_n$ takes value in the countable set $\mathcal{S}$. We denote by $\mathtt{P}_{p,q}$ the law of $(\mathtt{S}_n)_{n\geq 1}$ when $(\mathfrak{t},\sigma)$ is a Boltzmann Ising-triangulation of the (p,q)-gon.

As stated in the introduction, $\mathtt{P}_{p,q}$ converges weakly to probability distributions when $q \to \infty$ and then $p \to \infty$. In this section we first construct the limit distributions $\mathtt{P}_{p,\infty}$, $\mathtt{P}_{\infty,\infty}$ and establish their basic properties. Then we move on to prove the scaling limits of the perimeter processes stated in Theorem V.2 and V.3. For convenience, we will denote by $\mathcal{L}_{p,q}X$ (resp. $\mathcal{L}_{p,\infty}X$ and $\mathcal{L}_{\infty,\infty}X$) a random variable with the same law as the random variable X under $\mathtt{P}_{p,q}$ (reps. under $\mathtt{P}_{p,\infty}$ and $\mathtt{P}_{\infty,\infty}$).

4.1 Construction of $\mathtt{P}_{p,\infty}$ and $\mathtt{P}_{\infty,\infty}$

Proposition V.5 (Convergence of the sequence of peeling events)**.** *We have the following weak convergence with respect to the product topology:* $\mathtt{P}_{p,q} \xrightarrow[q\to\infty]{} \mathtt{P}_{p,\infty} \xrightarrow[p\to\infty]{} \mathtt{P}_{\infty,\infty}$*, where* $\mathtt{P}_{p,\infty}$ *and* $\mathtt{P}_{\infty,\infty}$ *are probability measures on the sequences of peeling events* $(\mathtt{S}_n)_{n\geq 1}$.

Since the first n terms of the process $(\mathtt{S}_n)_{n\geq 1}$ live in a countable space, the weak convergence of $\mathtt{P}_{p,q}$ boils down to the convergence of the probability mass of each point. In the proof below we will compute explicitly the limit of each of these masses, and verify that the resulting distribution is normalized.

Lemma V.6 (Convergence of the first peeling event)**.** *Assume $p \geq 1$. The limits*

$$\mathtt{P}_{p,\infty}(\mathtt{S}_1 = \mathtt{s}) := \lim_{q\to\infty} \mathtt{P}_{p,q}(\mathtt{S}_1 = \mathtt{s}) \qquad \text{and} \qquad \mathtt{P}_{\infty,\infty}(\mathtt{S}_1 = \mathtt{s}) := \lim_{p\to\infty} \mathtt{P}_{p,\infty}(\mathtt{S}_1 = \mathtt{s})$$

exist for all $\mathtt{s} \in \mathcal{S}$, *and we have* $\sum_{\mathtt{s}\in\mathcal{S}} \mathtt{P}_{p,\infty}(\mathtt{S}_1 = \mathtt{s}) = \sum_{\mathtt{s}\in\mathcal{S}} \mathtt{P}_{\infty,\infty}(\mathtt{S}_1 = \mathtt{s}) = 1.$

Proof. The existence of the limits can be easily checked using the expression of $\mathtt{P}_{p,q}(\mathtt{S}_1 = \mathtt{s})$ in Table V.1 and the asymptotics of $z_{p,q}$ provided by Theorem V.1. The explicit expressions of these limits are summarized in Table V.2.

It is clear that $\sum_{\mathtt{s}\in\mathcal{S}} \mathtt{P}_{p,\infty}(\mathtt{S}_1 = \mathtt{s}) = 1$ for all $p \geq 1$ if and only if

$$\sum_{p\geq 0} a_{p+1} u^p \;=\; \sum_{p\geq 0} \sum_{\mathtt{s}\in\mathcal{S}} a_{p+1} \mathtt{P}_{p+1,\infty}(\mathtt{S}_1 = \mathtt{s}) u^p$$

(a)

$\mathtt{s}$	$\mathtt{P}_{p+1,\infty}(\mathtt{S}_1 = \mathtt{s})$	(X_1, Y_1)	$\mathtt{s}$	$\mathtt{P}_{p+1,\infty}(\mathtt{S}_1 = \mathtt{s})$	(X_1, Y_1)	
$\mathtt{C}^+$	$\nu_c t_c \frac{a_{p+2}}{a_{p+1}}$	$(1,0)$	$\mathtt{C}^-$	$t_c \frac{a_p}{a_{p+1}} \frac{1}{u_c^2}$	$(-1,2)$	
$\mathtt{L}_k^+$	$\nu_c t_c z_{1,k} u_c^k$	$(0,-k)$	$\mathtt{L}_k^-$	$t_c z_{0,k+1} \frac{a_p}{a_{p+1}} u_c^{k-1}$	$(-1,-k+1)$	$(k \geq 0)$
$\mathtt{R}_k^+$	$\nu_c t_c z_{k+1,0} \frac{a_{p-k+1}}{a_{p+1}}$	$(-k,0)$	$\mathtt{R}_k^-$	$t_c z_{k,1} \frac{a_{p-k}}{a_{p+1}} \frac{1}{u_c}$	$(-k-1,1)$	$(0 \leq k \leq p)$
$\mathtt{R}_{p+k}^+$	$\nu_c t_c z_{p+1,k} \frac{a_1}{a_{p+1}} u_c^k$	$(-p,-k)$	$\mathtt{R}_{p+k}^-$	$t_c z_{p,k+1} \frac{a_0}{a_{p+1}} u_c^{k-1}$	$(-p-1,-k+1)$	$(k > 0)$

(b)

$\mathtt{s}$	$\mathtt{P}_{\infty,\infty}(\mathtt{S}_1 = \mathtt{s})$	(X_1, Y_1)	$\mathtt{s}$	$\mathtt{P}_{\infty,\infty}(\mathtt{S}_1 = \mathtt{s})$	(X_1, Y_1)	
$\mathtt{C}^+$	$\frac{\nu_c t_c}{u_c}$	$(1,0)$	$\mathtt{C}^-$	$\frac{t_c}{u_c}$	$(-1,2)$	
$\mathtt{L}_k^+$	$\nu_c t_c u_c^k z_{1,k}$	$(0,-k)$	$\mathtt{L}_k^-$	$t_c u_c^k z_{0,k+1}$	$(-1,-k+1)$	$(k \geq 0)$
$\mathtt{R}_k^+$	$\nu_c t_c u_c^k z_{k+1,0}$	$(-k,0)$	$\mathtt{R}_k^-$	$t_c u_c^k z_{k,1}$	$(-k-1,1)$	$(k \geq 0)$

Table V.2 – Law of the first peeling event $\mathtt{S}_1$ under $\mathtt{P}_{p,\infty}$, $\mathtt{P}_{\infty,\infty}$ and the corresponding (X_1, Y_1).

as formal power series in u. With a straightforward (but tedious) calculation using the data in Table V.2(a), one can show that the above condition is equivalent to

$$\begin{aligned}\Delta_u A(u) &= \nu_c t_c \Big(Z_0(u)\Delta_u^2 A(u) + Z_1(u_c)\Delta_u A(u) + a_1 \Delta_u Z(u,u_c) \Big) \\ &\quad + \frac{t_c}{u_c^2}\Big(Z_0(u_c)A(u) + u_c Z_1(u_c)A(u) + a_0\Big(Z(u,u_c) - Z_0(u_c) - u_c Z_1(u_c)\Big)\Big) \end{aligned} \tag{V.20}$$

where Δ_u is the discrete derivative operator defined below (V.1). Recall that when $v \to u_c$, we have $Z(u,v) = Z(u,u_c) + \partial_v Z(u,u_c)(v-u_c) + A(u)(1-\frac{v}{u_c})^{4/3} + O\left((1-\frac{v}{u_c})^{5/3}\right)$. Then one can write down the expansion at $v = u_c$ of the first equation in (V.1), and verify that the coefficient of the dominant singular term $(1-\frac{v}{u_c})^{4/3}$ gives exactly (V.20). This proves that $\sum_{\mathtt{s}\in\mathcal{S}} \mathtt{P}_{p,\infty}(\mathtt{S}_1 = \mathtt{s}) = 1$ for all $p \geq 1$.

Similarly, using the data in Table V.2(b) one can show that $\sum_{\mathtt{s}\in\mathcal{S}} \mathtt{P}_{\infty,\infty}(\mathtt{S}_1 = \mathtt{s}) = 1$ if and only if $(\nu_c+1)t_c\left(\frac{Z_0(u_c)}{u_c} + Z_1(u_c)\right) = 1$. This equation can be obtained as the coefficient of $(1-\frac{u}{u_c})^{1/3}$ in the expansion of (V.20) at $u = u_c$. This completes the proof of the lemma. □

Proof of Proposition V.5. Usually, to have the convergence $\mathtt{P}_{p,q} \to \mathtt{P}_{p,\infty}$ with respect to the product topology, we need to define

$$\mathtt{P}_{p,\infty}(\mathtt{S}_1 = \mathtt{s}_1, \cdots, \mathtt{S}_n = \mathtt{s}_n) \;:=\; \lim_{q\to\infty} \mathtt{P}_{p,q}(\mathtt{S}_1 = \mathtt{s}_1, \cdots, \mathtt{S}_n = \mathtt{s}_n) \tag{V.21}$$

for all $n \geq 1$ and all $s_1, \cdots, s_n \in \mathcal{S}$. However here the processes may be terminated in finite time T_0, so to in addition to the above limit, we must also have

$$\mathtt{P}_{p,\infty}(\mathtt{S}_1 = \mathtt{s}_1, \cdots, \mathtt{S}_m = \mathtt{s}_m, T_0 = m) \;:=\; \lim_{q\to\infty} \mathtt{P}_{p,q}(\mathtt{S}_1 = \mathtt{s}_1, \cdots, \mathtt{S}_m = \mathtt{s}_m, T_0 = m) \tag{V.22}$$

for all $m \leq n$. (Alternatively, one can consider the process $(\mathtt{S}_n)_{n\geq 0}$ to jump to some cemetery state after T_0. Then (V.21) and (V.22) together give the joint distribution of the n first terms of the process $(\mathtt{S}_n)_{n\geq 0}$.)

Now let us verify that this defines a probability distribution. As we have seen at the end of Section 2.2, the peeling events $(\mathtt{s}_k)_{1\leq k\leq n}$ completely determines the perimeter variations $(x_k, y_k)_{1\leq k\leq n}$, independently of the initial condition (p,q). So according to the spatial Markov property, (V.21) is equivalent to

$$\begin{aligned}\mathtt{P}_{p,\infty}(\mathtt{S}_1 = \mathtt{s}_1, \cdots, \mathtt{S}_n = \mathtt{s}_n) &= \lim_{q\to\infty} \mathtt{P}_{p,q}(\mathtt{S}_1 = \mathtt{s}_1)\mathtt{P}_{p+x_1,q+y_1}(\mathtt{S}_1 = \mathtt{s}_2)\cdots \mathtt{P}_{p+x_{n-1},q+y_{n-1}}(\mathtt{S}_1 = \mathtt{s}_n) \\ &= \mathtt{P}_{p,\infty}(\mathtt{S}_1 = \mathtt{s}_1)\cdot \mathtt{P}_{p+x_1,\infty}(\mathtt{S}_1 = \mathtt{s}_2)\cdots \mathtt{P}_{p+x_{n-1},\infty}(\mathtt{S}_1 = \mathtt{s}_n)\end{aligned}$$

The right hand side of (V.22) is almost identical, except that the last factor in the above product must be replaced by $\mathtt{P}_{p+x_{m-1},\infty}(\mathtt{S}_1 = \mathtt{s}_m)\cdot \lim_{q\to\infty} \mathtt{P}_{p+x_m,q+y_m}(T_0 = 0)$. By definition, we have $T_0 = 0$ in an unexplored triangulation $\mathfrak{u}$ of the (p,q)-gon either when $p = 0$ (the unexplored triangulation has no + boundary edge) or when $p+q = 0$ and that $\mathfrak{u}$ is the edge map. When $q \to \infty$, the second case never occur. This leaves us with

$$\begin{aligned}&\mathtt{P}_{p,\infty}(\mathtt{S}_1 = \mathtt{s}_1, \cdots, \mathtt{S}_m = \mathtt{s}_m, T_0 = m) \\ &= \mathtt{P}_{p,\infty}(\mathtt{S}_1 = \mathtt{s}_1)\cdot \mathtt{P}_{p+x_1,\infty}(\mathtt{S}_1 = \mathtt{s}_2)\cdots \mathtt{P}_{p+x_{m-1},\infty}(\mathtt{S}_1 = \mathtt{s}_m)\delta_{p+x_m,0}\end{aligned}$$

Then Lemma V.6 implies that the distribution $\mathtt{P}_{p,\infty}$ on the process $(\mathtt{S}_n)_{n\geq 1}$ defined by (V.21) and (V.22) is normalized. In particular, $T_0 = \inf\{n \geq 1 : P_n = 0\}$ almost surely under $\mathtt{P}_{p,\infty}$.

Similarly, we take the limit $p \to \infty$ in the above equations, and define $\mathtt{P}_{\infty,\infty}$ by

$$\mathtt{P}_{\infty,\infty}(\mathtt{S}_1 = \mathtt{s}_1, \cdots, \mathtt{S}_n = \mathtt{s}_n) \;:=\; \mathtt{P}_{\infty,\infty}(\mathtt{S}_1 = \mathtt{s}_1) \cdots \mathtt{P}_{\infty,\infty}(\mathtt{S}_1 = \mathtt{s}_n).$$

Observe that in this limit $\delta_{p+x_m,0}$ vanishes, so $T_0 = \infty$ almost surely under $\mathtt{P}_{\infty,\infty}$. □

The above construction of $\mathtt{P}_{p,\infty}$ and $\mathtt{P}_{\infty,\infty}$ implies immediately the following corollary.

Corollary V.7 (Markov property of $\mathtt{P}_{p,\infty}$ and $\mathtt{P}_{\infty,\infty}$). *Under $\mathtt{P}_{p,\infty}$, conditionally on $(\mathtt{S}_k)_{1\leq k\leq n}$ and provided that $n < T_0$, the shifted sequence $(\mathtt{S}_{n+k})_{k\geq 0}$ has the law $\mathtt{P}_{p+X_n,\infty}$. Moreover, $(P_n)_{n\geq 0}$ is a Markov chain and $T_0 = \inf\{n \geq 1 : P_n = 0\}$ almost surely.*
Under $\mathtt{P}_{\infty,\infty}$ and conditionally on $(\mathtt{S}_k)_{1\leq k\leq n}$, the shifted sequence $(\mathtt{S}_{n+k})_{k\geq 0}$ has the law $\mathtt{P}_{\infty,\infty}$. Moreover, $(X_n, Y_n)_{n\geq 0}$ is a random walk and $T_0 = \infty$ almost surely.

From the construction of $\mathtt{P}_{p,\infty}$ it is not obvious whether T_0 is finite almost surely. The following lemma answer this question positively by giving an upper bound for the tail of the distribution of T_0. It will be used as a technical ingredient in Appendix A.3.

Lemma V.8 (Tail of the law of T_0 under $\mathtt{P}_{p,\infty}$). *There exists $\gamma > 0$ such that $\mathtt{P}_{p,\infty}(T_0 > Cp) \leq C^{-\gamma}$ for all $p \geq 1$ and $C > 0$. In particular, T_0 is finite $\mathtt{P}_{p,\infty}$-almost surely.*

Proof. From Table V.2(a), we read $\mathtt{P}_{p,\infty}(\mathtt{S}_1 = \mathtt{R}^-_{p-1}) = \frac{t_c}{u_c} a_0 \frac{z_{p-1,1}}{a_p}$ for all $p \geq 1$. By Theorem V.1, the right hand side decays like p^{-1} when $p \to \infty$. Hence there exists $c > 0$ such that

$$\mathtt{P}_{p,\infty}(T_0 = 1) \;\geq\; \mathtt{P}_{p,\infty}(\mathtt{S}_1 = \mathtt{R}^-_{p-1}) \;\geq\; \frac{c}{p}$$

for all $p \geq 1$. On the other hand, P_n increases at most by 2 at each step, therefore $P_n \leq p+2n$ for all $n \geq 0$ almost surely under $\mathtt{P}_{p,\infty}$. It follows that for all $n \geq 0$,

$$\mathtt{P}_{p,\infty}(T_0 > n+1) \;=\; \mathtt{E}_{p,\infty}\Big[\mathtt{P}_{P_n,\infty}(T_0 \neq 1)\mathbb{1}_{\{T_0>n\}}\Big] \;\leq\; \Big(1 - \frac{c}{p+2n}\Big)\mathtt{P}_{p,\infty}(T_0 > n)\,.$$

By induction, we have $\mathtt{P}_{p,\infty}(T_0 > n) \;\leq\; \prod_{k=0}^{n-1}\left(1 - \frac{c}{p+2k}\right)$ for all $n \geq 0$. Use the inequality $\log(1-x) \leq -x$ for $0 < x < 1$ and bound sum by its Riemann integral, we get

$$\mathtt{P}_{p,\infty}(T_0 > Cp) \;\leq\; \exp\left(-\sum_{k=0}^{Cp-1} \frac{c}{p+2k}\right) \;\leq\; \exp\left(-\int_0^C \frac{c\,\mathrm{d}x}{1+2x}\right) \;=\; (1+2C)^{-c/2}. \quad □$$

4.2 The random walk $\mathcal{L}_{\infty,\infty}(X_n, Y_n)_{n\geq 0}$

The distribution of the first step $\mathcal{L}_{\infty,\infty}(X_1, Y_1)$ of this random walk can be readily read from Table V.2(b). From there it is not hard to compute explicitly its drift and tails, and deduce Theorem V.2 by standard invariance principles.

Proof of Theorem V.2. First, notice that the law of $\mathcal{L}_{\infty,\infty}(X_1+Y_1)$ has a particularly simple expression given by

$$\begin{aligned}
\mathtt{P}_{\infty,\infty}(X_1 + Y_1 = 1) \;&=\; \mathtt{P}_{\infty,\infty}(\mathtt{S}_1 \in \{\mathtt{C}^+, \mathtt{C}^-\}) &&=\; (\nu_c+1)t_c u_c^{-1}\\
\forall k \geq 0,\ \mathtt{P}_{\infty,\infty}(X_1 + Y_1 = -k) \;&=\; \mathtt{P}_{\infty,\infty}(\mathtt{S}_1 \in \{\mathtt{L}^+_k, \mathtt{L}^-_k, \mathtt{R}^+_k, \mathtt{R}^-_k\}) &&=\; (\nu_c+1)t_c u_c^k(z_{k+1,0} + z_{k,1})\,.
\end{aligned}$$

It follows that

$$\begin{aligned}\mathtt{E}_{\infty,\infty}[X_1+Y_1] &= (\nu_c+1)t_c\Big(-\sum_{k=0}^{\infty}(k-1)u_c^{k-1}z_{k,0}-\sum_{k=0}^{\infty}ku_c^k z_{k,1}\Big)\\ &= (\nu_c+1)t_c\Big(\frac{Z_0(u_c)}{u_c}-Z_0'(u_c)-u_cZ_1'(u_c)\Big) \;=\; \frac{1}{2\sqrt{7}}\end{aligned} \tag{V.23}$$

where the derivatives are computed using the chain rule $Z_0'(u_c)=\frac{\hat{Z}_0'(1)}{\hat{u}'(1)}$ and (V.16). Similarly, we deduce from Table V.2(b) and (V.16) the following expression and value of $\mathtt{E}_{\infty,\infty}[X_1]$.

$$\mathtt{E}_{\infty,\infty}[X_1]=t_c\left((\nu_c-1)\frac{Z_0(u_c)}{u_c}-Z_1(u_c)-\nu_cZ_0'(u_c)-u_cZ_1'(u_c)\right)=\frac{1}{4\sqrt{7}}\,. \tag{V.24}$$

We refer to the accompanying Maple file for the computation of the numerical values above. It follows that $\mathtt{E}_{\infty,\infty}[X_1]=\mathtt{E}_{\infty,\infty}[Y_1]$. This is not obvious *a priori*, since under $\mathtt{P}_{\infty,\infty}$ the peeling process always chooses to reveal a triangle adjacent to a + boundary edge, breaking the symmetry between + and -.

Again from Table V.2(b) we read that $\mathtt{P}_{\infty,\infty}(X_1=-k)=\left(\nu_c z_{k+1,0}+\frac{z_{k-1,1}}{u_c}\right)t_cu_c^k$ and $\mathtt{P}_{\infty,\infty}(Y_1=-k)=(\nu_c z_{k,1}+u_cz_{k+2,0})\,t_cu_c^k$ for all $k\geq 2$. By Theorem V.1, their asymptotics is

$$\mathtt{P}_{\infty,\infty}(X_1=-k)\underset{k\to\infty}{\sim}\frac{c_x}{k^{7/3}} \quad\text{and}\quad \mathtt{P}_{\infty,\infty}(Y_1=-k)\underset{k\to\infty}{\sim}\frac{c_y}{k^{7/3}}$$

$$\text{where}\quad c_x=\left(\nu_c\frac{a_0}{u_c}+a_1\right)\frac{t_c}{\Gamma(-4/3)} \quad\text{and}\quad c_y=\left(\frac{a_0}{u_c}+\nu_ca_1\right)\frac{t_c}{\Gamma(-4/3)}\,, \tag{V.25}$$

or explicitly, $c_x=\frac{1}{8\,\Gamma(-4/3)}\frac{2+3\sqrt{7}}{7+\sqrt{7}}\left(\frac{3}{2}\right)^{1/3}$ and $c_y=\frac{1}{8\,\Gamma(-4/3)}\frac{2+\sqrt{7}}{7+\sqrt{7}}\left(\frac{3}{2}\right)^{1/3}$. Observe that $c_x>c_y$. It follows from a standard invariance principle (see e.g. [JS03, Theorem VIII.3.57]) that the two components of the random walk $(X_n,Y_n)_{n\geq0}$, after renormalization, converge respectively to the Lévy processes $\mathcal{X}$ and $\mathcal{Y}$ in Theorem V.2.

Now let us show that these two convergences hold jointly, and that the limits $\mathcal{X}$ and $\mathcal{Y}$ are independent. For this we can adapt the proof of a similar result for the peeling of a UIPT ([Cur15, Proposition 2]). Our proof is based on the observation that the steps of the random walk satisfy $-2\leq\max(X_1,Y_1)\leq 2$, so that $(X_n)_{n\geq0}$ and $(Y_n)_{n\geq0}$ never jump simultaneously. Let us decompose (X,Y) as the sum of two random walks $(X^{(0)},Y^{(0)})$ and $(X^{(1)},Y^{(1)})$ of respective step distributions

$$(X_1^{(0)},Y_1^{(0)})=\mathbb{1}_{\{X_1<-2\}}(X_1,Y_1) \qquad\text{and}\qquad (X_1^{(1)},Y_1^{(1)})=\mathbb{1}_{\{X_1\geq-2\}}(X_1,Y_1)\,.$$

According to the above observation, $(X^{(0)},Y^{(0)})$ only jumps along the x-axis, and $(X^{(1)},Y^{(1)})$ only jumps along the y-axis. (More precisely, $\left|Y_k^{(0)}-Y_{k-1}^{(0)}\right|\leq 2$ and $\left|X_k^{(1)}-X_{k-1}^{(1)}\right|\leq 2$ for all $k\geq1$.) Thus according to the same invariance principle as before, we have

$$\left(\frac{X^{(0)}_{\lfloor nt\rfloor}-\mathbb{E}[X^{(0)}_{\lfloor nt\rfloor}]}{n^{3/4}},\frac{Y^{(0)}_{\lfloor nt\rfloor}-\mathbb{E}[Y^{(0)}_{\lfloor nt\rfloor}]}{n^{3/4}}\right)_{t\geq0}\xrightarrow[n\to\infty]{}(\mathcal{X}_t,0)_{t\geq0}$$

in distribution with respect to the Skorokhod topology. Here we have the joint convergence of the two components because the limit of the second component is a constant. Similarly, the random walk $(X^{(1)},Y^{(1)})$ converges to $(0,\mathcal{Y}_t)_{t\geq0}$ after renormalization.

The random walks $(X^{(0)}, Y^{(0)})$ and $(X^{(1)}, Y^{(1)})$ are still correlated. To recover independence, consider their poissonization defined by $(\tilde{X}_t^{(i)}, \tilde{Y}_t^{(i)}) = (X_{N_t}^{(i)}, Y_{N_t}^{(i)})$, where $i \in \{0,1\}$ and $(N_t)_{t\geq 0}$ is an integer-valued Poisson point process of intensity 1. According to Lemma V.9, the poissonized random walks converge to the same limit after renormalization, namely

$$\left(\frac{\tilde{X}_{nt}^{(0)} - \mathbb{E}[\tilde{X}_{nt}^{(0)}]}{n^{3/4}}, \frac{\tilde{Y}_{nt}^{(0)} - \mathbb{E}[\tilde{Y}_{nt}^{(0)}]}{n^{3/4}} \right)_{t\geq 0} \xrightarrow[n\to\infty]{} (\mathcal{X}_t, 0)_{t\geq 0}\,,$$

and similarly for $(\tilde{X}^{(1)}, \tilde{Y}^{(1)})$. By the splitting property of compound Poisson processes, $(\tilde{X}^{(0)}, \tilde{Y}^{(0)})$ and $(\tilde{X}^{(1)}, \tilde{Y}^{(1)})$ are independent (See [Nel95, Proposition 6.7]). Therefore their sum $(\tilde{X}, \tilde{Y})$, after renormalization, converges in distribution to the couple of independent Lévy processes $(\mathcal{X}, \mathcal{Y})$. Then we apply Lemma V.9 again to recover the convergence in Theorem V.2. (Notice that $\mathtt{E}_{\infty,\infty}[X_{\lfloor nt\rfloor}] = \mathtt{E}_{\infty,\infty}[Y_{\lfloor nt\rfloor}] = \mu \lfloor nt\rfloor$.) $\square$

Lemma V.9 (poissonization and depoissonization)**.** *Let $(W_n)_{n\geq 0}$ be a discrete-time random process in $\mathbb{R}^d$ $(d \geq 1)$ and $(a_n)_{n\geq 0}$ be a sequence of positive real numbers such that*

$$\frac{1}{n^{1/2} a_n} \sup_{t\in[0,T]} \| W_{\lfloor nt\rfloor} \| \xrightarrow[n\to\infty]{} 0$$

in probability for all fixed $T > 0$. If $(N_t)_{t\geq 0}$ is a Poisson counting process of intensity 1 and independent of $(W_n)_{n\geq 0}$, then we have

$$d_{D_\infty}(a_n^{-1} W_{\lfloor nt\rfloor}, a_n^{-1} W_{N_{nt}}) \xrightarrow[n\to\infty]{} 0$$

in probability, where d_{D_∞} is the Skorokhod distance on the space of functions on $[0,\infty)$ which are right-continuous and have left limits at every point.

Proof. For $t \geq 0$, let $W^{(n)}(t) = a_n^{-1} W_{\lfloor nt\rfloor}$ and $\tilde{W}^{(n)}(t) = a_n^{-1} W_{N_{nt}}$. Recall that d_{D_∞} is constructed using d_{D_m}, the Skorokhod distance on the space of functions on $[0,m]$ that are right-continuous and have left limits at every point. According to the construction of d_{D_∞} in [Bil99, Section 16], the conclusion of the lemma is equivalent to

$$d_{D_m}(g_m W^{(n)}, g_m \tilde{W}^{(n)}) \xrightarrow[n\to\infty]{} 0$$

in probability for all integers $m \geq 1$, where $g_m : [0,m] \to [0,1]$ is the regularization function defined by $g_m(t) = \min(1, m-t)$. From the definition of d_{D_m}, one sees that the left hand side is bounded by

$$\max\left(\sup_{t\leq m} |\lambda(t) - t| \;,\; \sup_{t\leq m} \left\| (g_m W^{(n)})(\lambda(t)) - (g_m \tilde{W}^{(n)})(t) \right\| \right) \tag{V.26}$$

where λ is any increasing homeomorphism from $[0,m]$ onto itself.

Let $\lambda^{(n)}$ be the increasing homeomorphism from $[0,\infty)$ onto itself defined by linearly interpolating the function $t \mapsto n^{-1} N_{nt}$ between the times of its jumps. Then we have $W^{(n)}(\lambda^{(n)}(t)) = \tilde{W}^{(n)}(t)$ for all $t \geq 0$. For each m, we modify $\lambda^{(n)}$ to produce a homeomorphism $\lambda_m^{(n)}$ from $[0,m]$ onto itself as follows: let t_m be the x-coordinate of the point where the graph of the function $\lambda^{(n)}$ exits the square $[0, m-1/n]^2$. Define $\lambda_m^{(n)}$ by $\lambda_m^{(n)}(t) = \lambda^{(n)}(t)$ for $t \in [0, t_m]$, and by linear interpolation for $t \in [t_m, m]$ so that $\lambda_m^{(n)}(m) = m$. Now consider

(V.26) when $\lambda = \lambda_m^{(n)}$. Using the property of $\lambda^{(n)}$ and the fact that g_m is 1-Lipschitz, we can simplify the bound to get

$$d_{D_m}(g_m W^{(n)}, g_m \tilde{W}^{(n)}) \;\le\; \left(\frac{1}{n} + \sup_{t\le m} |\lambda_m^{(n)}(t) - t|\right) \cdot \max\left(1,\, \sup_{t\le m} \|W^{(n)}(t)\|\right)$$

By central limit theorem, $\sqrt{n}\sup_{t\le m} |\lambda_m^{(n)}(t) - t|$ converges in distribution to a finite random variable as $n\to\infty$. Thus the assumption of the lemma implies that the right hand side of the above inequality converges to zero in probability. This completes the proof. □

4.3 The Markov chain $\mathcal{L}_{p,\infty}(P_n)_{n\ge 0}$

When p is large, $\mathcal{L}_{p,\infty}(P_n)_{n\ge 0}$ approximates the random walk $p+\mathcal{L}_{\infty,\infty}(X_n)_{n\ge 0}$, which has a strictly positive drift μ. This seems to suggest that $\mathcal{L}_{p,\infty}(P_n)_{n\ge 0}$ escapes to $+\infty$ with positive probability (indeed, as P_n increases, the transition probabilities of $\mathcal{L}_{p,\infty}(P_n)_{n\ge 0}$ gets closer to those of $p+\mathcal{L}_{\infty,\infty}(X_n)_{n\ge 0}$). However, as stated in Theorem V.3, $\mathcal{L}_{p,\infty}(P_n)_{n\ge 0}$ hits zero with probability one. There is no contradiction because, despite the weak convergence $\mathtt{P}_{p,\infty}\to\mathtt{P}_{\infty,\infty}$, the expectation $\mathtt{E}_{p,\infty}[X_1]$ *does not* converge to $\mathtt{E}_{\infty,\infty}[X_1]$ as $p\to\infty$.

What happens is that with high probability, the process $\mathcal{L}_{p,\infty}(P_n)_{n\ge 0}$ stays close to the straight line $p_n = p+\mu n$ up to a time of order $\Theta(p)$, and then jump to a neighborhood of zero in one single step. The jump occurs because the peeling events of type $\mathtt{R}^{\pm}_{p+k}$, for any fixed $k\in\mathbb{Z}$, occur with a probability of order $\Theta(p^{-1})$ (See Table V.2(a)). To formalize this phenomenon, let us consider the following stopping times:

$$T_m \;=\; \inf\{n\ge 0:\; P_n\le m\}$$

$$\tau_x^{\epsilon} \;=\; \inf\{n\ge 0:\; |P_n - P_0 - \mu n| > x+\epsilon n\}\;.$$

where $m\ge 0$ is an integer, and $x,\epsilon>0$ are real numbers. The definition of T_m generalizes that of T_0 under $\mathtt{P}_{p,\infty}$. The following lemma affirms the one-jump behavior described above. Its proof is based on technical estimates on the transition probabilities of $\mathcal{L}_{p,\infty}(P_n)_{n\ge 0}$ and will be left to Appendix A.3.

Lemma V.10 (One jump to zero)**.** *For all $\epsilon>0$, $\limsup_{p\to\infty} \mathtt{P}_{p,\infty}(\tau_x^{\epsilon} < T_m)\to 0$ when $x,m\to\infty$.*

Proposition V.11. *For all $m\in\mathbb{N}$, the jump time T_m has the same scaling limit as follows.*

$$\forall t>0\,,\qquad \lim_{p\to\infty} \mathtt{P}_{p,\infty}\left(T_m > tp\right) = (1+\mu t)^{-4/3}. \tag{V.27}$$

Proof. First observe that $T_0\ge T_m$, so by strong Markov property,

$$\mathtt{P}_{p,\infty}(T_0 - T_m > n) \;=\; \mathtt{E}_{p,\infty}\left[\mathtt{P}_{P_{T_m},\infty}(T_0>n)\right] \;\le\; \max_{p'\le m} \mathtt{P}_{p',\infty}(T_0>n) \xrightarrow[n\to\infty]{} 0\,.$$

In particular, $\mathtt{P}_{p,\infty}(T_0 - T_m > \epsilon p) \xrightarrow[p\to\infty]{} 0$ for all $m\in\mathbb{N}$ and $\epsilon>0$. This explains why the scaling limit of $p^{-1}T_m$ does not depend on m.

The rest of the proof is basically a refinement of the estimate of $\mathtt{P}_{p,\infty}(T_0 > tp)$ given in Lemma V.8. The idea is that, before time T_m, the Markov chain $(P_n)_{n\ge 0}$ stays close to the line $P_n = p + \mu n$. Therefore at time n there is a probability roughly $\mathbb{P}_{p+\mu n}(P_1 \le m)$ to jump below level m at the next step. On the other hand, from Table V.2(a) we can read the exact expression of $\mathtt{P}_{p,\infty}(P_1 \le m)$ and show that for all $m \ge 0$, there is a constant c_m such that

$$\mathtt{P}_{p,\infty}(P_1 \le m) \underset{p\to\infty}{\sim} c_m\, p^{-1}.$$

Then (V.27) is obtained by summing the above estimate over all steps up to time tp.

More precisely, let us fix $x > 0$, $m \in \mathbb{N}$ and $\epsilon \in (0, \mu)$. Take p large enough so that $\mathtt{P}_{p,\infty}$-almost surely, $\tau_x^\epsilon \le T_m$. Let $\mathcal{E} = \{\tau_x^\epsilon < T_m\}$ be the event of small probability in Lemma V.10, where the $(P_n)_{n\ge 0}$ deviates significantly from $p + \mu n$ before jumping close to zero. ($\mathcal{E}$ for "exceptional"). Also let $\mathcal{N}_n = \{\tau_x^\epsilon > n\}$ be the event that the trajectory of $(P_n)_{n\ge 0}$ stays close to the line $p_n = p + \mu n$ up to time n. ($\mathcal{N}$ for "normal"). Obviously $(\mathcal{N}_n)_{n\ge 0}$ is an decreasing sequence. Moreover, one can check that

$$\mathcal{N}_{n+1} \;\subset\; \mathcal{N}_n \setminus \{T_m = n+1\} \;\subset\; \mathcal{N}_{n+1} \cup \mathcal{E}\,. \tag{V.28}$$

On event $\mathcal{N}_n$, we have $|P_n - (P_0 + \mu n)| \le \epsilon n + x$. Combine this with the asymptotics of $\mathtt{P}_{p,\infty}(P_1 \le m)$, we obtain that for P_0 large enough,

$$\frac{c_m - \epsilon}{P_0 + \mu n + (\epsilon n + x)} \;\le\; \mathtt{P}_{P_n,\infty}(P_1 \le m) \;\le\; \frac{c_m + \epsilon}{P_0 + \mu n - (\epsilon n + x)}\,.$$

By Markov property, $\mathtt{P}_{p,\infty}(\mathcal{N}_n \setminus \{T_m = n+1\}) = \mathtt{P}_{p,\infty}(\mathcal{N}_n) - \mathtt{E}_{p,\infty}\left[\mathbb{1}_{\mathcal{N}_n} \mathtt{P}_{P_n,\infty}(Q_1 \le m)\right]$. Therefore

$$\begin{aligned}\left(1 - \frac{c_m + \epsilon}{p + \mu n - (\epsilon n + x)}\right) \mathtt{P}_{p,\infty}(\mathcal{N}_n) \;&\le\; \mathtt{P}_{p,\infty}(\mathcal{N}_n \setminus \{T_m = n+1\}) \\ &\le\; \left(1 - \frac{c_m - \epsilon}{p + \mu n + (\epsilon n + x)}\right) \mathtt{P}_{p,\infty}(\mathcal{N}_n)\,.\end{aligned}$$

Combine these estimates with the two inclusions in (V.28), we obtain that on the one hand,

$$\mathtt{P}_{p,\infty}(\mathcal{N}_{n+1}) \;\le\; \left(1 - \frac{c_m - \epsilon}{p + \mu n + (\epsilon n + x)}\right) \mathtt{P}_{p,\infty}(\mathcal{N}_n)\,.$$

And on the other hand,

$$\begin{aligned}\mathtt{P}_{p,\infty}(\mathcal{N}_{n+1} \cup \mathcal{E}) \;&\ge\; \mathtt{P}_{p,\infty}\left((\mathcal{N}_n \setminus \{T_m = n+1\}) \cup \mathcal{E}\right) \\ &\ge\; \mathtt{P}_{p,\infty}(\mathcal{N}_n \setminus \{T_m = n+1\}) + \mathtt{P}_{p,\infty}(\mathcal{E} \setminus \mathcal{N}_n) \\ &\ge\; \left(1 - \frac{c_m + \epsilon}{p + \mu n - (\epsilon n + x)}\right) \mathtt{P}_{p,\infty}(\mathcal{N}_n) + \mathtt{P}_{p,\infty}(\mathcal{E} \setminus \mathcal{N}_n) \\ &\ge\; \left(1 - \frac{c_m + \epsilon}{p + \mu n - (\epsilon n + x)}\right) \mathtt{P}_{p,\infty}(\mathcal{N}_n \cup \mathcal{E})\,.\end{aligned}$$

Notice that $\mathcal{N}_n \subset \{T_m > n\} \subset \mathcal{N}_n \cup \mathcal{E}$ up to a $\mathtt{P}_{p,\infty}$-negligible set. Thus we have by induction

$$\begin{aligned}\prod_{n=0}^{N-1} \left(1 - \frac{c_m + \epsilon}{p + \mu n - (\epsilon n + x)}\right) - \mathtt{P}_{p,\infty}(\mathcal{E}) \;&\le\; \mathtt{P}_{p,\infty}(\mathcal{N}_n \cup \mathcal{E}) - \mathtt{P}_{p,\infty}(\mathcal{E}) \\ \le\; \mathtt{P}_{p,\infty}(T_m > N) \;&\le\; \prod_{k=0}^{N-1} \left(1 - \frac{c_m - \epsilon}{p + \mu n + (\epsilon n + x)}\right) + \mathtt{P}_{p,\infty}(\mathcal{E})\,.\end{aligned}$$

From the Taylor series of the logarithm we see that for all $x \geq 0$, $-x-x^2 \leq \log(1-x) \leq -x$. Therefore for any positive sequence $(x_n)_{n\geq 0}$,

$$\exp\left(-\sum_{n=0}^{N-1} x_n - \sum_{n=0}^{N-1} x_n^2\right) \;\leq\; \prod_{n=0}^{N-1}(1-x_n) \;\leq\; \exp\left(-\sum_{n=0}^{N-1} x_n\right).$$

On the other hand, in the limit $p\to\infty$ we have $\frac{c_m\pm\epsilon}{p+\mu n\pm(\epsilon n+x)} = \frac{c_m\pm\epsilon}{p+\mu n}(1+o(1))$ where $o(1)$ is uniform over all $n\in[0,tp]$, for any fixed $t>0$. It follows that

$$\sum_{n=0}^{tp} \frac{c_m\pm\epsilon}{p+\mu n\pm(\epsilon n+x)} \;=\; (c_m\pm\epsilon)\int_0^{tp}\frac{\mathrm{d}s}{p+\mu s}(1+o(1)) \;\xrightarrow[p\to\infty]{}\; \frac{c_m\pm\epsilon}{\mu}\log(1+\mu t)\,.$$

We also have $\sum_{n=0}^{tp}(\frac{c_m+\epsilon}{p+\mu n-(\epsilon n+x)})^2 \xrightarrow[p\to\infty]{} 0$. Combine this with the last three displays, we conclude that

$$\begin{aligned}(1+\mu t)^{-\frac{c_m+\epsilon}{\mu}} \;&\leq\; \liminf_{p\to\infty} \mathtt{P}_{p,\infty}(T_m > tp)\\ &\leq\; \limsup_{p\to\infty} \mathtt{P}_{p,\infty}(T_m > tp) \;\leq\; (1+\mu x)^{-\frac{c_m-\epsilon}{\mu}} + \limsup_{p\to\infty}\mathtt{P}_{p,\infty}(\mathcal{E})\,.\end{aligned}$$

Now take the limit $m,x\to\infty$. The last term on the right tends to zero thanks to Lemma V.10. The middle terms $\liminf \mathtt{P}_{p,\infty}(T_m > tp)$ and $\limsup \mathtt{P}_{p,\infty}(T_m > tp)$ do not depend on m because of the limit $\mathtt{P}_{p,\infty}(T_0 - T_m > \epsilon p) \xrightarrow[p\to\infty]{} 0$ seen at the beginning of the proof. Moreover, the increasing sequence $(c_m)_{m\geq 0}$ has a limit c_∞. Thus by sending $\epsilon\to 0$, we obtain

$$\lim_{p\to\infty}\mathtt{P}_{p,\infty}(T_m > tp) = (1+\mu t)^{-\frac{c_\infty}{\mu}}\,.$$

Now it remains to show that in fact we have $c_\infty = \frac{4}{3}\mu$. Using $c_m = \lim\limits_{p\to\infty} p\,\mathtt{P}_{p,\infty}(P_1\leq m)$ and the data in Table V.2(a), c_∞ can be written as

$$\begin{aligned} c_\infty = \lim_{m\to\infty} c_m &= \lim_{m\to\infty}\lim_{p\to\infty} p\left(\mathtt{P}_{p+1,\infty}(P_1 = 0) + \sum_{k=1}^{m}\mathtt{P}_{p+1,\infty}(P_1 = k)\right)\\ &= \lim_{p\to\infty} p\sum_{k=0}^{\infty}\mathtt{P}_{p+1,\infty}\left(\mathtt{S}_1\in\{\mathtt{R}^+_{p+k},\mathtt{R}^-_{p+k}\}\right) + \sum_{k=1}^{\infty}\lim_{p\to\infty} p\,\mathtt{P}_{p+1,\infty}\left(\mathtt{S}_1\in\{\mathtt{R}^+_{p-k},\mathtt{R}^-_{p-k}\}\right)\end{aligned}$$

The probabilities can be read from Table V.2(a), which gives

$$\begin{aligned} &\mathtt{P}_{p+1,\infty}\left(\mathtt{S}_1\in\{\mathtt{R}^+_{p+k},\mathtt{R}^-_{p+k}\}\right) \;=\; \nu_c t_c z_{p+1,k}\frac{a_1}{a_{p+1}}u_c^k + t_c z_{p,k+1}\frac{a_0}{a_{p+1}}u_c^{k-1}\\ \text{and}\quad &\mathtt{P}_{p+1,\infty}\left(\mathtt{S}_1\in\{\mathtt{R}^+_{p-k},\mathtt{R}^-_{p-k}\}\right) \;=\; \nu_c t_c z_{p-k+1,0}\frac{a_{k+1}}{a_{p+1}} + t_c z_{p-k,1}\frac{a_k}{a_{p+1}}\frac{1}{u_c}\end{aligned}$$

for all $k\geq 0$. Then we can evaluate explicitly c_∞ using Theorem V.1 and the asymptotics (V.19). After a tedious calculation with several miraculous factorizations by the end, we obtain

$$c_\infty \;=\; \frac{t_c\,\Gamma(-1/3)}{b\,\Gamma(-4/3)}(\nu_c+1)\left(\frac{a_0}{u_c}+a_1\right)(A(u_c)-a_0). \tag{V.29}$$

The right hand side can be evaluated using the rational parametrization of $A(u)$, and we find indeed $c_\infty = \frac{1}{3\sqrt{7}} = \frac{4}{3}\mu$. $\square$

Remark. With our approach, it is quite amazing to find such a simple exponent 4/3 for the scaling limit of the jump time T_m. Currently we do not have any explanation of this exponent apart from the computation above. Going one step back, one can see that the value 4/3 relies on the algebraic identity

$$\mu \;=\; \frac{(\nu_c+1)t_c}{2}\left(\frac{Z_0(u_c)}{u_c}-Z_0'(u_c)-u_cZ_1'(u_c)\right) \;=\; -\frac{(\nu_c+1)t_c}{b}\left(\frac{a_0}{u_c}+a_1\right)(A(u_c)-a_0)\,,$$

together with the fact that $\mathtt{E}_{\infty,\infty}[X_1]=\mathtt{E}_{\infty,\infty}[Y_1]$. More importantly, we expect the same phenomenon to appear in any reasonable model of Ising-decorated maps, because the exponent 4/3, which describes the believed scaling limit of an Ising-decorated map, ought to be universal. In a work in progress, we have checked that this is indeed the case when we consider Boltzmann Ising-triangulations with spins on the vertices. It would be very interesting to have an algebraic or probabilistic explanation of this universality.

5 Discussion

In this section we discuss in more detail how our results should be interpreted geometrically, and provide a route map for the upcoming proof of the convergence in distribution of the Boltzmann Ising-triangulations of (p,q)-gon with respect to the local distance.

Structure of the explored region. We define the peeling process so that it explores the bicolored triangulation $(\mathfrak{t},\sigma)$ along the right-most interface $\mathcal{I}$ from ρ to $\rho^\dagger$. The explored region consists of faces which are directly revealed at a peeling step, and of faces which are swallowed when revealing another face (See Figure V.2).

The revealed faces are those which are adjacent to the interface $\mathcal{I}$, provided that "adjacent" is interpreted with a little nuance: an internal face with spin + is revealed by the peeling exploration as soon as it shares a vertex with $\mathcal{I}$, while an internal face with spin − is revealed only when it shares an edge with $\mathcal{I}$. This asymmetry is still due to our choice of peeling a boundary edge with spin + at each step: locally, the peeling exploration turns around a vertex on $\mathcal{I}$ in the anti-clockwise order until it finds the next non-monochromatic edge, as illustrated in Figure V.4. On the other hand, faces are swallowed when a peeling event of type $\mathtt{L}_k^{\pm}$ or $\mathtt{R}_k^{\pm}$ occurs. The swallowed region is always a Boltzmann Ising-triangulation which, conditionally on the values of the spins on its boundary, is independent of the unexplored region.

We have seen at the end of Section 2.2 that the first n peeling events $(\mathtt{S}_k)_{1\le k\le n}$ determines (X_n,Y_n). The same reasoning shows that $(\mathtt{S}_k)_{1\le k\le n}$ also determines (the law of) the explored region at time n. Thus Proposition V.5 should be interpreted as the convergence in distribution of explored region at any fixed time n, with respect to the discrete topology on the (countable) set of all possible configurations.

Recall that T_0, the killing time of our peeling process, is the first time that the explored region cover all the + boundary edges of the original bicolored triangulation. Under $\mathtt{P}_{p,\infty}$, we have $T_0<\infty$ almost surely, in other words, the peeling process finishes exploring the interface $\mathcal{I}$ in finite time, leaving an unexplored region with infinite monochromatic boundary. On the other hand, $T_0=\infty$ almost surely under $\mathtt{P}_{\infty,\infty}$. So in this case $\mathcal{I}$ is infinite and the peeling process, as discussed after Theorem V.2, gets further and further from the

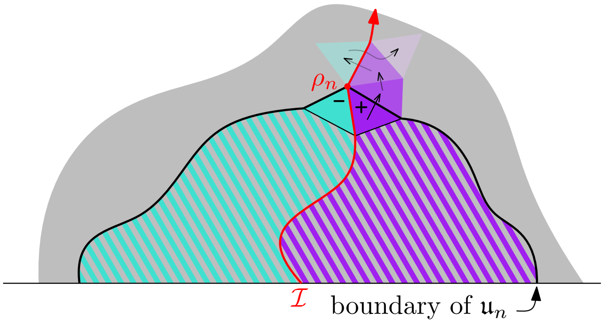

Figure V.4 – *Since the peeling process always chooses to peel the boundary edge with spin* + *on the boundary of the unexplored map* $\mathfrak{u}_n$*, the exploration turns anti-clockwise around each vertex on the right-most interface* $\mathcal{I}$*, until it finds the next edge on* $\mathcal{I}$*.*

boundary. In the limit $n \to \infty$, it leaves *two* unexplored region with infinite monochromatic boundaries on both sides of $\mathcal{I}$. See Figure V.5.

Geometric interpretation of the time of the peeling process. Intuitively, the peeling process explores the right-more interface $\mathcal{I}$ at a constant speed. Therefore the time n should be proportional to L_n, the length of the portion of $\mathcal{I}$ explored up to time n. To make this precise, let us consider the effect of a peeling event $\mathtt{S}_n$ on L_n. As shown in Figure V.6, when $\mathtt{S}_n$ is of type $\mathtt{L}_k^+$ or $\mathtt{R}_k^-$, a piece of the interface $\mathcal{I}$ of variable length is hidden in the region swallowed by the newly revealed triangle, increasing L_n by a random amount. And in all the other cases, L_n increases by either 0 or 1. To summarize, the variation of L_n conditionally on $\mathtt{S}_n$ is given by (assuming that $n < T_0$):

$$L_n - L_{n-1} = \begin{cases} 0 & \text{if } \mathtt{S}_n = \mathtt{C}^+ \text{ or } \mathtt{R}_k^+ \\ 1 & \text{if } \mathtt{S}_n = \mathtt{C}^- \text{ or } \mathtt{L}_k^- \\ \eta_{1,k} & \text{if } \mathtt{S}_n = \mathtt{L}_k^+ \\ 1 + \eta_{k,1} & \text{if } \mathtt{S}_n = \mathtt{R}_k^- \end{cases}$$

where $\eta_{k,l}$ denotes a random variable having the law of the total length of the interface $\mathcal{I}$ under $\mathbb{P}_{k,l}$ for $k, l \geq 0$.

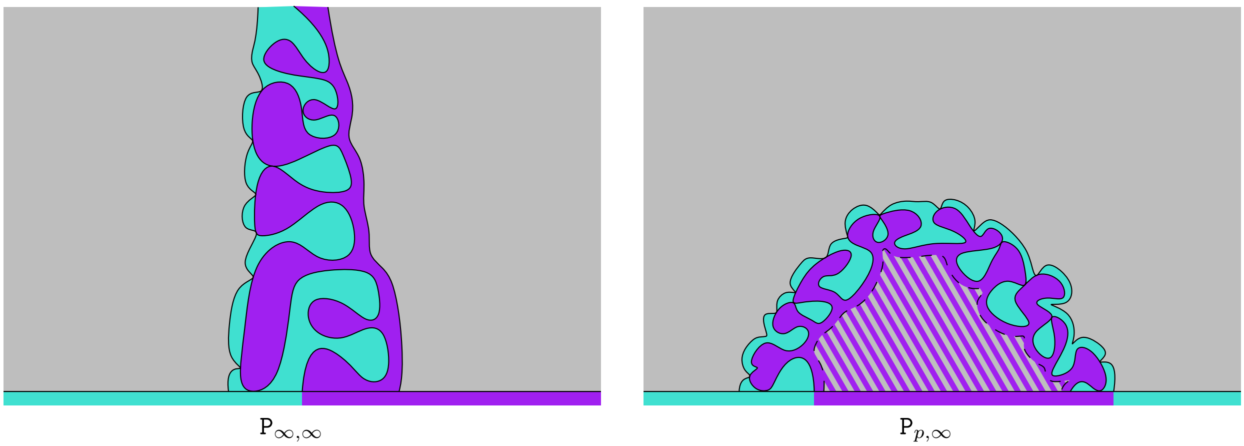

Figure V.5 – *Topology of the region explored by the peeling process up to time* T_0*.*

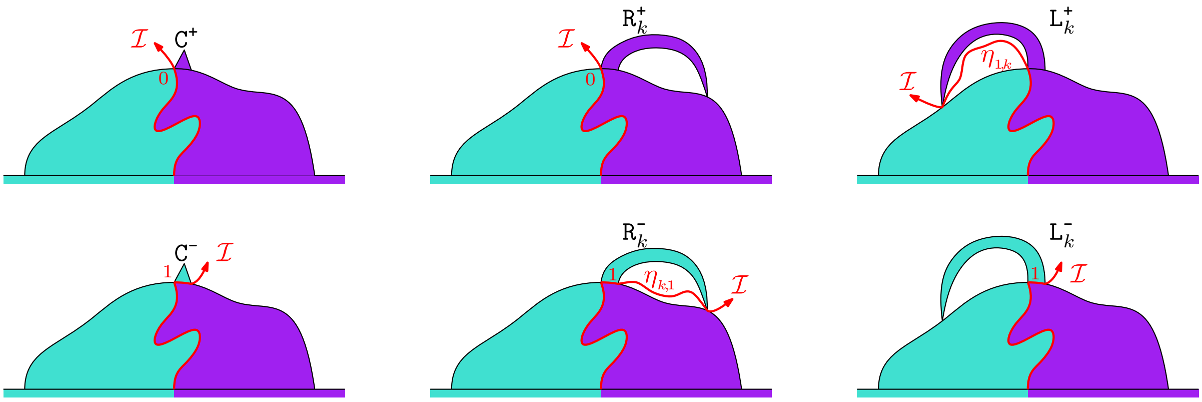

Figure V.6 – *The increment in the length of $\mathcal{I}$ resulted from each type of peeling step.*

Under $\mathtt{P}_{\infty,\infty}$, the peeling events $(\mathtt{S}_n)_{n\geq 1}$ are i.i.d., so are the increments $(L_n - L_{n-1})_{n\geq 1}$. So by the law of large numbers, we have simply $L_n \sim \mathtt{E}_{\infty,\infty}[L_1]\cdot n$ when $n\to\infty$, provided that the expectation $\mathtt{E}_{\infty,\infty}[L_1]$ is finite. A sufficient condition for that to hold is:

Conjecture. $\sup_{k\geq 0}\mathbb{E}[\eta_{1,k}] < \infty$ and $\sup_{k\geq 0}\mathbb{E}[\eta_{k,1}] < \infty$.

Under $\mathtt{P}_{p,\infty}$, the law of $\mathtt{S}_n$ depends on P_{n-1}. However, according to Theorem V.3, in the limit $p\to\infty$ and up to time T_m for some large m, the value of P_n will stay large with high probability. So intuitively the laws of the peeling events $\mathtt{S}_n$ under $\mathtt{P}_{p,\infty}$ remain close to its limit when $p\to\infty$. Then the random time ζ in Theorem V.3 has the following interpretation:

Conjecture. The interface length $\eta_{p,\infty}$ has the following scaling limit in distribution:

$$\frac{\eta_{p,\infty}}{p} \xrightarrow[p\to\infty]{} \mathtt{E}_{\infty,\infty}[L_1]\cdot\zeta \qquad \text{where} \qquad \mathbb{P}(\zeta > t) = (1+\mu t)^{-4/3}.$$

In particular, the exponent $4/3$ is intrinsic to the geometry of the Ising interface in the scaling limit.

Route map for the proof of local limit The first step of proving the local convergence of a Boltzmann Ising-triangulation of (p,q)-gon would be the construction of (a candidate for) the limit distribution $\mathbb{P}_{p,\infty}$ and $\mathbb{P}_{\infty,\infty}$. We will denote by $\mathcal{L}_{p,\infty}(\mathfrak{t},\sigma)$ (resp. $\mathcal{L}_{\infty,\infty}(\mathfrak{t},\sigma)$) a random (infinite) bicolored triangulation having the law $\mathbb{P}_{p,\infty}$ (resp. $\mathbb{P}_{\infty,\infty}$).

We have seen in Figure V.5 that under $\mathtt{P}_{p,\infty}$ or $\mathtt{P}_{\infty,\infty}$, the peeling process does *not* cover every finite ball around the origin before being killed. Instead, it leaves either one (under $\mathtt{P}_{p,\infty}$) or two (under $\mathtt{P}_{\infty,\infty}$) unexplored regions with infinite monochromatic boundaries. So By spatial Markov property, the natural candidate for $\mathcal{L}_{p,\infty}(\mathfrak{t},\sigma)$ (resp. $\mathcal{L}_{\infty,\infty}(\mathfrak{t},\sigma)$) should be constructed by gluing one (resp. two independent copies of) infinite Boltzmann Ising-triangulation to the unexplored region left behind by the peeling process under $\mathtt{P}_{p,\infty}$ (resp. $\mathtt{P}_{\infty,\infty}$). From its boundary condition, we see that this infinite Boltzmann Ising-triangulation must be $\mathcal{L}_{0,\infty}(\mathfrak{t},\sigma)$.

The construction of $\mathcal{L}_{0,\infty}(\mathfrak{t},\sigma)$ will rely on a modified peeling process. Since $\mathbb{P}_{0,\infty}$ is invariant by translation of the origin ρ along the boundary, the modified peeling process has the freedom to peel any edge on the boundary, and do so as long as the boundary of the unexplored map remains monochromatic (with spin -). When the process discovers a face of spin +, the boundary of the unexplored region becomes non-monochromatic, then we can continue peeling using our old peeling process up to the time when the boundary becomes monochromatic again. In this way, the boundary condition of the unexplored region follows a renewal process, whose holding time is almost surely finite thanks to Lemma V.8.

By choosing carefully the edge to peel when the boundary of the unexplored region is monochromatic, one can steer the modified peeling process so that it covers any finite ball almost surely in finite time. This determines the law of $\mathcal{L}_{0,\infty}(\mathfrak{t},\sigma)$ as a function of the transition probabilities of the modified peeling process. Then, $\mathcal{L}_{p,\infty}(\mathfrak{t},\sigma)$ is obtained by gluing an independent copy of $\mathcal{L}_{0,\infty}(\mathfrak{t},\sigma)$ to the finite triangulation constructed using $\mathtt{P}_{p,\infty}$. And $\mathcal{L}_{\infty,\infty}(\mathfrak{t},\sigma)$ is obtained by gluing a copy of $\mathcal{L}_{0,\infty}(\mathfrak{t},\sigma)$ and a copy of $\mathcal{L}_{\infty,0}(\mathfrak{t},\sigma)$ to a "ribbon" of bicolored triangles constructed using $\mathtt{P}_{\infty,\infty}$. (See Figure V.5.)

A Appendix

A.1 Elimination of the second catalytic variable in Tutte's equation

In Section 3.1 we showed how to eliminate one of the two catalytic variables (u,v) in Tutte's equation by extracting appropriate coefficients of the series $Z(u,v)$. In the end we obtained an algebraic equation with one catalytic variable of the form

$$Z_0(u) = 1 + \nu u^2 + t\,\mathcal{R}(Z_0(u), u, z_1, z_3; \nu, t) \tag{V.11'}$$

where $\mathcal{R}(y,u,z_1,z_3;\nu,t)$, given explicitly by (V.12), is a polynomial in $\frac{y}{u}, u, z_1, z_3, t$ and ν.

To eliminate the second catalytic variable u, we use a generalization of the quadratic method used by Tutte in his study of properly colored triangulations [Tut82, Tut95]. It is later adapted in [BBM11, Section 12] to treat bicolored maps with monochromatic boundary condition. In our setting, this method consists of finding two rational functions $J(u,y)$, $L(u,y)$ and a polynomial $C(x)$ whose coefficients do not depend on u or $Z_0(u)$, such that (V.11') can be written in the form

$$A \cdot L(u, Z_0(u))^2 = C(J(u, Z_0(u)))$$

where A is some polynomial that may depend on all the variables. Then the square factor on the left hand side would suggest that $C(x)$ has a double root, in the same way as the classical quadratic method (see e.g. [GJ83, Section 2.9]).

With some trial-and-errors, we discovered the following choice of J and L:

$$\begin{aligned} J(u,y) &= (\nu-1)\left(tu + \left(\frac{ty}{u}\right)^2\right) - \frac{ty}{u}\,, \\ L(u,y) &= 2\frac{ty}{u} + (\nu+1)J(u,y)\,. \end{aligned}$$

Notice that the mapping $(u,y) \mapsto (J,L)$ is invertible. Thus we can make the reverse change of variable and rewrite (V.11') as a polynomial equation satisfied by the variables J and L, with coefficients in the space of formal power series $\mathbb{C}(\nu)[[t]]$. As shown in [CAS], we obtain the following equation as the result:

$$L^4 - 2C_2(J)\,L^2 = C_0(J) \tag{V.30}$$

where $L = L(u, Z_0(u))$, $J = J(u, Z_0(u))$, and C_2, C_0 are the following polynomials with coefficients in $\mathbb{C}(\nu)[[t]]$:

$$C_2(J) \;=\; (\nu+1)^2 J^2 + \frac{2(\nu+3)}{\nu-1} J - 2(\nu^2-1)t^2 + \frac{2}{(\nu-1)^2}\,, \tag{V.31}$$

$$\begin{aligned} C_0(J) \;=\; & -(\nu+1)^2 \left(\left((\nu+1)J^2 - 2(\nu-1)t^2 \right)^2 + 4J^3 + 16(\nu-1)(t^3 z_1)J \right) \\ & - 4J^2 \;+\; 16(\nu+1)\nu t^2 J \;+\; 16w \end{aligned} \tag{V.32}$$

where $w = -(\nu^2-1)^2 t^5 z_3 + (\nu^2-1)^2 \left(2t^5 z_1^3 - \frac{3}{\nu+1} t^4 z_1^2 - \frac{3}{4} t^4 \right) + (\nu-3)\nu t^3 z_1 + t^2$. Notice that $z_3 \mapsto w$ is just a linear change of variable for fixed z_1.

Now we derive heuristically an algebraic equation satisfied by z_1 and t. We will check *a posteriori* that they lead to the right solution. We can write (V.30) in two ways:

$$(L^2 - 2C_2(J))L^2 = C_0(J) \qquad \text{and} \qquad (L^2 - C_2(J))^2 = C_0(J) + C_2^2(J)$$

If we view t and J as two independent variables, and view L as a function of (t, J). Then the above equations suggest that both C_0 and $C_0 + C_2^2$, viewed as polynomials of J, have double roots. It is well known that this is characterized by their discriminants being zero.

$$D_1 = \mathtt{Discriminant}_J(C_0) = 0 \qquad \text{and} \qquad D_2 = \mathtt{Discriminant}_J(C_0 + C_2^2) = 0$$

D_1 and D_2 are polynomials in t, z_1 and the auxiliary variable w. Since they both vanish for the same value of w, their resultant with respect to w must be zero. This provides a polynomial equation R_w satisfied by $z_1(t)$ and t. We compute this equation in [CAS]. After removing irrelevant factors, we get an equation of degree 15 in z_1 and t. Since $z_1(t)$ is an odd function of t, one can make the change of variable $\tilde{z}_1 = t^3 z_1$ and $\tilde{t} = t^2$ in the equation satisfied by $z_1(t)$. This leads to an equation of degree 6 in $\tilde{z}_1$ and $\tilde{t}$, see [CAS].

The discriminant $D_2 = 0$ provides an equation that relates $z_3(t)$ to $z_1(t)$ and t. Under the change of variables $\tilde{z}_3 = t^9 z_3$, $\tilde{z}_1 = t^3 z_1$ and $\tilde{t} = t^2$ and after removing irrelevant factors, it gives a quadratic equation for $\tilde{z}_3$. In [CAS] we check that this equation, as well as the equation of degree 6 relating $\tilde{z}_1$ to $\tilde{t}$, are both satisfied by the rational parametrizations (V.15).

A.2 Singularity analysis via rational parametrization

In this section we present a method to locate the dominant singularity of a combinatorial generating function from a proper rational parametrization of it. First let us clarify the definition of a rational parametrization.

Definition. Let $\mathcal{E} \in \mathbb{C}[x, y]$ be an irreducible polynomial. A couple of rational functions $\mathcal{P} = (\hat{x}, \hat{y})$ is an *(affine) rational parametrization* of the curve $\mathcal{E}(x, y) = 0$ if $\mathcal{E}(\hat{x}(s), \hat{y}(s)) = 0$ for all but finitely many $s \in \mathbb{C}$. Here a rational function is seen as a continuous mapping from $\overline{\mathbb{C}}$ to $\overline{\mathbb{C}}$. The rational parametrization $\mathcal{P}$ is

- *real* if $\hat{x}$ and $\hat{y}$ can be written with real coefficients.
- *proper* if $\mathcal{P}(s) = (x, y)$ has a unique solution s for all but finitely many (x, y) on $\mathcal{E} = 0$.

We call $s \in \mathbb{C}$ a *critical point* of $\mathcal{P}$ if either $\hat{x}'(s) = 0$ or $\hat{y}(s) = \infty$.

Proper parametrizations are minimal in the following sense. For all irreducible polynomial $\mathcal{E}(x, y)$, if $\mathcal{E} = 0$ has a rational parametrization, then it also has a proper one, and if $\mathcal{P}$ is one proper parametrization of $\mathcal{E} = 0$, then every rational parametrization of $\mathcal{E} = 0$ is of the form $\mathcal{P} \circ h$ with some non-constant rational function h [SWPD08, Lemma 4.17]. It is not hard to see that $\mathcal{P} \circ h$ is itself proper if and only if $h(s) = \frac{a+bs}{c+ds}$. One can use this property to move the poles of $\hat{x}(s)$, e.g. to place one pole at $s = \infty$, while keeping the parametrization proper. It is also easy determine whether a given rational parametrization is proper by looking at its degrees [SWPD08, Theorem 4.21]. One can check that all univariate rational parametrizations used in Section 3 are real and proper.

A rational parametrization $\mathcal{P} = (\hat{x}, \hat{y})$ is defined with respect to an algebraic equation $\mathcal{E} = 0$. But it is not immediately clear how $\mathcal{P}$ is related to the value of a function ϕ satisfying $\mathcal{E}(x, \phi(x)) = 0$, since a solution of the equation does not necessarily lie on the graph of the function. To study properties of the function, we want the relation $\hat{y} = \phi \circ \hat{x}$. If this relation holds in a neighborhood of $s_* \in \mathbb{C}$, we say that $(\mathcal{P}, s_*)$ *parametrizes* ϕ *locally at* $x_* = \hat{x}(s_*)$.

Lemma V.12. *Assume that $\mathcal{P} = (\hat{x}, \hat{y})$ is a proper parametrization of $\mathcal{E}(x, y) = 0$.*

(i) If a function ϕ satisfies $\mathcal{E}(x, \phi(x)) = 0$ in a neighborhood of $x_* \in \mathbb{C} \setminus \{\hat{x}(\infty)\}$, then there exists a unique $s_* \in \mathbb{C}$ such that $(\mathcal{P}, s_*)$ parametrizes ϕ locally at x_*.

(ii) For all $s_* \in \mathbb{C}$ such that $x_* := \hat{x}(s_*) \neq \infty$, $(\mathcal{P}, s_*)$ parametrizes a finite-valued function ϕ locally if and only if s_* is not a critical point of $\mathcal{P}$. In this case, ϕ is analytic at x_*.

Proof. (i) *Existence.* Consider a sequence $(x_n)_{n\geq 0}$ of distinct complex numbers converging to x_* such that $\mathcal{E}(x_n, \phi(x_n)) = 0$ for all n. According to the definition of proper parametrization, for all n large enough there exists $s_n \in \mathbb{C}$ such that $(x_n, \phi(x_n)) = (\hat{x}(s_n), \hat{y}(s_n))$. Let s_* be an accumulation point of $(s_n)_{n\geq n_0}$ in $\overline{\mathbb{C}}$. By the continuity of $\hat{x} : \overline{\mathbb{C}} \to \overline{\mathbb{C}}$, $x_* = \hat{x}(s_*) \neq \hat{x}(\infty)$, thus $s_* \in \mathbb{C}$. The analytic functions $\hat{y}$ and $\phi \circ \hat{x}$ coincide on a sequence of distinct points converging to s_*, so they must be equal in a neighborhood of s_*.

Uniqueness. Assume that $(\mathcal{P}, s_*)$ parametrize ϕ locally at x_*. Since a rational function is an open mapping, there exists a neighborhood V of x_* such that for all $x \in V$, $\mathcal{P}(s) = (x, \phi(x))$ has a solution close to s_*. But these solutions are unique except for finitely many values of x. Thus there is at most one $s_* \in \mathbb{C}$ having the above property.

(ii) If $\hat{x}'(s_*) \neq 0$ and $\hat{y}(s_*) \neq \infty$, then by the implicit function theorem, $\phi := \hat{y} \circ (\hat{x}^{-1})$ is a well defined analytic function such that $\hat{y} = \phi \circ \hat{x}$ in a neighborhood of s_*.

Inversely, assume $\hat{y} = \phi \circ \hat{x}$ in a neighborhood of s_* for some finite-valued function ϕ. Then $\hat{y}(s_*) = \phi(x_*) \neq \infty$. If $\hat{x}'(s_*) = 0$, then for all $x \neq x_*$ in some neighborhood of x_*, $\hat{x}(s) = x$ has at least two distinct solutions. But this gives two distinct solutions to $\mathcal{P}(s) = (x, \phi(x))$ for infinitely many x, contradicting the properness of $\mathcal{P}$. Thus $\hat{x}'(s_*) \neq 0$. $\square$

Proposition V.13. *Let $\phi(x) = \sum \phi_n x^n$ be a non-polynomial analytic function in a neighborhood of 0 such that $\phi_n \geq 0$ for all n. Assume that ϕ satisfies an algebraic equation $\mathcal{E}(x, y) = 0$ which has a real proper rational parametrization $\mathcal{P} = (\hat{x}, \hat{y})$ such that $\hat{x}(\infty) = \infty$.*

(i) There is a unique $s_0 \in \mathbb{R}$ such that $(\mathcal{P}, s_0)$ parametrizes ϕ locally at 0.

(ii) *ϕ has a dominant singularity at $x_c := \hat{x}(s_c)$, where $s_c \in \mathbb{R}$ is the critical point of $\mathcal{P}$ characterized by $\hat{x}(s_c) > 0$ and that $\mathcal{P}$ has no other critical point between s_0 and s_c.*

(iii) *If s_c is the only critical point of $\mathcal{P}$ such that $|\hat{x}(s)| = x_c$, then there exists a neighborhood V of s_0 such that $s_c \in \partial V$ and $\hat{x}|_V$ is a conformal bijection from V onto a slit disk at x_c. Moreover, ϕ has an analytic continuation on this slit disk.*

Proof. (i) The existence and uniqueness of s_0 is guaranteed by Lemma V.12. But since $\mathcal{P}$ and ϕ are real, $\bar{s}_0$ is also a solution to the problem. So we have $s_0 = \bar{s}_0$ by uniqueness.

(ii) Up to the change of variable $s \leftarrow -s$, we can assume that $\hat{x}'(s_0) > 0$. Let $s_c = \inf\{s \geq s_0 : \hat{x}'(s) = 0 \text{ or } \hat{y}(s) = \infty\}$ and $x_c = \hat{x}(s_c)$, then $\hat{y} \circ (\hat{x}^{-1})$ is an analytic continuation of ϕ on $[0, x_c)$. By Pringhseim's theorem, the radius of convergence of ϕ is at least x_c. It is well known that the only entire functions that satisfy algebraic equations are polynomials. Therefore $x_c < \infty = \hat{x}(\infty)$ according to the hypothesis that ϕ is not polynomial. It follows that $s_c < \infty$ and s_c is a critical point of $\mathcal{P}$.

If ϕ is analytic at x_c, then by analytic continuation, the relation $\hat{y} = \phi \circ \hat{x}$ holds in a neighborhood of s_c, i.e. $(\mathcal{P}, s_c)$ parametrizes ϕ locally at x_c. This contradicts Lemma V.12(ii). Therefore x_c is a dominant singularity of $\phi(x)$.

(iii) Recall that D_r is the open disk of radius r centered at 0. Let U be the connected component of $\hat{x}^{-1}(D_{x_c})$ containing s_0. By continuity, all s on the boundary of U satisfy $|\hat{x}(s)| = x_c$. By analytic continuation, $\hat{y} = \phi \circ \hat{x}$ on U, therefore Lemma V.12 implies that U contains no critical point of $\mathcal{P}$. As $\hat{x}(\infty) = \infty$, U is bounded, i.e. its closure $\overline{U}$ is compact.

Assume that s_c is the only critical point of $\mathcal{P}$ such that $|\hat{x}(s)| = x_c$. Since there are only finitely many critical points, there exists a neighborhood N of $\overline{U}$ in which s_c is the only critical point. Since $\hat{x}$ is an open mapping, $\hat{x}(N)$ contains a neighborhood of $\overline{D}_{x_c}$, in particular contains some slit disk $D_{x_c}^{|\epsilon}$. Let V be the connected component of $\hat{x}^{-1}(D_{x_c}^{|\epsilon})$ containing s_0. By construction, V contains no critical point of the parametrization $\mathcal{P}$. In particular, $\hat{x}'$ does not vanish on V. Combining the open mapping theorem and the fact $\hat{x}(\infty) = \infty$, one can show that $\hat{x}|_V$ is a proper mapping from V to $D_{x_c}^{|\epsilon}$. Then by Hadamard's global inversion theorem [KP13, Theorem 6.2.8], $\hat{x}|_V$ is a conformal bijection from V onto $D_{x_c}^{|\epsilon}$. In particular, $\phi = \hat{y} \circ (\hat{x}^{-1})$ defines an analytic function on $D_{x_c}^{|\epsilon}$. ☐

Proof of Lemma V.4. Recall that we derived in Section 3.3 a rational parametrization of Z of the form $(u, v) = (\hat{u}(H), \hat{u}(K))$ and $Z = \hat{Z}(H, K)$. We obtain a rational parametrization of $u \mapsto Z(u, u)$ by taking $K = H$:

$$\begin{cases} u = \hat{u}(H) & = \dfrac{u_c}{3} H(10 - 12H + 6H^2 - H^3) \\ Z = \hat{Z}(H, H) & = \dfrac{10 - 12H + 6H^2 - H^3}{10 - 14H + 7H^2 - H^3} Q(H)\,, \end{cases} \tag{V.33}$$

where Q is some polynomial of degree 6. In [CAS], we check by explicit computation that

(1) $H_0 = 0$ is the only value of H such that $\hat{Z}(H, H) = 1$ and $\hat{u}(H) = 0$.

(2) $H_c = 1$ is the (unique) real critical point of the rational parametrization (V.33) such that $\hat{u}(H) > 0$ and that there are no other critical points on $[H_0, H_c] = [0, 1]$.

(3) $H_c = 1$ is the unique critical point of (V.33) such that $|\hat{u}(H)| = u_c$.

Therefore by Proposition V.13, there is a neighborhood V of $H_0 = 0$ such that $H_c = 1 \in \partial V$ and that $\hat{u}|_V$ is a conformal bijection from V onto a slit disk $D_{u_c}^{|\epsilon}$ at u_c. It is clear that $\hat{u}(H) \uparrow u_c$ when $H \uparrow 1$ on the real axis. This proves (ii) of Lemma V.4.

To prove (i), we notice that the coefficients $z_{p,q}$ are all positive. Thus the monotone convergence theorem implies

$$\sum_{p,q\geq 0} z_{p,q} u_c^{p+q} \;=\; \lim_{u\uparrow u_c} Z(u,u) \;=\; \lim_{H\uparrow 1} \hat{Z}(H,H) \;<\; \infty\,.$$

And it follows that $\sum_{p,q\geq 0} z_{p,q} u^p v^q$ is absolutely convergent for all $(u,v) \in \overline{D}_{u_c}^2$. On the other hand, if the series is absolutely convergent for some (u,v) with $|u| > u_c$, then by monotonicity the series $Z_0(u) = Z(u,0)$ will have a radius of convergence strictly larger than u_c. This is not the case because the rational parametrization (V.16) implies that $Z_0(u)$ has a singularity of type $(u_c - u)^{4/3}$ at $u = u_c$.

Now let us fix a $u \in \overline{D}_{u_c}$ and prove (iii). Since the coefficients of the series $v \mapsto Z(u,v)$ are not necessarily non-negative, Proposition V.13 does not apply. Instead, we will check (iii) directly using the formula $Z(u,v) = \hat{Z}(\hat{u}^{-1}(u), \hat{u}^{-1}(v))$ and the analytic properties of the function $\hat{u}$. Recall that $\hat{u}$ induces a conformal bijection from some neighborhood V of $H = 0$ onto a slit disk $D_{u_c}^{|\epsilon}$ at u_c, which extends bi-continuously to $H = 1$ by $\hat{u}(1) = u_c$. Let $\overline{U}$ be the preimage of $\overline{D}_{u_c}$ by $\hat{u}|_{V\cup\{1\}}$, then it suffices to show that

(iii') for each $H \in \overline{U}$, $K \mapsto \hat{Z}(H,K)$ has no pole in $\overline{U} \setminus \{1\}$.

Indeed, since the poles of a *univariate* rational function are isolated, (iii') implies that $K = 1$ is the only possible pole of $K \mapsto \hat{Z}(H,K)$ in some neighborhood U' of the compact $\overline{U}$. Its image $\hat{u}(U')$ is a neighborhood of the disk $\overline{D}_{u_c}$. Since $\hat{u}$ is a conformal bijection onto $D_{u_c}^{|\epsilon}$, the composed function $v \mapsto \hat{Z}(\hat{u}^{-1}(u), \hat{u}^{-1}(v))$ is analytic on the intersection $\hat{u}(U') \cap D_{u_c}^{|\epsilon}$, which contains a slit disk at u_c. On the other hand, $v \mapsto Z(u,v)$ must have a singularity at u_c, otherwise its radius of convergence would be strictly larger than u_c, contradicting (i). We conclude that u_c is the unique dominant singularity of $v \mapsto Z(u,v)$ for all $u \in \overline{D}_{u_c}$.

In order to prove (iii'), we will show the following stronger statement: the denominator of $\hat{Z}(H,K)$ has no zero in $\overline{U}^2$ except at $(H,K) = (1,1)$. We denote by N and D the numerator and the denominator of $\hat{Z}$ written in reduced form. The polynomial D cannot have a zero $(H,K) \in \overline{U}^2$ which is not a zero of N, otherwise we would have $Z(u,v) \to \infty$ when $(u,v) \to (\hat{u}(H), \hat{u}(K)) \in \overline{D}_{u_c}^2$, contradicting the fact that $|Z(u,v)| \leq Z(u_c,u_c) < \infty$ for all $(u,v) \in \overline{D}_{u_c}^2$. Now assume that (H,K) is a common zero of D and N in $\overline{U}^2$. Then H must be a zero of $Res(H)$, the resultant of $D(H,K)$ and $N(H,K)$ with respect to K. In [CAS], we check by explicit computation that $H = 0$ and $H = 1$ are the only zeros of $Res(H)$ in $\overline{U}$. Moreover, $D(0,K)$ and $N(0,K)$ has no common zero in $\overline{U}$, and $K = 1$ is the only common zero of $D(1,K)$ and $N(1,K)$. We conclude that on $\overline{U}^2$, the denominator $D(H,K)$ only vanishes at $(H,K) = (1,1)$, therefore (iii') is true.

The assertion (iv) follows from Proposition V.13 thanks to the known properties of $\hat{u}$ and the fact that $\hat{A}$ has no pole on $[H_0, H_c] = [0,1]$. The application of Proposition V.13 here assumes that the coefficients of the series $A(u) = \sum_{p\geq 0} a_p u^p$ are non-negative. This is derived in Section 3.3 using only (i)-(iii) of Lemma V.4. □

A.3 A one-jump lemma for the Markov chain $\mathcal{L}_{p,\infty}(P_n)_{n\geq 0}$

Notation: We will denote by $x \wedge y$ the minimum of x and y, and by $x \vee y$ their maximum. When $A(\lambda)$ and $B(\lambda)$ are two families of positive numbers indexed by all λ in some set Λ, we use the following notations:

$$\begin{aligned} A(\lambda) \preccurlyeq B(\lambda) \quad &\Leftrightarrow \quad \exists\, C > 0 \text{ such that } \forall\, \lambda \in \Lambda,\ A(\lambda) \leq C B(\lambda)\,, \\ A(\lambda) \asymp B(\lambda) \quad &\Leftrightarrow \quad A(\lambda) \preccurlyeq B(\lambda) \text{ and } B(\lambda) \preccurlyeq A(\lambda)\,. \end{aligned}$$

The proof of following properties of $\preccurlyeq$ and $\asymp$ is left as a simple exercise.

Proposition V.14. *(a) If $A_1 \preccurlyeq B_1$ and $A_2 \preccurlyeq B_2$, then $A_1A_2 \preccurlyeq B_1B_2$ and $A_1+A_2 \preccurlyeq B_1+B_2$.*
(b) More generally, if $A(\lambda) \preccurlyeq B(\lambda)$ for $\lambda \in \Lambda = \bigcup_{i\in I} \Lambda_i$, where I is some arbitrary index set, then $\sum_{\lambda\in\Lambda_i} A(\lambda) \preccurlyeq \sum_{\lambda\in\Lambda_i} B(\lambda)$ for $i \in I$. The same is true when $\preccurlyeq$ is replaced by $\asymp$.
(c) If $\Lambda = \mathbb{N}$, then $A(\lambda) \preccurlyeq B(\lambda)$ is equivalent to $A(\lambda) = O(B(\lambda))$ in the limit $\lambda \to \infty$.
In particular, $A(\lambda) \underset{\lambda\to\infty}{\sim} B(\lambda)$ implies $A(\lambda) \asymp B(\lambda)$.

Our proof of Lemma V.10 is based on the following estimates on the transition probabilities of the Markov chain $\mathcal{L}_{p,\infty}(P_n)_{n\geq 0}$. Recall that $X_n = P_n - P_0$.

Lemma V.15. *We have for all $p \geq 2$ and $-2 \leq k \leq p$,*

$$\mathsf{P}_{p,\infty}(X_1 = -k) \;\asymp\; f_p(k) := \begin{cases} (k+3)^{-7/3} & \text{if } -2 \leq k \leq p/2 \\ p^{-1}(p-k+1)^{-4/3} & \text{if } p/2 < k \leq p \end{cases}.$$

And for all $k \geq -2$, $\mathsf{P}_{\infty,\infty}(X_1 = -k) \asymp (k+3)^{-7/3}$.
In particular, $\mathsf{P}_{p,\infty}(X_1 = -k) \asymp \mathsf{P}_{\infty,\infty}(X_1 = -k)$ for all $p \geq 2$ and $-2 \leq k \leq p/2$.

Remark. One can replace the $p/2$'s in the lemma by θq for any fixed $0 < \theta < 1$. The same applies to all subsequent lemmas.

Proof. Assume $p \geq 2$. We have seen in the proof of Theorem V.2 that $\mathsf{P}_{\infty,\infty}(X_1 = -k) \sim c_x k^{-7/3}$ as $k \to \infty$ for some numerical constant c_x. Therefore by the last property of $\asymp$, we have

$$\mathsf{P}_{\infty,\infty}(X_1 = -k) \asymp (k+3)^{-7/3}\,.$$

Similarly, we have seen in the proof of Proposition V.11 that $\mathsf{P}_{p,\infty}(X_1 = -p) \sim c_0\, p^{-1}$ and $\mathsf{P}_{p,\infty}(X_1 = -p+1) \sim (c_1 - c_0)p^{-1}$ as $p \to \infty$, so $\mathsf{P}_{p,\infty}(X_1 = -p) \asymp \mathsf{P}_{p,\infty}(X_1 = -p+1) \asymp p^{-1}$. On the other hand, for $-2 \leq k \leq p-2$, one can check from Table V.2(a) that

$$\mathsf{P}_{p,\infty}(X_1 = -k) = \mathsf{P}_{\infty,\infty}(X_1 = -k)\frac{a_{p-k}u_c^{p-k}}{a_p u_c^p}\,.$$

Moreover, the asymptotic of $(a_p)_{p\geq 0}$ gives $a_p u_c^p \asymp p^{-4/3}$. Thus for $p \geq 2$ and $-2 \leq k \leq p$,

$$\mathsf{P}_{p,\infty}(X_1 = -k) \asymp \left.\begin{cases} (k+3)^{-7/3}\frac{(p-k)^{-4/3}}{p^{-4/3}} & \text{if } k \leq p-2 \\ p^{-1} & \text{if } k \in \{p-1, p\} \end{cases}\right\} \asymp f_p(k)\,. \qquad \square$$

Lemma V.10 states that with high probability as $p \to \infty$, the process $\mathcal{L}_{p,\infty}(P_n)_{n\geq 0}$ stays around its drift within the linear barrier $|p_n - (p + \mu n)| \leq \epsilon n + x$ up to T_m, the first time it jumps to a neighborhood of zero. This would be a classical result if $\mathcal{L}_{p,\infty}(P_n)_{n\geq 0}$ was replaced by the random walk $p + \mathcal{L}_{\infty,\infty}(X_n)_{n\geq 0}$, and we could find its proof in for example [BB08]. But by the very definition of the random walk $\mathcal{L}_{\infty,\infty}(X_n)_{n\geq 0}$, the transition probabilities of $\mathcal{L}_{p,\infty}(P_n)_{n\geq 0}$ are close to that of $p + \mathcal{L}_{\infty,\infty}(X_n)_{n\geq 0}$ as long as P_n is far from zero. The basic idea of our proof is to quantify this closeness between the processes $\mathcal{L}_{p,\infty}(P_n)_{n\geq 0}$ and $p + \mathcal{L}_{\infty,\infty}(X_n)_{n\geq 0}$.

The mean technical difficulty is that *a priori*, the convergence of the transition probabilities only implies the convergence of the process $\mathcal{L}_{p,\infty}(P_n)_{n\geq 0}$ to $p+\mathcal{L}_{\infty,\infty}(X_n)_{n\geq 0}$ up to finite time. But we want an estimate about the behavior of $\mathcal{L}_{p,\infty}(P_n)_{n\geq 0}$ up to time T_m, which is of order $\Theta(p)$. For this we need to estimate the error committed when we approximate $\mathcal{L}_{p,\infty}X_1$ by $\mathcal{L}_{\infty,\infty}X_1$, and control the propagation of this error through the proof that leads to the random walk result.

As in [BB08], our proof comes in three steps. First, we give an estimate to the following truncated exponential moment of the distribution of $\mathcal{L}_{p,\infty}X_1$, defined for all $x > 0$ and $p \in \mathbb{N} \cup \{\infty\}$.

$$\varphi_p^x(\lambda) = \mathtt{E}_{p,\infty}\left[e^{\lambda(\mu - X_1)}\mathbb{1}_{\{\mu - X_1 < x\}}\right]$$

Lemma V.16. *For all $\delta > 0$, there exist constants p_δ, x_δ such that uniformly in $p \geq p_\delta$ (including $p = \infty$), $x \in [x_\delta, p/2]$ and $\lambda \in [2x^{-1}, 1]$, we have*

$$\begin{aligned} e^{-\lambda\delta}\varphi_p^x(-\lambda) - 1 &\preccurlyeq \lambda^{4/3} \\ \text{and} \qquad e^{-\lambda\delta}\varphi_p^x(\lambda) - 1 &\preccurlyeq \lambda^{4/3}e^{\lambda x/2} + x^{-4/3}e^{\lambda x}\,. \end{aligned}$$

Proof. To simplify notation, let $\check{X}_1 = \mu - X_1$. Summing the uniform bound $\mathtt{P}_{p,\infty}(X_1 = -k) \asymp (k+3)^{-7/3}$ in Lemma V.15 over $k \leq p/2$, we obtain that uniformly in $x \geq 1$ and $p \geq 2x$,

$$\mathtt{P}_{p,\infty}\left(x \leq \check{X}_1 \leq \frac{p}{2}\right) \preccurlyeq x^{-4/3}\,,\ \mathtt{E}_{p,\infty}\left[\check{X}_1\mathbb{1}_{\{x\leq \check{X}_1 \leq \frac{p}{2}\}}\right] \preccurlyeq x^{-1/3} \ \text{ and } \ \mathtt{E}_{p,\infty}\left[\check{X}_1^2\mathbb{1}_{\{\check{X}_1 \leq x\}}\right] \preccurlyeq x^{2/3}. \tag{V.34}$$

Writing $e^x = 1 + x + (e^x - 1 - x)$, we get that for all $\lambda \in \mathbb{R}$,

$$\varphi_p^x(\lambda) \leq 1 + \lambda I_1 + I_2(\lambda) \tag{V.35}$$

where $I_1 = \mathtt{E}_{p,\infty}\left[\check{X}_1\mathbb{1}_{\{\check{X}_1 < x\}}\right]$ and $I_2(\lambda) = \mathtt{E}_{p,\infty}\left[\left(e^{\lambda\check{X}_1} - 1 - \lambda\check{X}_1\right)\mathbb{1}_{\{\check{X}_1 < x\}}\right]$. By the definitions of μ and $\mathcal{L}_{\infty,\infty}X_1$, we have $\mathtt{E}_{\infty,\infty}[\check{X}_1] = 0$ and $\mathtt{P}_{p,\infty}(X_1 = x_1) \xrightarrow[p\to\infty]{} \mathtt{P}_{\infty,\infty}(X_1 = x_1)$ for all fixed x_1. Summing over $x_1 \in [\mu - x, 2] \cap \mathbb{Z}$, we get

$$I_1 = \mathtt{E}_{p,\infty}\left[\check{X}_1\mathbb{1}_{\{\check{X}_1 < x\}}\right] \xrightarrow[p\to\infty]{} \mathtt{E}_{\infty,\infty}\left[\check{X}_1\mathbb{1}_{\{\check{X}_1 < x\}}\right] = -\mathtt{E}_{\infty,\infty}\left[\check{X}_1\mathbb{1}_{\{\check{X}_1 \geq x\}}\right] \xrightarrow[x\to\infty]{} 0\,.$$

Thus for any fixed $\delta > 0$, there exist x_δ, p_δ large enough so that for all $p \geq p_\delta$ or $p = \infty$,

$$\left|\mathtt{E}_{p,\infty}\left[\check{X}_1\mathbb{1}_{\{\check{X}_1 < x_\delta\}}\right]\right| \leq \delta/2 \qquad \text{and} \qquad \left|\mathtt{E}_{p,\infty}\left[\check{X}_1\mathbb{1}_{\{x_\delta \leq \check{X}_1 \leq p/2\}}\right]\right| \leq \delta/2$$

where the second bound comes from the second estimate in (V.34). Since I_1 is increasing in x, it follows that $|I_1| \leq \delta$ for all $x \in [x_\delta, p/2]$. Combine this with the fact that $e^{-|t|}(1+t) \leq 1$ ($t \in \mathbb{R}$), we deduce from (V.35) that for all $p \geq p_\delta$ or $p = \infty$, $x \in [x_\delta, p/2]$ and $\lambda \geq 0$,

$$e^{-\lambda\delta}\varphi_p^x(-\lambda) - 1 \leq I_2(-\lambda) \qquad \text{and} \qquad e^{-\lambda\delta}\varphi_p^x(\lambda) - 1 \leq I_2(\lambda)\,.$$

Now take $\lambda \in [2x^{-1}, 1]$. Since $e^t - 1 - t \le 2t^2$ for all $t \le 2$, we have

$$\begin{aligned} I_2(-\lambda) &= \mathtt{E}_{p,\infty}\left[(e^{-\lambda \check{X}_1} - 1 + \lambda \check{X}_1)\mathbb{1}_{\{\mu-2 \le \check{X}_1 \le \frac{1}{\lambda}\}}\right] + \mathtt{E}_{p,\infty}\left[(e^{-\lambda \check{X}_1} - 1 + \lambda \check{X}_1)\mathbb{1}_{\{\frac{1}{\lambda} < \check{X}_1 < x\}}\right] \\ &\le 2\lambda^2\, \mathtt{E}_{p,\infty}\left[\check{X}_1^2 \mathbb{1}_{\{\check{X}_1 \le \frac{1}{\lambda}\}}\right] + \lambda\, \mathtt{E}_{p,\infty}\left[\check{X}_1 \mathbb{1}_{\{\frac{1}{\lambda} < \check{X}_1 \le p/2\}}\right] \end{aligned}$$

Using (V.34), we conclude that $I_2(-\lambda) \preccurlyeq \lambda^2 \cdot \lambda^{-2/3} + \lambda \cdot \lambda^{1/3} \asymp \lambda^{4/3}$.

Similarly, by cutting the interval of $\check{X}_1$ at $\frac{1}{\lambda}$ and $x/2$, we get

$$\begin{aligned} I_2(\lambda) &\le \lambda^2\, \mathtt{E}_{p,\infty}\left[\check{X}_1^2 \mathbb{1}_{\{\check{X}_1 \le \frac{1}{\lambda}\}}\right] + \mathtt{E}_{p,\infty}\left[e^{\lambda \check{X}_1} \mathbb{1}_{\{\frac{1}{\lambda} < \check{X}_1 < x/2\}}\right] + \mathtt{E}_{p,\infty}\left[e^{\lambda \check{X}_1} \mathbb{1}_{\{x/2 \le \check{X}_1 < x\}}\right] \\ &\le \lambda^2\, \mathtt{E}_{p,\infty}\left[\check{X}_1^2 \mathbb{1}_{\{\check{X}_1 \le \frac{1}{\lambda}\}}\right] + e^{\lambda x/2}\, \mathtt{P}_{p,\infty}\left(\lambda^{-1} \le \check{X}_1 \le p/2\right) + e^{\lambda x}\, \mathtt{P}_{p,\infty}\left(x/2 \le \check{X}_1 \le p/2\right) \\ &\preccurlyeq \lambda^{4/3} + e^{\lambda x/2}\lambda^{4/3} + e^{\lambda x} x^{-4/3} \\ &\asymp \lambda^{4/3} e^{\lambda x/2} + x^{-4/3} e^{\lambda x}. \end{aligned}$$

□

The second step in the proof of Lemma V.10 is to show that the process $\mathcal{L}_{p,\infty}(P_n)_{n\ge 0}$ stays around its mean within the constant barrier $|p_n - (p+\mu n)| \le x$ up to a time that is linear in x. Once this is done, we will be in a good position to show that the process stays within the linear barrier $|p_n - (p+\mu n)| \le \epsilon n + x$ up to a time of order $\Theta(p)$ using the Markov property. For $x > 0$, let $\tau_x = \tau_x^{\epsilon=0} = \inf\{n \ge 0 : |P_n - P_0 - \mu n| \ge x\}$.

Lemma V.17. *For all $\epsilon > 0$, denote $N = 2x/\epsilon$. Then there exist constants x_ϵ and p_ϵ such that uniformly in $p \ge p_\epsilon$, $x \in [x_\epsilon, p/2]$ and $m \ge 1$,*

$$\mathtt{P}_{p,\infty}(\tau_x < (N+1) \wedge T_m) \preccurlyeq x^{-1/6} + \frac{N}{p} m^{-1/3}.$$

Proof. Consider the first time that the process $(P_n)_{n\ge 0}$ makes a large (negative) jump of order x: $J_x = \inf\{n \ge 1 : X_n - X_{n-1} \le \mu - x\}$. We bound the probability of the event $\{\tau_x < (N+1) \wedge T_m\}$ separately in the case $\{J_x \le \tau_x\}$ (large jump estimate) and in the case $\{\tau_x < J_x\}$ (small jump estimate) by writing

$$\mathtt{P}_{p,\infty}(\tau_x < (N+1)\wedge T_m) \le \mathtt{P}_{p,\infty}(J_x < (N+1)\wedge T_m \text{ and } J_x \le \tau_x) + \mathtt{P}_{p,\infty}(\tau_x < (N+1)\wedge J_x)$$

Large jump estimate: union bound.

$$\begin{aligned} \mathtt{P}_{p,\infty}(J_x < (N+1) \wedge T_m \text{ and } J_x \le \tau_x) &= \sum_{n=1}^{N} \mathtt{P}_{p,\infty}(J_x = n < T_m \text{ and } n \le \tau_x) \\ &\le \sum_{n=1}^{N} \mathtt{P}_{p,\infty}(X_n - X_{n-1} \le \mu - x, P_n > m \text{ and } P_{n-1} > p - x) \qquad \text{(union bound)} \\ &= \sum_{n=1}^{N} \mathtt{E}_{p,\infty}\left[\mathbb{P}_{P_{n-1}}(X_1 \le \mu - x \text{ and } P_1 > m)\mathbb{1}_{\{P_{n-1} > p-x\}}\right] \quad \text{(Markov property)} \\ &\le N \sup_{p' > p-x} \mathtt{P}_{p',\infty}(x - \mu \le -X_1 < p' - m) \end{aligned}$$

According to Lemma V.15,

$$\begin{aligned} \mathtt{P}_{p',\infty}(x - \mu \le -X_1 < p' - m) \asymp \sum_{k=x-\mu}^{p'-m} f_p(k) &\le \sum_{k=x-\mu}^{\infty} (k+3)^{-7/3} + \sum_{k'=m}^{\infty} p'^{-1}(k'+1)^{-4/3} \\ &\preccurlyeq x^{-4/3} + p'^{-1} m^{-1/3} \end{aligned}$$

Recall that $x \le p/2$, so $p'^{-1} \asymp p^{-1}$ uniformly for all $p' > p - x$. It follows that

$$\mathtt{P}_{p,\infty}(J_x < (N+1) \wedge T_m \text{ and } J_x \le \tau_x) \ \preccurlyeq\ N\Big(x^{-4/3} + p^{-1}m^{-1/3}\Big) \ \preccurlyeq\ x^{-1/3} + \frac{N}{p}m^{-1/3}.$$

Small jump estimate: Chernoff bound. Consider the stopping times

$$\tau_x^- = \inf\{n \ge 0 : X_n \le \mu n - x\} \qquad \text{and} \qquad \tau_x^+ = \inf\{n \ge 0 : X_n \ge \mu n + x\}.$$

Obviously, $\tau_x = \tau_x^+ \wedge \tau_x^-$. Let us first bound the probability of $\{\tau_x^- < (N+1) \wedge J_x\}$ using

$$\mathtt{P}_{p,\infty}(\tau_x^- < (N+1) \wedge J_x) \ = \ \sum_{n=1}^{N} \mathtt{P}_{p,\infty}(\tau_x^- = n \text{ and for all } k \le n,\ \mu - (X_k - X_{k-1}) < x).$$

Since $\mathcal{L}_{p,\infty}X_1 \to \mathcal{L}_{\infty,\infty}X_1$ in distribution and $\varphi_p^x(\lambda)$ is the $\mathtt{E}_{p,\infty}$-expectation of a compactly supported function of X_1, we have $\varphi_{p'}^x(\lambda) \to \varphi_\infty^x(\lambda)$ as $p' \to \infty$. In other words, the function $p' \mapsto \varphi_{p'}^x(\lambda)$ is continuous on the compact $K = \{p' : p' \ge p - x\} \cup \{\infty\}$. Hence there exists $p^* = p^*(\lambda, x) \in K$ such that

$$\varphi_{p^*}^x(\lambda) = \sup_{p' \ge p-x} \varphi_{p'}^x(\lambda).$$

Consider an i.i.d. sequence of random variables $(X_n^*)_{n\ge0}$ independent of $(X_n)_{n\ge0}$, such that $\mathcal{L}_{p,\infty}X_1^* = \mathcal{L}_{p^*}X_1$ in distribution. Let

$$\check{X}_n = \begin{cases} \mu - (X_n - X_{n-1}) & \text{if } n \le \tau_x^- \\ \mu - X_n^* & \text{if } n > \tau_x^- \end{cases}.$$

On $\{\tau_x^- = n\}$, we have $X_n - (\mu n - x) = x - (\check{X}_1 + \cdots + \check{X}_n) \le 0$. Therefore for all $\lambda \ge 0$,

$$\begin{aligned}
\mathtt{P}_{p,\infty}(\tau_x^- < (N+1) \wedge J_x) \ &\le\ \sum_{n=1}^{N} \mathtt{E}_{p,\infty}\left[e^{\lambda(\check{X}_1+\cdots+\check{X}_n - x)} \mathbb{1}_{\{\tau_x^-=n\}} \prod_{k=1}^{n} \mathbb{1}_{\{\check{X}_k < x\}}\right] && \text{(Chernoff bound)}\\
&=\ e^{-\lambda x} \sum_{n=1}^{N} \mathtt{E}_{p,\infty}\left[\mathbb{1}_{\{\tau_x^-=n\}} \prod_{k=1}^{n} \left(e^{\lambda \check{X}_k} \mathbb{1}_{\{\check{X}_k < x\}}\right)\right]\\
&=\ e^{-\lambda x} \sum_{n=1}^{N} \varphi_{p^*}^x(\lambda)^{-N+n} \cdot \mathtt{E}_{p,\infty}\left[\mathbb{1}_{\{\tau_x^-=n\}} \prod_{k=1}^{N} \left(e^{\lambda \check{X}_k} \mathbb{1}_{\{\check{X}_k < x\}}\right)\right] && \text{(Markov)}\\
&\le\ e^{-\lambda x} \cdot (1 \vee \varphi_{p^*}^x(\lambda)^{-N}) \cdot \mathtt{E}_{p,\infty}\left[\prod_{k=1}^{N} \left(e^{\lambda \check{X}_k} \mathbb{1}_{\{\check{X}_k < x\}}\right)\right]. && \text{(V.36)}
\end{aligned}$$

Let $\check{\mathcal{F}}$ be the natural filtration of the process $(\check{X}_n)_{n\ge0}$. Then τ_x^- is also a $\check{\mathcal{F}}$-stopping time. Moreover, on the event $\{\tau_x^- > k\}$, we have $\mathtt{P}_{p,\infty}$-almost surely $P_k \ge P_0 + \mu k - x \ge p - x$ and thus $\varphi_{P_k}^x(\lambda) \le \varphi_{p^*}^x(\lambda)$ according to the definition of p^*. So by Markov property,

$$\mathtt{E}_{p,\infty}\left[e^{\lambda \check{X}_{k+1}} \mathbb{1}_{\{\check{X}_{k+1} < x\}} \,\middle|\, \check{\mathcal{F}}_k\right] \ = \ \mathbb{1}_{\{\tau_x^- \le k\}} \cdot \varphi_{p^*}^x(\lambda) + \mathbb{1}_{\{\tau_x^- > k\}} \cdot \varphi_{P_k}^x(\lambda) \ \le\ \varphi_{p^*}^x(\lambda).$$

Use this bound N times in (V.36), we get

$$\mathtt{P}_{p,\infty}(\tau_x^- < (N+1) \wedge J_x) \ \le\ e^{-\lambda x} \cdot (\varphi_{p^*}^x(\lambda)^N \vee 1).$$

Recall that $N = 2x/\epsilon$ and $\log(t) < t-1$ for all $t \geq 0$. By Lemma V.16 with $\delta = \epsilon/4$, there exist constants x_ϵ and p_ϵ such that uniformly in $p \geq p_\epsilon$, $x \in [x_\epsilon, p/2]$ and $\lambda \in [2x^{-1}, 1]$,

$$\log\left(e^{-\lambda x/2}\varphi^x_{p^*}(\lambda)^N\right) \;=\; N\log\left(e^{-\lambda\delta}\varphi^x_{p^*}(\lambda)\right) \preccurlyeq\; x\left(\lambda^{4/3}e^{\lambda x/2} + x^{-4/3}e^{\lambda x}\right).$$

When x_ϵ is large enough, we can take $\lambda = \frac{\log(x)}{3}x^{-1} \in [2x^{-1}, 1]$, so that $e^{\lambda x} = x^{1/3}$. Then the right hand side of the above inequality is equal to $(\frac{\log(x)}{3})^{4/3}x^{-1/6} + 1$, which is bounded when $x \geq x_\epsilon$. So with this choice of λ and for all $p \geq p_\epsilon$ and $x \in [x_\epsilon, p/2]$, $e^{-\lambda x/2}\varphi^x_{p^*}(\lambda)^N$ is bounded by a constant that depends only on ϵ. It follows that

$$\mathsf{P}_{p,\infty}(\tau_x^- < (N+1)\wedge J_x) \;\preccurlyeq\; e^{-\lambda x/2} \vee e^{-\lambda x} = x^{-1/6}.$$

Following exactly the same steps, we can prove the same bound for $\mathsf{P}_{p,\infty}(\tau_x^+ < (N+1)\wedge J_x)$ using the estimate for $\varphi^x_p(-\lambda)$ in Lemma V.16. Combine this with the large jump estimate, we conclude that

$$\mathsf{P}_{p,\infty}(\tau_x < (N+1)\wedge T_m) \;\preccurlyeq\; x^{-1/6} + \frac{N}{p}m^{-1/3}. \qquad \square$$

Proof of Lemma V.10. Consider $x > 0$ and $\epsilon \in (0, \mu)$. Let $x_k = (2^k - 1)x$ and $N_k = (2^k - 2)\frac{x}{\epsilon}$ so that we have $x_1 = x$, $N_1 = 0$ and for all $k \geq 0$,

$$x_{k+1} - x_k = 2^k x\,, \quad N_{k+1} - N_k = 2^k x/\epsilon \qquad \text{and} \qquad x_k = x + \epsilon N_k\,.$$

Without loss of generality, we assume that $(N_k)_{k\geq 0}$ are integers. $(x_k)_{k\geq 1}$ and $(N_k)_{k\geq 0}$ define a sequence of disjoint boxes $B_k = \{(n, X_n) : n \in (N_k, N_{k+1}] \text{ and } |X_n - \mu n| \leq x_k\}$, which are all contained in the region $|X_n - \mu n| \leq \epsilon n + x$ thanks to the relation $x_k = x + \epsilon N_k$ above. See Figure V.7. Let $K^\epsilon_{x,m}$ be the index of the first box exited by $(X_n)_{n\geq 0}$ before T_m. More precisely, let

$$K^\epsilon_{x,m} = \inf\left\{k \geq 1 : \exists\, n \in (N_k, N_{k+1}] \text{ such that } n < T_m \text{ and } |X_n - \mu n| > x_k\right\}.$$

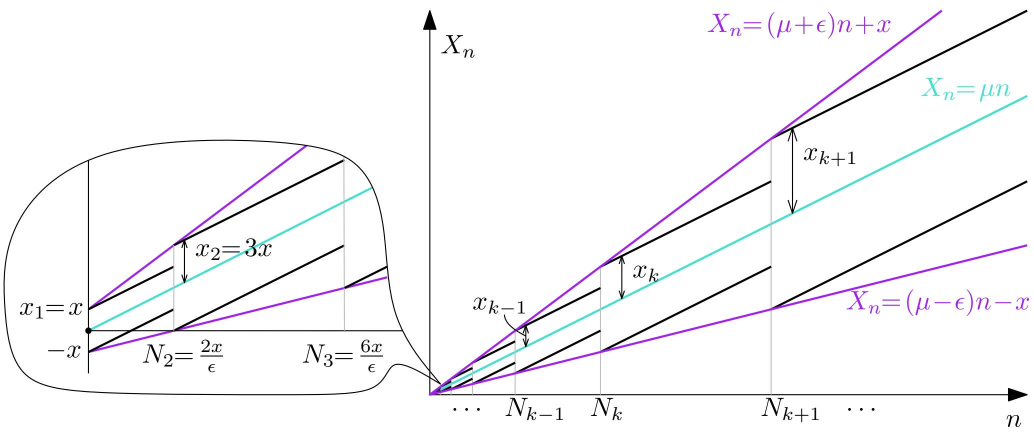

Figure V.7 – *The boxes B_k are parallelograms centered around the line $X_n = \mu n$. They are all contained between the lines $X_n = (\mu+\epsilon)n + x$ and $X_n = (\mu-\epsilon)n - x$.*

Then we have $\{\tau_x^\epsilon < T_m\} \subset \{K_{x,m}^\epsilon < \infty\}$. So it suffices to bound the probability of the latter event. For any $k \geq 1$, we use the Markov property at time N_k to write

$$\begin{aligned}
\mathtt{P}_{p,\infty}(K_{x,m}^\epsilon = k) &\leq \mathtt{P}_{p,\infty}\left(|X_{N_k} - \mu N_k| \leq x_{k-1} \text{ and } \exists\, n \in (N_k, N_{k+1}] \text{ s.t. } n < T_m\,, |X_n - \mu n| > x_k\right) \\
&\leq \sup_{|\delta| \leq x_{k-1}} \mathbb{P}_{p+\mu N_k+\delta}\Big(\exists\, n < (N_{k+1} - N_k + 1) \wedge T_m \text{ s.t. } |X_n - \mu n + \delta| > x_k\Big)
\end{aligned}$$

Using triangular inequality $|X_n - \mu n| \geq |X_n - \mu n + \delta| - |\delta|$ and the fact that $\mu N_k - x_{k-1} \geq 0$ for all $k \geq 1$, we can continue the above inequality with

$$\begin{aligned}
&\leq \sup_{p' \geq p} \mathtt{P}_{p',\infty}\Big(\exists\, n < (N_{k+1} - N_k + 1) \wedge T_m \text{ s.t. } |X_n - \mu n| > x_k - x_{k-1}\Big) \\
&= \sup_{p' \geq p} \mathtt{P}_{p',\infty}(\tau_{x_k - x_{k-1}} < (N_{k+1} - N_k + 1) \wedge T_m)
\end{aligned}$$

Notice that $N_{k+1} - N_k = 2(x_k - x_{k-1})/\epsilon$. Moreover, let $k_0 = k_0(p,x) = \lfloor \log_2(p/x) \rfloor$ so that $x_k - x_{k-1} = 2^{k-1}x \in [x, p/2]$ for all $1 \leq k \leq k_0$. Then by Lemma V.17, there exist constants x_ϵ and p_ϵ such that uniformly in $p \geq p_\epsilon$, $x \in [x_\epsilon, p/2]$, $1 \leq k < k_0$ and $m \geq 1$,

$$\mathtt{P}_{p,\infty}(K_{x,m}^\epsilon = k) \;\preccurlyeq\; (2^k x)^{-1/6} + \frac{N_{k+1} - N_k}{p} m^{-1/3}\,.$$

Summing over k, we get $\mathtt{P}_{p,\infty}(K_{x,m}^\epsilon < k_0) \preccurlyeq x^{-1/6} + (N_{k_0}/p) \cdot m^{-1/3}$. On the other hand, we read from the definition of $K_{x,m}^\epsilon$ that $\mathtt{P}_{p,\infty}(k_0 \leq K_{x,m}^\epsilon < \infty) \leq \mathtt{P}_{p,\infty}(T_m > N_{k_0}) \leq (N_{k_0}/p)^{-\gamma_0}$, where $\gamma_0 > 0$ is the absolute constant provided by Lemma V.8. Notice that the definition of k_0 implies $\frac{N_{k_0}}{p} = \frac{(2^{k_0}-2)x}{\epsilon p} \in [(2\epsilon)^{-1}, \epsilon^{-1}]$ provided that $x \leq p/2$. Hence by combining the two previous estimates, we conclude that there is a constant C_ϵ depending only on ϵ, such that for all $p \geq p_\epsilon$, $x \in [x_\epsilon, p/2]$ and $m \geq 1$,

$$\mathtt{P}_{p,\infty}(K_{x,m}^\epsilon < \infty) \;\leq\; C_\epsilon(x^{-1/6} + m^{-1/3}) + (2\epsilon)^{\gamma_0}\,.$$

Since $\{\tau_x^\epsilon < T_m\} \subset \{K_{x,m}^\epsilon < \infty\}$, it follows that $\limsup_{m,x\to\infty} \limsup_{p\to\infty} \mathtt{P}_{p,\infty}(\tau_x^\epsilon < T_m) \leq (2\epsilon)^{\gamma_0}$. But the left hand side is a decreasing function of ϵ, so it must be zero for all $\epsilon > 0$. $\square$

Bibliography

[ABA17] Louigi Addario-Berry and Marie Albenque. The scaling limit of random simple triangulations and random simple quadrangulations. *Ann. Probab.*, 45(5):2767–2825, 2017. arXiv:1306.5227.

[Abr16] Céline Abraham. Rescaled bipartite planar maps converge to the Brownian map. *Ann. Inst. Henri Poincaré Probab. Stat.*, 52(2):575–595, 2016. arXiv:1312.5959.

[ABW17] Louigi Addario-Berry and Yuting Wen. Joint convergence of random quadrangulations and their cores. *Ann. Inst. Henri Poincaré Probab. Stat.*, 53(4):1890–1920, 2017. arXiv:1503.06738.

[AC15] Omer Angel and Nicolas Curien. Percolations on random maps I: Half-plane models. *Ann. Inst. Henri Poincaré Probab. Stat.*, 51(2):405–431, 2015. arXiv:1301.5311.

[ADJ97] Jan Ambjørn, Bergfinnur Durhuus, and Thordur Jonsson. *Quantum geometry: a statistical field theory approach*. Cambridge Monographs on Mathematical Physics. Cambridge University Press, Cambridge, 1997.

[Ald91] David Aldous. The continuum random tree. II. An overview. In *Stochastic analysis (Durham, 1990)*, volume 167 of *London Math. Soc. Lecture Note Ser.*, pages 23–70. Cambridge Univ. Press, Cambridge, 1991.

[AS03] Omer Angel and Oded Schramm. Uniform infinite planar triangulations. *Comm. Math. Phys.*, 241(2-3):191–213, 2003. arXiv:math/0207153.

[AS11] Elie Aïdékon and Zhan Shi. Martingale ratio convergence in the branching random walk. *arXiv:1102.0217*, 2011.

[BB08] A. A. Borovkov and K. A. Borovkov. *Asymptotic analysis of random walks: Heavy-tailed distributions*, volume 118 of *Encyclopedia of Mathematics and its Applications*. Cambridge University Press, Cambridge, 2008. Translated from the Russian by O. B. Borovkova.

[BBCK16] Jean Bertoin, Timothy Budd, Nicolas Curien, and Igor Kortchemski. Martingales in self-similar growth-fragmentations and their connections with random planar maps. *arXiv:1605.00581*, may 2016.

[BBD16] Gaëtan Borot, Jérémie Bouttier, and Bertrand Duplantier. Nesting statistics in the $O(n)$ loop model on random planar maps. *arXiv:1605.02239*, 2016.

[BBG12a] G. Borot, Jérémie Bouttier, and Emmanuel Guitter. Loop models on random maps via nested loops: the case of domain symmetry breaking and application to the Potts model. *J. Phys. A*, 45(49):494017, 35, 2012. arXiv:1207.4878.

[BBG12b] G. Borot, Jérémie Bouttier, and Emmanuel Guitter. More on the $O(n)$ model on random maps via nested loops: loops with bending energy. *J. Phys. A*, 45(27):275206, 32, 2012. arXiv:1202.5521.

[BBG12c] G. Borot, Jérémie Bouttier, and Emmanuel Guitter. A recursive approach to the $O(n)$ model on random maps via nested loops. *J. Phys. A*, 45(4):045002, 38, 2012. arXiv:1106.0153.

[BBI01] Dmitri Burago, Yuri Burago, and Sergei Ivanov. *A course in metric geometry*, volume 33 of *Graduate Studies in Mathematics*. American Mathematical Society, Providence, RI, 2001.

[BBM11] Olivier Bernardi and Mireille Bousquet-Mélou. Counting colored planar maps: algebraicity results. *J. Combin. Theory Ser. B*, 101(5):315–377, 2011.

[BBM17] Olivier Bernardi and Mireille Bousquet-Mélou. Counting coloured planar maps: differential equations. *Comm. Math. Phys.*, 354(1):31–84, 2017. arXiv:1507.02391.

[BC12] Itai Benjamini and Nicolas Curien. Ergodic theory on stationary random graphs. *Electron. J. Probab.*, 17:no. 93, 20, 2012. arXiv:1011.2526.

[BC17] Timothy Budd and Nicolas Curien. Geometry of infinite planar maps with high degrees. *Electron. J. Probab.*, 22:Paper No. 35, 37, 2017. arXiv: 1602.01328.

[BCP03] Jean Bertoin, Loïc Chaumont, and Jim Pitman. Path transformations of first passage bridges. *Electron. Comm. Probab.*, 8:155–166 (electronic), 2003.

[BDC16] Vincent Beffara and Hugo Duminil-Copin. Critical point and duality in planar lattice models. In *Probability and statistical physics in St. Petersburg*, volume 91 of *Proc. Sympos. Pure Math.*, pages 51–98. Amer. Math. Soc., Providence, RI, 2016. Lecture notes of the St Petersburg summer School 2012.

[BDFG04] Jérémie Bouttier, Philippe Di Francesco, and Emmanuel Guitter. Planar maps as labeled mobiles. *Electron. J. Combin.*, 11(1):Research Paper 69, 27, 2004. arXiv:math/0405099.

[Ber96] Jean Bertoin. *Lévy processes*, volume 121 of *Cambridge Tracts in Mathematics*. Cambridge University Press, Cambridge, 1996.

[Ber07] Olivier Bernardi. Bijective counting of tree-rooted maps and shuffles of parenthesis systems. *Electron. J. Combin.*, 14(1):Research Paper 9, 36, 2007. arXiv:math/0601684.

[Bet10] Jérémie Bettinelli. Scaling limits for random quadrangulations of positive genus. *Electron. J. Probab.*, 15:no. 52, 1594–1644, 2010. arXiv:1002.3682.

[Bet12] Jérémie Bettinelli. The topology of scaling limits of positive genus random quadrangulations. *Ann. Probab.*, 40(5):1897–1944, 2012. arXiv:1012.3726.

[Bet15a] Jérémie Bettinelli. A bijection for nonorientable general maps. *arXiv:1512.02208*, 2015.

[Bet15b] Jérémie Bettinelli. Scaling limit of random planar quadrangulations with a boundary. *Ann. Inst. Henri Poincaré Probab. Stat.*, 51(2):432–477, 2015. arXiv:1111.7227.

[Big79] John D. Biggins. Growth rates in the branching random walk. *Z. Wahrsch. Verw. Gebiete*, 48(1):17–34, 1979.

[Big92] John D. Biggins. Uniform convergence of martingales in the branching random walk. *Ann. Probab.*, 20(1):137–151, 1992.

[Bil99] Patrick Billingsley. *Convergence of probability measures.* Wiley Series in Probability and Statistics: Probability and Statistics. John Wiley & Sons, Inc., New York, second edition, 1999. A Wiley-Interscience Publication.

[BIPZ78] Édouard Brézin, Claude Itzykson, Giorgio Parisi, and Jean-Bernard Zuber. Planar diagrams. *Comm. Math. Phys.*, 1978.

[BJM14] Jérémie Bettinelli, Emmanuel Jacob, and Grégory Miermont. The scaling limit of uniform random plane maps, *via* the Ambjørn-Budd bijection. *Electron. J. Probab.*, 19:no. 74, 16, 2014. arXiv:1312.5842.

[BK87] D. V. Boulatov and V. A. Kazakov. The Ising model on a random planar lattice: the structure of the phase transition and the exact critical exponents. *Phys. Lett. B*, 186(3-4):379–384, 1987.

[BK04] John D. Biggins and A. E. Kyprianou. Measure change in multitype branching. *Adv. in Appl. Probab.*, 36(2):544–581, 2004.

[BLG13] Johel Beltran and Jean-François Le Gall. Quadrangulations with no pending vertices. *Bernoulli*, 19:1150–1175, 2013.

[BLR17] Nathanaël Berestycki, Benoît Laslier, and Gourab Ray. Critical exponents on Fortuin-Kasteleyn weighted planar maps. *Comm. Math. Phys.*, 355(2):427–462, 2017.

[BM17] Jérémie Bettinelli and Grégory Miermont. Compact Brownian surfaces I: Brownian disks. *Probab. Theory Related Fields*, 167(3-4):555–614, 2017.

[BMJ06] Mireille Bousquet-Mélou and Arnaud Jehanne. Polynomial equations with one catalytic variable, algebraic series and map enumeration. *J. Combin. Theory Ser. B*, 96(5):623–672, 2006.

[BMR16] Erich Baur, Grégory Miermont, and Gourab Ray. Classification of scaling limits of uniform quadrangulations with a boundary. *arXiv:1608.01129*, 2016.

[BMS02] Mireille Bousquet-Mélou and Gilles Schaeffer. The degree distribution in bipartite planar maps: applications to the Ising model. *arXiv:0211070*, 2002.

[Bro63] William G. Brown. Enumeration of non-separable planar maps. *Canad. J. Math.*, 15:526–545, 1963.

[Bro64] William G. Brown. Enumeration of triangulations of the disk. *Proc. London Math. Soc. (3)*, 14:746–768, 1964.

[Bro65a] William G. Brown. Enumeration of quadrangular dissections of the disk. *Canad. J. Math.*, 17:302–317, 1965.

[Bro65b] William G. Brown. On the existence of square roots in certain rings of power series. *Math. Ann.*, 158:82–89, 1965.

[Bro16] Tova Brown. *Asymptotics and Dynamics of Map Enumeration Problems*. PhD thesis, University of Arizona, 2016.

[BS01] Itai Benjamini and Oded Schramm. Recurrence of distributional limits of finite planar graphs. *Electron. J. Probab.*, 6:no. 23, 13 pp. (electronic), 2001.

[BS14] Jakob E. Björnberg and Sigurdur Ö. Stefánsson. Recurrence of bipartite planar maps. *Electron. J. Probab.*, 19:no. 31, 40, 2014. arXiv:1311.0178.

[BT64] W. G. Brown and W. T. Tutte. On the enumeration of rooted non-separable planar maps. *Canad. J. Math.*, 16:572–577, 1964.

[Bud17] Timothy Budd. The peeling process on random planar maps coupled to an $O(n)$ loop model. *In preparation*, 2017. With an appendix jointly with Linxiao Chen.

[CAS] Mathematica notebook accompanying the last chapter. Available at `https://www.dropbox.com/s/ofqk77f85vvatgz/Ising-IPT_CAS.nb?dl=0` , and in PDF at `https://www.dropbox.com/s/depynsozur9op0g/Ising-IPT_CAS.pdf?dl=0`.

[CCM17] Linxiao Chen, Nicolas Curien, and Pascal Maillard. The perimeter cascade in critical boltzmann quadrangulations decorated by an $O(n)$ loop model. *arXiv:1702.06916*, 2017.

[CD06] Philippe Chassaing and Bergfinnur Durhuus. Local limit of labeled trees and expected volume growth in a random quadrangulation. *Ann. Probab.*, 34(3):879–917, 2006.

[Che17] Linxiao Chen. Basic properties of the infinite critical-FK random map. *Ann. Inst. Henri Poincaré D*, 4(3):245–271, 2017. arXiv:1502.01013.

[CK15] Nicolas Curien and Igor Kortchemski. Percolation on random triangulations and stable looptrees. *Probab. Theory Related Fields*, 163(1-2):303–337, 2015. arXiv:1307.6818.

[CLG14] Nicolas Curien and Jean-François Le Gall. The Brownian plane. *J. Theoret. Probab.*, 27(4):1249–1291, 2014.

[CMM13] Nicolas Curien, Laurent Ménard, and Grégory Miermont. A view from infinity of the uniform infinite planar quadrangulation. *Lat. Am. J. Probab. Math. Stat.*, 10(1):45–88, 2013.

[CPV⁺08] Annie Cuyt, Vigdis Brevik Petersen, Brigitte Verdonk, Haakon Waadeland, and William B. Jones. *Handbook of continued fractions for special functions*. Springer, New York, 2008. With contributions by Franky Backeljauw and Catherine Bonan-Hamada, Verified numerical output by Stefan Becuwe and Cuyt.

[CS12] Dmitry Chelkak and Stanislav Smirnov. Universality in the 2D Ising model and conformal invariance of fermionic observables. *Invent. Math.*, 189(3):515–580, 2012.

[CT17] Linxiao Chen and Joonas Turunen. Infinite half-planar Ising-triangulations: Dobrushin boundary condition. *In preparation*, 2017.

[Cur15] Nicolas Curien. A glimpse of the conformal structure of random planar maps. *Commun. Math. Phys.*, 333:1417–1463, 2015.

[Cur16] Nicolas Curien. Planar stochastic hyperbolic triangulations. *Probab. Theory Related Fields*, 165(3-4):509–540, 2016.

[Cur17] Nicolas Curien. Peeling random planar maps (lecture notes), 2017. Lecture notes of Cours Peccot at Collège de France.

[CV81] Robert Cori and Bernard Vauquelin. Planar maps are well labeled trees. *Canad. J. Math.*, 33(5):1023–1042, 1981.

[Dei99] P. A. Deift. *Orthogonal polynomials and random matrices: a Riemann-Hilbert approach*, volume 3 of *Courant Lecture Notes in Mathematics*. New York University, Courant Institute of Mathematical Sciences, New York; American Mathematical Society, Providence, RI, 1999.

[DJW07] Bergfinnur Durhuus, Thordur Jonsson, and John F. Wheater. The spectral dimension of generic trees. *J. Stat. Phys.*, 128(5):1237–1260, 2007.

[DKRV16] François David, Antti Kupiainen, Rémi Rhodes, and Vincent Vargas. Liouville quantum gravity on the Riemann sphere. *Comm. Math. Phys.*, 342(3):869–907, 2016.

[DMS14] Bertrand Duplantier, Jason Miller, and Scott Sheffield. Liouville quantum gravity as a mating of trees. *arXiv:1409.7055*, 2014.

[DS11] Bertrand Duplantier and Scott Sheffield. Liouville quantum gravity and KPZ. *Invent. Math.*, 185(2):333–393, 2011.

[DZ10] Amir Dembo and Ofer Zeitouni. *Large deviations techniques and applications*, volume 38 of *Stochastic Modelling and Applied Probability*. Springer-Verlag, Berlin, 2010. Corrected reprint of the second (1998) edition.

[EB99] B. Eynard and G. Bonnet. The Potts-q random matrix model: loop equations, critical exponents, and rational case. *Phys. Lett. B*, 463(2-4):273–279, 1999.

[EK95] B. Eynard and C. Kristjansen. Exact solution of the O(n) model on a random lattice. *Nuclear Phys. B*, 455(3):577–618, 1995.

[EMOT53] Arthur Erdélyi, Wilhelm Magnus, Fritz Oberhettinger, and Francesco G. Tricomi. *Higher transcendental functions. Vols. I, II.* McGraw-Hill Book Company, Inc., New York-Toronto-London, 1953. Based, in part, on notes left by Harry Bateman.

[EMOT54] A. Erdélyi, W. Magnus, F. Oberhettinger, and F. G. Tricomi. *Tables of integral transforms. Vol. I.* McGraw-Hill Book Company, Inc., New York-Toronto-London, 1954. Based, in part, on notes left by Harry Bateman.

[EO05] Bertrand Eynard and Nicolas Orantin. Mixed correlation functions in the 2-matrix model, and the Bethe ansatz. *J. High Energy Phys.*, (8):028, 36, 2005.

[Eyn16] Bertrand Eynard. *Counting surfaces*, volume 70 of *Progress in Mathematical Physics*. Birkhäuser/Springer, [Cham], 2016. CRM Aisenstadt chair lectures.

[FK72] C. M. Fortuin and P. W. Kasteleyn. On the random-cluster model. I. Introduction and relation to other models. *Physica*, 57:536–564, 1972.

[FS09] Philippe Flajolet and Robert Sedgewick. *Analytic combinatorics*. Cambridge University Press, Cambridge, 2009.

[Fus15] Éric Fusy. *A master bijection method for planar maps (Habilitation thesis)*. Université Paris 11 Orsay, 2015.

[GGN13] Ori Gurel-Gurevich and Asaf Nachmias. Recurrence of planar graph limits. *Ann. of Math. (2)*, 177(2):761–781, 2013. arXiv:1206.0707.

[GJ83] I. P. Goulden and D. M. Jackson. *Combinatorial enumeration*. A Wiley-Interscience Publication. John Wiley & Sons Inc., New York, 1983. With a foreword by Gian-Carlo Rota, Wiley-Interscience Series in Discrete Mathematics.

[GJSZJ12] A. Guionnet, V. F. R. Jones, D. Shlyakhtenko, and P. Zinn-Justin. Loop models, random matrices and planar algebras. *Comm. Math. Phys.*, 316(1):45–97, 2012.

[GKMW16] Ewain Gwynne, Adrien Kassel, Jason Miller, and David B. Wilson. Active spanning trees with bending energy on planar maps and SLE-decorated Liouville quantum gravity for $\kappa > 8$. *arXiv:1603.09722*, 2016.

[GMS15] Ewain Gwynne, Cheng Mao, and Xin Sun. Scaling limits for the critical Fortuin-Kasteleyn model on a random planar map I: cone times. *arXiv:1502.00546*, 2015.

[Gri06] Geoffrey Grimmett. *The random-cluster model*, volume 333 of *Grundlehren der Mathematischen Wissenschaften [Fundamental Principles of Mathematical Sciences]*. Springer-Verlag, Berlin, 2006.

[GS15] Ewain Gwynne and Xin Sun. Scaling limits for the critical Fortuin-Kasteleyn model on a random planar map III: finite volume case. *arXiv:1510.06346*, 2015.

[GS17] Ewain Gwynne and Xin Sun. Scaling limits for the critical Fortuin-Kasteleyn model on a random planar map II: local estimates and empty reduced word exponent. *Electron. J. Probab.*, 22:Paper No. 45, 56, 2017. arXiv:1505.03375.

[Hen77] Peter Henrici. *Applied and computational complex analysis. Vol. 2.* Wiley Interscience [John Wiley & Sons], New York-London-Sydney, 1977. Special functions—integral transforms—asymptotics—continued fractions.

[JS03] Jean Jacod and Albert N. Shiryaev. *Limit theorems for stochastic processes*, volume 288 of *Grundlehren der Mathematischen Wissenschaften [Fundamental Principles of Mathematical Sciences]*. Springer-Verlag, Berlin, second edition, 2003.

[JS11] Thordur Jonsson and Sigurdur Örn Stefánsson. Condensation in nongeneric trees. *J. Stat. Phys.*, 142(2):277–313, 2011.

[JS15] Svante Janson and Sigurdur Örn Stefánsson. Scaling limits of random planar maps with a unique large face. *Ann. Probab.*, 43(3):1045–1081, 2015. arXiv:1212.5072.

[Kaz86] V. A. Kazakov. Ising model on a dynamical planar random lattice: exact solution. *Phys. Lett. A*, 119(3):140–144, 1986.

[Kor15] Igor Kortchemski. Limit theorems for conditioned non-generic Galton-Watson trees. *Ann. Inst. Henri Poincaré Probab. Stat.*, 51(2):489–511, 2015.

[Kos89] I. K. Kostov. O(n) vector model on a planar random lattice: spectrum of anomalous dimensions. *Modern Phys. Lett. A*, 4(3):217–226, 1989.

[KP13] Steven G. Krantz and Harold R. Parks. *The implicit function theorem.* Modern Birkhäuser Classics. Birkhäuser/Springer, New York, 2013. History, theory, and applications, Reprint of the 2003 edition.

[KPZ88] V. G. Knizhnik, A. M. Polyakov, and A. B. Zamolodchikov. Fractal structure of 2D-quantum gravity. *Modern Phys. Lett. A*, 3(8):819–826, 1988.

[Kri06] Maxim Krikun. Local structure of random quadrangulations. *arXiv:math/0512304*, 2006.

[KS92] Ivan K. Kostov and Matthias Staudacher. Multicritical phases of the O(n) model on a random lattice. *Nuclear Phys. B*, 384(3):459–483, 1992. arXiv:hep-th/9203030.

[Kyp98] A. E. Kyprianou. Slow variation and uniqueness of solutions to the functional equation in the branching random walk. *J. Appl. Probab.*, 35(4):795–801, 1998.

[LG13] Jean-François Le Gall. Uniqueness and universality of the Brownian map. *Ann. Probab.*, 41:2880–2960, 2013.

[LGM11] Jean-François Le Gall and Grégory Miermont. Scaling limits of random planar maps with large faces. *Ann. Probab.*, 39(1):1–69, jan 2011.

[LGP08] Jean-François Le Gall and Frédéric Paulin. Scaling limits of bipartite planar maps are homeomorphic to the 2-sphere. *Geom. Funct. Anal.*, 18(3):893–918, 2008.

[Lyo97] Russell Lyons. A simple path to Biggins' martingale convergence for branching random walk. In *Classical and modern branching processes (Minneapolis, MN, 1994)*, volume 84 of *IMA Vol. Math. Appl.*, pages 217–221. Springer, New York, 1997. arXiv:math/9803100.

[LZ04] Sergei K. Lando and Alexander K. Zvonkin. *Graphs on surfaces and their applications*, volume 141 of *Encyclopaedia of Mathematical Sciences*. Springer-Verlag, Berlin, 2004. With an appendix by Don B. Zagier, Low-Dimensional Topology, II.

[Mar16] Cyril Marzouk. Scaling limits of random bipartite planar maps with a prescribed degree sequence. *arXiv:1612.08618*, 2016.

[Mén10] Laurent Ménard. The two uniform infinite quadrangulations of the plane have the same law. *Ann. Inst. H. Poincaré Probab. Statist.*, 46(1):190–208, 2010.

[Mie13] Grégory Miermont. The Brownian map is the scaling limit of uniform random plane quadrangulations. *Acta Math.*, 210(2):319–401, 2013.

[Mie14] Grégory Miermont. Aspects of random maps. *Lecture notes of the 2014 Saint-Flour Probability Summer School, available at http://perso.ens-lyon.fr/gregory.miermont/*, 2014.

[MM07] Jean-François Marckert and Grégory Miermont. Invariance principles for random bipartite planar maps. *Ann. Probab.*, 35(5):1642–1705, 2007. arXiv:math/0504110.

[MS15] Jason Miller and Scott Sheffield. Liouville quantum gravity spheres as matings of finite-diameter trees. *Preprint*, page 52, 2015. arXiv:1506.03804.

[MSW17] Jason Miller, Scott Sheffield, and Wendelin Werner. CLE percolations. *Forum Math. Pi*, 5:e4, 102, 2017. arXiv:1602.03884.

[MT01] Bojan Mohar and Carsten Thomassen. *Graphs on surfaces*. Johns Hopkins Studies in the Mathematical Sciences. Johns Hopkins University Press, Baltimore, MD, 2001.

[MWW16] Jason Miller, Samuel S. Watson, and David B. Wilson. Extreme nesting in the conformal loop ensemble. *Ann. Probab.*, 44(2):1013–1052, 2016. arXiv:1401.0217.

[Nag79] S. V. Nagaev. Large deviations of sums of independent random variables. *Ann. Probab.*, 7(5):745–789, 1979.

[Nel95] Randolph Nelson. *Probability, stochastic processes, and queueing theory*. Springer-Verlag, New York, 1995. The mathematics of computer performance modeling.

[OLBC10] Frank W. J. Olver, Daniel W. Lozier, Ronald F. Boisvert, and Charles W. Clark, editors. *NIST handbook of mathematical functions*. U.S. Department of Commerce, National Institute of Standards and Technology, Washington, DC; Cambridge University Press, Cambridge, 2010. With 1 CD-ROM (Windows, Macintosh and UNIX).

[Pit06] J. Pitman. *Combinatorial stochastic processes*, volume 1875 of *Lecture Notes in Mathematics*. Springer-Verlag, Berlin, 2006. Lectures from the 32nd Summer School on Probability Theory held in Saint-Flour, July 7–24, 2002, With a foreword by Jean Picard.

[Pol81] A. M. Polyakov. Quantum geometry of bosonic strings. *Phys. Lett. B*, 103(3):207–210, 1981.

[Ric17] Loïc Richier. *Géométrie et percolation sur des cartes à bord aléatoire*. PhD thesis, L'École Normale Supérieure de Lyon, 2017.

[Sch98] Gilles Schaeffer. *Conjugaison d'arbres et cartes combinatoires aléatoires*. PhD thesis, Université de Bordeaux 1, 1998.

[She16a] Scott Sheffield. Conformal weldings of random surfaces: SLE and the quantum gravity zipper. *Ann. Probab.*, 44(5):3474–3545, 2016.

[She16b] Scott Sheffield. Quantum gravity and inventory accumulation. *Ann. Probab.*, 44(6):3804–3848, 2016. arXiv:1108.2241.

[Smi01] Stanislav Smirnov. Critical percolation in the plane: conformal invariance, Cardy's formula, scaling limits. *C. R. Acad. Sci. Paris Sér. I Math.*, 333(3):239–244, 2001.

[Smi10] Stanislav Smirnov. Conformal invariance in random cluster models. I. Holomorphic fermions in the Ising model. *Ann. of Math. (2)*, 172(2):1435–1467, 2010.

[SSW09] Oded Schramm, Scott Sheffield, and David B. Wilson. Conformal radii for conformal loop ensembles. *Communications in Mathematical Physics*, 288(1):43–53, 2009.

[Sta99] Richard P. Stanley. *Enumerative combinatorics. Vol. 2*, volume 62 of *Cambridge Studies in Advanced Mathematics*. Cambridge University Press, Cambridge, 1999. With a foreword by Gian-Carlo Rota and appendix 1 by Sergey Fomin.

[SWPD08] J. Rafael Sendra, Franz Winkler, and Sonia Pérez-Díaz. *Rational algebraic curves*, volume 22 of *Algorithms and Computation in Mathematics*. Springer, Berlin, 2008. A computer algebra approach.

[tH74] Gerard 't Hooft. A planar diagram theory for strong interactions. *Nuclear Physics B*, 72:461–473, 1974.

[Tut62a] W. T. Tutte. A census of Hamiltonian polygons. *Canad. J. Math.*, 14:402–417, 1962.

[Tut62b] W. T. Tutte. A census of planar triangulations. *Canad. J. Math.*, 14:21–38, 1962.

[Tut62c] W. T. Tutte. A census of slicings. *Canad. J. Math.*, 14:708–722, 1962.

[Tut63] W. T. Tutte. A census of planar maps. *Canad. J. Math.*, 15:249–271, 1963.

[Tut82] W. T. Tutte. Chromatic solutions. II. *Canad. J. Math.*, 34(4):952–960, 1982.

[Tut95] W. T. Tutte. Chromatic sums revisited. *Aequationes Math.*, 50(1-2):95–134, 1995.

[Wu82] F. Y. Wu. The Potts model. *Rev. Modern Phys.*, 54(1):235–268, 1982.

[Zol86] V. M. Zolotarev. *One-dimensional stable distributions*, volume 65 of *Translations of Mathematical Monographs*. American Mathematical Society, Providence, RI, 1986. Translated from the Russian by H. H. McFaden, Translation edited by Ben Silver.

université PARIS-SACLAY | École doctorale de mathématiques Hadamard (EDMH)

Titre : Cartes planaires aléatoires couplées aux systèmes de spins

Mots Clefs : Carte planaire aléatoire, modèle de boucles $O(n)$, percolation de Fortuin-Kasteleyn, modèle d'Ising, limite locale, géométrie d'interfaces.

Résumé : Cette thèse vise à améliorer notre compréhension des cartes planaires aléatoires décorées par les modèles de physique statistique. On examine trois modèles particuliers à l'aide des outils provenant de l'analyse, de la combinatoire et des probabilités. Dans une perspective géométrique, on se concentre sur les propriétés des interfaces et les limites locales des cartes aléatoires décorées.
Le premier modèle consiste en une famille de quadrangulations aléatoires du disque décorées par un modèle de boucles $O(n)$. Après avoir complété la preuve de son diagramme de phase initiée par [BBG12c] (chap. II), on étudie les longueurs et la structure d'imbrication des boucles dans la phase critique non-générique (chap. III). On montre que ces statistiques, décrites par un arbre étiqueté, convergent en loi vers une cascade multiplicative explicite lorsque la périmètre du disque tend vers l'infini. Le deuxième modèle (chap. IV) consiste en une carte planaire aléatoire décorée par la percolation de Fortuin-Kasteleyn. On complète la preuve de la convergence du modèle esquissée dans [She16b] et établit un certain nombre de propriétés de la limite. Le troisième modèle (chap. V) est celui des triangulations aléatoires du disque décorées par le modèle d'Ising. Il est étroitement lié au modèle des quadrangulations décorées par un modèle $O(n)$ quand $n = 1$. On calcule explicitement la fonction de partition du modèle muni des conditions au bord de Dobrushin au point critique, sous une forme exploitable pour les asymptotiques. à l'aide de ces asymptotiques, on étudie le processus d'épluchage le long de l'interface d'Ising dans la limite où la périmètre du disque tend vers l'infini.

Title : Random planar maps coupled to spin systems

Keys words : Random planar map, $O(n)$ loop model, Fortuin-Kasteleyn percolation, Ising model, local limit, interface geometry.

Abstract : The aim of this thesis is to improve our understanding of random planar maps decorated by statistical physics models. We examine three particular models using tools coming from analysis, combinatorics and probability. From a geometric perspective, we focus on the interface properties and the local limits of the decorated random maps.
The first model defines a family of random quadrangulations of the disk decorated by an $O(n)$-loop model. After completing the proof of its phase diagram initiated in [BBG12c] (Chap. II), we look into the lengths and the nesting structure of the loops in the non-generic critical phase (Chap. III). We show that these statistics, described as a labeled tree, converge in distribution to an explicit multiplicative cascade when the perimeter of the disk tends to infinity. The second model (Chap. IV) consists of random planar maps decorated by the Fortuin-Kasteleyn percolation. We complete the proof of its local convergence sketched in [She16b] and establish a number of properties of the limit. The third model (Chap. V) is that of random triangulations of the disk decorated by the Ising model. It is closely related to the $O(n)$-decorated quadrangulation when $n = 1$. We compute explicitly the partition function of the model with Dobrushin boundary conditions at its critical point, in a form ameneable to asymptotics. Using these asymptotics, we study the peeling process along the Ising interface in the limit where the perimeter of the disk tends to infinity.

Université Paris-Saclay
Espace Technologique / Immeuble Discovery
Route de l'Orme aux Merisiers RD 128 / 91190 Saint-Aubin, France